Adaptive and Neuroadaptive Control for Nonnegative and Compartmental Dynamical Systems

A Dissertation Presented to
The Academic Faculty of
The School of Aerospace Engineering

by

Kostyantyn Y. Volyanskyy

In Partial Fulfillment of
The Requirements for the Degree of
Doctor of Philosophy in Aerospace Engineering

Georgia Institute of Technology
August 2010

Adaptive and Neuroadaptive Control for Nonnegative and Compartmental Dynamical Systems

Approved by:

Dr. Wassim M. Haddad, Chairman
Aerospace Engineering
Georgia Institute of Technology

Dr. Panagiotis Tsiotras
Aerospace Engineering
Georgia Institute of Technology

Dr. J.V.R Prasad
Aerospace Engineering
Georgia Institute of Technology

Dr. Eric Feron
Aerospace Engineering
Georgia Institute of Technology

Dr. James M. Bailey
Department of Anesthesiology
Northeast Georgia Medical Center

Date Approved: June 23, 2010

To my family

Acknowledgements

It is my great pleasure to take this opportunity and express my sincere gratitude to several people who directly or indirectly played a key role in the successful completion of this work. Their constant support and encouragement was a tremendous help to me in many ways.

First, I would like to deeply thank my advisor Professor Wassim M. Haddad. As a scientist of unlimited intellectual frontiers, he has made a deep impact on my research and my future career. His passion for rigor, research, and discovery as well as his fervor for understanding the mysteries of nature, and the translation of these mysteries into the language of mathematics, has had a profound impact on my scientific vision. Besides his motivation and guidance through the different stages of my Ph.D research, I thank him for his patience and friendship. I am also grateful to his family for their hospitality and the great time we had together.

I also want to deeply thank Professor Anthony J. Calise, who was my advisor in the beginning of my Ph.D program at Georgia Tech, and with whom I started my research at Tech. I thank Professor Calise for helping me identify new areas of research, for his encouragement, and for his constant support. I greatly enjoyed our conversations on different subjects.

I would like to express my sincere and deep gratitude to Dr. James M. Bailey; Dr. Bailey was a tremendous source of knowledge when it came to the clinical aspects

of my research. Our discussions on pharmacokinetics and pharmacodymanics were of tremendous help for me to complete this dissertation.

I thank Professors Panagiotis Tsiotras, J. V. R. Prasad, and Eric Feron for taking the time to serve on my dissertation committee and providing helpful comments and suggestions to further improve this dissertation. I am grateful to the School of Aerospace Engineering for providing and fostering teaching and research excellence.

I would like to also thank Dr. Eugene Lavretsky for his help and encouragement. My special thanks also go to Dr. Naira Hovakimyan for sharing ideas and opinions about my research.

I have made many friends while pursuing my doctoral degree, all of whom made my graduate experience at Georgia Tech even more enjoyable. I thank them all for their friendship and support.

Finally, I would like to express my deepest gratitude, love, and respect to my family for their patience, support and encouragement.

I thank the Air Force Office of Scientific Research, the National Science Foundation, and the US Army Medical Research and Material Command for their financial support of this research.

Table of Contents

List of Tables

List of Figures

Summary

Neural networks have been extensively used for adaptive system identification as well as adaptive and neuroadaptive control of highly uncertain systems. The goal of adaptive and neuroadaptive control is to achieve system performance without excessive reliance on system models. To improve robustness and the speed of adaptation of adaptive and neuroadaptive controllers several controller architectures have been proposed in the literature. In this dissertation, we develop a new neuroadaptive control architecture for nonlinear uncertain dynamical systems. The proposed framework involves a novel controller architecture with additional terms in the update laws that are constructed using a moving window of the integrated system uncertainty. These terms can be used to identify the ideal system weights of the neural network as well as effectively suppress system uncertainty. Linear and nonlinear parameterizations of the system uncertainty are considered and state and output feedback neuroadaptive controllers are developed. Furthermore, we extend the developed framework to discrete-time dynamical systems. To illustrate the efficacy of the proposed approach we apply our results to an aircraft model with wing rock dynamics, a spacecraft model with unknown moment of inertia, and an unmanned combat aerial vehicle undergoing actuator failures, and compare our results with standard neuroadaptive control methods.

Nonnegative systems are essential in capturing the behavior of a wide range of dynamical systems involving dynamic states whose values are nonnegative. A sub-

class of nonnegative dynamical systems are compartmental systems. These systems are derived from mass and energy balance considerations and are comprised of homogeneous interconnected microscopic subsystems or compartments which exchange variable quantities of material via intercompartmental flow laws. In this dissertation, we develop direct adaptive and neuroadaptive control framework for stabilization, disturbance rejection and noise suppression for nonnegative and compartmental dynamical systems with noise and exogenous system disturbances. We then use the developed framework to control the infusion of the anesthetic drug propofol for maintaining a desired constant level of depth of anesthesia for surgery in the face of continuing hemorrhage and hemodilution.

Critical care patients, whether undergoing surgery or recovering in intensive care units, require drug administration to regulate physiological variables such as blood pressure, cardiac output, heart rate, and degree of consciousness. The rate of infusion of each administered drug is critical, requiring constant monitoring and frequent adjustments. In this dissertation, we develop a neuroadaptive output feedback control framework for nonlinear uncertain nonnegative and compartmental systems with nonnegative control inputs and noisy measurements. The proposed framework is Lyapunov-based and guarantees ultimate boundedness of the error signals. In addition, the neuroadaptive controller guarantees that the physical system states remain in the nonnegative orthant of the state space. Finally, the developed approach is used to control the infusion of the anesthetic drug propofol for maintaining a desired constant level of depth of anesthesia for surgery in the face of noisy electroencephalographic (EEG) measurements. Clinical trials demonstrate excellent regulation of unconsciousness allowing for a safe and effective administration of the anesthetic agent propofol.

Furthermore, a neuroadaptive output feedback control architecture for nonlin-

ear nonnegative dynamical systems with input amplitude and integral constraints is developed. Specifically, the neuroadaptive controller guarantees that the imposed amplitude and integral input constraints are satisfied and the physical system states remain in the nonnegative orthant of the state space. The proposed approach is used to control the infusion of the anesthetic drug propofol for maintaining a desired constant level of depth of anesthesia for noncardiac surgery in the face of infusion rate constraints and a drug dosing constraint over a specified period.

In addition, the aforementioned control architecture is used to control lung volume and minute ventilation with input pressure constraints that also accounts for spontaneous breathing by the patient. Specifically, we develop a pressure- and work-limited neuroadaptive controller for mechanical ventilation based on a nonlinear multi-compartmental lung model. The control framework does not rely on any averaged data and is designed to automatically adjust the input pressure to the patient's physiological characteristics capturing lung resistance and compliance modeling uncertainty. Moreover, the controller accounts for input pressure constraints as well as work of breathing constraints. The effect of spontaneous breathing is incorporated within the lung model and the control framework.

Finally, a neural network hybrid adaptive control framework for nonlinear uncertain hybrid dynamical systems is developed. The proposed hybrid adaptive control framework is Lyapunov-based and guarantees partial asymptotic stability of the closed-loop hybrid system; that is, asymptotic stability with respect to part of the closed-loop system states associated with the hybrid plant states. A numerical example is provided to demonstrate the efficacy of the proposed hybrid adaptive stabilization approach.

Chapter 1

Introduction

1.1. Adaptive and Neuroadaptive Control

One of the primary reasons for the large interest in neural networks is their capability to approximate a large class of continuous nonlinear maps from the collective action of very simple, autonomous processing units interconnected in simple ways. Neural networks have also attracted attention due to their inherently parallel and highly redundant processing architecture that makes it possible to develop parallel weight update laws. This parallelism makes it possible to effectively update a neural network on line. These properties make neural networks a viable paradigm for adaptive system identification and control of complex highly uncertain systems, and as a consequence the use of neural networks for identification and control has become an active area of research [19, 25, 27, 34, 40, 63, 82, 91–93, 104, 105, 108, 109, 114, 121, 129].

The goal of adaptive and neuroadaptive control is to achieve system performance without excessive reliance on system models. Both controller approaches directly or indirectly adjust feedback controller gains and improve system performance in the face of system uncertainty. Specifically, indirect adaptive and neuroadaptive controllers utilize parameter update laws to identify unknown system parameters and adjust feedback gains to account for system variation, while direct adaptive and neuroad-

aptive controllers adjust the controller gains in response to system variations. The fundamental difference between adaptive control and neuroadaptive control can be traced back to the modeling and treatment of the system uncertainties as well as the structure of the basis functions used in constructing the regressor vector. In particular, adaptive control is based on *constant*, *linearly parameterized* system uncertainty models of a known structure but unknown parameters [5, 66, 103]. This uncertainty characterization allows for the system nonlinearities to be parameterized by a *finite* linear combination of basis functions within a class of function approximators such as rational functions, spline functions, radial basis functions, sigmoidal functions, and wavelets. However, this linear parametrization with a given basis function cannot, in general, exactly capture the system uncertainty.

To approximate a larger class of nonlinear system uncertainty, the uncertainty can be expressed in terms of a neural network involving a parameterized nonlinearity. Hence, in contrast to adaptive control, neuroadaptive control is based on the universal function approximation property, wherein any continuous nonlinear system uncertainty can be *approximated* arbitrarily closely on a compact set using a neural network with appropriate size, structure, and weights [92, 129], all of which are not necessarily known a priori. Hence, while neuroadaptive control has advantages over standard adaptive control in the ability to capture a much larger class of uncertainties, further complexities arise when the basis functions are not known. In particular, the choice and the structure of the basis functions as well as the size of the neural network and the approximation error over a compact domain become important issues to address in neuroadaptive control. This difference in the modeling and treatment of the system uncertainties results in the ability of adaptive controllers to guarantee asymptotic closed-loop system stability versus ultimate boundness as is the case with neuroadaptive controllers [58].

In this dissertation, we develop a new neuroadaptive control architecture for nonlinear uncertain dynamical systems. Specifically, the proposed framework involves a new and novel controller architecture involving additional terms, or *Q-modification terms*, in the update laws that are constructed using a moving time window of the integrated system uncertainty. The Q-modification terms can be used to identify the ideal neural network system weights which can be used in the adaptive law. In addition, these terms effectively suppress system uncertainty. Furthermore, we develop a direct adaptive and neuroadaptive control framework for stabilization, disturbance rejection, and noise suppression of nonnegative and compartmental dynamical systems.

1.2. Nonnegative and Compartmental Dynamical Systems

Nonnegative systems are essential in capturing the behavior of a wide range of dynamical systems involving dynamic states whose values are nonnegative [13,35,47]. A subclass of nonnegative dynamical systems are compartmental systems [3, 14, 44, 47, 69, 70, 113]. These systems are derived from mass and energy balance considerations and are comprised of homogeneous interconnected microscopic subsystems or compartments which exchange variable quantities of material via intercompartmental flow laws. Since biological and physiological systems have numerous input, state, and output properties related to conservation, dissipation, and transport of mass and energy, nonnegative and compartmental systems are remarkably effective in describing the phenomenological behavior of these dynamical systems. The range of applications of nonnegative and compartmental systems is not limited to biological and medical systems. Their usage includes demographic, epidemic [69], ecological [100], economic [13], telecommunications [36], transportation, power, and large-scale systems [124].

In a recent series of papers [52–54] a direct adaptive control framework for linear and nonlinear nonnegative and compartmental systems was developed. The framework in [52–54] is Lyapunov-based and guarantees partial asymptotic set-point regulation, that is, asymptotic set point stability with respect to the closed-loop system states associated with the plant. In addition, the adaptive controllers in [52–54] guarantee that the physical system states remain in the nonnegative orthant of the state space.

In this dissertation, we develop direct adaptive and neuroadaptive control framework for stabilization, disturbance rejection, and noise suppression for nonnegative and compartmental dynamical systems with noise and exogenous system disturbances. We apply our results to automatically control anesthetic drug delivery for maintaining a desired constant level of depth of anesthesia for surgery in the face of continuing hemorrhage and hemodilution, noisy EEG measurements, and drug infusion rate and drug dosage constraints. Finally, we develop a neuroadaptive control architecture to control lung volume and minute ventilation with input pressure constraints that also accounts for spontaneous breathing by the patient.

1.3. Brief Outline of the Dissertation

The contents of the dissertation are as follows. In Chapter 2, we develop a new and novel architecture called Q-modification for adaptive and neuroadaptive control for nonlinear uncertain dynamical systems. In Chapter 3, we extend Q-modification architecture to discrete-time systems. In Chapter 4, we develop a direct adaptive disturbance rejection control framework for compartmental dynamical systems with exogenous bounded disturbances. In Chapter 5, we develop a neuroadaptive output feedback control framework for nonlinear uncertain nonnegative and compartmental systems with nonnegative control inputs and noisy measurements. In Chapter 6, we

design a neuroadaptive output feedback control architecture for nonlinear nonnegative dynamical systems with input amplitude and integral constraints. In Chapter 7, we extend the neuroadaptive output feedback control architecture of Chapter 6 to address the challenging problem of mechanical ventilation control. A neural network hybrid adaptive control framework for nonlinear uncertain hybrid dynamical systems is presented in Chapter 8. Finally, in Chapter 9 we give concluding remarks and discuss future extensions.

Chapter 2

A New Neuroadaptive Control Architecture for Nonlinear Uncertain Systems

2.1. Introduction

Neural networks have been extensively used for adaptive system identification as well as adaptive and neuroadaptive control of highly uncertain systems [19, 25, 27, 34, 40, 63, 82, 91–93, 104, 105, 108, 109, 114, 121, 129]. The goal of adaptive and neuroadaptive control is to achieve system performance without excessive reliance on system models. The fundamental difference between adaptive control and neuroadaptive control can be traced back to the modeling and treatment of the system uncertainties as well as the structure of the basis functions used in constructing the regressor vector. In particular, adaptive control is based on *constant*, *linearly parameterized* system uncertainty models of a known structure but unknown parameters [5, 66, 103]. This uncertainty characterization allows for the system nonlinearities to be parameterized by a *finite* linear combination of basis functions within a class of function approximators such as rational functions, spline functions, radial basis functions, sigmoidal functions, and wavelets. However, this linear parametrization with a given basis function cannot, in general, exactly capture the system uncertainty.

To approximate a larger class of nonlinear system uncertainty, the uncertainty

can be expressed in terms of a neural network involving a parameterized nonlinearity. Hence, in contrast to adaptive control, neuroadaptive control is based on the universal function approximation property, wherein any continuous nonlinear system uncertainty can be *approximated* arbitrarily closely on a compact set using a neural network with appropriate size, structure, and weights [92, 129], all of which are not necessarily known a priori. Hence, while neuroadaptive control has advantages over standard adaptive control in the ability to capture a much larger class of uncertainties, further complexities arise when the basis functions are not known. In particular, the choice and the structure of the basis functions as well as the size of the neural network and the approximation error over a compact domain become important issues to address in neuroadaptive control. This difference in the modeling and treatment of the system uncertainties results in the ability of adaptive controllers to guarantee asymptotic closed-loop system stability versus ultimate boundness as is the case with neuroadaptive controllers [58].

To improve robustness and the speed of adaptation of adaptive and neuroadaptive controllers several controller architectures have been proposed in the literature. These include the σ- and e-modification architectures used to keep the system parameter estimates from growing without bound in the face of system uncertainty [92, 129]. In this chapter, a new neuroadaptive control architecture for nonlinear uncertain dynamical systems is developed. Specifically, the proposed framework involves a new and novel controller architecture involving additional terms, or Q-*modification terms*, in the update laws that are constructed using a moving time window of the integrated system uncertainty. The Q-modification terms can be used to identify the ideal neural network system weights which can be used in the adaptive law. In addition, these terms effectively suppress system uncertainty.

Even though the proposed approach is reminiscent to the composite adaptive

control framework discussed in [127], the Q-modification framework does not involve filtered versions of the control input and system state in the update laws nor does it involve a least-squares exponential forgetting factor. Rather, the update laws involve auxiliary terms predicated on an estimate of the unknown neural network weights which in turn are characterized by an auxiliary equation involving the integrated error dynamics over a moving time interval. For a scalar linearly parameterized uncertainty structure, these ideas were first explored in [136, 137]. In this chapter, we extend the results in [136] to vector uncertainty structures with nonlinear parameterizations. In addition, state and output feedback controllers are developed. Finally, to illustrate the efficacy of the proposed approach we apply our results to an aircraft model with wing rock dynamics, a spacecraft model involving an unknown moment of inertia matrix, and an unmanned combat aerial vehicle undergoing actuator failures, and compare our results with standard neuroadaptive control methods.

2.2. Adaptive Control with a Q-Modification Architecture

In this section, we present the notion of the Q-modification architecture in adaptive control. Specifically, consider the adaptive control problem with error dynamics given by

$$\dot{e}(t) = Ae(t) + b[\Delta(x(t)) - \nu_{\rm ad}(t)], \quad e(0) = e_0, \quad t \geq 0, \tag{2.1}$$

where $e(t) \in \mathbb{R}^n$, $t \geq 0$, is the system error signal, $\Delta : \mathbb{R}^n \to \mathbb{R}$ is the system uncertainty, $x(t) \in \mathbb{R}^n$, $t \geq 0$, is the system state, $\nu_{\rm ad}(t)$ is the adaptive signal whose purpose is to suppress or cancel the effect of the system uncertainty, $A \in \mathbb{R}^{n \times n}$ is a known Hurwitz matrix, and $b = [0, \ldots, 0, 1]^{\rm T} \in \mathbb{R}^n$. For simplicity of exposition, in this section we consider the case where the system uncertainty $\Delta(x(t))$, $t \geq 0$, is a scalar function. Furthermore, in the first part of this section we assume

that the system uncertainty can be perfectly parameterized in terms of a constant *unknown* vector $W \in \mathbb{R}^N$ and a *known* vector of continuous basis functions $\theta(x(t)) = [\theta_1(x(t)), \ldots, \theta_N(x(t))]^{\mathrm{T}} \in \mathbb{R}^N$ such that $\theta_i(x(t))$, $i = 1, \ldots, N$, are bounded for all $t \geq 0$. In particular,

$$\Delta(x(t)) = W^{\mathrm{T}}\theta(x(t)), \quad t \geq 0. \tag{2.2}$$

The parametrization given by (2.2) suggests an adaptive control signal $\nu_{\mathrm{ad}}(t)$, $t \geq 0$, of the form

$$\nu_{\mathrm{ad}}(t) = \hat{W}^{\mathrm{T}}(t)\theta(x(t)), \tag{2.3}$$

where $\hat{W}(t) \in \mathbb{R}^N$, $t \geq 0$, is a vector of the adaptive weights. Hence, the dynamics in (2.1) can be rewritten as

$$\dot{e}(t) = Ae(t) + b[W - \hat{W}(t)]^{\mathrm{T}}\theta(x(t)), \quad e(0) = e_0, \quad t \geq 0. \tag{2.4}$$

The update law for $\hat{W}(t)$, $t \geq 0$, can be derived using standard Lyaupunov analysis by considering the Lyapunov function candidate

$$V(e, \tilde{W}) = \frac{1}{2}e^{\mathrm{T}}Pe + \frac{1}{2}\tilde{W}^{\mathrm{T}}\Gamma^{-1}\tilde{W}, \tag{2.5}$$

where $\tilde{W} \triangleq W - \hat{W}$, $\Gamma = \Gamma^{\mathrm{T}} > 0$, and $P > 0$ satisfies

$$0 = A^{\mathrm{T}}P + PA + R,$$

where $R = R^{\mathrm{T}} > 0$. Note that $V(0, 0) = 0$ and $V(e, \tilde{W}) > 0$ for all $(e, \tilde{W}) \neq (0, 0)$.

Now, differentiating (2.5) along the trajectories of (2.4) yields

$$\dot{V}(e(t), \tilde{W}(t)) = -\frac{1}{2}e^{\mathrm{T}}(t)Re(t) + e^{\mathrm{T}}(t)Pb\tilde{W}^{\mathrm{T}}(t)\theta(x(t)) - \tilde{W}^{\mathrm{T}}(t)\Gamma^{-1}\dot{\hat{W}}(t), \quad t \geq 0.$$

The standard choice of the update law is given by

$$\dot{\hat{W}}(t) = \Gamma e^{\mathrm{T}}(t)Pb\theta(x(t)), \quad \hat{W}(0) = \hat{W}_0, \quad t \geq 0, \tag{2.6}$$

so that $\dot{V}(e(t),\tilde{W}(t)) = -\frac{1}{2}e^{\mathrm{T}}(t)Re(t) \leq 0$, $t \geq 0$, which guarantees that the error signal $e(t)$, $t \geq 0$, and weight error $\tilde{W}(t)$, $t \geq 0$, are Lyapunov stable, and hence, are bounded for all $t \geq 0$. Since $e(t)$ and $\theta(x(t))$ are bounded for all $t \geq 0$, it follows that $\dot{e}(t)$, $t \geq 0$, is bounded, and hence, $\ddot{V}(e(t),\tilde{W}(t))$ is bounded for all $t \geq 0$. Now, it follows from Barbalat's lemma [48] that $e(t)$ converges to zero asymptotically.

The above analysis outlines the salient features of the classical adaptive control architecture. To improve the robustness properties of the adaptive controller (2.3) and (2.6) a σ-modification term of the form $\sigma(\hat{W} - W^0)$, where $\sigma > 0$ and W^0 is an approximation of the ideal neural network system weights, can be included to the update law (2.6) to keep the adaptive weight (i.e., parameter estimate) $\hat{W}$ from growing without bound in the face of the system uncertainty and system disturbances. However, in this case, when the error $e(t)$ is small, $\dot{\hat{W}}(t)$ is dominated by $\sigma(\hat{W} - W^0)$ which causes $\hat{W}$ to be driven to W^0. If W^0 is not a good approximation of the actual system parameters W, then the system error can increase. To circumvent this problem, an e-modification term of the form $\varepsilon(e)(\hat{W} - W^0)$, where, typically, $\varepsilon(e) = \sigma\|e\|$, can be included to the update law (2.6) in place of the σ-modification term. In both cases, however, the modification terms are predicated on W^0 involving a best guess for some $W \in \mathbb{R}^N$.

Next, we present a new and novel modification term that goes beyond the aforementioned modifications by using continuous learning of the unknown weights to improve system uncertainty suppression or achieve uncertainty cancelation without the need for persistency of excitation. Specifically, consider the error dynamics given by (2.4) and integrate (2.4) over the moving time interval $[t_{\mathrm{d}}, t]$, $t \geq 0$, where $t_{\mathrm{d}} \triangleq \max\{0, t - \tau_{\mathrm{d}}\}$ and $\tau_{\mathrm{d}} > 0$ is a design parameter. Premultiplying (2.4) by b^{T} and rearranging terms we obtain

$$W^{\mathrm{T}}q(t, t-\tau_{\mathrm{d}}) = c(t, t-\tau_{\mathrm{d}}), \quad t \geq 0, \quad \tau_{\mathrm{d}} > 0, \tag{2.7}$$

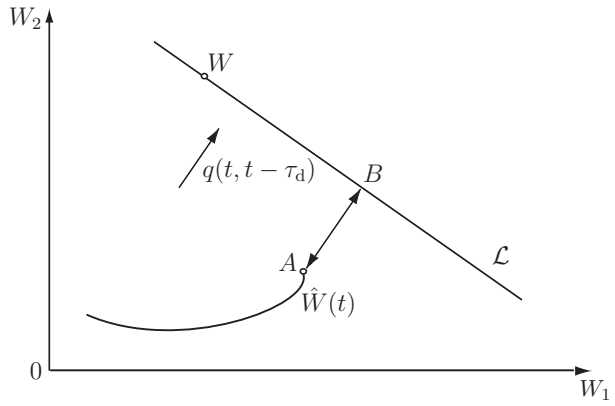

Figure 2.1: Visualization of Q-modification term.

where

$$c(t, t-\tau_{\rm d}) \triangleq b^{\rm T}\left[e(t) - e(t-\tau_{\rm d}) - \int_{t_{\rm d}}^{t} Ae(s){\rm d}s\right] + \int_{t_{\rm d}}^{t} \hat{W}^{\rm T}(s)\theta(x(s)){\rm d}s, \quad t \geq 0,\ \tau_{\rm d} > 0, \tag{2.8}$$

$$q(t, t-\tau_{\rm d}) \triangleq \int_{t_{\rm d}}^{t} \theta(x(s)){\rm d}s, \quad t \geq 0, \quad \tau_{\rm d} > 0. \tag{2.9}$$

Hence, although the vector W is *unknown*, W satisfies the *linear* equation (2.7). Geometrically, (2.7) characterizes an affine hyperplane $\mathcal{L}$ in $\mathbb{R}^N$. For example, in the case where $N = 2$, the affine hyperplane (2.7) is described by a line $\mathcal{L}$ with $q(t, t-\tau_{\rm d})$ being a normal vector to $\mathcal{L}$ as shown in Figure 2.1. Note that the distance from point A to point B shown in Figure 2.1, which is the shortest distance from the weight estimate $\hat{W}(t)$ to affine hyperplane $\mathcal{L}$ defined by (2.7), is given by $c(t, t-\tau_{\rm d}) - \hat{W}^{\rm T}(t)q(t, t-\tau_{\rm d})$.

Next, define the square of the distance from the weight estimate $\hat{W}(t)$, $t \geq 0$, to the affine hyperplane $\mathcal{L}$ by

$$\rho(\hat{W}(t),\, q(t, t-\tau_{\rm d}),\, c(t, t-\tau_{\rm d})) \triangleq \frac{1}{2}\left[\hat{W}^{\rm T}(t)q(t, t-\tau_{\rm d}) - c(t, t-\tau_{\rm d})\right]^2, \quad t \geq 0, \tag{2.10}$$

and note that the gradient of $\rho(\hat{W}(t),\, q(t, t-\tau_{\rm d}),\, c(t, t-\tau_{\rm d}))$, $t \geq 0$, with respect to

$\hat{W}(t)$, $t \geq 0$, is given by

$$\frac{\partial \rho(\hat{W}(t),\, q(t,t-\tau_{\mathrm{d}}),\, c(t,t-\tau_{\mathrm{d}}))}{\partial \hat{W}(t)} = \left[\hat{W}^{\mathrm{T}}(t)q(t,t-\tau_{\mathrm{d}}) - c(t,t-\tau_{\mathrm{d}})\right] q(t,t-\tau_{\mathrm{d}}). \tag{2.11}$$

Now, consider the modified update law for the adaptive weights $\hat{W}(t)$, $t \geq 0$, given by

$$\dot{\hat{W}}(t) = \Gamma \left[e^{\mathrm{T}}(t)Pb\theta(x(t)) + k\, Q(t)\right], \quad \hat{W}(0) = \hat{W}_0, \quad t \geq 0, \tag{2.12}$$

where $k > 0$ and

$$Q(t) \triangleq -\left[\hat{W}^{\mathrm{T}}(t)q(t,t-\tau_{\mathrm{d}}) - c(t,t-\tau_{\mathrm{d}})\right] q(t,t-\tau_{\mathrm{d}}), \quad t \geq 0.$$

In contrast to (2.6), the update law given by (2.12) contains the additional term $Q(t)$, $t \geq 0$, based on the gradient of $\rho(\hat{W}(t),\, q(t,t-\tau_{\mathrm{d}}),\, c(t,t-\tau_{\mathrm{d}}))$ with respect to $\hat{W}(t)$, $t \geq 0$. We call $Q(t)$, $t \geq 0$, a *Q-modification* term. Note that for every $t \geq 0$ the vector $Q(t)$ is directed opposite to the gradient $\frac{\partial \rho(\hat{W}(t),\, q(t,t-\tau_{\mathrm{d}}),\, c(t,t-\tau_{\mathrm{d}}))}{\partial \hat{W}(t)}$ and parallel to $q(t,t-\tau_{\mathrm{d}})$, which is a vector normal to the affine hyperplane defined by (2.7). Hence, $Q(t)$, $t \geq 0$, introduces a component in the update law (2.12) that drives the trajectory $\hat{W}(t)$, $t \geq 0$, in such a way so that the error given by (2.10) is minimized.

Note that if $\hat{W}(t)$, $t \geq 0$, satisfies

$$\hat{W}(t)^{\mathrm{T}} q(t,t-\tau_{\mathrm{d}}) = c(t,t-\tau_{\mathrm{d}}), \quad t \geq 0, \tag{2.13}$$

then $Q(t)$, $t \geq 0$, is zero and the weight estimates $\hat{W}(t)$, $t \geq 0$, lie on the affine hyperplane defined by (2.7). If the weight estimates $\hat{W}(t)$, $t \geq 0$, do not satisfy (2.13), then $Q(t)$, $t \geq 0$, is a nonzero vector that is orthogonal to the affine hyperplane (2.7) and points in the direction of the hyperplane. Thus, the Q-modification term drives the weight estimate trajectory $\hat{W}(t)$, $t \geq 0$, to the affine hyperplane characterized by (2.7), wherein the ideal weights W lie. As shown below, the Q-modification technique

can ensure convergence of the weight estimates $\hat{W}(t)$, $t \geq 0$, to the ideal weights W under persistency of excitation. However, it is important to note here that identifying the unknown weights is not a goal of this research, nor is this necessary for the Q-modification framework to achieve uncertainty suppression or uncertainty cancelation.

Next, we establish stability guarantees of the adaptive law (2.3) with (2.12).

Theorem 2.1. Consider the uncertain dynamical system given by (2.4). The adaptive feedback control law (2.3) with update law given by (2.12) guarantees that the solution $(e(t), \hat{W}(t)) \equiv (0, W)$ of the closed-loop system given by (2.4) and (2.12) is Lyapunov stable and $e(t) \to 0$ as $t \to \infty$ for all $e_0 \in \mathbb{R}^n$ and $\hat{W}_0 \in \mathbb{R}^n$.

Proof. Consider the Lyapunov function candidate given by (2.5) and note that using (2.7) the Lyapunov derivative $\dot{V}(e, \tilde{W})$ along the trajectories of the closed-loop system (2.4) is given by

$$
\begin{aligned}
&\dot{V}(e(t), \tilde{W}(t)) \\
&\quad = -\frac{1}{2} e^{\mathrm{T}}(t) R e(t) + e^{\mathrm{T}}(t) P b \tilde{W}^{\mathrm{T}}(t) \theta(x(t)) - \tilde{W}^{\mathrm{T}}(t) \Gamma^{-1} \dot{\hat{W}}(t) \\
&\quad = -\frac{1}{2} e^{\mathrm{T}}(t) R e(t) - k \tilde{W}^{\mathrm{T}}(t) Q(t) \\
&\quad = -\frac{1}{2} e^{\mathrm{T}}(t) R e(t) + k (W - \hat{W}(t))^{\mathrm{T}} \left[\hat{W}^{\mathrm{T}}(t) q(t, t - \tau_{\mathrm{d}}) - c(t, t - \tau_{\mathrm{d}}) \right] q(t, t - \tau_{\mathrm{d}}) \\
&\quad = -\frac{1}{2} e^{\mathrm{T}}(t) R e(t) \\
&\qquad + k \left[W^{\mathrm{T}} q(t, t - \tau_{\mathrm{d}}) - \hat{W}^{\mathrm{T}}(t) q(t, t - \tau_{\mathrm{d}}) \right] \left[\hat{W}^{\mathrm{T}}(t) q(t, t - \tau_{\mathrm{d}}) - c(t, t - \tau_{\mathrm{d}}) \right] \\
&\quad = -\frac{1}{2} e^{\mathrm{T}}(t) R e(t) - k \left| \hat{W}^{\mathrm{T}}(t) q(t, t - \tau_{\mathrm{d}}) - c(t, t - \tau_{\mathrm{d}}) \right|^2 \\
&\quad = -\frac{1}{2} e^{\mathrm{T}}(t) R e(t) - k \tilde{W}^{\mathrm{T}}(t) q(t, t - \tau_{\mathrm{d}}) q^{\mathrm{T}}(t, t - \tau_{\mathrm{d}}) \tilde{W}(t) \\
&\quad \leq 0, \quad t \geq 0,
\end{aligned} \tag{2.14}
$$

which proves Lyapunov stability of the closed-loop system (2.4) and (2.12). This guarantees that the error signal $e(t)$, $t \geq 0$, and the weight error $\tilde{W}(t)$, $t \geq 0$, are

Lyapunov stable, and hence, are bounded for all $t \geq 0$. The result now follows from Barbalat's lemma [48] using the fact that $\dot{e}(t)$, and hence, $\ddot{V}(e(t), \tilde{W}(t))$, are bounded for all $t \geq 0$. □

Remark 2.1. The nonnegative term $k\,|\hat{W}^{\mathrm{T}}(t)q(t, t-\tau_{\mathrm{d}}) - c(t, t-\tau_{\mathrm{d}})|^2$ in the derivative of the Lyapunov function (2.14) appears due to the Q-modification term in the update law (2.12) and is a measure of the (scaled) distance between the update weights $\hat{W}(t)$, $t \geq 0$, and the affine hyperplane given by (2.7).

Remark 2.2. The Q-modification architecture is reminiscent to the composite adaptation technique [126,127] and the combined direct and indirect adaptation technique [32]. As in the Q-modification framework, composite adaptation involves a linear equation of the unknown weights and uses a prediciton error-based estimation error method to construct additional terms in the update law. However, the key difference between the two methods is in how the linear equations involving the unknown weights are constructed. Specifically, in the Q-modification technique we use a moving time window of the integrated system uncertainty, whereas composite adaptation uses filtered versions of the control input and system state in the update law. In addition, composite adaptation involves a least squares approach with exponential forgetting.

Remark 2.3. The standard adaptive control algorithm of (6) adjusts the parameters in the direction defined by $\theta(x(t))$, $t \geq 0$. In the absence of noise, if $\theta(x(t))$, $t \geq 0$, is constant for some period of time, then the parameters would be adjusted along the vector $\theta(x(t))$, $t \geq 0$, until the error $e(t)$ is zero. In the presence of noise, however, the parameter would wiggle around in the vicinity of the hyperplane orthogonal to $\theta(x(t))$, $t \geq 0$, on which the error $e(t)$ is small. This still allows the parameter estimate $\hat{W}(t)$, $t \geq 0$, to grow without bound.

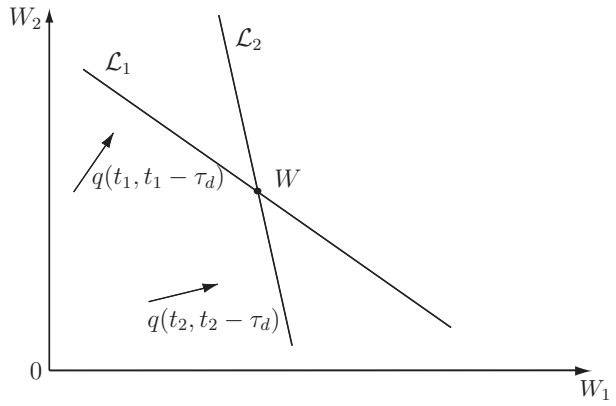

Figure 2.2: Weights identification using Q-modification architecture.

If N time intervals $[t_i - \tau_d,\, t_i]$, $i = 1, \ldots, N$, can be appropriately identified such that the corresponding vectors $q(t_i, t_i - \tau_d)$, $i = 1, \ldots, N$, given by (2.9) are linearly independent and

$$W^{\mathrm{T}} q(t_i, t_i - \tau_d) = c(t_i, t_i - \tau_d), \quad t_i \geq \tau_{\mathrm{d}}, \quad i = 1, \ldots, N, \tag{2.15}$$

where $c(t_i, t_i - \tau_d)$, $i = 1, \ldots, N$, are given by (2.8), then W can be identified *exactly* by solving the linear equation

$$MW = c, \tag{2.16}$$

where

$$M = \begin{bmatrix} q^{\mathrm{T}}(t_1, t_1 - \tau_d) \\ \vdots \\ q^{\mathrm{T}}(t_N, t_N - \tau_d) \end{bmatrix}, \quad c = \begin{bmatrix} c(t_1, t_1 - \tau_d) \\ \vdots \\ c(t_N, t_N - \tau_d) \end{bmatrix}. \tag{2.17}$$

In the case where $N = 2$, Figure 2.2 shows the ideal weight W is identified as the intersection of the two affine hyperplanes $\mathcal{L}_1$ and $\mathcal{L}_2$ characterized by the linearly independent normal (to $\mathcal{L}_1$ and $\mathcal{L}_2$) vectors given by $q(t_1, t_1 - \tau_d)$ and $q(t_2, t_2 - \tau_d)$, respectively.

If the ideal weights can be identified, then no further adaptation is necessary. In this case, we can drive the trajectory $\hat{W}(t)$, $t \geq 0$, to the point W satisfying (2.16) and

setting $\hat{W}(t) = W$ for all $t \geq T$, where $T > \max_{i=1,\ldots,N}\{t_i\}$, so that the uncertainty $\Delta(x)$ in (2.1) is completely canceled by the adaptive signal $\nu_{\rm ad}(t)$ for all $t \geq T$. This, of course, corresponds to an ideal situation. Although for simple problems it may be possible to identify the ideal weights using the technique discussed above, for most problems it is difficult to find N vectors $q(t_i, t_i - \tau_d)$, $i = 1, \ldots, N$, such that the matrix M given by (2.17) is nonsingular and well conditioned. Hence, if a batch solution for N time intervals cannot be appropriately identified such that (2.16) holds, then a moving time window of the integrated system uncertainty can be used to construct the affine hyperplane (2.7) containing W and drive the update weight trajectory $\hat{W}(t)$, $t \geq 0$, to this hyperplane.

As elucidated above, the Q-modification technique is based on a gradient minimization of the cost function defined by (2.10). However, there are other cost function measures based on the integral of the system uncertainty that can be used. For example, define the *accumulated* (or *batch*) *least squares error*

$$\kappa(t,\, \hat{W}(t),\, q_t,\, c_t) \triangleq \frac{1}{2}\int_0^t \left[\hat{W}^{\rm T}(t)q(s,0) - c(s,0)\right]^2 {\rm d}s, \quad t \geq 0, \tag{2.18}$$

where the notation $z_t \in \mathcal{C}$ denotes a function defined by $z_t = z(t + \tau, 0)$, $\tau \in [-t,\, 0]$, at time t corresponding to the *piece of the function* z between 0 and t or, equivalently, the *element* z_t in the space of continuous functions $\mathcal{C}$ defined on the interval $[-t,\, 0]$ and taking values in $\mathbb{R}^v$, where $v = N$ or 1. The gradient of this cost function with respect to $\hat{W}(t)$, $t \geq 0$, is given by

$$\frac{\partial \kappa(t,\, \hat{W}(t),\, q_t,\, c_t)}{\partial \hat{W}(t)} = L(t,\, q_t)\hat{W}(t) - h(t,\, q_t,\, c_t), \quad t \geq 0, \tag{2.19}$$

where

$$L(t,\, q_t) \triangleq \int_0^t q(s,0)q^{\rm T}(s,0){\rm d}s, \quad h(t,\, q_t,\, c_t) \triangleq \int_0^t c(s,0)q(s,0){\rm d}s, \quad t \geq 0. \tag{2.20}$$

For the statement of the next result define $\hat{L}(t) \triangleq L(t,\, q_t)$, $t \geq 0$, and $\hat{h}(t) \triangleq$

$h(t,\, q_t, c_t)$, $t \geq 0$, and consider the update law

$$\dot{\hat{W}}(t) = \Gamma \left[e^{\mathrm{T}}(t) P b \theta(x(t)) + k \left(\hat{h}(t) - \hat{L}(t) \hat{W}(t) \right) \right], \quad \hat{W}(0) = \hat{W}_0, \quad t \geq 0, \tag{2.21}$$

where $\Gamma = \Gamma^{\mathrm{T}} > 0$ and $k > 0$. Furthermore, let $\lambda_{\min}(\cdot)$ and $\lambda_{\max}(\cdot)$ denote the minimum and maximum eigenvalues of a Hermitian matrix, respectively.

Theorem 2.2. Consider the linear uncertain dynamical system given by (2.4). The adaptive feedback control law (2.3) with update law given by (2.21) guarantees that the solution $(e(t), \hat{W}(t)) \equiv (0, W)$ of the closed-loop system given by (2.4) and (2.21) is Lyapunov stable and $e(t) \to 0$ as $t \to \infty$ for all $e_0 \in \mathbb{R}^n$ and $\hat{W}_0 \in \mathbb{R}^n$. Moreover, if $q(t, 0)$, $t \geq 0$, is persistently excited, that is, there exists $T > 0$ such that

$$\int_t^{t+T} q(s,0) q^{\mathrm{T}}(s,0) \mathrm{d}s \geq \alpha I_N, \quad t \geq 0, \tag{2.22}$$

where I_N is the $N \times N$ identity matrix and $\alpha > 0$, then $e(t) \to 0$ and $\hat{W}(t) \to W$ exponentially as $t \to \infty$ with degree not less than

$$K = \frac{\min\{\lambda_{\min}(R),\, 2k\alpha\}}{\max\{\lambda_{\max}(P), \lambda_{\min}(\Gamma)\}}. \tag{2.23}$$

Proof. To show Lyapunov stability of the closed-loop system (2.4) and (2.21) consider the Lyapunov function candidate given by (2.5). Note that since $W^{\mathrm{T}} q(t, 0) = c(t, 0)$, $t \geq 0$, $\hat{h}(t)$, $t \geq 0$, can be rewritten as $\hat{h}(t) = \hat{L}(t) W$, $t \geq 0$. Hence, the time derivative of the Lyapunov function candidate (2.5) along the trajectories of the closed-loop system is given by

$$\dot{V}(e(t), \tilde{W}(t)) = -\frac{1}{2} e^{\mathrm{T}}(t) R e(t) - k\, \tilde{W}^{\mathrm{T}}(t) \hat{L}(t) \tilde{W}(t), \quad t \geq 0. \tag{2.24}$$

Since $\hat{L}(t)$, $t \geq 0$, is nonnegative definite, it follows from (2.24) that $\dot{V}(e(t), \tilde{W}(t)) \leq 0$ for all $t \geq 0$, which proves Lyapunov stability of the closed-loop system (2.4) and (2.21). Hence, $e(t)$, $t \geq 0$, and $\tilde{W}(t)$, $t \geq 0$, are bounded for all $t \geq 0$. Furthermore,

since $\dot{e}(t)$, $t \geq 0$, and $\dot{\tilde{W}}(t)$, $t \geq 0$, are bounded, it follows that $\ddot{V}(e(t), \tilde{W}(t))$ is bounded for all $t \geq 0$. Now, it follows from Barbalat's lemma [48] that $e(t) \to 0$ as $t \to \infty$.

Next, if $q(t, 0)$, $t \geq 0$, is persistently excited, then there exists $\hat{t} > 0$ such that $\hat{L}(t)$ is positive definite for all $t \geq \hat{t}$, that is, there exists $\alpha > 0$ such that $L(t) \geq \alpha I_N > 0$, $t \geq \hat{t}$. Hence,

$$\frac{\dot{V}(e(t), \tilde{W}(t))}{V(e(t), \tilde{W}(t))} = -\frac{\left[e^{\mathrm{T}}(t),\, \tilde{W}^{\mathrm{T}}(t)\right]^{\mathrm{T}} \left[\begin{array}{cc} \frac{1}{2}R & 0 \\ 0 & k\,\hat{L}(t) \end{array}\right] \left[\begin{array}{c} e(t) \\ \tilde{W}(t) \end{array}\right]}{\left[e^{\mathrm{T}}(t),\, \tilde{W}^{\mathrm{T}}(t)\right]^{\mathrm{T}} \left[\begin{array}{cc} \frac{1}{2}P & 0 \\ 0 & \frac{1}{2}\Gamma^{-1} \end{array}\right] \left[\begin{array}{c} e(t) \\ \tilde{W}(t) \end{array}\right]} \leq -K, \quad t \geq \hat{t}, \quad (2.25)$$

where K is given by (2.23). This proves that $e(t)$ and $\tilde{W}(t)$ converge to zero exponentially as $t \to \infty$, which completes the proof. □

Remark 2.4. It follows from Theorem 2.2 that if $q(t, 0)$, $t \geq 0$, is persistently excited, then $\hat{W}(t)$ approaches W exponentialy, where the point W is the optimal solution that would result from a batch solution when N time intervals are appropriately identified and (2.16) holds. In the absence of persistency of excitation, the update weights converge to the affine hyperplane (2.7) containing W.

Next, we show the efficacy of the Q-modification technique in addressing uncertainty cancelation or suppression. Specifically, suppose that the weight estimates $\hat{W}(t)$ satisfy (2.13) for some $t \geq 0$ and the vector $\theta(x(t))$ is parallel to $q(t, t - \tau_{\mathrm{d}})$, that is, there exists $k > 0$ such that $\theta(x(t)) = k\, q(t, t - \tau_{\mathrm{d}})$. In this case, the uncertainty $\Delta(x(t))$ is perfectly canceled by the adaptive signal $\nu_{\mathrm{ad}}(t)$. To see this, note that it follows from (2.7) that

$$\Delta(x(t)) - \nu_{\mathrm{ad}}(t) = k\,(W - \hat{W}(t))^{\mathrm{T}} q(t, t - \tau_{\mathrm{d}}) = c(t, t - \tau_{\mathrm{d}}) - c(t, t - \tau_{\mathrm{d}}) = 0, \quad t \geq 0, \quad (2.26)$$

which shows uncertainty cancelation.

To show uncertainty suppression, note that since $\theta_i(x(t))$, $i = 1, \ldots, N$, are bounded continuous functions for all $t \geq 0$, it follows from the mean value theorem [48] that, for every $i \in \{1, \ldots, N\}$ and interval $[t_{\rm d}, t]$, $t \geq 0$, there exists $\bar{s}_i \in [t_{\rm d}, t]$ such that

$$q_i(t, t-\tau_{\rm d}) = \int_{t_{\rm d}}^{t} \theta_i(x(s)){\rm d}s = \theta_i(x(\bar{s}_i))\tau_{\rm d}, \quad t \geq 0. \tag{2.27}$$

Hence, for all $t \geq 0$ and each $i \in \{1, \ldots, N\}$,

$$q_i(t, t-\tau_{\rm d}) = \theta_i(x(t))\tau_{\rm d} + \varepsilon_i(t, \tau_{\rm d}), \tag{2.28}$$

where $\varepsilon_i(t, \tau_{\rm d}) \triangleq \tau_{\rm d}\left[\theta_i(x(\bar{s}_i)) - \theta_i(x(t))\right]$, or, in vector form,

$$q(t, t-\tau_{\rm d}) = \tau_{\rm d}\theta(x(t)) + \varepsilon(t, \tau_{\rm d}), \quad t \geq 0, \tag{2.29}$$

where $\varepsilon(t, \tau_{\rm d}) \triangleq [\varepsilon_1(t, \tau_{\rm d}), \ldots, \varepsilon_N(t, \tau_{\rm d})]^{\rm T}$.

If $\hat{W}(t)$, $t \geq 0$, satisfies (2.13), then

$$\begin{aligned} |\Delta(x(t)) - \nu_{\rm ad}(t)| &= \left|W^{\rm T}\theta(x(t)) - \hat{W}(t)^{\rm T}\theta(x(t))\right| \\ &= \left|\frac{1}{\tau_{\rm d}}\tilde{W}^{\rm T}(t)q(t, t-\tau_{\rm d}) - \frac{1}{\tau_{\rm d}}\tilde{W}^{\rm T}(t)\varepsilon(t, \tau_{\rm d})\right| \\ &= \left|-\frac{1}{\tau_{\rm d}}\tilde{W}^{\rm T}(t)\varepsilon(t, \tau_{\rm d})\right| \\ &\leq \frac{1}{\tau_{\rm d}}\|\tilde{W}^{\rm T}(t)\|\|\varepsilon(t, \tau_{\rm d})\|, \quad t \geq 0, \end{aligned} \tag{2.30}$$

where $\|\cdot\|$ denotes the Euclidean vector norm on $\mathbb{R}^N$. Now, if $\tau_{\rm d}$ is chosen such that $\frac{1}{\tau_{\rm d}}\|\varepsilon(t, \tau_{\rm d})\|$ is sufficiently small, then it follows from (2.30) that $|\Delta(x(t)) - \nu_{\rm ad}(t)|$ can be made sufficiently small regardless of the magnitude of $\|\tilde{W}(t)\|$, $t \geq 0$. Hence, the Q-modification technique, which ensures that $\hat{W}(t)$, $t \geq 0$, satisfies (2.13), guarantees system uncertainty suppression. Finally, note that since $\frac{1}{\tau_{\rm d}}\varepsilon(t, \tau_{\rm d}) = [\,\theta_1(x(\bar{s}_1)) - \theta_1(x(t)), \ldots, \theta_N(x(\bar{s}_N)) - \theta_N(x(t))\,]^{\rm T}$, the choice of $\tau_{\rm d}$ can be made to depend on the

time rate of change of $\theta(x(t))$, $t \geq 0$. Hence, if we assume $\tau_{\mathrm{d}}(\cdot)$ is a time-varying design parameter, then we can derive an optimal choice for $\tau_{\mathrm{d}}(\cdot)$ as a function of the rate of change of $\theta(x(t))$, $t \geq 0$. This extension will be considered in a future research.

The Q-modification technique described above involves the integration of the system uncertainty. To see this, note that (2.7) can be rewritten as

$$\int_{t-\tau_{\mathrm{d}}}^{t} \Delta(x(s))\mathrm{d}s = c(t, t-\tau_{\mathrm{d}}), \quad t \geq 0, \tag{2.31}$$

where the integration is performed over a moving time window of fixed length $[t-\tau_{\mathrm{d}}, t]$, $t \geq 0$. When the system uncertainty can be perfectly parameterized as in (2.2), integration over the time interval $[0, t]$, $t \geq 0$, can be used instead of integration over a moving time window of fixed length. Since perfect system uncertainty parametrization eliminates approximation errors, integration over the time interval $[0, t]$, $t \geq 0$, does not introduce any distortion of the information of unknown weights W given by (2.7). However, in most practical problems, system uncertainty cannot be perfectly parameterized. In this case, neural networks can be used to approximate uncertain nonlinear continuous functions over a compact domain with a bounded error [92].

In particular, let $\Delta : \mathbb{R}^n \to \mathbb{R}$ be given by

$$\Delta(x(t)) = W^{\mathrm{T}}\theta(x(t)) + \varepsilon(x(t)), \quad t \geq 0, \tag{2.32}$$

where $\varepsilon : \mathcal{D}_x \to \mathbb{R}$, $\mathcal{D}_x \subset \mathbb{R}^n$, is the modeling error such that $|\varepsilon(x(t))| \leq \varepsilon^*$, $\varepsilon^* > 0$, for all $x(t) \in \mathcal{D}_x$, $t \geq 0$, where $\mathcal{D}_x$ is a compact set. In this case, integration of the system uncertainty over the time interval $[0, t]$ gives

$$W^{\mathrm{T}}q(t, 0) = c(t, 0) + \int_0^t \varepsilon(x(s))\mathrm{d}s, \quad t \geq 0, \tag{2.33}$$

where the term $\int_0^t \varepsilon(x(s))\mathrm{d}s$ can become very large over time. Hence, (2.33) cannot be used effectively in the update law (2.12) with the appropriate modifications. Alternatively, if the system uncertainty is integrated over a moving time window $[t-\tau_{\mathrm{d}}, t]$,

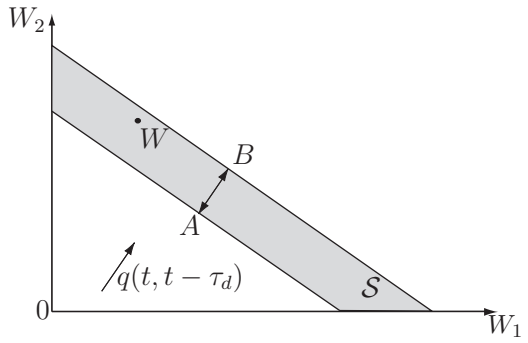

Figure 2.3: Visualization of Q-modification with modeling errors.

$t \geq 0$, then the unknown weights W satisfy

$$W^{\mathrm{T}} q(t, t-\tau_{\mathrm{d}}) = c(t, t-\tau_{\mathrm{d}}) + \int_{t-\tau_{\mathrm{d}}}^{t} \varepsilon(x(s))\mathrm{d}s, \quad t \geq 0, \tag{2.34}$$

where the term $\int_{t-\tau_{\mathrm{d}}}^{t} \varepsilon(x(s))\mathrm{d}s$ is bounded by $\varepsilon^*\tau_{\mathrm{d}}$. By choosing τ_{d} appropriately, one can guarantee that $\varepsilon^*\tau_{\mathrm{d}}$ is sufficiently small. Note that (2.34) defines a collection of parallel affine hyperplanes in $\mathbb{R}^N$, or a *boundary layer*, where the ideal weights W lie. Figure 2.3 shows such a collection of affine hyperplanes $\mathcal{S}$ for the case where $N = 2$. Note that in Figure 2.3 the width of the boundary layer, that is, the distance between points A and B, is $2\tau_{\mathrm{d}}\varepsilon^*$. In the subsequent sections we consider the case of non-perfect parametrizations of the system uncertainty and show how the Q-modification technique can be used to develop static and dynamic neuroadaptive controllers using (2.34).

For illustrative purposes, in this section we considered a simplified version of an adaptive control problem wherein the system uncertainty is a scalar function and the adaptive weight is a vector. Our main goal in this section was to illustrate the main idea of the Q-modification technique by focusing on the salient features of the technical details. In the subsequent sections we develop the Q-modification technique for general nonlinear dynamical systems with vector uncertainty structures, nonlinear uncertainty parameterization, and state and output feedback neuroadaptive controllers.

2.3. Neuroadaptive Full-State Feedback Control for Nonlinear Uncertain Dynamical Systems with a Q-modification Architecture

In this section, we consider the problem of characterizing neuroadaptive full-state feedback control laws for nonlinear uncertain dynamical systems to achieve reference model trajectory tracking. Specifically, consider the controlled nonlinear uncertain dynamical system $\mathcal{G}$ given by

$$\dot{x}(t) = A_0x(t) + B\Lambda\left[G(x(t))u(t) + f(x(t),\hat{u}(t)) + Ax(t)\right], \quad x(0) = x_0, \quad t \geq 0, \tag{2.35}$$

where $x(t) \in \mathbb{R}^n$, $t \geq 0$, is the state vector, $u(t) \in \mathbb{R}^m$, $t \geq 0$, is the control input, $\hat{u}(t) \triangleq [\,u(t-\tau),\, u(t-2\tau),\, \ldots,\, u(t-p\tau)]$ is a vector of p-delayed values of the control input with $p \geq 1$ and $\tau > 0$ given, $A_0 \in \mathbb{R}^{n\times n}$ and $B \in \mathbb{R}^{n\times m}$ are known matrices, $\Lambda \in \mathbb{R}^{m\times m}$ is an *unknown* positive-definite matrix, $G : \mathbb{R}^n \to \mathbb{R}^{m\times m}$ is a known input matrix function such that $\det G(x) \neq 0$ for all $x \in \mathbb{R}^n$, $f : \mathbb{R}^n \times \mathbb{R}^{mp} \to \mathbb{R}^m$ is Lipschitz continuous and bounded in a neighborhood of the origin in $\mathbb{R}^n \times \mathbb{R}^{mp}$ but otherwise *unknown*, and $A \in \mathbb{R}^{m\times n}$ is *unknown*. Furthermore, we assume that $x(t)$, $t \geq 0$, is available for feedback and the control input $u(\cdot)$ in (2.35) is restricted to the class of *admissible controls* consisting of measurable functions such that $u(t) \in \mathbb{R}^m$, $t \geq 0$.

In order to achieve trajectory tracking, we construct a reference system $\mathcal{G}_{\rm ref}$ given by

$$\dot{x}_{\rm ref}(t) = A_{\rm ref}x_{\rm ref}(t) + B_{\rm ref}r(t), \quad x_{\rm ref}(0) = x_{\rm ref_0}, \quad t \geq 0, \tag{2.36}$$

where $x_{\rm ref}(t) \in \mathbb{R}^n$, $t \geq 0$, is the reference state vector, $r(t) \in \mathbb{R}^r$, $t \geq 0$, is a bounded piecewise continuous reference input, $A_{\rm ref} \in \mathbb{R}^{n\times n}$ is Hurwitz, and $B_{\rm ref} \in \mathbb{R}^{n\times r}$. The goal here is to develop an adaptive control signal $u(t)$, $t \geq 0$, that guarantees that

$\|x(t) - x_{\rm ref}(t)\| < \gamma$, $t \geq T$, where $\|\cdot\|$ denotes the Euclidean vector norm on $\mathbb{R}^n$ and $\gamma > 0$ is sufficiently small.

Consider the control law given by

$$u(t) = G^{-1}(x(t))\left[u_{\rm n}(t) + u_{\rm ad}(t)\right], \quad t \geq 0, \tag{2.37}$$

where $u_{\rm n}(t)$, $t \geq 0$, and $u_{\rm ad}(t)$, $t \geq 0$, are defined below. Using the parameterization $\Lambda = \hat{\Lambda} + \delta\Lambda$, where $\hat{\Lambda} \in \mathbb{R}^{m\times m}$ is a known positive-definite matrix that can be chosen and $\delta\Lambda \in \mathbb{R}^{m\times m}$ is an unknown symmetric matrix such that $\hat{\Lambda}+\delta\Lambda$ is positive definite, the dynamics in (2.35) can be rewritten as

$$\begin{aligned}\dot{x}(t) = A_0 x(t) + B\left[\hat{\Lambda}u_{\rm ad}(t) + \Lambda f(x(t),\hat{u}(t)) + \Lambda A x(t) + \delta\Lambda u_{\rm n}(t) + \delta\Lambda u_{\rm ad}(t)\right]\\ +B\hat{\Lambda}u_{\rm n}(t), \qquad x(0) = x_0, \quad t \geq 0.\end{aligned} \tag{2.38}$$

The following matching conditions are needed for the main results of this section.

Assumption 2.1. There exist $K_{\rm x} \in \mathbb{R}^{m\times n}$ and $K_{\rm r} \in \mathbb{R}^{m\times r}$ such that $A_0 + B\hat{\Lambda}K_{\rm x} = A_{\rm ref}$ and $B\hat{\Lambda}K_{\rm r} = B_{\rm ref}$.

Now, let $u_{\rm n}(t)$, $t \geq 0$, in (2.37) be given by

$$u_{\rm n}(t) = K_{\rm x}x(t) + K_{\rm r}r(t), \quad t \geq 0. \tag{2.39}$$

In this case, the system dynamics (2.38) can be rewritten as

$$\begin{aligned}\dot{x}(t) = A_{\rm ref}x(t) + B\left[\hat{\Lambda}u_{\rm ad}(t) + \Lambda f(x(t),\hat{u}(t)) + \Lambda A x(t) + \delta\Lambda u_{\rm n}(t) + \delta\Lambda u_{\rm ad}(t)\right]\\ +B_{\rm ref}r(t), \qquad x(0) = x_0, \quad t \geq 0.\end{aligned}$$

Defining the tracking error $e(t) \triangleq x(t) - x_{\rm ref}(t)$, $t \geq 0$, the error dynamics is given by

$$\begin{aligned}\dot{e}(t) = A_{\rm ref}e(t) + B(\hat{\Lambda}u_{\rm ad}(t) + \Lambda f(x(t),\hat{u}(t)) + \Lambda A x(t) + \delta\Lambda u_{\rm n}(t) + \delta\Lambda u_{\rm ad}(t)),\\ e(0) = e_0, \quad t \geq 0,\end{aligned} \tag{2.40}$$

where $e_0 \triangleq x_0 - x_{\mathrm{ref}_0}$. We assume that the function $f(x, \hat{u})$ can be approximated over a compact set $\mathcal{D}_x \times \mathcal{D}_{\hat{u}}$ by a nonlinear in the parameters neural network up to a desired accuracy. In this case, there exists $\tilde{\varepsilon} : \mathbb{R}^n \times \mathbb{R}^{mp} \to \mathbb{R}^m$ such that $\|\tilde{\varepsilon}(x, \hat{u})\| < \tilde{\varepsilon}^*$, $(x, \hat{u}) \in \mathcal{D}_x \times \mathcal{D}_{\hat{u}}$, where $\tilde{\varepsilon}^* > 0$, and

$$f(x, \hat{u}) = W_f^{\mathrm{T}} \hat{\sigma}(V_f^{\mathrm{T}} \eta(x, \hat{u})) + \tilde{\varepsilon}(x, \hat{u}), \quad (x, \hat{u}) \in \mathcal{D}_x \times \mathcal{D}_{\hat{u}}, \tag{2.41}$$

where $W_f \in \mathbb{R}^{s \times m}$ and $V_f \in \mathbb{R}^{l \times (s-1)}$ are optimal *unknown* (constant) weights that minimize the approximation error over $\mathcal{D}_x \times \mathcal{D}_{\hat{u}}$, $\hat{\sigma}(V_f^{\mathrm{T}} \eta(x, \hat{u})) \triangleq [1,\ \sigma_1(V_{f_1}^{\mathrm{T}} \eta(x, \hat{u})), \sigma_2(V_{f_2}^{\mathrm{T}} \eta(x, \hat{u})), \ldots,\ \sigma_{s-1}(V_{f_{s-1}}^{\mathrm{T}} \eta(x, \hat{u}))]^{\mathrm{T}} \in \mathbb{R}^s$, $\sigma_i(z) \triangleq \frac{1}{1+\exp(-a_i z)}$, $a_i > 0$, $i = 1, \ldots, s-1$, $V_{f_i}^{\mathrm{T}}$ denotes the ith row of V_f^{T}, $i = 1, \ldots, s-1$, $\eta : \mathcal{D}_x \times \mathcal{D}_{\hat{u}} \to \mathbb{R}^l$, and $\tilde{\varepsilon}(\cdot, \cdot)$ is the modeling error.

Since $f(\cdot, \cdot)$ is continuous on $\mathbb{R}^n \times \mathbb{R}^{mp}$, we can choose $\hat{\sigma}(\eta(\cdot, \cdot))$ from a linear space $\mathcal{X}$ of continuous functions that forms an algebra and separates points in $\mathcal{D}_x \times \mathcal{D}_{\hat{u}}$. In this case, it follows from the Stone-Weierstrass theorem [111, p. 212] that $\mathcal{X}$ is a dense subset of the set of continuous functions on $\mathcal{D}_x \times \mathcal{D}_{\hat{u}}$. Now, as is the case in the standard neuroadaptive control literature [92], we can construct a signal involving the estimates of the optimal weights and basis functions as our adaptive control signal. It is important to note here that we assume that we know both the structure and the size of the approximator. This is a standard assumption in the neural network adaptive control literature. In online neural network training, the size and the structure of the optimal approximator are not known and are often chosen by the rule that the larger the size of the neural network and the richer the distribution class of the basis functions over a compact domain, the tighter the resulting approximation error bound $\tilde{\varepsilon}(\cdot, \cdot)$. This goes back to the Stone-Weierstrass theorem which only provides an existence result without any constructive guidelines.

Next, define

$$W_1 \triangleq W_f\Lambda, \quad W_2 \triangleq A^{\mathrm{T}}\Lambda, \quad W_3 \triangleq \delta\Lambda^{\mathrm{T}}, \tag{2.42}$$

and let $u_{\mathrm{ad}}(t)$, $t \geq 0$, in (2.37) be given by

$$u_{\mathrm{ad}}(t) = -\left[\hat{\Lambda} + \hat{W}_3^{\mathrm{T}}(t)\right]^{-1}\left[\hat{W}_1^{\mathrm{T}}(t)\hat{\sigma}(\hat{V}_f^{\mathrm{T}}(t)\eta(x(t),\hat{u}(t))) + \hat{W}_2^{\mathrm{T}}(t)x(t) + \hat{W}_3^{\mathrm{T}}(t)u_{\mathrm{n}}(t)\right], \quad t \geq 0, \tag{2.43}$$

where $\hat{W}_1(t) \in \mathbb{R}^{s\times m}$, $t \geq 0$, $\hat{W}_2(t) \in \mathbb{R}^{n\times m}$, $t \geq 0$, $\hat{W}_3(t) \in \mathbb{R}^{m\times m}$, $t \geq 0$, and $\hat{V}_f(t) \in \mathbb{R}^{l\times(s-1)}$, $t \geq 0$, are update weights. Using (2.41) and (2.42), it follows from (2.43) that the error dynamics (2.40) can be rewritten as

$$\begin{aligned}\dot{e}(t) = {} & A_{\mathrm{ref}}e(t) + B\left[W_1^{\mathrm{T}}\hat{\sigma}(V_f^{\mathrm{T}}\eta(x(t),\hat{u}(t))) - \hat{W}_1^{\mathrm{T}}(t)\hat{\sigma}(\hat{V}_f^{\mathrm{T}}(t)\eta(x(t),\hat{u}(t)))\right] \\ & + \bar{\varepsilon}(x(t),\hat{u}(t)) + B(W_2^{\mathrm{T}} - \hat{W}_2^{\mathrm{T}}(t))x(t) + B(W_3^{\mathrm{T}} - \hat{W}_3^{\mathrm{T}}(t))v(t), \quad e(0) = e_0, \quad t \geq 0, \end{aligned} \tag{2.44}$$

where $\bar{\varepsilon}(x,\hat{u}) \triangleq B\Lambda\tilde{\varepsilon}(x,\hat{u})$. Define $\tilde{W}_i(t) \triangleq W_i - \hat{W}_i(t)$, $i = 1, 2, 3$, $t \geq 0$, and $\tilde{V}_f(t) \triangleq V_f - \hat{V}_f(t)$, $t \geq 0$. As it is often done in the neural network literature, for $(x(t),\hat{u}(t)) \in \mathcal{D}_x \times \mathcal{D}_{\hat{u}}$ and $t \geq 0$, using a Taylor series expansion about $(\hat{W}_1^{\mathrm{T}}(t),\ \hat{V}_f^{\mathrm{T}}(t))$ for $t \in [0,\infty)$ (see [93] for details) it follows that

$$\begin{aligned} & W_1^{\mathrm{T}}\hat{\sigma}(V_f^{\mathrm{T}}\eta(x(t),\hat{u}(t))) - \hat{W}_1^{\mathrm{T}}(t)\hat{\sigma}(\hat{V}_f^{\mathrm{T}}(t)\eta(x(t),\hat{u}(t))) \\ & \quad = \tilde{W}_1^{\mathrm{T}}(t)\left[\hat{\sigma}(\hat{V}_f^{\mathrm{T}}(t)\eta(x(t),\hat{u}(t))) - \hat{\sigma}'(\hat{V}_f^{\mathrm{T}}(t),\eta(x(t),\hat{u}(t)))\hat{V}_f^{\mathrm{T}}(t)\eta(x(t),\hat{u}(t))\right] \\ & \qquad + \hat{W}_1^{\mathrm{T}}(t)\hat{\sigma}'(\hat{V}_f^{\mathrm{T}}(t),\eta(x(t),\hat{u}(t)))\tilde{V}_f^{\mathrm{T}}(t)\eta(x(t),\hat{u}(t)) \\ & \qquad + \tilde{W}_1^{\mathrm{T}}(t)\hat{\sigma}'(\hat{V}_f^{\mathrm{T}}(t),\eta(x(t),\hat{u}(t)))V_f^{\mathrm{T}}(t)\eta(x(t),\hat{u}(t)) + W_1^{\mathrm{T}}\mathcal{O}(\|\tilde{V}_f(t)\|^2), \end{aligned} \tag{2.45}$$

where $\sigma'(\hat{V}_f^{\mathrm{T}}(t),\eta(x(t),\hat{u}(t))) \in \mathbb{R}^{s\times(s-1)}$ is the Jacobian of $\hat{\sigma} : \mathbb{R}^s \to \mathbb{R}^{s\times(s-1)}$ given by

$$\sigma'(\hat{V}_f^{\mathrm{T}}(t),\eta(x(t),\hat{u}(t))) = \left[\begin{array}{ccc} 0 & \cdots & 0 \\ \frac{d\sigma_1(z_1(t))}{dz} & \cdots & 0 \\ \vdots & \ddots & \vdots \\ 0 & \cdots & \frac{d\sigma_{s-1}(z_{s-1}(t))}{dz} \end{array}\right], \tag{2.46}$$

where $z_i(t) = \hat{V}_{f_i}^{\mathrm{T}}(t)\eta(x(t),\hat{u}(t))$, $i = 1, \ldots, s-1$, and $\mathcal{O}(\|\tilde{V}_f\|)/\|\tilde{V}_f\| \to 0$ as $\|\tilde{V}_f\| \to 0$. Since the update laws for $\hat{W}_1(t)$, $t \geq 0$, and $\hat{V}_f(t)$, $t \geq 0$, will be predicated on the projection operator, it follows that $\tilde{W}_1(t)$, $t \geq 0$, and $\tilde{V}_f(t)$, $t \geq 0$, are bounded. Hence, for all $t \geq 0$ and $(x(t),\hat{u}(t)) \in \mathcal{D}_x \times \mathcal{D}_{\hat{u}}$, there exists $\gamma^* > 0$ such that $\|\gamma(t)\| \leq \gamma^*$, where $\gamma(t) \triangleq B\tilde{W}_1^{\mathrm{T}}(t)\hat{\sigma}'(\hat{V}_f^{\mathrm{T}}(t),\eta(x(t),\hat{u}(t)))V_f^{\mathrm{T}}(t)\eta(x(t),\hat{u}(t)) + BW_1^{\mathrm{T}}\mathcal{O}(\|\tilde{V}_f(t)\|^2)$, $t \geq 0$.

Using (2.45) the error dynamics (2.44) are given by

$$\begin{aligned}\dot{e}(t) = {} & A_{\mathrm{ref}}e(t) + B\tilde{W}_2^{\mathrm{T}}(t)x(t) + B\tilde{W}_3^{\mathrm{T}}(t)v(t) + B\tilde{W}_1^{\mathrm{T}}(t)\Big[\hat{\sigma}(\hat{V}_f^{\mathrm{T}}(t)\eta(x(t),\hat{u}(t))) \\ & -\hat{\sigma}'(\hat{V}_f^{\mathrm{T}}(t),\eta(x(t),\hat{u}(t)))\hat{V}_f^{\mathrm{T}}(t)\eta(x(t),\hat{u}(t))\Big] + \bar{\varepsilon}(x(t),\hat{u}(t)) + \gamma(t) \\ & +B\hat{W}_1^{\mathrm{T}}(t)\hat{\sigma}'(\hat{V}_f^{\mathrm{T}}(t),\eta(x(t),\hat{u}(t)))\tilde{V}_f^{\mathrm{T}}(t)\eta(x(t),\hat{u}(t)), \quad e(0) = e_0, \quad t \geq 0.\end{aligned} \tag{2.47}$$

Defining

$$\begin{aligned}\bar{\sigma}(\hat{V}_f(t),x(t),\hat{u}(t)) \triangleq {} & \hat{\sigma}(\hat{V}_f^{\mathrm{T}}(t)\eta(x(t),\hat{u}(t))) \\ & -\hat{\sigma}'(\hat{V}_f^{\mathrm{T}}(t),\eta(x(t),\hat{u}(t)))\hat{V}_f^{\mathrm{T}}(t)\eta(x(t),\hat{u}(t)), \quad t \geq 0,\end{aligned} \tag{2.48}$$

$$H(\hat{W}_1(t),\hat{V}_f(t),x(t),\hat{u}(t)) \triangleq \hat{W}_1^{\mathrm{T}}(t)\hat{\sigma}'(\hat{V}_f^{\mathrm{T}}(t),\eta(x(t),\hat{u}(t))), \quad t \geq 0, \tag{2.49}$$

and using (2.48) and (2.49), the error dynamics (2.47) can be rewritten as

$$\begin{aligned}\dot{e}(t) = {} & A_{\mathrm{ref}}e(t) + B\tilde{W}_1^{\mathrm{T}}(t)\bar{\sigma}(\hat{V}_f(t),x(t),\hat{u}(t)) \\ & +B\,H(\hat{W}_1(t),\hat{V}_f(t),x(t),\hat{u}(t))\tilde{V}_f^{\mathrm{T}}(t)\eta(x(t),\hat{u}(t)) + B\tilde{W}_2^{\mathrm{T}}(t)x(t) \\ & +B\tilde{W}_3^{\mathrm{T}}(t)v(t) + \bar{\varepsilon}(x(t),\hat{u}(t)) + \gamma(t), \quad e(0) = e_0, \quad t \geq 0.\end{aligned} \tag{2.50}$$

Next, we develop a neuroadaptive control architecture which involves additional terms in the update laws that are predicated on auxiliary terms involving an estimate of the unknown weights W_1, V_f, W_2, and W_3. In particular, by integrating the error

dynamics (2.47) over the moving time interval $[t_{\rm d}, t]$, where $t_{\rm d} \triangleq \max\{0, t-\tau_{\rm d}\}$ and $\tau_{\rm d} > 0$, we obtain

$$B\left[W_1^{\rm T},\ \Sigma(t)V_f^{\rm T},\ W_2^{\rm T},\ W_3^{\rm T}\right] q(t, t-\tau_{\rm d}) = c(t, t-\tau_{\rm d}) - \delta(t, t-\tau_{\rm d}), \quad t \geq 0, \quad (2.51)$$

where

$$\Sigma(t) \triangleq \int_{t_{\rm d}}^{t} H(\hat{W}_1(\xi), \hat{V}_f(\xi), x(\xi), \hat{u}(\xi))\mathrm{d}\xi, \quad q(t, t-\tau_{\rm d}) \triangleq \int_{t_{\rm d}}^{t} \mu(\xi)\mathrm{d}\xi, \quad t \geq 0, \quad (2.52)$$

$$\mu(t) \triangleq \left[\bar{\sigma}^{\rm T}(\hat{V}_f(t), x(t), \hat{u}(t))\ \ \eta^{\rm T}(x(t), \hat{u}(t))\ \ x^{\rm T}(t))\ \ v^{\rm T}(t)\right]^{\rm T}, \quad t \geq 0, \quad (2.53)$$

$$\begin{aligned} c(t, t-\tau_{\rm d}) \triangleq & \int_{t_{\rm d}}^{t} B\left[\hat{W}_1^{\rm T}(\xi),\ H(\hat{W}_1(\xi), \hat{V}_f(\xi), x(\xi), \hat{u}(\xi))\hat{V}_f^{\rm T}(\xi),\ \hat{W}_2^{\rm T}(\xi),\ \hat{W}_3^{\rm T}(\xi)\right] \\ & \cdot\mu(\xi)\mathrm{d}\xi + e(t) - e(t_{\rm d}) - \int_{t_{\rm d}}^{t} A_{\rm ref} e(\xi)\mathrm{d}\xi, \quad t \geq 0, \end{aligned} \quad (2.54)$$

$$\begin{aligned} \delta(t, t-\tau_{\rm d}) \triangleq & \int_{t_{\rm d}}^{t} \Big[B\, H(\hat{W}_1(\xi), \hat{V}_f(\xi), x(\xi), \hat{u}(\xi))V_f^{\rm T}\eta(x(\xi), \hat{u}(\xi)) \\ & + \bar{\varepsilon}(x(\xi), \hat{u}(\xi)) + \gamma(\xi)\Big]\mathrm{d}\xi - B\Sigma(t)V_f^{\rm T}\int_{t_{\rm d}}^{t} \eta(x(\xi), \hat{u}(\xi))\mathrm{d}\xi, \ t \geq 0. \end{aligned} \quad (2.55)$$

Note that $\Sigma(t)$, $q(t, t-\tau_{\rm d})$, and $c(t, t-\tau_{\rm d})$ are computable, whereas $\delta(t, t-\tau_{\rm d})$ is an *unknown* integrated modeling error such that $\|\delta(t, t-\tau_{\rm d})\| \leq \tau_{\rm d}\left(\|B\Lambda\|'\tilde{\varepsilon}^* + \gamma^* + \delta_1\right)$, where $\delta_1 > 0$ is such that

$$\begin{aligned} \left\|\int_{t_{\rm d}}^{t} [BH(\hat{W}_1(\xi), \hat{V}_f(\xi), x(\xi), \hat{u}(\xi))V_f^{\rm T}\eta(x(\xi), \hat{u}(\xi))\mathrm{d}\xi - B\Sigma(t)V_f^{\rm T}\int_{t_{\rm d}}^{t} \eta(x(\xi), \hat{u}(\xi))]\mathrm{d}\xi\right\| \\ \leq \delta_1\tau_{\rm d}, \quad t \geq 0, \end{aligned}$$

where $\|\cdot\|' : \mathbb{R}^{n\times m} \to \mathbb{R}$ is the matrix norm induced by the vector norms $\|\cdot\|'' : \mathbb{R}^n \to \mathbb{R}$ and $\|\cdot\|''' : \mathbb{R}^m \to \mathbb{R}$.

For the statement of next result, define the projection operator $\mathrm{Proj}(\tilde{W}, Y)$ given by

$$\mathrm{Proj}(\tilde{W}, Y) \triangleq \begin{cases} Y & \text{if } \mu(\tilde{W}) < 0, \\ Y & \text{if } \mu(\tilde{W}) \geq 0 \text{ and } \mu'(\tilde{W})Y \leq 0, \\ Y - \frac{\mu'(\tilde{W})Y}{\mu'(\tilde{W})\mu'^{\rm T}(\tilde{W})}\mu'^{\rm T}(\tilde{W}) & \text{otherwise,} \end{cases}$$

where $\tilde{W} \in \mathbb{R}^{s\times m}$, $Y \in \mathbb{R}^{n\times m}$, $\mu(\tilde{W}) \triangleq \frac{\operatorname{tr}\tilde{W}^{\mathrm{T}}\tilde{W}-\tilde{w}_{\max}^2}{\varepsilon_{\tilde{W}}}$, $\tilde{w}_{\max} \in \mathbb{R}$ is the norm bound imposed on $\tilde{W}$, and $\varepsilon_{\tilde{W}} > 0$, and $(\cdot)'$ denotes the Fréchet derivative. Note that for a given matrix $\tilde{W} \in \mathbb{R}^{s\times m}$ and $Y \in \mathbb{R}^{n\times m}$, it follows that

$$\begin{aligned}\operatorname{tr}[(\tilde{W}-W)^{\mathrm{T}}(\operatorname{Proj}(\tilde{W},Y)-Y)]&\\ &=\sum_{i=1}^{n}[\operatorname{col}_i(\tilde{W}-W)]^{\mathrm{T}}[\operatorname{Proj}(\operatorname{col}_i(\tilde{W}),\operatorname{col}_i(Y))-\operatorname{col}_i(Y)]\\ &\leq 0,\end{aligned}$$

where $\operatorname{col}_i(X)$ denotes the ith column of the matrix X.

Next, we choose $\tau_{\mathrm{d}} \geq 0$ such that $\|q(t,t-\tau_{\mathrm{d}})\| \leq q_{\max}$ and $\|c(t,t-\tau_{\mathrm{d}})\| \leq c_{\max}$ for all $t \geq 0$. Define

$$\Phi(t) \triangleq \left[W_1^{\mathrm{T}},\ \Sigma(t)V_f^{\mathrm{T}},\ W_2^{\mathrm{T}},\ W_3^{\mathrm{T}}\right] \in \mathbb{R}^{m\times(s+l+n+m)}, \quad t \geq 0, \tag{2.56}$$

$$\hat{\Phi}(t) \triangleq \left[\hat{W}_1^{\mathrm{T}}(t),\ \Sigma(t)\hat{V}_f^{\mathrm{T}}(t),\ \hat{W}_2^{\mathrm{T}}(t),\ \hat{W}_3^{\mathrm{T}}(t)\right] \in \mathbb{R}^{m\times(s+l+n+m)}, \quad t \geq 0, \tag{2.57}$$

and note that it follows from (2.51) that

$$B\Phi(t)q(t,t-\tau_{\mathrm{d}}) = c(t,t-\tau_{\mathrm{d}}) - \delta(t,t-\tau_{\mathrm{d}}), \quad t \geq 0. \tag{2.58}$$

Now, using (2.58) it follows that, for every $k > 0$ and $\Gamma = \Gamma^{\mathrm{T}} > 0$,

$$\begin{aligned}&\operatorname{tr}\left[(\Phi(t)-\hat{\Phi}(t))\Gamma^{-1}\left[k\,\Gamma q(t,t-\tau_{\mathrm{d}})(B\hat{\Phi}(t)q(t,t-\tau_{\mathrm{d}})-c(t,t-\tau_{\mathrm{d}}))^{\mathrm{T}}B\right]\right]\\ &\quad= k\operatorname{tr}\left[B(\Phi(t)-\hat{\Phi}(t))q(t,t-\tau_{\mathrm{d}})\left(B\hat{\Phi}(t)q(t,t-\tau_{\mathrm{d}})-c(t,t-\tau_{\mathrm{d}})\right)^{\mathrm{T}}\right]\\ &\quad= -k\left\|B\hat{\Phi}(t)q(t,t-\tau_{\mathrm{d}})-c(t,t-\tau_{\mathrm{d}})\right\|^2 - k\left(B\hat{\Phi}(t)q(t,t-\tau_{\mathrm{d}})-c(t,t-\tau_{\mathrm{d}})\right)^{\mathrm{T}}\\ &\qquad\cdot\delta(t,t-\tau_{\mathrm{d}})\\ &\quad\leq -k\left\|B\hat{\Phi}(t)q(t,t-\tau_{\mathrm{d}})-c(t,t-\tau_{\mathrm{d}})\right\|^2\\ &\qquad+k(\|B\|'\hat{\Phi}_{\max}q_{\max}+c_{\max})(\|B\Lambda\|'\tilde{\varepsilon}^*+\gamma^*+\delta_1)\tau_{\mathrm{d}}, \quad t \geq 0,\end{aligned} \tag{2.59}$$

where $\hat{\Phi}_{\max}$ is the norm bound imposed on $\hat{\Phi}(t)$, $t \geq 0$. Next, define the Q-

modification term $Q^{\rm nl}(t)$ by

$$Q^{\rm nl}(t) = \left[\begin{array}{c} Q_1^{\rm nl}(t) \\ Q_2^{\rm nl}(t) \\ Q_3^{\rm nl}(t) \\ Q_4^{\rm nl}(t) \end{array} \right] \triangleq q(t, t-\tau_{\rm d}) \left(B\hat{\Phi}^{\rm T}(t) q(t, t-\tau_{\rm d}) - c(t, t-\tau_{\rm d}) \right)^{\rm T} B, \quad t \geq 0, \tag{2.60}$$

where for $t \geq 0$, $Q^{\rm nl}(t) \in \mathbb{R}^{(s+l+n+m)\times m}$, $Q_1^{\rm nl}(t) \in \mathbb{R}^{s\times m}$, $Q_2^{\rm nl}(t) \in \mathbb{R}^{l\times m}$, $Q_3^{\rm nl}(t) \in \mathbb{R}^{n\times m}$, and $Q_4^{\rm nl}(t) \in \mathbb{R}^{m\times m}$.

Consider the feedback control law (2.37) with $u_{\rm n}(t)$ and $u_{\rm ad}(t)$ given by (2.39) and (2.43), and update laws given by

$$\dot{\hat{W}}_1(t) = \Gamma_1 {\rm Proj}[\hat{W}_1(t), \bar{\sigma}(\hat{V}_f^{\rm T}(t), x(t), \hat{u}(t)) e^{\rm T}(t) PB - k\, h(\bar{W}(t)) Q_1^{\rm nl}(t)], \quad \hat{W}_1(0) = \hat{W}_{10}, \quad t \geq 0, \tag{2.61}$$

$$\dot{\hat{V}}_f(t) = \Gamma_f {\rm Proj}[\hat{V}_f(t), \eta(x(t), \hat{u}(t)) e^{\rm T}(t) PBH(\hat{W}_1(t), \hat{V}_f^{\rm T}(t), x(t), \hat{u}(t)) - k\, h(\bar{W}(t)) Q_2^{\rm nl}(t) \Sigma(t)], \quad \hat{V}_f(0) = \hat{V}_{f0}, \tag{2.62}$$

$$\dot{\hat{W}}_2(t) = \Gamma_2 {\rm Proj}[\hat{W}_2(t), x(t) e^{\rm T}(t) PB - k\, h(\bar{W}(t)) Q_3^{\rm nl}(t)], \quad \hat{W}_2(0) = \hat{W}_{20}, \tag{2.63}$$

$$\dot{\hat{W}}_3(t) = \Gamma_3 {\rm Proj}[\hat{W}_3(t), v(t) e^{\rm T}(t) PB - k\, h(\bar{W}(t)) Q_4^{\rm nl}(t)], \quad \hat{W}_3(0) = \hat{W}_{30}, \tag{2.64}$$

where $\Gamma_1 \in \mathbb{R}^{s\times s}$, $\Gamma_f \in \mathbb{R}^{l\times l}$, $\Gamma_2 \in \mathbb{R}^{n\times n}$, and $\Gamma_3 \in \mathbb{R}^{m\times m}$ are positive-definite matrices, $P \in \mathbb{R}^{n\times n}$ is the positive-definite solution of the Lyapunov equation

$$0 = A_{\rm ref}^{\rm T} P + P A_{\rm ref} + R, \tag{2.65}$$

$k > 0$, $\bar{\sigma}(\hat{V}_f^{\rm T}(t), x(t), \hat{u}(t))$ and $H(\hat{W}_1(t), \hat{V}_f(t), x(t), \hat{u}(t))$ are given by (2.48) and (2.49), respectively, $Q_1^{\rm nl}(t)$, $Q_2^{\rm nl}(t)$, $Q_3^{\rm nl}(t)$ and $Q_4^{\rm nl}(t)$ are given by (2.60), $\bar{W}(t) \triangleq (\hat{W}_1(t), \hat{V}_f(t), \hat{W}_2(t), \hat{W}_3(t))$, and $h : \mathbb{R}^{(s+l+n+m)\times m} \to \mathbb{R}$ is a bounded nonnegative function taking values between 0 and 1 such that if ${\rm tr}\, \hat{W}_i^{\rm T}(t) \hat{W}_i(t) = \hat{w}_{i\,\max}^2$, for $i = 1$, 2, or 3, or ${\rm tr}\, \hat{V}_f^{\rm T}(t) \hat{V}_f(t) = \hat{v}_{f\max}^2$, then $h(\bar{W}(t)) = 0$, where $\hat{w}_{i\,\max}^2$, $i = 1$, 2, 3, and $\hat{v}_{f\max}^2$ are the norm bounds imposed on $\hat{W}_i(t)$, $i = 1$, 2, 3, $t \geq 0$, and $\hat{V}_f(t)$, $t \geq 0$, respectively.

Theorem 2.3. Consider the nonlinear uncertain dynamical system $\mathcal{G}$ given by (2.35) with $u(t)$, $t \geq 0$, given by (2.37) and $u_{\mathrm{n}}(t)$ and $u_{\mathrm{ad}}(t)$ given by (2.39) and (2.43), respectively, and reference model given by (2.36) with the tracking error dynamics given by (2.50). Assume Assumption 2.1 holds. Then there exists a compact positively invariant set $\mathcal{D}_\alpha \subset \mathbb{R}^n \times \mathbb{R}^{s\times m} \times \mathbb{R}^{l\times(s-1)} \times \mathbb{R}^{n\times m} \times \mathbb{R}^{m\times m}$ such that $(0, W_1, V_f, W_2, W_3) \in \mathcal{D}_\alpha$, where $W_1 \in \mathbb{R}^{s\times m}$, $V_f \in \mathbb{R}^{l\times(s-1)}$, $W_2 \in \mathbb{R}^{n\times m}$, and $W_2 \in \mathbb{R}^{m\times m}$, and the solution $(e(t), \hat{W}_1(t), \hat{W}_2(t), \hat{W}_3(t))$, $t \geq 0$, of the closed-loop system given by (2.50) and (2.61)–(2.64) is ultimately bounded for all $(e(0), \hat{W}_1(0), \hat{V}_f(0), \hat{W}_2(0), \hat{W}_3(0)) \in \mathcal{D}_\alpha$ with ultimate bound $\|e(t)\| < \theta$, $t \geq T$, where

$$\theta > \Big[(\rho + \sqrt{\rho^2 + \nu})^2 + \lambda_{\max}(\Gamma_1^{-1})\hat{w}_{1\max}^2 + \lambda_{\max}(\Gamma_f^{-1})\hat{v}_{f\max}^2 + \lambda_{\max}(\Gamma_2^{-1})\hat{w}_{2\max}^2 + \lambda_{\max}(\Gamma_3^{-1})\hat{w}_{3\max}^2\Big]^{\frac{1}{2}}, \tag{2.66}$$

$$\rho \triangleq \lambda_{\min}^{-1}(R)\|P\|'(\|B\Lambda\|'\tilde{\varepsilon}^* + \gamma^*), \tag{2.67}$$

$$\nu \triangleq 2k\lambda_{\min}^{-1}(R)(\|B\|'\hat{\Phi}_{\max}q_{\max} + c_{\max})(\|B\Lambda\|'\tilde{\varepsilon}^* + \gamma^* + \delta_1)\tau_{\mathrm{d}}, \tag{2.68}$$

$\hat{w}_{i\max}$, $i = 1, 2, 3$ and $\hat{v}_{f\max}$, are norm bounds imposed on $\hat{W}_i$, and $\hat{V}_f$, respectively, and $P \in \mathbb{R}^{n\times n}$ is the positive-definite solution of the Lyapunov equation (2.65).

Proof. To show ultimate boundedness of the closed-loop system (2.50), (2.37), (2.39), (2.43), (2.61)–(2.64), and (2.60) consider the Lyapunov-like function

$$V(e, \tilde{W}_1, \tilde{V}_f, \tilde{W}_2, \tilde{W}_3) = e^{\mathrm{T}}Pe + \operatorname{tr}\tilde{W}_1^{\mathrm{T}}\Gamma_1^{-1}\tilde{W}_1 + \operatorname{tr}\tilde{V}_f^{\mathrm{T}}\Gamma_f^{-1}\tilde{V}_f + \operatorname{tr}\tilde{W}_2^{\mathrm{T}}\Gamma_2^{-1}\tilde{W}_2 + \operatorname{tr}\tilde{W}_3^{\mathrm{T}}\Gamma_3^{-1}\tilde{W}_3, \tag{2.69}$$

where $P > 0$ satisfies (2.65). Note that (2.69) satisfies $\alpha(\|z\|) \leq V(z) \leq \beta(\|z\|)$ with $z = [e^{\mathrm{T}}, (\operatorname{vec}\tilde{W}_1)^{\mathrm{T}}, (\operatorname{vec}\tilde{V}_f)^{\mathrm{T}}, (\operatorname{vec}\tilde{W}_2)^{\mathrm{T}}, (\operatorname{vec}\tilde{W}_3)^{\mathrm{T}}]^{\mathrm{T}}$ and $\alpha(\|z\|) = \beta(\|z\|) = \|z\|^2$, where $\|z\|^2 \triangleq e^{\mathrm{T}}Pe + \operatorname{tr}\tilde{W}_1^{\mathrm{T}}\Gamma_1^{-1}\tilde{W}_1 + \tilde{V}_f^{\mathrm{T}}\Gamma_f^{-1}\tilde{V}_f + \operatorname{tr}\tilde{W}_2^{\mathrm{T}}\Gamma_2^{-1}\tilde{W}_2 + \operatorname{tr}\tilde{W}_3^{\mathrm{T}}\Gamma_3^{-1}\tilde{W}_3$ and $\operatorname{vec}(\cdot)$ denotes the column stacking operator. Furthermore, note that $\alpha(\cdot)$ and $\beta(\cdot)$ are class $\mathcal{K}_\infty$ functions. Now, letting $e(t)$, $t \geq 0$, denote the solution to (2.50) and

using (2.61)–(2.64), it follows that the time derivative of $V(e, \tilde{W}_1, \tilde{V}_f\tilde{W}_2, \tilde{W}_3)$ along the closed-loop system trajectories is given by

$$
\begin{aligned}
&\dot{V}(e(t), \tilde{W}_1(t), \tilde{V}_f(t), \tilde{W}_2(t), \tilde{W}_3(t)) \\
&= 2e^{\mathrm{T}}(t)P\Big[A_{\mathrm{ref}}e(t) + B\tilde{W}_1^{\mathrm{T}}(t)\bar{\sigma}(\hat{V}_f(t), x(t), \hat{u}(t)) + B\tilde{W}_2^{\mathrm{T}}(t)x(t) + B\tilde{W}_3^{\mathrm{T}}(t)v(t) \\
&\quad + B\,H(\hat{W}_1(t), \hat{V}_f(t), x(t), \hat{u}(t))\tilde{V}_f^{\mathrm{T}}(t)\eta(x(t), \hat{u}(t)) + \bar{\varepsilon}(x(t), \hat{u}(t)) + \gamma(t)\Big] \\
&\quad - 2\mathrm{tr}\,\tilde{W}_1^{\mathrm{T}}(t)\Gamma_1^{-1}\dot{\hat{W}}_1(t) - 2\mathrm{tr}\,\tilde{V}_f^{\mathrm{T}}(t)\Gamma_f^{-1}\dot{\hat{V}}_f(t) - 2\mathrm{tr}\,\tilde{W}_2^{\mathrm{T}}(t)\Gamma_2^{-1}\dot{\hat{W}}_2(t) \\
&\quad - 2\mathrm{tr}\,\tilde{W}_3^{\mathrm{T}}(t)\Gamma_3^{-1}\dot{\hat{W}}_3(t) \\
&= -e^{\mathrm{T}}(t)Re(t) \\
&\quad + 2\mathrm{tr}\,\tilde{W}_2^{\mathrm{T}}(t)\Big[x(t)e^{\mathrm{T}}(t)PB - \mathrm{Proj}[\hat{W}_2(t), x(t)e^{\mathrm{T}}(t)PB - k\,h(\bar{W}(t))Q_3^{\mathrm{nl}}(t)]\Big] \\
&\quad + 2\mathrm{tr}\,\tilde{W}_3^{\mathrm{T}}(t)\Big[v(t)e^{\mathrm{T}}(t)PB - \mathrm{Proj}[\hat{W}_3(t), v(t)e^{\mathrm{T}}(t)PB - k\,h(\bar{W}(t))Q_4^{\mathrm{nl}}(t)]\Big] \\
&\quad + 2\mathrm{tr}\,\tilde{W}_1^{\mathrm{T}}(t)\Big[\bar{\sigma}(\hat{V}_f(t), x(t), \hat{u}(t))e^{\mathrm{T}}(t)PB - \mathrm{Proj}[\hat{W}_1(t), \bar{\sigma}(\hat{V}_f(t), x(t), \hat{u}(t))e^{\mathrm{T}}(t)PB \\
&\quad - k\,h(\bar{W}(t))Q_1^{\mathrm{nl}}(t)]\Big] + 2\mathrm{tr}\,\tilde{V}_f^{\mathrm{T}}(t)\Big[\eta(x(t), \hat{u}(t))e^{\mathrm{T}}(t)PB\,H(\hat{W}_1(t), \hat{V}_f(t), x(t), \hat{u}(t)) \\
&\quad - \mathrm{Proj}[\hat{V}_f(t), \eta(x(t), \hat{u}(t))e^{\mathrm{T}}(t)PB\,H(\hat{W}_1(t), \hat{V}_f(t), x(t), \hat{u}(t)) \\
&\quad - k\,h(\bar{W}(t))Q_2^{\mathrm{nl}}(t)\Sigma(t)]\Big] + 2e^{\mathrm{T}}(t)P\,(\bar{\varepsilon}(x(t), \hat{u}(t)) + \gamma(t)) \\
&\le -\lambda_{\min}(R)\|e(t)\|^2 + 2k\,h(\bar{W}(t))\Big[\mathrm{tr}\,\tilde{W}_1^{\mathrm{T}}(t)Q_1^{\mathrm{nl}}(t) + \mathrm{tr}\,\Sigma(t)\tilde{V}_f^{\mathrm{T}}(t)Q_2^{\mathrm{nl}}(t) \\
&\quad + \mathrm{tr}\,\tilde{W}_2^{\mathrm{T}}(t)Q_3^{\mathrm{nl}}(t) + \mathrm{tr}\,\tilde{W}_3^{\mathrm{T}}(t)Q_4^{\mathrm{nl}}(t)\Big] + 2\|e(t)\|\|P\|'(\|B\Lambda\|'\tilde{\varepsilon}^* + \gamma^*) \\
&\le -\|e(t)\|\Big(\lambda_{\min}(R)\|e(t)\| - 2\|P\|'\Big(\|B\Lambda\|'\tilde{\varepsilon}^* + \gamma^*\Big)\Big) \\
&\quad + 2k\,h(\bar{W}(t))\mathrm{tr}\,\Big[[\tilde{W}_1^{\mathrm{T}}(t)\ \Sigma(t)\tilde{V}_f^{\mathrm{T}}(t)\ \tilde{W}_2^{\mathrm{T}}(t)\ \tilde{W}_3^{\mathrm{T}}(t)\ ]Q^{\mathrm{nl}}\Big], \quad t \ge 0. \qquad (2.70)
\end{aligned}
$$

Next, using (2.56), (2.57), and (2.59), the time derivative of $V(e, \tilde{W}_1, \tilde{V}_f\tilde{W}_2, \tilde{W}_3)$ along the closed-loop system trajectories satisfies

$$
\begin{aligned}
&\dot{V}(e(t), \tilde{W}_1(t), \tilde{W}_2(t), \tilde{W}_3(t)) \\
&\qquad \le -\|e(t)\|\Big(\lambda_{\min}(R)\|e(t)\| - 2\|P\|'\Big(\|B\Lambda\|'\tilde{\varepsilon}^* + \gamma^*\Big)\Big) \\
&\qquad\quad + 2k\,h(\bar{W}(t))\mathrm{tr}\,\Big[\Big(\Phi(t) - \hat{\Phi}(t)\Big)\,Q^{\mathrm{nl}}(t)\Big]
\end{aligned}
$$

$$\leq -\|e(t)\|\Big(\lambda_{\min}(R)\|e(t)\| - 2\|P\|'\Big(\|B\Lambda\|'\tilde{\varepsilon}^* + \gamma^*\Big)\Big)$$
$$-2k\, h(\bar{W}(t))\, \|B\hat{\Phi}(t)q(t, t-\tau_{\rm d}) - c(t, t-\tau_{\rm d})\|^2$$
$$+2k(\|B\|'\hat{\Phi}_{\max}q_{\max} + c_{\max})(\|B\Lambda\|'\tilde{\varepsilon}^* + \gamma^* + \delta_1)\tau_{\rm d}, \tag{2.71}$$

Now, for $\|e(t)\| \geq \alpha_e \triangleq \rho + \sqrt{\rho^2 + \nu}$, where ρ and ν are given by (2.67) and (2.68), it follows that $\dot{V}(e(t), \tilde{W}_1(t), \tilde{V}_f(t), \tilde{W}_2(t), \tilde{W}_3(t)) \leq 0$ for all $t \geq 0$, that is, $\dot{V}(e(t), \tilde{W}_1(t), \tilde{V}_f(t), \tilde{W}_2(t), \tilde{W}_3(t)) \leq 0$ for all $(e(t), \tilde{W}_1(t), \tilde{V}_f(t), \tilde{W}_2(t), \tilde{W}_3(t)) \in \tilde{\mathcal{D}}_{\rm e} \backslash \tilde{\mathcal{D}}_{\rm r}$ and $t \geq 0$, where

$$\tilde{\mathcal{D}}_{\rm e} \triangleq \Big\{(e, \tilde{W}_1, \tilde{V}_f, \tilde{W}_2, \tilde{W}_3) \in \mathbb{R}^n \times \mathbb{R}^{s\times m} \times \mathbb{R}^{l\times(s-1)} \times \mathbb{R}^{m\times n} \times \mathbb{R}^{m\times m} : x \in \mathcal{D}_{\rm c}\Big\},$$
$$\tilde{\mathcal{D}}_{\rm r} \triangleq \Big\{(e, \tilde{W}_1, \tilde{V}_f, \tilde{W}_2, \tilde{W}_3) \in \mathbb{R}^n \times \mathbb{R}^{s\times m} \times \mathbb{R}^{l\times(s-1)} \times \mathbb{R}^{m\times n} \times \mathbb{R}^{m\times m} : \|e\| \leq \alpha_e\Big\}.$$

Finally, define

$$\tilde{\mathcal{D}}_\alpha \triangleq \Big\{(e, \tilde{W}_1, \tilde{V}_f, \tilde{W}_2, \tilde{W}_3) \in \mathbb{R}^n \times \mathbb{R}^{s\times m} \times \mathbb{R}^{l\times(s-1)} \times \mathbb{R}^{m\times n} \times \mathbb{R}^{m\times m} :$$
$$V(e, \tilde{W}_1, \tilde{V}_f, \tilde{W}_2, \tilde{W}_3) \leq \alpha\Big\},$$

where α is the maximum value such that $\tilde{\mathcal{D}}_\alpha \subseteq \tilde{\mathcal{D}}_{\rm e}$, and define

$$\tilde{\mathcal{D}}_\eta \triangleq \Big\{(e, \tilde{W}_1, \tilde{V}_f, \tilde{W}_2, \tilde{W}_3) \in \mathbb{R}^n \times \mathbb{R}^{s\times m} \times \mathbb{R}^{l\times(s-1)} \times \mathbb{R}^{m\times n} \times \mathbb{R}^{m\times m} :$$
$$V(e, \tilde{W}_1, \tilde{V}_f, \tilde{W}_2, \tilde{W}_3) \leq \eta\Big\},$$

where

$$\eta > \beta(\mu) = \mu^2 = \lambda_{\max}(P)\alpha_e^2 + \lambda_{\max}(\Gamma_1^{-1})\hat{w}_{1\max}^2 + \lambda_{\max}(\Gamma_f^{-1})\hat{v}_{f\max}\lambda_{\max}(\Gamma_2^{-1})\hat{w}_{2\max}^2$$
$$+\lambda_{\max}(\Gamma_3^{-1})\hat{w}_{3\max}^2. \tag{2.72}$$

To show ultimate boundedness of the closed-loop system (2.50) and (2.61)–(2.64) assume[1] that $\tilde{\mathcal{D}}_\eta \subset \tilde{\mathcal{D}}_\alpha$. Now, since $\dot{V}(e, \tilde{W}_1, \tilde{V}_f, \tilde{W}_2, \tilde{W}_3) \leq 0$ for all $(e, \tilde{W}_1, \tilde{V}_f, \tilde{W}_2, \tilde{W}_3) \in$

[1]This assumption is standard in the neural network literature and ensures that in the error space $\tilde{\mathcal{D}}_{\rm e}$ there exists at least one Lyapunov level set $\tilde{\mathcal{D}}_\eta \subset \tilde{\mathcal{D}}_\alpha$. In the case where the neural network approximation holds in $\mathbb{R}^n$ with delayed values, this assumption is automatically satisfied.

$\tilde{\mathcal{D}}_{\mathrm{e}} \backslash \tilde{\mathcal{D}}_{\mathrm{r}}$ and $\tilde{\mathcal{D}}_{\mathrm{r}} \subset \tilde{\mathcal{D}}_{\alpha}$, it follows that $\tilde{\mathcal{D}}_{\alpha}$ is positively invariant. Hence, if $(e(0), \tilde{W}_1(0), \tilde{V}_f(0), \tilde{W}_2(0), \tilde{W}_3(0)) \in \tilde{\mathcal{D}}_{\alpha}$, then it follows from Corollary 4.4 of [48] that the solution $(e(t), \tilde{W}_1(t), \tilde{V}_f(0), \tilde{W}_2(t), \tilde{W}_3(t))$, $t \geq 0$, to (2.50) and (2.61)–(2.64) is ultimately bounded with respect to $(e, \tilde{W}_1, \tilde{V}_f, \tilde{W}_2, \tilde{W}_3)$ with ultimate bound given by $\gamma = \alpha^{-1}(\eta) = \sqrt{\eta}$, which yields (2.66). This completes the proof. □

Remark 2.5. Note that since $e(t)$, $t \geq 0$, and $x_{\mathrm{ref}}(t)$, $t \geq 0$, are bounded, it follows that $x(t)$, $t \geq 0$, is bounded, and hence, $u_{\mathrm{n}}(t)$, $t \geq 0$, given by (2.39) is bounded. Furthermore, since $\hat{W}_3(t)$ is bounded for all $t \geq 0$, it is always possible to choose $\hat{\Lambda}$ and $\hat{w}_{3\max}^2$ so that $\left[\hat{\Lambda} + \hat{W}_3^{\mathrm{T}}(t)\right]^{-1}$ exists and is bounded for all $t \geq 0$. This follows from the fact that for any two square matrices A and B, $\det(A + B) \neq 0$ if and only if there exists $\alpha > 0$ such that $\sigma_{\min}(A) > \alpha$ and $\sigma_{\max}(B) \leq \alpha$. Hence, it follows that for $A = \hat{\Lambda}$ and $B = \hat{W}_3^{\mathrm{T}}(t)$, $t \in [0, \infty)$, $\left[\hat{\Lambda} + \hat{W}_3^{\mathrm{T}}(t)\right]^{-1}$ exists for all $t \geq 0$ if $\hat{w}_{3\max}^2$ is sufficiently small. Hence, the adaptive signal $u_{\mathrm{ad}}(t)$, $t \geq 0$, given by (2.43) is bounded. Since $u_{\mathrm{n}}(t)$, $t \geq 0$, and $u_{\mathrm{ad}}(t)$, $t \geq 0$ are bounded, and $\det G(x) \neq 0$ for all $x \in \mathbb{R}^n$, it follows that control input $u(t)$, $t \geq 0$, given by (2.37) is bounded for all $t \geq 0$.

Remark 2.6. It is straightforward to show that the Q-modification framework can be incorporated within a radial basis function neural network-based adaptive controller and combined with the robust adaptive control laws discussed in [66], such as σ- or e-modifications.

Remark 2.7. Note that the Q-modification terms in the update laws (2.61)–(2.64) drive the trajectories of the neural network weights to a collection of affine hyperplanes characterized by (2.51) involving the unknown neural network weights.

2.4. Output Feedback Control for Nonlinear Uncertain Dynamical Systems with a Q-modification Architecture

In this section, we consider the problem of characterizing neuroadaptive dynamic output feedback control laws for nonlinear uncertain dynamical systems to achieve reference model trajectory tracking. Specifically, consider the controlled nonlinear uncertain dynamical system $\mathcal{G}$ given by

$$\dot{x}(t) = A_0 x(t) + B\Lambda \left[u(t) + f(x(t), \hat{u}(t))\right], \quad x(0) = x_0, \quad t \geq 0, \tag{2.73}$$

$$y(t) = Cx(t) + W_y^{\mathrm{T}} \sigma_y(\hat{y}(t), \hat{u}(t)), \tag{2.74}$$

where $x(t) \in \mathbb{R}^n$, $t \geq 0$, is the state vector, $u(t) \in \mathbb{R}^m$, $t \geq 0$, is the control input, $y(t) \in \mathbb{R}^m$, $t \geq 0$, is the system output, $\hat{u}(t) \triangleq [\, u(t - \tau_u),\, u(t - 2\tau_u),\, \ldots,\, u(t - p\tau_u)]$ is a vector of p-delayed values of the control input with $p \geq 1$ and $\tau_u > 0$ given, $\hat{y}(t) \triangleq [\, y(t - \tau_y),\, y(t - 2\tau_y),\, \ldots,\, y(t - q\tau_y)]$ is a vector of q-delayed values of the system output with $q \geq 1$ and $\tau_y > 0$ given, $A_0 \in \mathbb{R}^{n \times n}$, $B \in \mathbb{R}^{n \times m}$, and $C \in \mathbb{R}^{m \times n}$ are known matrices with A_0 Hurwitz, $\Lambda \in \mathbb{R}^{m \times m}$ is an *unknown* positive-definite matrix, $f : \mathbb{R}^n \times \mathbb{R}^{mp} \to \mathbb{R}^m$ is Lipschitz continuous and bounded in a neighborhood of the origin in $\mathbb{R}^n \times \mathbb{R}^{mp}$ but otherwise *unknown*, $W_y \in \mathbb{R}^{k \times m}$ is an *unknown* matrix, and $\sigma_y : \mathbb{R}^{mq} \times \mathbb{R}^{mp} \to \mathbb{R}^k$ is a known bounded Lipschitz continuous function. Furthermore, we assume that the control input $u(\cdot)$ in (2.73) is restricted to the class of *admissible controls* consisting of measurable functions such that $u(t) \in \mathbb{R}^m$, $t \geq 0$.

In order to achieve trajectory tracking, we construct a reference system $\mathcal{G}_{\mathrm{ref}}$ given by

$$\dot{x}_{\mathrm{ref}}(t) = A_{\mathrm{ref}} x_{\mathrm{ref}}(t) + B_{\mathrm{ref}} r(t), \quad x_{\mathrm{ref}}(0) = x_{\mathrm{ref}_0}, \quad t \geq 0, \tag{2.75}$$

$$y_{\mathrm{ref}}(t) = Cx_{\mathrm{ref}}(t), \tag{2.76}$$

where $x_{\mathrm{ref}}(t) \in \mathbb{R}^n$, $t \geq 0$, is the reference state vector, $r(t) \in \mathbb{R}^r$, $t \geq 0$, is a bounded piecewise continuous reference input, $y_{\mathrm{ref}}(t) \in \mathbb{R}^m$, $t \geq 0$, is the reference output,

$A_{\rm ref} \in \mathbb{R}^{n\times n}$ is Hurwitz, and $B_{\rm ref} \in \mathbb{R}^{n\times r}$. The goal of the controller design is to develop an adaptive control signal $u(t)$, $t \geq 0$, predicated on the system measurement $y(t)$, $t \geq 0$, such that $\|y(t) - y_{\rm ref}(t)\| < \gamma$, for all $t \geq T$, where $T \in [0, \infty)$ and $\gamma > 0$ is sufficiently small.

The following matching conditions are needed for the main results of this section.

Assumption 2.2. There exist $K_{\rm y} \in \mathbb{R}^{m\times m}$ and $K_{\rm r} \in \mathbb{R}^{m\times r}$ such that $A_0 + BK_{\rm y}C = A_{\rm ref}$ and $BK_{\rm r} = B_{\rm ref}$.

Consider the control law given by

$$u(t) = \hat{\Lambda}^{-1}(u_{\rm n}(t) + u_{\rm ad}(t)), \quad t \geq 0, \tag{2.77}$$

where $\hat{\Lambda} \in \mathbb{R}^{m\times m}$ is positive-definite matrix, and $u_{\rm n}(t)$, $t \geq 0$, and $u_{\rm ad}(t)$, $t \geq 0$, are defined below. Using the parameterization $\Lambda = \hat{\Lambda} + \delta\Lambda$, where $\delta\Lambda \in \mathbb{R}^{m\times m}$ is an unknown symmetric matrix, the dynamics in (2.73) can be rewritten as

$$\dot{x}(t) = A_0x(t) + Bu_{\rm n}(t) + B\left[u_{\rm ad}(t) + \Lambda f(x(t), \hat{u}(t)) + \delta\Lambda u(t)\right], \ x(0) = x_0, \ t \geq 0. \tag{2.78}$$

Now, let $u_{\rm n}(t)$, $t \geq 0$, in (2.77) be given by

$$u_{\rm n}(t) = K_{\rm y}y(t) + K_{\rm r}r(t), \quad t \geq 0. \tag{2.79}$$

In this case, using Assumption 2.2 the system dynamics (2.78) can be rewritten as

$$\dot{x}(t) = A_{\rm ref}x(t) + B\left[u_{\rm ad}(t) + \Lambda f(x(t), \hat{u}(t)) + \delta\Lambda u(t) + K_{\rm y}W_y^{\rm T}\sigma_y(\hat{y}(t), \hat{u}(t))\right], \\ +B_{\rm ref}r(t)x(0) = x_0, \quad t \geq 0. \tag{2.80}$$

Defining the tracking error $e(t) \triangleq x(t) - x_{\rm ref}(t)$, $t \geq 0$, the error dynamics is given by

$$\dot{e}(t) = A_{\rm ref}e(t) + B\left[u_{\rm ad}(t) + \Lambda f(x(t), \hat{u}(t)) + \delta\Lambda u(t) + K_{\rm y}W_y^{\rm T}\sigma_y(\hat{y}(t), \hat{u}(t))\right], \\ e(0) = e_0, \quad t \geq 0, \tag{2.81}$$

where $e_0 \triangleq x_0 - x_{\mathrm{ref}_0}$.

As in Section 2.3, we approximate the unknown function $f(x, \hat{u})$, $(x, \hat{u}) \in \mathcal{D}_x \times \mathcal{D}_{\hat{u}}$, by a nonlinear in the parameters neural network. In particular, we assume that the function $f(x, \hat{u})$ can be approximated over a compact set $\mathcal{D}_x \times \mathcal{D}_{\hat{u}}$ by a nonlinear in the parameters neural network up to a desired accuracy. In this case, (2.41) holds.

In order to develop an *output* feedback neural network, we use the approach developed in [87] for reconstructing the system states via the system delayed inputs and outputs. Specifically, we use a *memory unit* as a particular form of a tapped delay line that takes a scalar time series input and provides an $(2mn-r)$-dimensional vector output consisting of the present values of the system outputs and system inputs, and their $2(n-1)m - r$ delayed values given by

$$\begin{aligned}\zeta(t) \triangleq\ & [y_1(t), y_1(t-d), \ldots, y_1(t-(n-1)d), \ldots, y_m(t), y_m(t-d), \ldots,\\ & y_m(t-(n-1)d); u_1(t), u_1(t-d), \ldots, u_1(t-(n-r_1-1)d), \ldots, u_m(t),\\ & u_m(t-d), \ldots, u_m(t-(n-r_m-1)d)]^{\mathrm{T}}, \quad t \geq 0, \end{aligned} \tag{2.82}$$

where r_i denotes the relative degree of $\mathcal{G}$ with respect to the output y_i, $i = 1, \ldots, m$, $r \triangleq r_1 + \cdots + r_m$ is the (vector) relative degree of $\mathcal{G}$, and $d > 0$.

Analogous to (2.43), consider the adaptive signal $u_{\mathrm{ad}}(t)$, $t \geq 0$, given by

$$\begin{aligned}u_{\mathrm{ad}}(t) = -\left[I_m + \hat{W}_2^{\mathrm{T}}(t)\hat{\Lambda}^{-1}\right]^{-1} & \left[\hat{W}_1^{\mathrm{T}}(t)\hat{\sigma}(\hat{V}_f^{\mathrm{T}}(t)\hat{\eta}(\zeta(t), \hat{u}(t))) + \hat{W}_2^{\mathrm{T}}(t)\hat{\Lambda}^{-1}u_{\mathrm{n}}(t)\right.\\ & \left. + \hat{W}_y^{\mathrm{T}}(t)\sigma_y(\hat{y}(t), \hat{u}(t))\right], \quad t \geq 0, \end{aligned} \tag{2.83}$$

where $\hat{W}_1(t) \in \mathbb{R}^{s \times m}$, $t \geq 0$, $\hat{W}_2(t) \in \mathbb{R}^{m \times m}$, $t \geq 0$, $\hat{W}_y(t) \in \mathbb{R}^{k \times m}$, $t \geq 0$, and $\hat{V}_f(t) \in \mathbb{R}^{l \times (s-1)}$, $t \geq 0$, are update weights, and $\hat{\eta} : \mathcal{D}_\zeta \times \mathcal{D}_{\hat{u}} \to \mathbb{R}^l$ is continuous and bounded on $\mathcal{D}_\zeta \times \mathcal{D}_{\hat{u}}$, where $\mathcal{D}_\zeta \subset \mathbb{R}^{2mn-r}$ is a compact set. Furthermore, define $W_1 \triangleq W_f\Lambda$ and $W_2 \triangleq \delta\Lambda^{\mathrm{T}}$.

Using (2.41), it follows from (2.83) that the error dynamics (2.81) can be rewritten

as

$$\begin{aligned}\dot{e}(t) = {} & A_{\mathrm{ref}}e(t) + B\left[W_1^{\mathrm{T}}\hat{\sigma}(V_f^{\mathrm{T}}\hat{\eta}(\zeta(t),\hat{u}(t))) - \hat{W}_1^{\mathrm{T}}(t)\hat{\sigma}(\hat{V}_f^{\mathrm{T}}(t)\hat{\eta}(\zeta(t),\hat{u}(t)))\right] \\ & + \bar{\varepsilon}(x(t),\hat{u}(t)) + B(W_2 - \hat{W}_2(t))^{\mathrm{T}}u(t) + BK_{\mathrm{y}}(W_y - \hat{W}_y(t))^{\mathrm{T}}\sigma_y(\hat{y}(t),\hat{u}(t)) \\ & + BW_1^{\mathrm{T}}\left[\hat{\sigma}(V_f^{\mathrm{T}}\eta(x(t),\hat{u}(t))) - \hat{\sigma}(V_f^{\mathrm{T}}\hat{\eta}(\zeta(t),\hat{u}(t))\right],\ e(0) = e_0,\ t \geq 0, \quad (2.84)\end{aligned}$$

where $\bar{\varepsilon}(x,\hat{u}) \triangleq B\Lambda\tilde{\varepsilon}(x,\hat{u})$. Define $\tilde{W}_i(t) \triangleq W_i - \hat{W}_i(t)$, $i = 1, 2$, $t \geq 0$, $\tilde{V}_f(t) \triangleq V_f - \hat{V}_f(t)$, $t \geq 0$, and $\tilde{W}_y(t) \triangleq W_y - \hat{W}_y(t)$, $t \geq 0$. As in Section 2.3 , for $(\zeta(t),\hat{u}(t)) \in \mathcal{D}_\zeta \times \mathcal{D}_{\hat{u}}$ and $t \geq 0$, using a Taylor series expansion about $(\hat{W}_1^{\mathrm{T}}(t),\ \hat{V}_f^{\mathrm{T}}(t))$ for $t \in [0,\infty)$ (see [93] for details) it follows that

$$\begin{aligned}& W_1^{\mathrm{T}}\hat{\sigma}(V_f^{\mathrm{T}}\hat{\eta}(\zeta(t),\hat{u}(t))) - \hat{W}_1^{\mathrm{T}}(t)\hat{\sigma}(\hat{V}_f^{\mathrm{T}}(t)\hat{\eta}(\zeta(t),\hat{u}(t))) \\ & \quad = \tilde{W}_1^{\mathrm{T}}(t)\left[\hat{\sigma}(\hat{V}_f^{\mathrm{T}}(t)\hat{\eta}(\zeta(t),\hat{u}(t))) - \hat{\sigma}'(\hat{V}_f^{\mathrm{T}}(t),\hat{\eta}(\zeta(t),\hat{u}(t)))\hat{V}_f^{\mathrm{T}}(t)\hat{\eta}(\zeta(t),\hat{u}(t))\right] \\ & \qquad + \hat{W}_1^{\mathrm{T}}(t)\hat{\sigma}'(\hat{V}_f^{\mathrm{T}}(t),\hat{\eta}(\zeta(t),\hat{u}(t)))\tilde{V}_f^{\mathrm{T}}(t)\hat{\eta}(\zeta(t),\hat{u}(t)) \\ & \qquad + \tilde{W}_1^{\mathrm{T}}(t)\hat{\sigma}'(\hat{V}_f^{\mathrm{T}}(t),\hat{\eta}(\zeta(t),\hat{u}(t)))V_f^{\mathrm{T}}(t)\hat{\eta}(\zeta(t),\hat{u}(t)) + W_1^{\mathrm{T}}\mathcal{O}(\|\tilde{V}_f(t)\|^2), \quad (2.85)\end{aligned}$$

where $\sigma'(\hat{V}_f^{\mathrm{T}}(t),\hat{\eta}(\zeta(t),\hat{u}(t))) \in \mathbb{R}^{s\times(s-1)}$ is the Jacobian of $\hat{\sigma} : \mathbb{R}^s \to \mathbb{R}^{s\times(s-1)}$ given by

$$\sigma'(\hat{V}_f^{\mathrm{T}}(t),\hat{\eta}(\zeta(t),\hat{u}(t))) = \begin{bmatrix} 0 & \cdots & 0 \\ \frac{d\sigma_1(z_1(t))}{dz} & \cdots & 0 \\ \vdots & \ddots & \vdots \\ 0 & \cdots & \frac{d\sigma_{s-1}(z_{s-1}(t))}{dz} \end{bmatrix}, \quad (2.86)$$

where $z_i(t) = \hat{V}_{f_i}^{\mathrm{T}}(t)\hat{\eta}(\zeta(t),\hat{u}(t))$, $i = 1, \ldots, s-1$. Since the update laws for $\hat{W}_1(t)$, $t \geq 0$, and $\hat{V}_f(t)$, $t \geq 0$, will be predicated on the projection operator, it follows that $\tilde{W}_1(t)$, $t \geq 0$, and $\tilde{V}_f(t)$, $t \geq 0$, are bounded. Hence, for all $t \geq 0$ and $(\zeta(t),\hat{u}(t)) \in \mathcal{D}_\zeta \times \mathcal{D}_{\hat{u}}$, there exists $\gamma^* > 0$ such that $\|\gamma(t)\| \leq \gamma^*$, where $\gamma(t) \triangleq B\tilde{W}_1^{\mathrm{T}}(t)\hat{\sigma}'(\hat{V}_f^{\mathrm{T}}(t),\hat{\eta}(\zeta(t),\hat{u}(t)))V_f^{\mathrm{T}}(t)\hat{\eta}(\zeta(t),\hat{u}(t)) + BW_1^{\mathrm{T}}\mathcal{O}(\|\tilde{V}_f(t)\|^2)$, $t \geq 0$.

Using (2.85) the error dynamics (2.84) are given by

$$\dot{e}(t) = B\tilde{W}_1^{\mathrm{T}}(t)\left[\hat{\sigma}(\hat{V}_f^{\mathrm{T}}(t)\hat{\eta}(\zeta(t),\hat{u}(t))) - \hat{\sigma}'(\hat{V}_f^{\mathrm{T}}(t),\hat{\eta}(\zeta(t),\hat{u}(t)))\hat{V}_f^{\mathrm{T}}(t)\hat{\eta}(\zeta(t),\hat{u}(t))\right]$$

$$+A_{\rm ref}e(t) + B\hat{W}_1^{\rm T}(t)\hat{\sigma}'(\hat{V}_f^{\rm T}(t),\hat{\eta}(\zeta(t),\hat{u}(t)))\tilde{V}_f^{\rm T}(t)\hat{\eta}(\zeta(t),\hat{u}(t)) + B\tilde{W}_2^{\rm T}(t)u(t)$$
$$+BK_{\rm y}\tilde{W}_y^{\rm T}(t)\sigma_y(\hat{y}(t),\hat{u}(t)) + BW_1^{\rm T}\left[\hat{\sigma}(V_f^{\rm T}\eta(x(t),\hat{u}(t))) - \hat{\sigma}(V_f^{\rm T}\hat{\eta}(\zeta(t),\hat{u}(t))\right]$$
$$+\bar{\varepsilon}(x(t),\hat{u}(t)) + \gamma(t), \quad e(0) = e_0, \quad t \geq 0. \tag{2.87}$$

Defining

$$\bar{\sigma}(\hat{V}_f(t),\zeta(t),\hat{u}(t)) \triangleq \hat{\sigma}(\hat{V}_f^{\rm T}(t)\hat{\eta}(\zeta(t),\hat{u}(t)))$$
$$-\hat{\sigma}'(\hat{V}_f^{\rm T}(t),\hat{\eta}(\zeta(t),\hat{u}(t)))\hat{V}_f^{\rm T}(t)\hat{\eta}(\zeta(t),\hat{u}(t)), \quad t \geq 0, \tag{2.88}$$
$$H(\hat{W}_1(t),\hat{V}_f(t),\zeta(t),\hat{u}(t)) \triangleq \hat{W}_1^{\rm T}(t)\hat{\sigma}'(\hat{V}_f^{\rm T}(t),\hat{\eta}(\zeta(t),\hat{u}(t))), \quad t \geq 0, \tag{2.89}$$

and using (2.88) and (2.89), the error dynamics (2.87) can be rewritten as

$$\begin{aligned}\dot{e}(t) = {} & A_{\rm ref}e(t) + B\tilde{W}_1^{\rm T}(t)\bar{\sigma}(\hat{V}_f(t),\zeta(t),\hat{u}(t)) \\ & +B\,H(\hat{W}_1(t),\hat{V}_f(t),\zeta(t),\hat{u}(t))\tilde{V}_f^{\rm T}(t)\hat{\eta}(\zeta(t),\hat{u}(t)) + B\tilde{W}_2^{\rm T}(t)u(t) \\ & +BK_{\rm y}\tilde{W}_y^{\rm T}(t)\sigma_y(\hat{y}(t),\hat{u}(t)) + \varepsilon(x(t),\zeta(t),\hat{u}(t)),\ e(0) = e_0,\ t \geq 0, \end{aligned} \tag{2.90}$$

where $\|\varepsilon(x(t),\zeta(t),\hat{u}(t))\| \leq \varepsilon^*$ as long as $(x(t),\zeta(t),\hat{u}(t)) \in \mathcal{D}_x \times \mathcal{D}_\zeta \times \mathcal{D}_{\hat{u}}$, where $\varepsilon^* \triangleq \|B\Lambda\|'\tilde{\varepsilon}^* + \gamma^* + 2\|BW_1\|'\sqrt{s}$.

In order to develop an *output* feedback neural network, consider the estimator given by

$$\dot{\xi}_{\rm c}(t) = A_{\rm ref}\xi_{\rm c}(t) + L\left[y(t) - y_{\rm c}(t) - y_{\rm ref}(t)\right], \quad \xi_{\rm c}(0) = \xi_{\rm c0}, \quad t \geq 0, \tag{2.91}$$
$$y_{\rm c}(t) = C\xi_{\rm c}(t) + \hat{W}_y^{\rm T}(t)\sigma_y(\hat{y}(t),\hat{u}(t)), \tag{2.92}$$

where $\xi_{\rm c}(t) \in \mathbb{R}^n$, $t \geq 0$, $L \in \mathbb{R}^{n\times m}$ is such that $A_{\rm ref} - LC$ is Hurwitz, and define $\tilde{y}(t) \triangleq y(t) - y_{\rm ref}(t)$. It follows from (2.74) and (2.76) that

$$Ce(t) = \tilde{y}(t) - W_y^{\rm T}\sigma_y(\hat{y}(t),\hat{u}(t)). \tag{2.93}$$

Premultiplying (2.90) by C and integrating the resulting equation over the moving time interval $[t_{\rm d},t]$, where $t_{\rm d} \triangleq \max\{0, t-\tau_{\rm d}\}$ and $\tau_{\rm d} \geq 0$, and using (2.93), we obtain

$$B_1\left[W_1^{\rm T},\ \Sigma(t)V_f^{\rm T},\ W_2^{\rm T},\ K_{\rm y}W_y^{\rm T}\right]q(t,t-\tau_{\rm d}) = c(t,t-\tau_{\rm d}) - \delta(t,t-\tau_{\rm d}),\ t \geq 0, \tag{2.94}$$

where

$$\Sigma(t) \triangleq \int_{t_{\rm d}}^{t} H(\hat{W}_1(\xi), \hat{V}_f(\xi), \zeta(\xi), \hat{u}(\xi))\mathrm{d}\xi, \quad q(t, t-\tau_{\rm d}) \triangleq \int_{t_{\rm d}}^{t} \mu(\xi)\mathrm{d}\xi, \quad t \geq 0, \tag{2.95}$$

$$\mu(t) \triangleq \left[\bar{\sigma}^{\rm T}(\hat{V}_f(t), \zeta(t), \hat{u}(t)) \;\; \hat{\eta}^{\rm T}(\zeta(t), \hat{u}(t)) \;\; u^{\rm T}(t) \;\; \sigma_y^{\rm T}(\hat{y}(t), \hat{u}(t))\right]^{\rm T}, \; t \geq 0, \tag{2.96}$$

$$\begin{aligned} c(t, t-\tau_{\rm d}) \triangleq \; & B_1 \int_{t_{\rm d}}^{t} \left[\hat{W}_1^{\rm T}(\xi), \; H(\hat{W}_1(\xi), \hat{V}_f(\xi), \zeta(\xi), \hat{u}(\xi))\hat{V}_f^{\rm T}(\xi), \; \hat{W}_2^{\rm T}(\xi), \; K_{\rm y}\hat{W}_y^{\rm T}(\xi)\right] \\ & \cdot \mu(\xi)\mathrm{d}\xi + \tilde{y}(t) - \tilde{y}(t_{\rm d}) - CA_{\rm ref}\int_{t_{\rm d}}^{t} \xi_{\rm c}(\xi)\mathrm{d}\xi, \quad t \geq 0, \end{aligned} \tag{2.97}$$

$$\begin{aligned} \delta(t, t-\tau_{\rm d}) \triangleq \; & W_y^{\rm T}\left[\sigma_y(\hat{y}(t), \hat{u}(t)) - \sigma_y(\hat{y}(t_{\rm d}), \hat{u}(t-\tau_{\rm d})\right] + CA_{\rm ref}\int_{t_{\rm d}}^{t} (e(\xi) - \xi_{\rm c}(\xi))\mathrm{d}\xi \\ & + B_1 \int_{t_{\rm d}}^{t} H(\hat{W}_1(\xi), \hat{V}_f(\xi), \zeta(\xi), \hat{u}(\xi))V_f^{\rm T}\hat{\eta}(\zeta(\xi), \hat{u}(\xi))\mathrm{d}\xi \\ & - B_1\Sigma(t)V_f^{\rm T}\int_{t_{\rm d}}^{t} \hat{\eta}(\zeta(\xi), \hat{u}(\xi))\mathrm{d}\xi + C\int_{t_{\rm d}}^{t} \varepsilon(x(\xi), \zeta(\xi), \hat{u}(\xi))\mathrm{d}\xi, \quad t \geq 0, \end{aligned} \tag{2.98}$$

and $B_1 \triangleq CB$. Note that $\Sigma(t)$, $q(t, t-\tau_{\rm d})$, and $c(t, t-\tau_{\rm d})$ are computable, whereas $\delta(t, t-\tau_{\rm d})$ is an *unknown* term such that $\|\delta(t, t-\tau_{\rm d})\| \leq 2\|W_y\|'\sigma_y^* + \tau_{\rm d}\varepsilon^*\|C\|' + \|CA_{\rm ref}\|'\tau_{\rm d}\max_{s\in[t_{\rm d},t]}\|e(s) - \xi(s)\| + \tau_d\delta_1$, where σ_y^* is such that $\|\sigma_y(\hat{y}, \hat{u})\| \leq \sigma_y^*$ for all $\hat{y} \in \mathbb{R}^{mq}$ and $\hat{u} \in \mathbb{R}^{mp}$, and $\delta_1 > 0$ is such that

$$\left\|B_1\int_{t_{\rm d}}^{t}[H(\hat{W}_1(\xi), \hat{V}_f(\xi), \zeta(\xi), \hat{u}(\xi))V_f^{\rm T}\hat{\eta}(\zeta(\xi), \hat{u}(\xi))\mathrm{d}\xi - B_1\Sigma(t)V_f^{\rm T}\int_{t_{\rm d}}^{t}\hat{\eta}(\zeta(\xi), \hat{u}(\xi))]\mathrm{d}\xi\right\| \leq \delta_1\tau_{\rm d}, \quad t \geq 0.$$

As in Section 2.3, we choose $\tau_{\rm d} \geq 0$ such that $\|q(t, t-\tau_{\rm d})\| \leq q_{\max}$ and $\|c(t, t-\tau_{\rm d})\| \leq c_{\max}$ for all $t \geq 0$. Define

$$\Phi(t) \triangleq \left[W_1^{\rm T}, \; \Sigma(t)V_f^{\rm T}, \; W_2^{\rm T}, \; K_{\rm y}W_y^{\rm T}\right] \in \mathbb{R}^{m\times(s+l+m+k)}, \quad t \geq 0, \tag{2.99}$$

$$\hat{\Phi}(t) \triangleq \left[\hat{W}_1^{\rm T}(t), \; \Sigma(t)\hat{V}_f^{\rm T}(t), \; \hat{W}_2^{\rm T}(t), \; K_{\rm y}\hat{W}_y^{\rm T}(t)\right] \in \mathbb{R}^{m\times(s+l+m+k)}, \quad t \geq 0, \tag{2.100}$$

and note that it follows from (2.94) that

$$B_1\Phi(t)q(t,t-\tau_{\rm d})=c(t,t-\tau_{\rm d})-\delta(t,t-\tau_{\rm d}),\quad t\geq 0. \tag{2.101}$$

Now, using (2.101) it follows that, for every $k>0$ and $\Gamma=\Gamma^{\rm T}>0$,

$$\begin{aligned}
&\mathrm{tr}\left[(\Phi(t)-\hat{\Phi}(t))\Gamma^{-1}\left(k\,\Gamma q(t,t-\tau_{\rm d})(B_1\hat{\Phi}(t)q(t,t-\tau_{\rm d})-c(t,t-\tau_{\rm d}))^{\rm T}B_1\right)\right]\\
&\quad=k\,\mathrm{tr}\left[B_1(\Phi(t)-\hat{\Phi}(t))q(t,t-\tau_{\rm d})\left(B_1\hat{\Phi}(t)q(t,t-\tau_{\rm d})-c(t,t-\tau_{\rm d})\right)^{\rm T}\right]\\
&\quad=-k\left\|B_1\hat{\Phi}(t)q(t,t-\tau_{\rm d})-c(t,t-\tau_{\rm d})\right\|^2-k\left(B_1\hat{\Phi}(t)q(t,t-\tau_{\rm d})-c(t,t-\tau_{\rm d})\right)^{\rm T}\\
&\qquad\cdot\delta(t,t-\tau_{\rm d})\\
&\quad\leq-k\left\|B_1\hat{\Phi}(t)q(t,t-\tau_{\rm d})-c(t,t-\tau_{\rm d})\right\|^2+\psi^*,\quad t\geq 0,
\end{aligned} \tag{2.102}$$

where $\psi^*\triangleq k(\|CA_{\rm ref}\|'\tau_{\rm d}\max_{s\in[t_{\rm d},t]}\|e(s)-\xi(s)\|+\tau_{\rm d}\varepsilon^*\|C\|'+2\|W_y\|'\sigma_y^*)(\|B_1\|'\hat{\Phi}_{\max}\cdot q_{\max}+c_{\max})$, and $\hat{\Phi}_{\max}$ is the norm bound imposed on $\hat{\Phi}(t)$, $t\geq 0$. Next, define the Q-modification term $Q^{\rm nl}(t)$ by

$$Q^{\rm nl}(t)=\left[\begin{array}{c}Q_1^{\rm nl}(t)\\Q_2^{\rm nl}(t)\\Q_3^{\rm nl}(t)\\Q_4^{\rm nl}(t)\end{array}\right]\triangleq q(t,t-\tau_{\rm d})\left(B_1\hat{\Phi}^{\rm T}(t)q(t,t-\tau_{\rm d})-c(t,t-\tau_{\rm d})\right)^{\rm T}B_1,\quad t\geq 0, \tag{2.103}$$

where for $t\geq 0$, $Q^{\rm nl}(t)\in\mathbb{R}^{(s+l+m+k)\times m}$, $Q_1^{\rm nl}(t)\in\mathbb{R}^{s\times m}$, $Q_2^{\rm nl}(t)\in\mathbb{R}^{l\times m}$, $Q_3^{\rm nl}(t)\in\mathbb{R}^{m\times m}$, and $Q_4^{\rm nl}(t)\in\mathbb{R}^{k\times m}$.

Consider the feedback control law (2.77) with $u_{\rm n}(t)$ and $u_{\rm ad}(t)$ given by (2.79) and (2.83), and update laws given by

$$\dot{\hat{W}}_1(t)=\Gamma_1\mathrm{Proj}[\hat{W}_1(t),\bar{\sigma}(\hat{V}_f^{\rm T}(t),\zeta(t),\hat{u}(t))\xi_{\rm c}^{\rm T}(t)PB-k\,h(\bar{W}(t))Q_1^{\rm nl}(t)],\quad \hat{W}_1(0)=\hat{W}_{10},\quad t\geq 0, \tag{2.104}$$

$$\begin{aligned}\dot{\hat{V}}_f(t)=\Gamma_f\mathrm{Proj}[\hat{V}_f(t),\hat{\eta}(\zeta(t),\hat{u}(t))\xi_{\rm c}^{\rm T}(t)PBH(\hat{W}_1(t),\hat{V}_f^{\rm T}(t),\zeta(t),\hat{u}(t))\\ -k\,h(\bar{W}(t))Q_2^{\rm nl}(t)\Sigma(t)],\quad \hat{V}_f(0)=\hat{V}_{f0},\end{aligned} \tag{2.105}$$

$$\dot{\hat{W}}_2(t) = \Gamma_2 \mathrm{Proj}[\hat{W}_2(t), u(t)\xi_{\mathrm{c}}^{\mathrm{T}}(t)PB - k\,h(\bar{W}(t))Q_3^{\mathrm{nl}}(t)], \quad \hat{W}_2(0) = \hat{W}_{20}, \tag{2.106}$$

$$\dot{\hat{W}}_y(t) = \Gamma_y \mathrm{Proj}[\hat{W}_y(t), \sigma_y(\hat{y}(t), \hat{u}(t))\xi_{\mathrm{c}}^{\mathrm{T}}(t)(PBK_{\mathrm{y}} + \tilde{P}L) - k\,h(\bar{W}(t))Q_4^{\mathrm{nl}}(t)],$$

$$\hat{W}_y(0) = \hat{W}_{y0}, \tag{2.107}$$

where $\Gamma_1 \in \mathbb{R}^{s\times s}$, $\Gamma_f \in \mathbb{R}^{l\times l}$, $\Gamma_2 \in \mathbb{R}^{m\times m}$, and $\Gamma_3 \in \mathbb{R}^{k\times k}$ are positive-definite matrices, $P \in \mathbb{R}^{n\times n}$ is the positive-definite solution to (2.65), and $\tilde{P} \in \mathbb{R}^{n\times n}$ is the positive-definite solution to the Lyapunov equation

$$0 = (A - LC)^{\mathrm{T}}\tilde{P} + \tilde{P}(A - LC) + \tilde{R}, \tag{2.108}$$

where $R > 0$, $k > 0$, $\bar{\sigma}(\hat{V}_f^{\mathrm{T}}(t), \zeta(t), \hat{u}(t))$ and $H(\hat{W}_1(t), \hat{V}_f^{\mathrm{T}}(t), \zeta(t), \hat{u}(t))$ are given by (2.88) and (2.89), respectively, $Q_1^{\mathrm{nl}}(t)$, $Q_2^{\mathrm{nl}}(t)$, $Q_3^{\mathrm{nl}}(t)$, and $Q_4^{\mathrm{nl}}(t)$ are given by (2.103), $\bar{W}(t) \triangleq (\hat{W}_1(t), \hat{V}_f(t), \hat{W}_2(t), \hat{W}_y(t))$, and $h : \mathbb{R}^{(s+l+m+k)\times m} \to \mathbb{R}$ is a bounded nonnegative function taking values between 0 and 1 such that if $\mathrm{tr}\,\hat{W}_i^{\mathrm{T}}(t)\hat{W}_i(t) = \hat{w}_{i\max}^2$, for $i = 1$, 2, or y, or $\mathrm{tr}\,\hat{V}_f^{\mathrm{T}}(t)\hat{V}_f(t) = \hat{v}_{f\max}^2$, then $h(\bar{W}(t)) = 0$, where $\hat{w}_{i\max}^2$, $i = 1$, 2, or y, and $\hat{v}_{f\max}^2$ are the norm bounds imposed on $\hat{W}_i(t)$, $i = 1$, 2, or y, $t \geq 0$, and $\hat{V}_f(t)$, $t \geq 0$, respectively. Note that projection operator guarantees boundness of $\hat{W}_i(t)$, $i = 1$, 2, $t \geq 0$, $\hat{V}_f^{\mathrm{T}}(t)$, $t \geq 0$, and $\hat{W}_y(t)$, $t \geq 0$. In addition, we choose the parameters $\hat{w}_{2\max}$ and $\hat{\Lambda}$ such that the inverse $\left[I_m + \hat{W}_2^{\mathrm{T}}(t)\hat{\Lambda}^{-1}\right]^{-1}$ in (2.83) exists for all $t \geq 0$. In particular, there exists $\nu > 0$ such that

$$\|I_m + \hat{W}_2^{\mathrm{T}}(t)\hat{\Lambda}^{-1}\|' \leq \nu, \quad t \geq 0. \tag{2.109}$$

Next, we introduce several bounds needed to formulate the main result of this section. Since $\hat{\eta}(\zeta(t), \hat{(t)})$ and $\sigma_y(\hat{y}(t), \hat{u}(t))$ are bounded for all $t \geq 0$, there exist $\eta^* > 0$ and $\sigma_y^* > 0$ such that $\|\hat{\eta}(\zeta(t), \hat{u}(t))\| \leq \eta^*$, $t \geq 0$, and $\|\sigma_y(\hat{y}(t), \hat{u}(t))\| \leq \sigma_y^*$, $t \geq 0$. Hence, there exist $\bar{\sigma}^* > 0$ and $H^* > 0$ such that $\|\bar{\sigma}(\hat{V}_f(t), \zeta(t), \hat{u}(t))\| \leq \bar{\sigma}^*$, $t \geq 0$, and $\|H(\hat{W}_1(t), \hat{V}_f(t), \zeta(t), \hat{u}(t))\|' \leq H^*$, $t \geq 0$. Furthermore, there exist $x_{\mathrm{ref}}^* > 0$ and $r^* > 0$ such that $\|x_{\mathrm{ref}}(t)\| \leq x_{\mathrm{ref}}^*$, $t \geq 0$, and $\|r(t)\| \leq r^*$, $t \geq 0$. It

follows from (2.77), (2.79), and (2.83) that there exist $\alpha_u > 0$ and $\beta_u > 0$ such that

$$\|u(t)\| \leq \alpha_u + \beta_u \|e(t)\|, \quad t \geq 0, \tag{2.110}$$

$$\alpha_u \leq \|\hat{\Lambda}^{-1}\|' \Big[\nu(\hat{w}_{1\max}\sqrt{s} + \hat{w}_{y\max}\sigma_y^*) + (1 + \hat{w}_{2\max}\|\hat{\Lambda}^{-1}\|')(\|K_y C\|' x_{\mathrm{ref}}^* + \|K_y W_y\|'\sigma_y^* + \|K_y\|' r^*) \Big], \tag{2.111}$$

$$\beta_u \leq \|\hat{\Lambda}^{-1}\|'(1 + \hat{w}_{2\max}\|\hat{\Lambda}^{-1}\|')\|K_y C\|'. \tag{2.112}$$

Finally, define

$$\alpha_e \triangleq \lambda_{\min}(R) - 1 - \beta_u \|PB\|' \left(\|W_2\|' + \hat{w}_{2\max}\right), \tag{2.113}$$

$$\alpha_\xi \triangleq \lambda_{\min}(\tilde{R}) - \|\tilde{P}LC\|'^2 - \beta_u \|PB\|'(\|W_2\|' + \hat{w}_{2\max}), \tag{2.114}$$

$$\beta_e \triangleq \|P\|'\varepsilon^* + \|PB\|' \left(\|W_1\|' + \hat{w}_{2\max}\bar{\sigma}^*\right) + \alpha_u \|PB\|' \left(\|W_2\|' + \hat{w}_{2\max}\right) + \|PB\|' H^* \left(\|V_f\|' + \hat{v}_{f\max}\right)\eta^* + \|PBK_y\|' H^* \left(\|W_y\|' + \hat{w}_{y\max}\right)\sigma_y^*, \tag{2.115}$$

$$\beta_\xi \triangleq \beta_e - \|P\|'\varepsilon^*. \tag{2.116}$$

Theorem 2.4. Consider the nonlinear uncertain dynamical system $\mathcal{G}$ given by (2.73) and (2.74) with $u(t)$, $t \geq 0$, given by (2.77). Assume Assumption 2.2 holds, $\alpha_e > 0$, and $\alpha_\xi > 0$. Then there exists a compact positively invariant set $\mathcal{D}_\alpha \subset \mathbb{R}^n \times \mathbb{R}^n \times \mathbb{R}^{s\times m} \times \mathbb{R}^{k\times s} \times \mathbb{R}^{m\times m} \times \mathbb{R}^{l\times m}$ such that $(0, 0, W_1, V_f, W_2, W_y) \in \mathcal{D}_\alpha$ and the solution $(x(t), \xi_{\mathrm{c}}(t), \hat{W}_1(t), \hat{V}_f(t), \hat{W}_2(t), \hat{W}_y(t))$, $t \geq 0$, of the closed-loop system given by (2.73), (2.74), (2.91), (2.92), (2.104)–(2.107), is ultimately bounded for all $(x(0), \xi_{\mathrm{c}}(0), \hat{W}_1(0), \hat{V}_f(0), \hat{W}_2(0), \hat{W}_y(0)) \in \mathcal{D}_\alpha$ with ultimate bound $\|y(t) - y_{\mathrm{ref}}(t)\|^2 < \varepsilon$, $t \geq T$, where

$$\varepsilon > \left[\left(\sqrt{\frac{\mu}{\alpha_e}} + \beta_e \right)^2 + \left(\sqrt{\frac{\mu}{\alpha_\xi}} + \beta_\xi \right)^2 + \lambda_{\max}(\Gamma_1^{-1})\hat{w}_{1\max}^2 + \lambda_{\max}(\Gamma_f^{-1})\hat{w}_{f\max}^2 + \lambda_{\max}(\Gamma_2^{-1})\hat{w}_{2\max}^2 + \lambda_{\max}(\Gamma_y^{-1})\hat{w}_{y\max}^2 \right]^{\frac{1}{2}}, \tag{2.117}$$

$$\nu \triangleq \alpha_e \beta_e^2 + \alpha_\xi \beta_\xi^2 + \psi^*. \tag{2.118}$$

Proof. Ultimate boundness can be established by considering the Lyapunov-like function

$$V(e,\xi_{\mathrm{c}},\tilde{W}_1,\tilde{V}_f,\tilde{W}_2,\tilde{W}_y) = e^{\mathrm{T}}Pe+\xi_{\mathrm{c}}^{\mathrm{T}}\tilde{P}\xi_{\mathrm{c}}+\operatorname{tr}\tilde{W}_1^{\mathrm{T}}\Gamma_1^{-1}\tilde{W}_1+\operatorname{tr}\tilde{V}_f^{\mathrm{T}}\Gamma_f^{-1}\tilde{V}_f$$
$$+\operatorname{tr}\tilde{W}_2^{\mathrm{T}}\Gamma_2^{-1}\tilde{W}_2+\operatorname{tr}\tilde{W}_y^{\mathrm{T}}\Gamma_y^{-1}\tilde{W}_y.$$

The remainder of the proof is similar to the proof of Theorem 2.3 and, hence, is omitted. □

2.5. Illustrative Numerical Examples

In this section, we present three numerical examples to demonstrate the utility and efficacy of the proposed Q-modification architecture for neuroadaptive stabilization and command following.

Example 2.1 Consider the uncertain dynamical system describing wing rock aircraft dynamics [20] given by

$$\dot{x}_1(t) = x_2(t), \quad x_1(0) = x_{10}, \quad t \geq 0, \tag{2.119}$$

$$\dot{x}_2(t) = u(t)+\Delta(x(t)), \quad x_2(0) = x_{20}, \tag{2.120}$$

where $x = [x_1,\ x_2]^{\mathrm{T}}$, x_1 represents the roll angle, x_2 represents the roll rate, and $\Delta(x) = \theta_1+\theta_2x_1+\theta_3x_2+\theta_4|x_1|x_2+\theta_5|x_2|x_2+\theta_6x_1^3$, where θ_i, $i = 1,\ \ldots,\ 6$, are unknown parameters. For our simulation we set $\theta_1 = 0$, $\theta_2 = -0.01859521$, $\theta_3 = 0.015162375$, $\theta_4 = -0.06245153$, $\theta_5 = 0.00954708$, and $\theta_6 = 0.02145291$. These parameters are derived from the aircraft aerodynamic coefficients. The initial conditions are $x_1(0) = 6^\circ$ and $x_2(0) = 3^\circ/\mathrm{sec}$. A reference model is chosen in the form of (2.36) with

$$A_{\mathrm{ref}} = \begin{bmatrix} 0 & 1 \\ -\omega_n^2 & -2\omega_n\zeta \end{bmatrix}, \quad B_{\mathrm{ref}} = \begin{bmatrix} 0 \\ \omega_n^2 \end{bmatrix},$$

where $\omega_n = 0.5$ rad/sec and $\zeta = 0.707$, $x_{\mathrm{ref}_0} = [0,\ 0]^{\mathrm{T}}$, and the roll command is set to zero so that $r(t) \equiv 0$. Here, the control objective is to eliminate the oscillations

caused by the wing rock phenomenon and to stabilize the roll dynamics to the trim flight condition $(x_1, x_2) = (0, 0)$. For this example, we let

$$A_0 = \begin{bmatrix} 0 & 1 \\ -\omega_n^2 & -2\omega_n\zeta \end{bmatrix}, \quad B = \begin{bmatrix} 0 \\ 1 \end{bmatrix},$$

$\Lambda = 1$ which is assumed to be known, $\hat{\Lambda} = \Lambda$, $G(x(t)) \equiv 1$, $A = 0$, and $f(x, \hat{u}) = W^{\mathrm{T}}\sigma(x)$, where $W = [\theta_1,\ \theta_2{+}\omega_n^2,\ \theta_3{+}2\omega_n\zeta,\ \theta_4, \theta_5,\ \theta_6]^{\mathrm{T}}$ and $\sigma(x) = [1,\ x_1,\ x_2,\ |x_1|x_2,\ |x_2|x_2,\ x_1^3]^{\mathrm{T}}$. Hence, $K_x = [0,\ 0]$, $K_r = \omega_n^2$, and $u_{\mathrm{n}}(t) = 0$, $t \geq 0$.

Figure 2.4 shows the phase portrait of the uncontrolled and controlled (with $k = 0$) system. Note that the uncontrolled system results in a limit cycle instability, whereas the case where $k = 0$ corresponds to the Q-modification term turned off in the adaptive controller. Figure 2.4 shows that for $k = 0$, adaptation takes place very slowly for small gains and the system transient response exhibits large oscillations. Figure 2.5 shows the phase portrait of the controlled system with the Q-modification term active, with $\tau_{\mathrm{d}} = 1$ sec and different values of k. Finally, Figures 2.6 and 2.7 show the update weights versus time. Note that for $k = 0$ the update weights exhibit oscillations and involve high gains, whereas with the Q-modification terms present the update weights converge to their steady state values much faster and without exhibiting excessive oscillations.

Example 2.2 This example considers a nonlinear dynamical system representing a controlled rigid spacecraft given by

$$\dot{x}(t) = -I_{\mathrm{b}}^{-1}X(t)I_{\mathrm{b}}x(t) + I_{\mathrm{b}}^{-1}u(t), \quad x(0) = x_0, \quad t \geq 0, \tag{2.121}$$

where $x = [x_1,\ x_2,\ x_3]^{\mathrm{T}}$ represents the angular velocities of the spacecraft with respect to the body-fixed frame, $I_{\mathrm{b}} \in \mathbb{R}^3$ is an *unknown* positive-definite inertia matrix of the spacecraft, $u = [u_1,\ u_2,\ u_3]^{\mathrm{T}}$ is a control vector with control inputs providing body-fixed torques about three mutually perpendicular axes defining the body-fixed

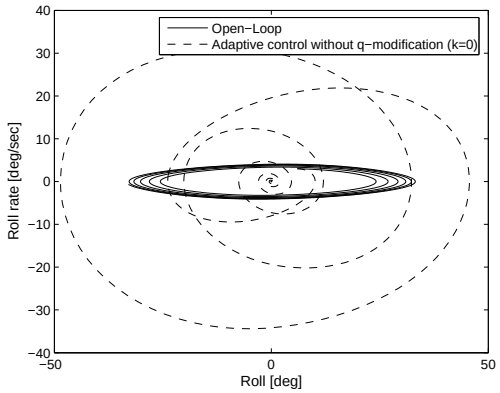

Figure 2.4: Phase portrait of uncontrolled and controlled system without Q-modification terms.

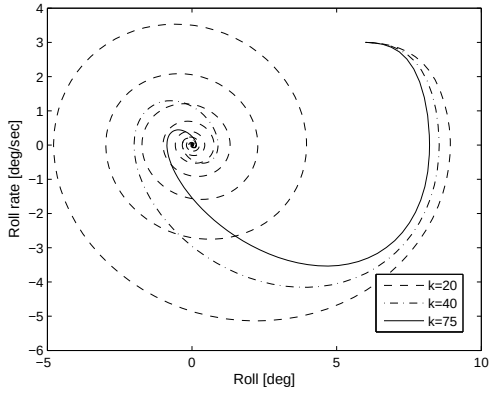

Figure 2.5: Phase portrait of controlled system with Q-modification terms active.

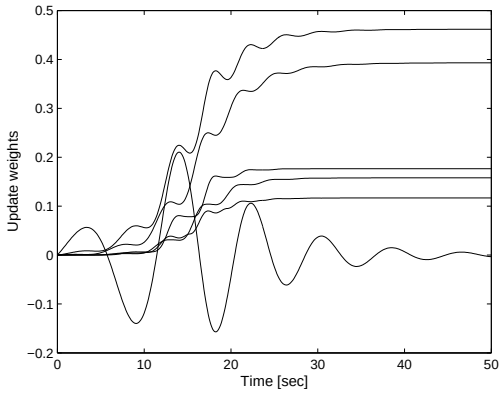

Figure 2.6: Neural network weighting functions versus time without Q-modification.

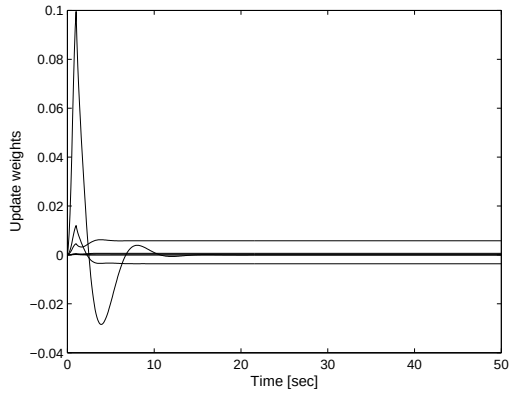

Figure 2.7: Neural network weighting functions versus time with Q-modification.

frame of the spacecraft, and $X(t)$ denotes the skew-symmetric matrix

$$X \triangleq \begin{bmatrix} 0 & -x_3 & x_2 \\ x_3 & 0 & -x_1 \\ -x_2 & x_1 & 0 \end{bmatrix}.$$

Note that (2.121) can be rewritten in state-space form (2.35) with $A_0 \in \mathbb{R}^{3\times 3}$, $B = I_3$, $\Lambda = I_{\rm b}^{-1}$, $G(x(t)) \equiv I_3$, $f(x(t), \hat{u}(t)) = -X(t)I_{\rm b}x(t) - I_{\rm b}A_0x(t)$, and $A = 0_{3\times 3}$.

Next, we use Theorem 2.3 to design a neuroadaptive controller given by (2.37) with $u_{\rm n}(t)$ and $u_{\rm ad}(t)$ given by (2.39) and (2.43), respectively. Here, we used 6 nodes ($s = 2$, $m = 3$) in the outer layer and 3 nodes ($l = 1$, $m = 3$) in the hidden layer of the neural network. For our simulation we used $A_{\rm ref} = {\rm diag}[-1, -2, -3]$, $A_0 = 0.99A_{\rm ref}$, $B_{\rm ref} = I_3$, $r(t) \equiv 0$, $x_{\rm ref_0} = [0, 0, 0]^{\rm T}$,

$$\hat{\Lambda} = \begin{bmatrix} 0.0351 & 0 & -0.0021 \\ 0 & 0.0412 & 0 \\ -0.0021 & 0 & 0.0468 \end{bmatrix},$$

$\hat{W}_1(t) \in \mathbb{R}^{2\times 3}$, $\hat{V}_f(t) \in \mathbb{R}^{3\times 1}$, $\eta(x(t), \hat{u}(t)) = x(t)$, $t \geq 0$, $a = 0.01$, $\hat{W}_2(t) \equiv 0$, $\hat{W}_3(t) \in \mathbb{R}^{3\times 3}$, $\hat{W}_{10}(t) = 0_{2\times 3}$, $\hat{V}_f(t) = [0, 0, 0]^{\rm T}$, $\hat{W}_{30}(t) = 0_{3\times 3}$, $\Gamma_1 = 0.1I_2$, $\Gamma_f = 0.1I_3$, $\Gamma_3 = 0.01I_3$, $P = {\rm diag}[0.05, 0.25, 0.0167]$, and $\tau_{\rm d} = 0.1\,{\rm sec}$. With the above data Assumption 2.1 holds with

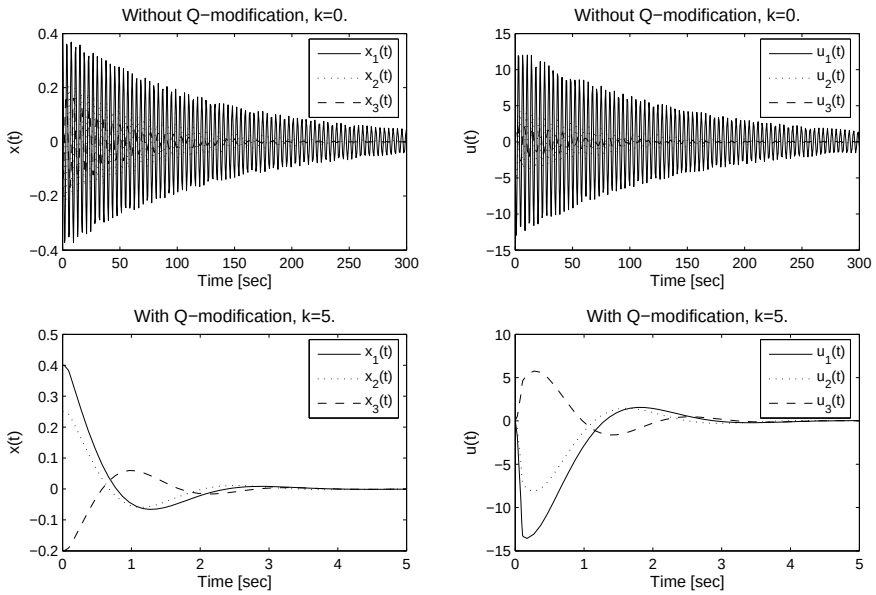

Figure 2.8: Angular velocities and control signals versus time.

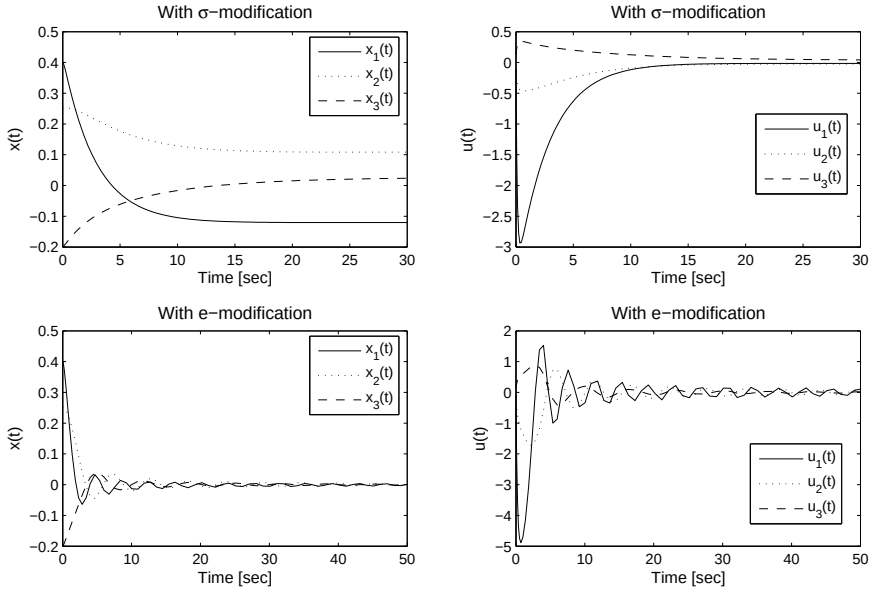

Figure 2.9: Angular velocities and control signals versus time with σ- and e-modification controllers.

$$K_{\mathrm{x}} = \begin{bmatrix} -0.2857 & 0 & -0.0386 \\ 0 & -0.4857 & 0 \\ -0.0129 & 0 & -0.6429 \end{bmatrix}, \quad K_{\mathrm{r}} = \begin{bmatrix} 28.5714 & 0 & 1.2857 \\ 0 & 24.2857 & 0 \\ 1.2857 & 0 & 21.4286 \end{bmatrix}.$$

Now, with

$$I_{\rm b} = \begin{bmatrix} 20 & 0 & 0.9 \\ 0 & 17 & 0 \\ 0.9 & 0 & 15 \end{bmatrix} \tag{2.122}$$

and initial conditions $x_0 = [0.4, 0.25, -0.2]^{\rm T}$, Figure 2.8 shows the controlled angular velocities and the control signals versus time with and without the Q-modification architecture. It is clear from these simulations that the Q-modification neuroadaptive controller achieves superior performance over a standard neuroadaptive controller. Finally, we compare the Q-modification controller with the σ- and e-modification schemes. For the σ- and e-modification schemes we modified the standard neural network update laws to include the terms $-\sigma(\hat{W} - W^0)$ and $-\sigma\|e\|(\hat{W} - W^0)$, respectively, where e is the state error. As expected, the performance of the σ- and e-modification controllers depend on the design parameter W^0. Assuming that the actual weights are unknown, here we let $V_f^0 = 0_{3\times 1}$ and $W_3^0 = 0_{3\times 3}$, and construct $W_1^0 \in \mathbb{R}^{2\times 3}$ as a random matrix with entries corresponding to a Gaussian distribution with zero mean and variance 0.01. In this case,

$$W_1^0 = \begin{bmatrix} 0.0591 & 0.0380 & -0.0020 \\ -0.0644 & -0.1009 & -0.0048 \end{bmatrix}.$$

With $\sigma = 0.1$, Figure 2.9 shows the angular velocities and the control signals versus time of the two approaches. Though the σ- and e-modification controllers can give better performance than the standard neural network controller, the Q-modification controller achieves superior performance as compared to all three designs.

Example 2.3 In this example, we design several neuroadaptive full-state feedback controllers based on the Q-modification architecture for the Boeing unmanned combat aerial vehicle (UCAV), and compare the performance of three controllers to *conventional* neural network controllers as well as σ- and e-modification neuroadaptive controllers. The UCAV consists of a tailless configuration with 3 elevon controls

on each wing, along with thrust vectoring for yaw control. A linearized model for the controlled UCAV at a single flight condition is given by [89, 137].

$$\dot{x}(t) = A_0 x(t) + B_1 \Lambda \left[u(t) + f(x_{\rm p}(t)) \right] + B_2 y_{\rm c}(t), \quad x(0) = 0, \quad t \geq 0, \quad (2.123)$$

where the state vector $x(t) = [x_{\rm p}^{\rm T}(t), x_{\rm c}^{\rm T}(t)]^{\rm T} \in \mathbb{R}^9,\ t \geq 0$, consists of the model and baseline controller states. The system dynamic states $x_{\rm p}(t) \in \mathbb{R}^5$ consist of the angle of attack $\alpha(t)$, sideslip angle $\beta(t)$, body roll rate $p(t)$, body pitch rate $q(t)$, and body yaw rate $r(t)$. The baseline controller states $x_{\rm c}(t) \in \mathbb{R}^4$ consist of the pitch integrator $q_{\rm c}(t)$, roll integrator $p_{\rm c}(t)$, yaw integrator $r_{\rm c}(t)$, and yaw rate washout filter signal $r_{\rm w}(t)$. The control input is given by $u(t) = u_{\rm n}(t) - u_{\rm ad}(t) \in \mathbb{R}^7,\ t \geq 0$, where $u_{\rm n}(t) = -K_{\rm x} x(t) + K_{\rm y_c} y_c(t)$, $K_{\rm x}$ and $K_{\rm y_c}$ are defined in the Appendix of [89], and $u_{\rm ad}(t)$ is given by 2.43. The signal $y_{\rm c}(t) \in \mathbb{R}^4,\ t \geq 0$, is the inner loop command vector and consists of the positive down vertical acceleration command $A_{\rm r}(t)$, the sideslip angle command $\beta_{\rm r}(t)$, the body roll rate command $p_{\rm r}(t)$, and the yaw integrator command $r_{\rm r}(t)$. In (2.123), $\Lambda \in \mathbb{R}^{7\times 7}$ is nominally an identity matrix, that is, $\hat{\Lambda} = I_7$, and a control failure is emulated by setting one of its diagonal entries to zero. The function $f : \mathbb{R}^5 \to \mathbb{R}^7$ is the matched uncertainty that depends on the UCAV model states and is nonlinearly parameterized as in (2.41) with $\eta(x(t), \hat{u}(t)) = x(t)$. The system matrices $A_0 \in \mathbb{R}^{9\times 9}$, $B_1 \in \mathbb{R}^{9\times 7}$, and $B_2 \in \mathbb{R}^{9\times 4}$ are defined in the Appendix of [89]. In addition, the reference system matrices in (2.36) can be given as $A_{\rm ref} = A_0 + B_1 \hat{\Lambda} K_{\rm x}$ and $B_{\rm ref} = B_2 + B_1 \hat{\Lambda} K_{\rm r}$.

With the aforementioned definitions, the error dynamics in (2.44) can be rewritten as

$$\dot{e}(t) = A_{\rm ref} e(t) + B \left[W_1^{\rm T} \hat{\sigma}(V_f^{\rm T} x(t)) - \hat{W}_1^{\rm T}(t) \hat{\sigma}(\hat{V}_f^{\rm T}(t) x(t)) \right] + B \left[W_3^{\rm T} - \hat{W}_3^{\rm T}(t) \right] u(t) + \bar{\varepsilon}(x(t)), \quad e(0) = 0, \quad t \geq 0,$$

which gives an appropriate error model for Q-modification approach. In our design, a

right-out elevon (ROE) failure is introduced at $t = 5$ sec by setting a diagonal entry of $\hat{\Lambda}$ to zero, and the design goal is to stabilize the closed-loop system under this failure while maintaining the nominal reference tracking performance.

Now, we design a neuroadaptive controller of the form given by (2.37) with $u_{\mathrm{n}}(t)$ and $u_{\mathrm{ad}}(t)$ given by (2.39) and (2.43), respectively. We used 35 nodes ($s = 5,\ m = 7$) in the outer layer, and 63 nodes ($l = 9,\ m = 7$) in the hidden layer of the neural network. The initial conditions for the system and controller states as well as the neural network weights were initialized at zero. Furthermore, the gains are selected to be $\Gamma_1 = I_5,\ \Gamma_f = I_9,$ and $\Gamma_3 = I_7$, and we used $R = I_9$ to solve the Lyapunov equation given by (2.65) for P. In addition, the Q-modification design parameters are selected to be $k = 10$ and $\tau_{\mathrm{d}} = 0.5$ sec.

Figures 2.10 and 2.11 show the nominal performance of the baseline controller for a sequence of commands $y_c(t)$. For the design, the positive down vertical acceleration $A_{\mathrm{z}}(t)$ is computed as the system output signal that tracks the command $A_{\mathrm{r}}(t)$ defined above [89]. Figures 2.12 and 2.13 show that the performance of the baseline controller is seriously degraded when a right-out elevon (ROE) failure is introduced at $t = 5$ sec. This shows that the baseline controller design does not make effective use of the available control redundancy. One approach to solving this problem might be to reconfigure the flight control system for this failure, however this presumes that the failure is detected and correctly identified. Therefore, an alternative approach that employs adaptation is pursued.

Figures 2.14–2.18 show the performance of a *conventional* neuroadaptive controller with ROE failure, that is, a controller with the adaptation law given by (2.61), (2.62), and (2.64) with $k = 0$ (without Q-modification). The weight histories for this case are shown in Figures 2.16 and 2.17. Clearly, the performance in Figures 2.14–2.18 is better than the performance in Figures 2.12 and 2.13. Consequently, using a

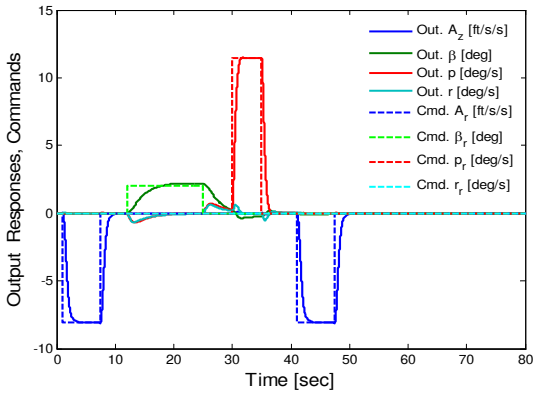

Figure 2.10: Nominal output response performance of the baseline controller.

conventional neuroadaptive controller improves the UCAV performance in the face of a ROE failure at $t = 5$ sec. Figures 2.19–2.23 show the improvement obtained when the Q-modification architecture is employed with $k = 10$ and $\tau_{\rm d} = 0.5$ sec. It is obvious from Figures 2.19–2.23 that the performance of the neuroadaptive controller with the Q-modification is superior to the *conventional* neuroadaptive controller. In addition, the behavior of the weight histories are also significantly improved.

Finally, we compare the Q-modification controller with an e- and σ-modification controllers. For the e- and σ modification controller design we modified the standard neural network update laws to include terms of the form $-\sigma\|e\|\widehat{W}$ and $-\sigma\widehat{W}$, respectively, where e is the system state error [65,102]. Figures 2.24 and 2.25 show that employing these modifications with $\sigma = 10$ degrades the performance of the *conventional* neuroadaptive controller. One can surmise from these results that the Q-modification controller provides superior performance to both the e- and σ-modification controllers when a system failure occurs for a wide range of system gains. In this case, the Q-modification controller performance monotonically improves, whereas the performance of both the e- and σ-modification controllers monotonically degrade over the range of the adaptation gains investigated.

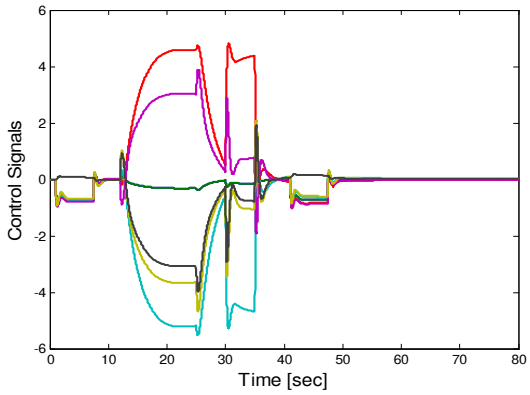

Figure 2.11: Nominal control response performance of the baseline controller.

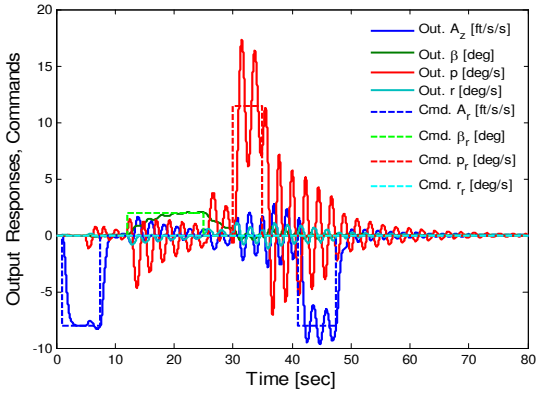

Figure 2.12: Output response of the baseline controller with a ROE failure.

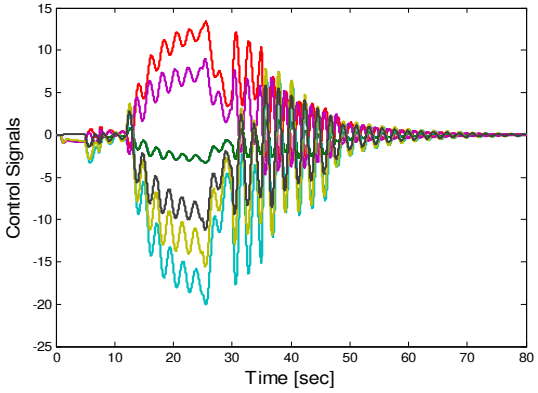

Figure 2.13: Control response of the baseline controller with a ROE failure.

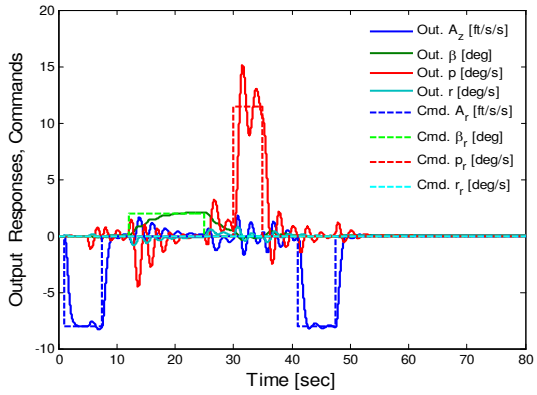

Figure 2.14: Output response of the neuroadaptive controller with ROE failure.

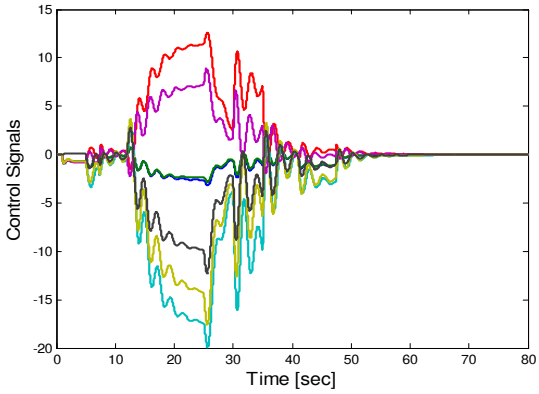

Figure 2.15: Control response of the neuroadaptive controller with ROE failure.

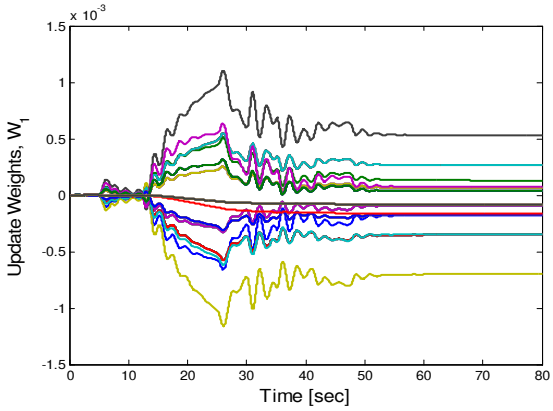

Figure 2.16: Update weights $\hat{W}_1(t)$ of the neuroadaptive controller with ROE failure.

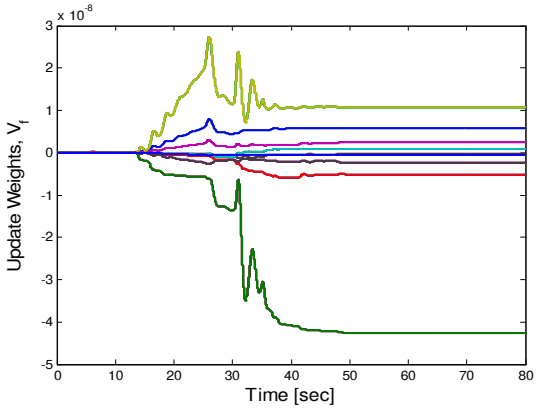

Figure 2.17: Update weights $\hat{V}_f(t)$ of the neuroadaptive controller with ROE failure.

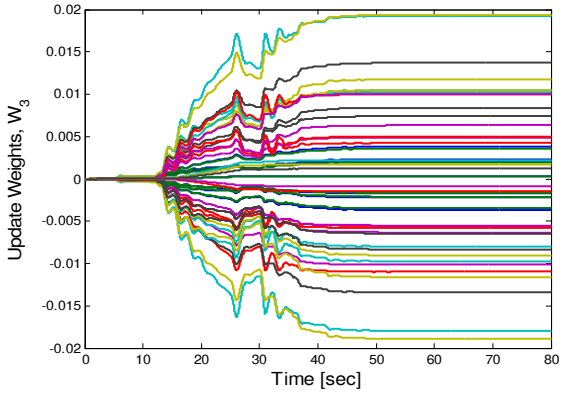

Figure 2.18: Update weights $\hat{W}_3(t)$ of the neuroadaptive controller with ROE failure.

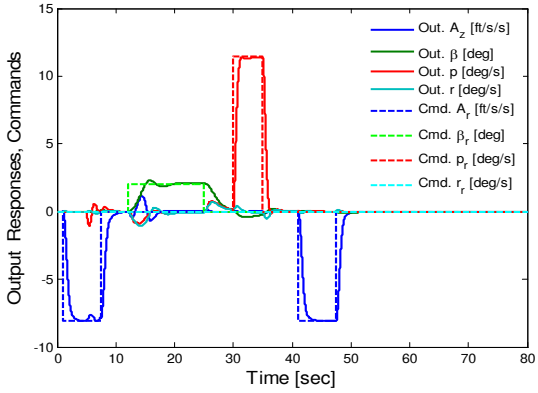

Figure 2.19: Output response of the neuroadaptive controller with Q-modification ($k = 10,\ \tau_{\rm d} = 0.5$ sec) with ROE failure.

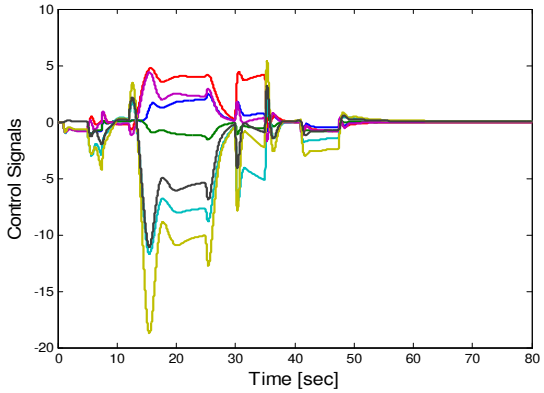

Figure 2.20: Control response of the neuroadaptive controller with Q-modification ($k = 10,\ \tau_{\mathrm{d}} = 0.5$ sec) with ROE failure.

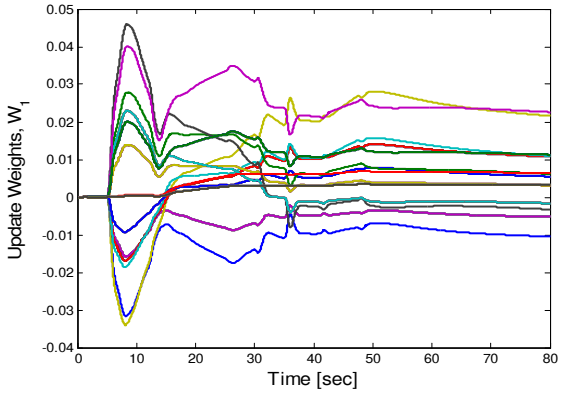

Figure 2.21: Update weights $\hat{W}_1(t)$ of the neuroadaptive controller with Q-modification ($k = 10,\ \tau_{\mathrm{d}} = 0.5$ sec) with ROE failure.

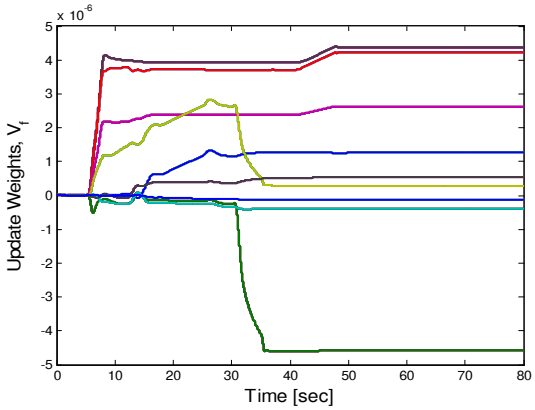

Figure 2.22: Update weights $\hat{V}_f(t)$ of the neuroadaptive controller with Q-modification ($k = 10,\ \tau_{\mathrm{d}} = 0.5$ sec) with ROE failure.

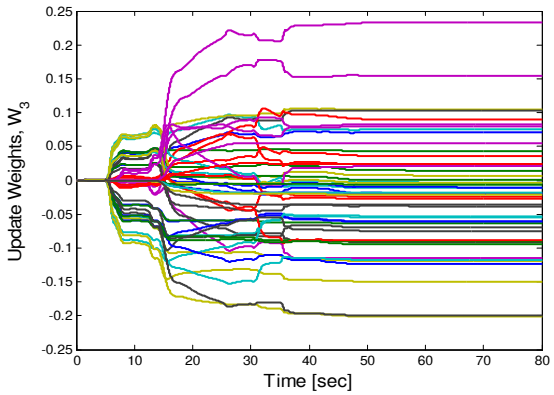

Figure 2.23: Update weights $\hat{W}_3(t)$ of the neuroadaptive controller with Q-modification ($k = 10,\ \tau_{\rm d} = 0.5$ sec) with ROE failure.

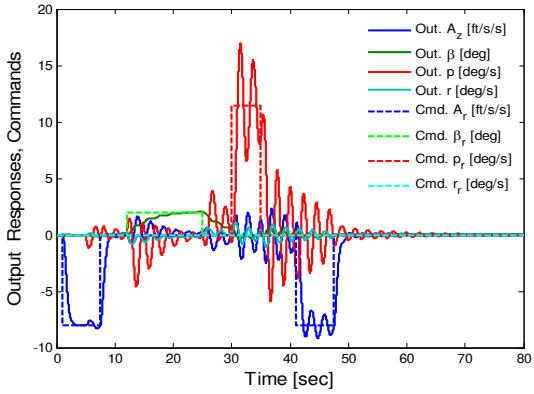

Figure 2.24: Output response of the neuroadaptive controller with e-modification ($\sigma = 10$) with ROE failure.

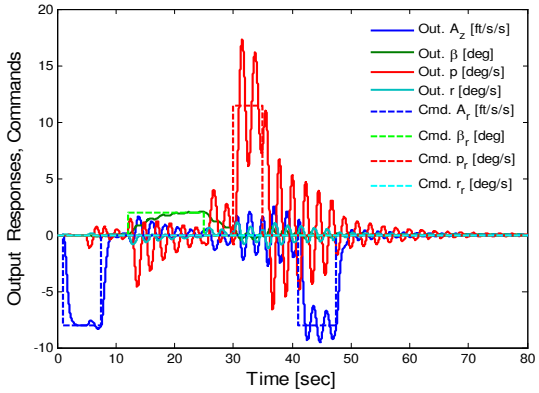

Figure 2.25: Output response of the neuroadaptive controller with σ-modification ($\sigma = 10$) with ROE failure.

Chapter 3

A Q-Modification Neuroadaptive Control Architecture for Discrete-Time Systems

3.1. Introduction

As discussed in Chapter 2, neural networks have been extensively used for adaptive system identification as well as adaptive and neuroadaptive control of highly uncertain continuous-time dynamical systems [25, 63, 91, 92, 104, 105, 108, 114, 129]. One of the primary reasons for the large interest in neural networks is their capability to approximate a large class of continuous nonlinear maps from the collective action of very simple, autonomous processing units interconnected in simple ways. Neural networks have also attracted attention due to their inherently parallel and highly redundant processing architecture that makes it possible to develop parallel weight update laws. This parallelism makes it possible to effectively update a neural network on line. Discrete-time extensions of neural network adaptive control methods have also appeared in the literature; see [26, 31, 38, 64, 71, 72, 74, 95, 129] and the references therein.

To improve robustness and the speed of adaptation of adaptive and neuroadaptive controllers several controller architectures have been proposed in the literature. These include the σ- and e-modification architectures used to keep the system pa-

rameter estimates from growing without bound in the face of system uncertainty and system disturbances [72, 92, 129]. In Chapter 2 (see also [138, 139]), a new neuroadaptive control architecture for nonlinear uncertain dynamical systems was developed. Specifically, the proposed framework involved a new and novel controller architecture involving additional terms, or *Q-modification terms*, in the update laws that were constructed using a moving time window of the integrated system uncertainty. The Q-modification terms were shown to effectively suppress and cancel system uncertainty without the need for persistency of excitation.

In this chapter, we extend some of the results of Chapter 2 to discrete-time uncertain dynamical systems. As in the continuous-time case, the discrete-time update laws involve auxiliary terms, or Q-modification terms, predicated on an estimate of the unknown neural network weights which in turn involve a set of auxiliary equations characterizing a set of affine hyperplanes. In addition, we show that the Q-modification terms in the update law are designed to minimize an error criterion involving a sum of squares of the distances between the update weights and the family of affine hyperplanes. The proposed approach thus uses a linear subspace projection scheme with a gradient-based search to estimate the neural network weights.

The notation used in this paper is fairly standard. Specifically, $\overline{\mathbb{Z}}_+$ denotes the set of nonnegative integers, $(\cdot)^{\mathrm{T}}$ denotes transpose, $(\cdot)^{\dagger}$ denotes the Moore-Penrose generalized inverse, $\mathrm{tr}(\cdot)$ denotes the trace operator, $\ln(\cdot)$ denotes the natural log operator, and $\|\cdot\|$ denotes the Euclidean norm.

3.2. Neuroadaptive Control for Discrete-Time Nonlinear Uncertain Dynamical Systems with a Q-modification Architecture

In this section, we consider the problem of characterizing neuroadaptive full-state feedback control laws for discrete-time nonlinear uncertain dynamical systems to achieve reference model trajectory tracking. Specifically, consider the controlled discrete-time nonlinear uncertain dynamical system $\mathcal{G}$ given by

$$x(k+1) = A_0x(k) + B\Delta(\hat{x}(k), \hat{u}(k)) + BG(x(k))u(k), \quad x(0) = x_0, \quad k \in \overline{\mathbb{Z}}_+, \tag{3.1}$$

where $x(k) \in \mathbb{R}^n$, $k \in \overline{\mathbb{Z}}_+$, is the state vector, $u(k) \in \mathbb{R}^m$, $k \in \overline{\mathbb{Z}}_+$, is the control input, $\hat{x}(k) \triangleq [\,x(k),\, x(k-1),\, \ldots,\, x(k-p+1)]$ is a vector of p-delayed values of the state vector with $p \geq 1$, $\hat{u}(k) \triangleq [\,u(k-1),\, u(k-2),\, \ldots,\, u(k-q)]$ is a vector of q-delayed values of the control input with $q \geq 1$, $A_0 \in \mathbb{R}^{n\times n}$ and $B \in \mathbb{R}^{n\times m}$ are known matrices, $G : \mathbb{R}^n \to \mathbb{R}^{m\times m}$ is a known input matrix function such that $\det G(x) \neq 0$ for all $x \in \mathbb{R}^n$, and $\Delta : \mathbb{R}^{np} \times \mathbb{R}^{mq} \to \mathbb{R}^m$ is an *unknown* nonlinear function representing system uncertainty. Dynamical systems with uncertainty structures given by (3.1) are discussed in [138].

We assume that $\Delta(\hat{x}(k), \hat{u}(k))$, $k \in \overline{\mathbb{Z}}_+$, can be perfectly parameterized as

$$\Delta(\hat{x}(k), \hat{u}(k)) = W^{\mathrm{T}}\sigma(\hat{x}(k), \hat{u}(k)), \quad k \in \overline{\mathbb{Z}}_+, \tag{3.2}$$

where $W \in \mathbb{R}^{l\times m}$ is an *unknown* matrix and $\sigma : \mathbb{R}^{np} \times \mathbb{R}^{mq} \to \mathbb{R}^l$ is a known bounded Lipschitz continuous function such that, for all $\hat{x}(k) \in \mathbb{R}^{np}$ and $\hat{u}(k) \in \mathbb{R}^{mq}$, $k \in \overline{\mathbb{Z}}_+$, $\|\sigma(\hat{x}, \hat{u})\| \leq \sigma^*$, where $\sigma^* > 0$. Furthermore, we assume that the state $x(k)$, $k \in \overline{\mathbb{Z}}_+$, is available for feedback.

In order to achieve trajectory tracking, we construct a reference system $\mathcal{G}_{\mathrm{ref}}$ given

by

$$x_{\rm ref}(k+1) = A_{\rm ref}x_{\rm ref}(k) + B_{\rm ref}r(k), \quad x_{\rm ref}(0) = x_{\rm ref_0}, \quad k \in \overline{\mathbb{Z}}_+, \tag{3.3}$$

where $x_{\rm ref}(k) \in \mathbb{R}^n$, $k \in \overline{\mathbb{Z}}_+$, is the reference state vector, $r(k) \in \mathbb{R}^r$, $k \in \overline{\mathbb{Z}}_+$, is a bounded reference input, $A_{\rm ref} \in \mathbb{R}^{n\times n}$ is Shur, and $B_{\rm ref} \in \mathbb{R}^{n\times r}$. Since all the eigenvalues of the matrix $A_{\rm ref}$ lie in the unit disk, it follows from Lemma 13.2 of [129] that there exists a positive-definite matrix $P \in \mathbb{R}^{n\times n}$ such that

$$P = A_{\rm ref}^{\rm T}PA_{\rm ref} + R, \tag{3.4}$$

where $R \in \mathbb{R}^{n\times n}$ is a positive-definite matrix. The goal here is to develop an adaptive control signal $u(k)$, $k \in \overline{\mathbb{Z}}_+$, that guarantees $x(k) \to x_{\rm ref}(k)$ as $k \to \infty$.

The following matching conditions are needed for the main result of this section.

Assumption 3.1. There exist gains $K_{\rm x} \in \mathbb{R}^{m\times n}$ and $K_{\rm r} \in \mathbb{R}^{m\times r}$ such that $A_0 + BK_{\rm x} = A_{\rm ref}$ and $BK_{\rm r} = B_{\rm ref}$.

Consider the control law given by

$$u(k) = G^{-1}(x(k))(u_{\rm n}(k) - u_{\rm ad}(k)), \quad k \in \overline{\mathbb{Z}}_+, \tag{3.5}$$

where

$$u_{\rm n}(k) = K_{\rm x}x(k) + K_{\rm r}r(k), \quad k \in \overline{\mathbb{Z}}_+, \tag{3.6}$$

and

$$u_{\rm ad}(k) = \hat{W}^{\rm T}(k)\sigma(\hat{x}(k), \hat{u}(k)), \quad k \in \overline{\mathbb{Z}}_+, \tag{3.7}$$

gives the output of the linearly parameterized neural network and $\hat{W}(k) \in \mathbb{R}^{l\times m}$, $k \in \overline{\mathbb{Z}}_+$, is an update weight matrix.

Using (3.5)–(3.7) and Assumption 3.1 the system dynamics (3.1) can be rewritten as

$$x(k+1) = A_{\mathrm{ref}}x(k) + B_{\mathrm{ref}}r(k) + B\tilde{W}^{\mathrm{T}}(k)\sigma(\hat{x}(k),\hat{u}(k)), \quad x(0) = x_0, \quad k \in \overline{\mathbb{Z}}_+, \tag{3.8}$$

where $\tilde{W}(k) \triangleq W - \hat{W}(k)$, $k \in \overline{\mathbb{Z}}_+$. Defining the tracking error $e(k) \triangleq x(k) - x_{\mathrm{ref}}(k)$, $k \in \overline{\mathbb{Z}}_+$, the error dynamics are given by

$$e(k+1) = A_{\mathrm{ref}}e(k) + B\tilde{W}^{\mathrm{T}}(k)\sigma(\hat{x}(k),\hat{u}(k)), \quad e(0) = e_0, \quad k \in \overline{\mathbb{Z}}_+, \tag{3.9}$$

where $e_0 \triangleq x_0 - x_{\mathrm{ref}_0}$.

Now, for every $k \in \overline{\mathbb{Z}}_+$, consider a linear subspace $\mathcal{L}_s$, where $s \leq \min\{l, k\}$, formed by s linearly independent vectors $q(i)$, $i = 1, \ldots, s$, such that

$$BW^{\mathrm{T}}q(i) = c(i), \quad i = 1, \ldots, s, \tag{3.10}$$

where

$$q(i) = \sigma(\hat{x}(i),\hat{u}(i)), \quad i = 1, \ldots, s, \tag{3.11}$$

$$c(i) = e(i+1) - A_{\mathrm{ref}}e(i) + B\hat{W}^{\mathrm{T}}(i)\sigma(\hat{x}(i),\hat{u}(i)), \quad i = 1, \ldots, s. \tag{3.12}$$

Note that (3.10) is a direct consequence of (3.9). Furthermore, note that $q(i)$, $i = 1, \ldots, s$, and $c(i)$, $i = 1, \ldots, s$, given by (3.11) and (3.12) are computable. Hence, although the matrix W is *unknown*, W satisfies a set of linear equations given by (3.10). Equation (3.10) represents a system of s equations in terms of the entries of W, where each of these equations characterizes an affine hyperplane. For example, in the case where $n = 1$, $m = 1$, $l = 2$, $s = 1$, $W = [W_1, W_2]^{\mathrm{T}}$, and $B = 1$, the affine hyperplane (3.10) is described by a line $\mathcal{L}_s$ with $q(i)$, $i = 1, \ldots, s$, being a normal vector to $\mathcal{L}_s$ as shown in Figure 3.1. Note that the distance from point A to point B

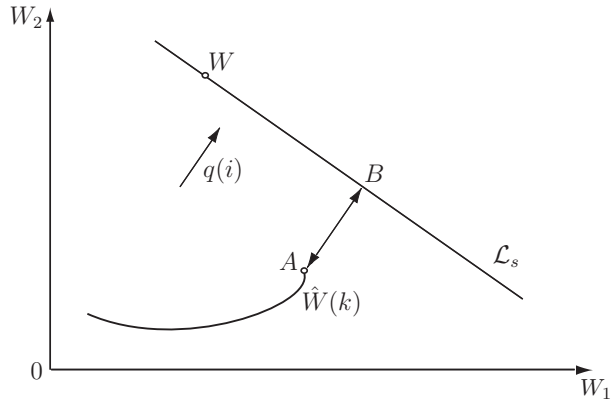

Figure 3.1: Visualization of Q-modification term.

shown in Figure 3.1, which is the shortest distance from the weight estimate $\hat{W}(k)$ to affine hyperplane $\mathcal{L}_s$ defined by (3.10), is given by $c(i) - \hat{W}^{\mathrm{T}}(k)q(i)$.

Next, define the error criterion

$$\rho(\hat{W}(k), \bar{q}(k), \bar{c}(k)) \triangleq \frac{\gamma_Q}{2}\mathrm{tr}\left[\bar{c}(k) - B\hat{W}^{\mathrm{T}}(k)\bar{q}(k)\right]\left[\bar{c}(k) - B\hat{W}^{\mathrm{T}}(k)\bar{q}(k)\right]^{\mathrm{T}}, \; k \in \overline{\mathbb{Z}}_+, \tag{3.13}$$

where $\gamma_Q > 0$, $\bar{q}(k) \triangleq \sum_{i=1}^{s} \alpha_i(k)q(i)$, $\bar{c}(k) \triangleq \sum_{i=1}^{s} \alpha_i(k)c(i)$, and $\alpha_i(k) \in \mathbb{R}$, $i = 1, \ldots, s$, $k \in \overline{\mathbb{Z}}_+$, are design parameters. Note that (3.13) is a weighted sum of squares of the distances between the update weights $\hat{W}(k)$, $k \in \overline{\mathbb{Z}}_+$, and the family of affine hyperplanes defined by (3.10). Now, note that the gradient of $\rho(\hat{W}(k), \bar{q}(k), \bar{c}(k))$, $k \in \overline{\mathbb{Z}}_+$, with respect to $\hat{W}(k)$, $k \in \overline{\mathbb{Z}}_+$, is given by

$$\frac{\partial \rho(\hat{W}(k), \bar{q}(k), \bar{c}(k))}{\partial \hat{W}(k)} = -\gamma_Q \bar{q}(k)\left[\bar{c}(k) - B\hat{W}^{\mathrm{T}}(k)\bar{q}(k)\right]^{\mathrm{T}} B, \quad k \in \overline{\mathbb{Z}}_+. \tag{3.14}$$

Next, define

$$H(k) \triangleq \gamma_Q \bar{q}(k)\left[\bar{c}(k) - B\hat{W}^{\mathrm{T}}(k)\bar{q}(k)\right]^{\mathrm{T}} B, \quad k \in \overline{\mathbb{Z}}_+, \tag{3.15}$$

and note that if $\hat{W}(k)$, $k \in \overline{\mathbb{Z}}_+$, satisfies

$$B\hat{W}^{\mathrm{T}}(k)\bar{q}(k) = \bar{c}(k), \quad k \in \overline{\mathbb{Z}}_+, \tag{3.16}$$

then $H(k)$, $k \in \overline{\mathbb{Z}}_+$, is zero and the weight estimates $\hat{W}(k)$, $k \in \overline{\mathbb{Z}}_+$, lie on the collection of the affine hyperplanes defined by (3.10). If the weight estimates $\hat{W}(k)$, $k \in \overline{\mathbb{Z}}_+$, do not satisfy (3.16), then each nonzero row of the matrix $H(k)$, $k \in \overline{\mathbb{Z}}_+$, is a vector that is orthogonal to the corresponding affine hyperplane defined by (3.10) and points in the direction of the hyperplane. Finally, using (3.10), it follows that

$$\operatorname{tr} H^{\mathrm{T}}(k)\tilde{W}(k) = \gamma_Q \left\| \bar{c}(k) - B\hat{W}^{\mathrm{T}}(k)\bar{q}(k) \right\|^2 \geq 0, \quad k \in \overline{\mathbb{Z}}_+. \tag{3.17}$$

Theorem 3.1. Consider the nonlinear uncertain dynamical system $\mathcal{G}$ given by (3.1). Assume Assumption 3.1 holds. Furthermore, assume that for a given $\gamma > 0$, there exist positive-definite matrices $P \in \mathbb{R}^{n\times n}$ and $E \in \mathbb{R}^{m\times m}$ such that

$$\frac{1}{\gamma(c + \sigma^{*2})} I_m > (E + B^{\mathrm{T}} P B), \tag{3.18}$$

where I_m is the $m \times m$ identity matrix and $c > 0$. Then, the neuroadaptive control law (3.5)–(3.7) with update law given by

$$\hat{W}(k+1) = \hat{W}(k) + \Phi(k+1) + Q(k+1), \quad \hat{W}(0) = \hat{W}_0, \quad k \in \overline{\mathbb{Z}}_+, \tag{3.19}$$

where $\Phi(k) \in \mathbb{R}^{l\times m}$, $k \in \overline{\mathbb{Z}}_+$, and $Q(k) \in \mathbb{R}^{l\times m}$, $k \in \overline{\mathbb{Z}}_+$, are given by

$$\Phi(k+1) = \frac{1}{c + \sigma^{\mathrm{T}}(\hat{x}(k), \hat{u}(k))\sigma(\hat{x}(k), \hat{u}(k))} \sigma(\hat{x}(k), \hat{u}(k)) \left[e(k+1) - A_{\mathrm{ref}} e(k) \right]^{\mathrm{T}} B^{\dagger}, \tag{3.20}$$

$$Q(k+1) = \begin{cases} H(k), & \text{if } g(k) > 0, \\ 0_{l\times m}, & \text{otherwise,} \end{cases}, \quad k \in \overline{\mathbb{Z}}_+, \tag{3.21}$$

and

$$g(k) \triangleq \gamma_Q \left\| \bar{c}(k) - B\hat{W}^{\mathrm{T}}(k)\bar{q}(k) \right\|^2 - \operatorname{tr} \Phi^{\mathrm{T}}(k) H(k) - \frac{1}{2} \operatorname{tr} H^{\mathrm{T}}(k) H(k), \quad k \in \overline{\mathbb{Z}}_+, \tag{3.22}$$

guarantees that there exists a positively invariant set $\mathcal{D}_\alpha \subset \mathbb{R}^n \times \mathbb{R}^{l\times m}$, with $(0, W) \in \mathcal{D}_\alpha$, such that the solution $(e(k), \hat{W}(k)) \equiv (0, W)$ of the closed-loop system given by (3.9), (3.5)–(3.7), and (3.19)–(3.21) is Lyapunov stable and $e(k) \to 0$ as $k \to \infty$ for all $(e_0, \hat{W}_0) \in \mathcal{D}_\alpha$.

Proof. To show Lyapunov stability of the closed-loop system (3.9), (3.5)–(3.7), and (3.19)–(3.21), consider the Lyapunov function candidate

$$V(e, \tilde{W}) = \ln(1 + e^{\mathrm{T}} P e) + \frac{1}{\gamma} \mathrm{tr}\, \tilde{W}^{\mathrm{T}} \tilde{W}, \tag{3.23}$$

where $P > 0$ satisfies (3.4) and $\gamma > 0$. Note that $V(0, 0) = 0$ and, since P is positive definite and $\gamma > 0$, $V(e, \tilde{W}) > 0$ for all $(e, \tilde{W}) \neq 0$. Now, letting $e(k)$, $k \in \overline{\mathbb{Z}}_+$, denote the solution to (3.9) and using (3.19)–(3.22), it follows that the Lyapunov difference along the closed-loop system trajectories is given by

$$\begin{aligned}
&\Delta V(e(k), \tilde{W}(k)) \\
&\quad \triangleq V(e(k+1), \tilde{W}(k+1)) - V(e(k), \tilde{W}(k)) \\
&\quad = \ln\left(1 + \left[A_{\mathrm{ref}} e(k) + B\tilde{W}^{\mathrm{T}}(k)\sigma(\hat{x}(k), \hat{u})\right]^{\mathrm{T}} P \left[A_{\mathrm{ref}} e(k) + B\tilde{W}^{\mathrm{T}}(k)\sigma(\hat{x}(k), \hat{u})\right]\right) \\
&\qquad - \ln\left(1 + e^{\mathrm{T}}(k) P e(k)\right) + \frac{1}{\gamma}\mathrm{tr}\, \tilde{W}^{\mathrm{T}}(k+1)\tilde{W}(k+1) - \frac{1}{\gamma}\mathrm{tr}\, \tilde{W}^{\mathrm{T}}(k)\tilde{W}(k) \\
&\quad = \ln\left(\frac{1 + \left[A_{\mathrm{ref}} e(k) + B\tilde{W}^{\mathrm{T}}(k)\sigma(\hat{x}(k), \hat{u})\right]^{\mathrm{T}} P \left[A_{\mathrm{ref}} e(k) + B\tilde{W}^{\mathrm{T}}(k)\sigma(\hat{x}(k), \hat{u})\right]}{1 + e^{\mathrm{T}}(k) P e(k)}\right) \\
&\qquad + \frac{1}{\gamma}\mathrm{tr}\, \left[\tilde{W}(k) - \Phi(k+1) - Q(k+1)\right]^{\mathrm{T}} \left[\tilde{W}(k) - \Phi(k+1) - Q(k+1)\right] \\
&\qquad - \frac{1}{\gamma}\mathrm{tr}\, \tilde{W}^{\mathrm{T}}(k)\tilde{W}(k) \\
&\quad = \ln\Big[\big(1 + e^{\mathrm{T}}(k) P e(k) - e^{\mathrm{T}}(k) P e(k) + e^{\mathrm{T}}(k) A_{\mathrm{ref}}^{\mathrm{T}} P A_{\mathrm{ref}} e(k) + 2 e^{\mathrm{T}}(k) A_{\mathrm{ref}}^{\mathrm{T}} P B \\
&\qquad \cdot \tilde{W}^{\mathrm{T}}(k)\sigma(\hat{x}(k), \hat{u}(k)) + \sigma^{\mathrm{T}}(\hat{x}(k), \hat{u}(k))\tilde{W}(k) B^{\mathrm{T}} P B \tilde{W}^{\mathrm{T}}(k)\sigma(\hat{x}(k), \hat{u}(k))\big)\Big] \\
&\qquad \cdot \left[1 + e^{\mathrm{T}}(k) P e(k)\right]^{-1} + \frac{1}{\gamma}\mathrm{tr}\, \tilde{W}^{\mathrm{T}}(k)\tilde{W}(k) - \frac{1}{\gamma}\mathrm{tr}\, \tilde{W}^{\mathrm{T}}(k)\tilde{W}(k) \\
&\qquad - \frac{1}{\gamma}\mathrm{tr}\, \left[\Phi(k+1) + Q(k+1)\right]^{\mathrm{T}} \left[2\tilde{W}(k) - \Phi(k+1) - Q(k+1)\right]
\end{aligned}$$

$$
\begin{aligned}
&= \ln\big[\big(1 + e^{\mathrm{T}}(k)Pe(k) + e^{\mathrm{T}}(k)(A_{\mathrm{ref}}^{\mathrm{T}}PA_{\mathrm{ref}} - P)e(k) + 2e^{\mathrm{T}}(k)A_{\mathrm{ref}}^{\mathrm{T}}PB \\
&\quad \cdot\tilde{W}^{\mathrm{T}}(k)\sigma(\hat{x}(k),\hat{u}(k)) + \sigma^{\mathrm{T}}(\hat{x}(k),\hat{u}(k))\tilde{W}(k)B^{\mathrm{T}}PB\tilde{W}^{\mathrm{T}}(k)\sigma(\hat{x}(k),\hat{u}(k))\big)\big] \\
&\quad \cdot\big[1 + e^{\mathrm{T}}(k)Pe(k)\big]^{-1} - \frac{1}{\gamma}\mathrm{tr}\,\big[\Phi(k+1) + Q(k+1)\big]^{\mathrm{T}} \\
&\quad \cdot\Big[2\tilde{W}(k) - \Phi(k+1) - Q(k+1)\Big] \\
&= \ln\Big(\big[1 + e^{\mathrm{T}}(k)Pe(k)\big]\,\big[1 + e^{\mathrm{T}}(k)Pe(k)\big]^{-1} + \Big(2e^{\mathrm{T}}(k)A_{\mathrm{ref}}^{\mathrm{T}}PB\tilde{W}^{\mathrm{T}}(k)\sigma(\hat{x}(k),\hat{u}(k)) \\
&\quad + e^{\mathrm{T}}(k)(A_{\mathrm{ref}}^{\mathrm{T}}PA_{\mathrm{ref}} - P)e(k) + \sigma^{\mathrm{T}}(\hat{x}(k),\hat{u}(k))\tilde{W}(k)B^{\mathrm{T}}PB\tilde{W}^{\mathrm{T}}(k)\sigma(\hat{x}(k),\hat{u}(k))\Big) \\
&\quad \cdot\big[1 + e^{\mathrm{T}}(k)Pe(k)\big]^{-1}\Big) - \frac{1}{\gamma}\mathrm{tr}\,\big[\Phi(k+1) + Q(k+1)\big]^{\mathrm{T}} \\
&\quad \cdot[2\tilde{W}(k) - \Phi(k+1) - Q(k+1)] \\
&= \ln\Big(1 + \Big[e^{\mathrm{T}}(k)\left(A_{\mathrm{ref}}^{\mathrm{T}}PA_{\mathrm{ref}} - P\right)e(k) + 2e^{\mathrm{T}}(k)A_{\mathrm{ref}}^{\mathrm{T}}PB\tilde{W}^{\mathrm{T}}(k)\sigma(\hat{x}(k),\hat{u}(k)) \\
&\quad + \sigma^{\mathrm{T}}(\hat{x}(k),\hat{u}(k))\tilde{W}(k)B^{\mathrm{T}}PB\tilde{W}^{\mathrm{T}}(k)\sigma(\hat{x}(k),\hat{u}(k))\Big]\,\big[1 + e^{\mathrm{T}}(k)Pe(k)\big]^{-1}\Big) \\
&\quad - \frac{1}{\gamma}\mathrm{tr}\left(\big[\Phi(k+1) + Q(k+1)\big]^{\mathrm{T}}\Big[2\tilde{W}(k) - \Phi(k+1) - Q(k+1)\Big]\right). \qquad (3.24)
\end{aligned}
$$

Next, let $R_1 > 0$ and $R_2 > 0$ be such that $R_1 + R_2 = R$ and define

$$
\eta(k) \triangleq \Big[e^{\mathrm{T}}(k), \sigma^{\mathrm{T}}(\hat{x}(k),\hat{u}(k))\tilde{W}(k)\Big]^{\mathrm{T}}, \quad k \in \overline{\mathbb{Z}}_+, \qquad (3.25)
$$

$$
M \triangleq \begin{bmatrix} R_2 & -A_{\mathrm{ref}}^{\mathrm{T}}PB \\ -B^{\mathrm{T}}PA_{\mathrm{ref}} & E \end{bmatrix} > 0. \qquad (3.26)
$$

Now, using (3.4) and the fact that $\ln(1+a) \leq a$, $a > -1$, it follows from (3.24) that

$$
\begin{aligned}
&\Delta V(e(k),\tilde{W}(k)) \\
&\quad \leq -\frac{e^{\mathrm{T}}(k)R_1e(k)}{1 + e^{\mathrm{T}}(k)Pe(k)} - \frac{1}{1 + e^{\mathrm{T}}(k)Pe(k)}\eta^{\mathrm{T}}(k)M\eta(k) \\
&\qquad + \frac{1}{1 + e^{\mathrm{T}}(k)Pe(k)}\sigma^{\mathrm{T}}(\hat{x}(k),\hat{u}(k))\tilde{W}(k)\left[E + B^{\mathrm{T}}PB\right]\tilde{W}^{\mathrm{T}}(k)\sigma(\hat{x}(k),\hat{u}(k)) \\
&\qquad - \frac{1}{\gamma}\mathrm{tr}\left(\big[\Phi(k+1) + Q(k+1)\big]^{\mathrm{T}}\Big[2\tilde{W}(k) - \Phi(k+1) - Q(k+1)\Big]\right). \qquad (3.27)
\end{aligned}
$$

Using (3.20), (3.21), and the fact that $\frac{\sigma^{\mathrm{T}}(\hat{x}(k),\hat{u}(k))\sigma(\hat{x}(k),\hat{u}(k))}{c + \sigma^{\mathrm{T}}(\hat{x}(k),\hat{u}(k))\sigma(\hat{x}(k),\hat{u}(k))} < 1$, $c > 0$, it follows that

$$
\Delta V(e(k),\tilde{W}(k))
$$

$$
\begin{aligned}
&\leq -\frac{e^{\mathrm{T}}(k)R_1e(k)}{1+e^{\mathrm{T}}(k)Pe(k)} - \frac{1}{1+e^{\mathrm{T}}(k)Pe(k)}\eta^{\mathrm{T}}(k)M\eta(k)\\
&\quad +\frac{1}{1+e^{\mathrm{T}}(k)Pe(k)}\sigma^{\mathrm{T}}(\hat{x}(k),\hat{u}(k))\tilde{W}(k)\left[E+B^{\mathrm{T}}PB\right]\tilde{W}^{\mathrm{T}}(k)\sigma(\hat{x}(k),\hat{u}(k))\\
&\quad -\frac{1}{\gamma}\frac{1}{c+\sigma^{\mathrm{T}}(\hat{x}(k),\hat{u}(k))\sigma(\hat{x}(k),\hat{u}(k))}\sigma^{\mathrm{T}}(\hat{x}(k),\hat{u}(k))\tilde{W}(k)\tilde{W}^{\mathrm{T}}(k)\sigma(\hat{x}(k),\hat{u}(k))\\
&\quad -\frac{2}{\gamma}\mathrm{tr}\left[Q^{\mathrm{T}}(k+1)\tilde{W}(k)-\Phi^{\mathrm{T}}(k+1)Q(k+1)-\frac{1}{2}Q^{\mathrm{T}}(k+1)Q(k+1)\right]. \qquad (3.28)
\end{aligned}
$$

Finally, using (3.18), (3.21), and (3.17), it follows that

$$
\Delta V(e(k),\tilde{W}(k)) \leq 0, \quad k \in \overline{\mathbb{Z}}_+. \qquad (3.29)
$$

Next, define

$$
\tilde{\mathcal{D}}_\alpha \triangleq \left\{(e,\tilde{W}) \in \mathbb{R}^n \times \mathbb{R}^{l\times m} : V(e,\tilde{W}) \leq \alpha\right\}, \quad \alpha > 0. \qquad (3.30)
$$

Since $\Delta V(e(k),\tilde{W}(k)) \leq 0$ for all $(e(k),\tilde{W}(k)) \in \tilde{\mathcal{D}}_\alpha$ and $k \in \overline{\mathbb{Z}}_+$, it follows that $\tilde{\mathcal{D}}_\alpha$ is positively invariant. Now, since $\tilde{\mathcal{D}}_\alpha$ is positively invariant, it follows that

$$
\mathcal{D}_\alpha \triangleq \left\{(e,\hat{W}) \in \mathbb{R}^n \times \mathbb{R}^{l\times m} : (e,\hat{W}-W) \in \tilde{\mathcal{D}}_\alpha\right\} \qquad (3.31)
$$

is also positively invariant. Furthermore, it follows from (3.29) and Theorem 13.10 of [48] that the solution $(e(k),\hat{W}(k)) \equiv (0,W)$ of the closed-loop system given by (3.9) and (3.19) is Lyapunov stable and $e(k) \to 0$ as $k \to \infty$ for all $(e_0,\hat{W}_0) \in \mathcal{D}_\alpha$. □

The term $Q(k)$, $k \in \overline{\mathbb{Z}}_+$, in (3.19) given by (3.21) is a discrete-time analogue of the Q-modification term introduced in Chapter 2 for continuous-time systems. As in the continuous-time case, $Q(k)$, $k \in \overline{\mathbb{Z}}_+$, is an additional term that is introduced to the update law that is designed to minimize the error criterion given by (3.13) and is constructed based on information of the unknown weights W given by (3.10) and the property given by (3.17). Note that for every $k \in \overline{\mathbb{Z}}_+$, the vector $Q(k)$ is directed opposite to the gradient $\frac{\partial\rho(\hat{W}(k),\bar{q}(k),\bar{c}(k))}{\partial\tilde{W}(k)}$ and, in the case where the system uncertainty

is a scalar function, is parallel to $\bar{q}(k)$, which involves a linear combination of vectors normal to affine hyperplanes defined by (3.10). Hence, $Q(k)$, $k \in \overline{\mathbb{Z}}_+$, introduces a component in the update law (3.19) that drives the trajectory $\hat{W}(k)$, $k \in \overline{\mathbb{Z}}_+$, in such a way so that the error criterion given by (3.13) is minimized.

3.3. Illustrative Numerical Example

In this section, we present a numerical example to demonstrate the utility and efficacy of the proposed Q-modification architecture for discrete-time neuroadaptive stabilization. Specifically, consider the following dynamical system given by

$$x(k+1) = A_0 x(k) + B\Delta(x(k)) + Bu(k), \quad x(0) = x_0, \quad k \in \overline{\mathbb{Z}}_+, \tag{3.32}$$

where

$$A_0 = \begin{bmatrix} 0 & 1 \\ -0.35 & -0.25 \end{bmatrix}, \quad B = \begin{bmatrix} 0 \\ 1 \end{bmatrix}, \quad \Delta(x(k)) = W^{\mathrm{T}}\sigma(x(k)), \quad k \in \overline{\mathbb{Z}}_+,$$

and $\sigma(x) = [\sin(x_1),\, \cos(x_2),\, \cos(x_1),\, \sin(x_2),\, x_1,\, x_1|x_1|]^{\mathrm{T}}$ is a known regressor vector. Note that eigenvalues of A_0 are $\lambda_1 = -0.1250 - 0.5783\jmath$ and $\lambda_2 = -0.1250 + 0.5783\jmath$, and hence, lie inside the unit disk.

Here our goal is to achieve stabilization of the uncertain system around the origin. Hence, the reference model is given by (3.3) with $A_{\mathrm{ref}} = A_0$, $B_{\mathrm{ref}} = B$, $x_{\mathrm{ref}_0} = [0,\, 0]^{\mathrm{T}}$, and $r(k) \equiv 0$. Next, we use Theorem 3.1 to design a neuroadaptive controller given by (3.5)–(3.7), with $u_{\mathrm{n}}(k) \equiv 0$ and update laws given by (3.19)–(3.21). Now, with initial conditions $x_0 = [3,\, 4]^{\mathrm{T}}$ and $\hat{W}_0 = 0_{6\times 1}$, and $W = [1.00,\, -1.50,\, 2.50,\, 3.50,\, 1.00,\, 0.50]^{\mathrm{T}}$, Figures 3.2–3.5 show the state trajectories, the control input, and the update weight trajectories versus time with and without the Q-modification term activated. It is clear that the Q-modification architecture results in a faster convergence and reduces system and weight oscillations. It is interesting to note that for this example the update weights for both controllers converge

to the same values. However, in the presence of persistency of excitation it can be shown that the update weights of the Q-modification controller converge to the ideal weights [138].

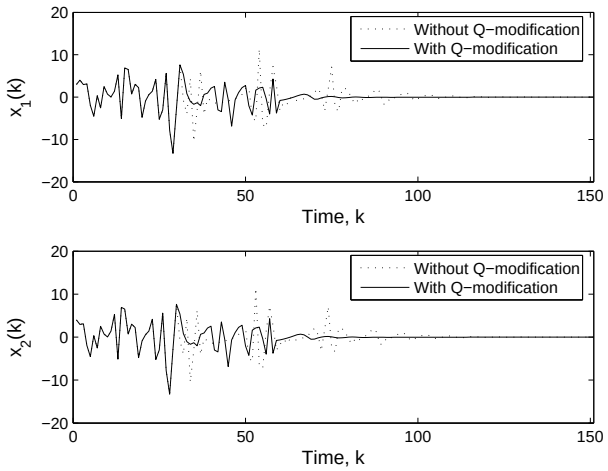

Figure 3.2: System states versus time with and without the Q-modification controller.

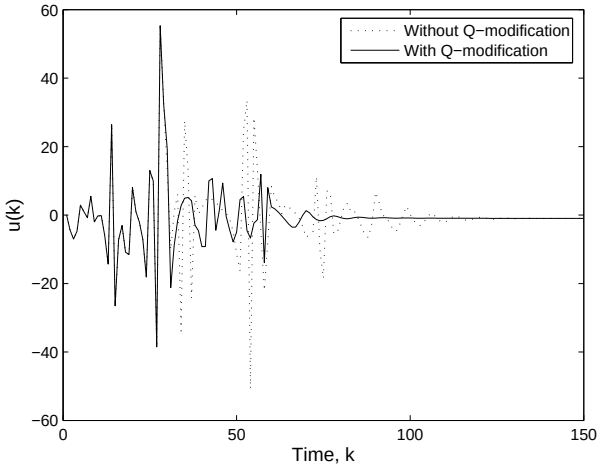

Figure 3.3: Control input versus time.

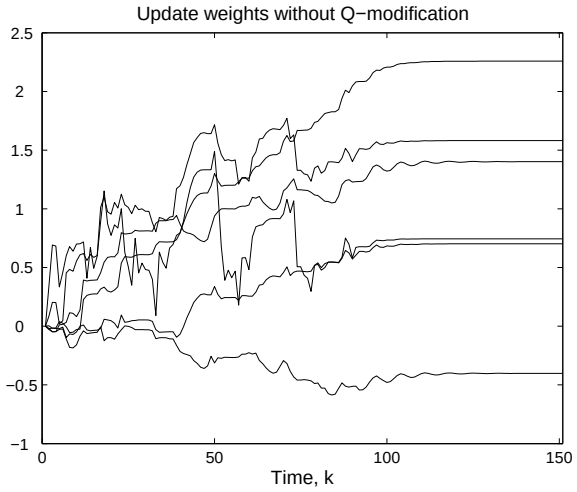

Figure 3.4: Update weights versus time without the Q-modification controller.

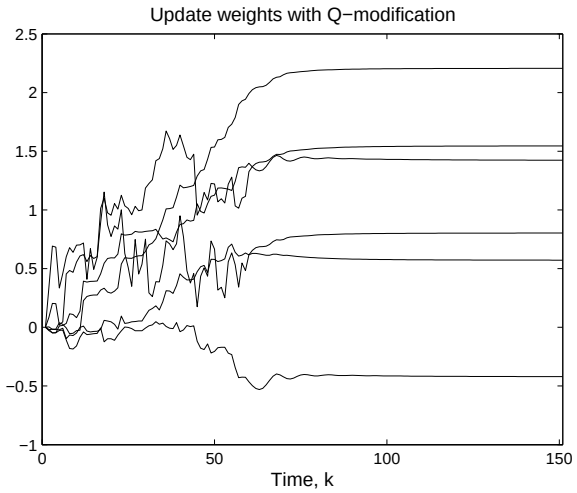

Figure 3.5: Update weights versus time with the Q-modification controller.

Chapter 4

Adaptive Disturbance Rejection Control for Compartmental Systems

4.1. Introduction

Nonnegative systems are essential in capturing the behavior of a wide range of dynamical systems involving dynamic states whose values are nonnegative [12,35,47]. A subclass of nonnegative dynamical systems are compartmental systems [3, 14, 44, 47, 69, 70, 113]. These systems are derived from mass and energy balance considerations and are comprised of homogeneous interconnected microscopic subsystems or compartments which exchange variable quantities of material via intercompartmental flow laws. Since biological and physiological systems have numerous input, state, and output properties related to conservation, dissipation, and transport of mass and energy, nonnegative and compartmental systems are remarkably effective in describing the phenomenological behavior of these dynamical systems. The range of applications of nonnegative and compartmental systems is not limited to biological and medical systems. Their usage includes demographic, epidemic [69], ecological [100], economic [13], telecommunications [36], transportation, power, and large-scale systems [124].

In a recent series of papers [52–54], a direct adaptive control framework for linear

and nonlinear nonnegative and compartmental systems was developed. The framework in [52–54] is Lyapunov-based and guarantees partial asymptotic set-point regulation, that is, asymptotic set point stability with respect to the closed-loop system states associated with the plant. In addition, the adaptive controllers in [52–54] guarantee that the physical system states remain in the nonnegative orthant of the state space. In this chapter, we extend the results of [53] to develop a direct adaptive control framework for adaptive stabilization and disturbance rejection for compartmental dynamical systems with exogenous system disturbances. The main challenge here is to construct nonlinear adaptive disturbance rejection controllers without requiring knowledge of the system dynamics or the system disturbances while guaranteeing that the physical system states remain in the nonnegative orthant of the state space.

While such an adaptive control framework can have wide applicability in areas such as economics, telecommunications, and power systems, its use in the specific field of anesthetic pharmacology is particularly noteworthy. Specifically, during stress (such as hemorrhage) in an acute care environment, such as the operating room, perfusion pressure falls and hypertonic saline solutions are typically intravenously administered to regulate hemodynamic effects and avoid hemorrhagic shock. This exogenous disturbance drives the system pharmacokinetics and pharmacodynamics and can be captured as a system disturbance. In addition, exogenous system disturbances can be used to capture unmodeled physiological and pharmacological system dynamics. Although the proposed framework develops adaptive controllers for general compartmental systems with exogenous disturbances, the specific focus of this chapter is on pharmacokinetic models with hemorrhage and hemodilution effects.

4.2. Mathematical Preliminaries

In this section, we introduce notation, several definitions, and some key results concerning linear nonnegative dynamical systems [12–14, 47] that are necessary for developing the main results of this and next two chapters. Specifically, for $x \in \mathbb{R}^n$ we write $x \geq\geq 0$ (resp., $x >> 0$) to indicate that every component of x is nonnegative (resp., positive). In this case, we say that x is *nonnegative* or *positive*, respectively. Likewise, $A \in \mathbb{R}^{n\times m}$ is *nonnegative*[2] or *positive* if every entry of A is nonnegative or positive, respectively, which is written as $A \geq\geq 0$ or $A >> 0$, respectively. Furthermore, let $\overline{\mathbb{R}}^n_+$ and $\mathbb{R}^n_+$ denote the nonnegative and positive orthants of $\mathbb{R}^n$, that is, if $x \in \mathbb{R}^n$, then $x \in \overline{\mathbb{R}}^n_+$ and $x \in \mathbb{R}^n_+$ are equivalent, respectively, to $x \geq\geq 0$ and $x >> 0$. Finally, $\mathbf{e} \in \mathbb{R}^n$ denotes the ones vector of order n, that is, $\mathbf{e} \triangleq [1, \ldots, 1]^{\mathrm{T}}$.

The following definition introduces the notion of a nonnegative (resp., positive) function.

Definition 4.1 . Let $T > 0$. A real function $u : [0, T] \to \mathbb{R}^m$ is a *nonnegative* (resp., *positive*) *function* if $u(t) \geq\geq 0$ (resp., $u(t) >> 0$) on the interval $[0, T]$.

The next definition introduces the notion of essentially nonnegative and compartmental matrices.

Definition 4.2 [14, 47]. Let $A \in \mathbb{R}^{n\times n}$. A is *essentially nonnegative* if $A_{(i,j)} \geq 0$, $i, j = 1, \ldots, n$, $i \neq j$. A is *compartmental* if A is essentially nonnegative and $A^{\mathrm{T}}\mathbf{e} \leq\leq 0$.

Next, consider the linear nonnegative dynamical system

$$\dot{x}(t) = Ax(t), \quad x(0) = x_0, \quad t \geq 0, \tag{4.1}$$

[2]In this dissertation it is important to distinguish between a square nonnegative (resp., positive) matrix and a nonnegative-definite (resp., positive-definite) matrix.

where $x(t) \in \mathbb{R}^n$, $t \geq 0$, and $A \in \mathbb{R}^{n\times n}$ is essentially nonnegative. The solution to (4.1) is standard and is given by $x(t) = e^{At}x(0)$, $t \geq 0$. The following lemma proven in [14] (see also [47]) shows that A is essentially nonnegative if and only if the state transition matrix e^{At} is nonnegative on $[0, \infty)$.

Proposition 4.1. Let $A \in \mathbb{R}^{n\times n}$. Then A is essentially nonnegative if and only if e^{At} is nonnegative for all $t \geq 0$. Hence, if A is essentially nonnegative and $x_0 \geq\geq 0$, then $x(t) \geq\geq 0$, $t \geq 0$, where $x(t)$, $t \geq 0$, denotes the solution to (4.1).

The following theorem gives necessary and sufficient conditions for asymptotic stability of a linear nonnegative dynamical system using a quadratic component decoupled Lyapunov function.

Theorem 4.1 [47]. Consider the linear dynamical system $\mathcal{G}$ given by (4.1) where $A \in \mathbb{R}^{n\times n}$ is essentially nonnegative. Then $\mathcal{G}$ is asymptotically stable if and only if there exist a positive diagonal matrix $P \in \mathbb{R}^{n\times n}$ and an $n \times n$ positive-definite matrix R such that

$$0 = A^{\mathrm{T}}P + PA + R. \tag{4.2}$$

Next, we note that every Hurwitz nonnegative matrix is equivalent, modulo a similarity transformation, to a compartmental matrix.

Proposition 4.2 [47]. Let $A \in \mathbb{R}^{n\times n}$ be Hurwitz. Then A is essentially nonnegative if and only if there exists an invertible diagonal matrix $S \in \mathbb{R}^{n\times n}$ such that SAS^{-1} is a compartmental matrix.

Finally, in this section we consider controlled dynamical systems of the form

$$\dot{x}(t) = Ax(t) + Bu(t), \quad x(0) = x_0, \quad t \geq 0, \tag{4.3}$$

where $x(t) \in \mathbb{R}^n$, $t \geq 0$, $u(t) \in \mathbb{R}^m$, $t \geq 0$, $A \in \mathbb{R}^{n \times n}$, and $B \in \mathbb{R}^{n \times m}$. The following definition and proposition are needed for the main results of the chapter.

Definition 4.3. The linear dynamical system given by (4.3) is *nonnegative* if, for every $x(0) \in \overline{\mathbb{R}}_+^n$ and $u(t) \geq\geq 0$, $t \geq 0$, the solution $x(t)$, $t \geq 0$, to (4.3) is nonnegative.

Proposition 4.3 [47]. The linear dynamical system given by (4.3) is nonnegative if and only if $A \in \mathbb{R}^{n \times n}$ is essentially nonnegative and $B \in \mathbb{R}^{n \times m}$ is nonnegative.

It follows from Proposition 4.3 that the weighted control input signal $Bu(t)$, $t \geq 0$, needs to be nonnegative to guarantee the nonnegativity of the state of (4.3). This is due to the fact that when the initial state of (4.3) belongs to the boundary of the nonnegative orthant, a negative input can destroy the nonnegativity of the state of (4.3). Since stabilization of nonnegative systems naturally deals with equilibrium points in the interior of the nonnegative orthant $\overline{\mathbb{R}}_+^n$, the following proposition provides necessary conditions for the existence of an interior equilibrium point $x_{\mathrm{e}} \in \mathbb{R}_+^n$ of (4.3) in terms of the stability properties of the system dynamics matrix A. For the next result recall that a matrix $M \in \mathbb{R}^{n \times n}$ is *semistable* if and only if $\lim_{t \to \infty} e^{Mt}$ exists [14, 15, 47].

Proposition 4.4 [53]. Consider the nonnegative dynamical system (4.3) and assume there exist $x_{\mathrm{e}} \in \mathbb{R}_+^n$ and $u_{\mathrm{e}} \in \overline{\mathbb{R}}_+^m$ such that

$$0 = Ax_{\mathrm{e}} + Bu_{\mathrm{e}}. \tag{4.4}$$

Then, A is semistable.

It follows from Proposition 4.4 that the existence of an equilibrium point $x_{\mathrm{e}} \in \mathbb{R}_+^n$ for (4.3) implies that the system matrix A is semistable. Hence, if (4.4) holds for

$x_{\rm e} \in \mathbb{R}^n_+$ and $u_{\rm e} \in \overline{\mathbb{R}}^m_+$, A is Hurwitz or $0 \in \spec(A)$, where $\spec(A)$ denotes the spectrum of A, is a semisimple eigenvalue of A and all other eigenvalues of A have negative real parts since $-A$ is an M-matrix [13]. In light of the above constraints, it was shown in [30] using Brockett's necessary condition for asymptotic stabilizability [17] that if $0 \in \spec(A)$, then there does *not* exist a *continuous* stabilizing *nonnegative* feedback for set-point regulation in $\mathbb{R}^n_+$ for a nonnegative system. However, that is not to say that asymptotic feedback regulation using *discontinuous* feedback is not possible.

Finally, we present a time-varying extension to Proposition 4.3 needed for the main theorems of this section. Specifically, we consider the linear time-varying dynamical system

$$\dot{x}(t) = A(t)x(t) + Bu(t), \quad x(0) = x_0, \quad t \geq 0, \tag{4.5}$$

where $A : [0, \infty) \to \mathbb{R}^{n\times n}$ is continuous. For the following result the definition of nonnegativity holds with (4.3) replaced by (4.5).

Proposition 4.5 . Consider the time-varying dynamical system (4.5) where $A : [0, \infty) \to \mathbb{R}^{n\times n}$ is continuous. If for every $t \in [0, \infty)$, $A : [0, \infty) \to \mathbb{R}^{n\times n}$ is essentially nonnegative, $B \in \mathbb{R}^{n\times m}$ is nonnegative, and $u(t)$ is nonnegative, then the solution $x(t)$, $t \geq 0$, to (4.5) is nonnegative.

Proof. The result is a direct consequence of the nonlinear analogue to Proposition 4.3 by representing the time-varying dynamical system (4.5) as an autonomous linear system by appending another state to represent time. See [53] for a similar proof. □

4.3. Compartmental Systems with Exogenous Disturbances

In this section, we develop an adaptive disturbance rejection control framework for asymptotic set point regulation of a disturbed linear compartmental system. Specifically, we consider uncertain dynamical systems $\mathcal{G}$ of the form

$$\dot{x}(t) = Ax(t) + Bu(t) + d(x(t), t), \quad x(0) = x_0, \quad t \geq 0, \tag{4.6}$$

where $x(t) \in \mathbb{R}^n$, $t \geq 0$, is the state vector, $x_0 \in \overline{\mathbb{R}}_+^n$, $u(t) \in \mathbb{R}^m$, $t \geq 0$, is the control input, $d(x(t), t) \in \mathbb{R}^n$, $t \geq 0$, is an *unknown* nonlinear disturbance signal, $A \in \mathbb{R}^{n \times n}$ is an *unknown* compartmental matrix, and $B \in \mathbb{R}^{n \times m}$ is an *unknown* matrix given by

$$B = \left[\begin{array}{c} B_u \\ 0_{(n-m) \times m} \end{array} \right], \ B_u = \mathrm{diag}[\, b_1, \ldots, b_m \,], \ b_i > 0, \ i = 1, 2, \ldots, m. \tag{4.7}$$

Here we assume that for all $i = 1, 2, \ldots, m$, b_i is *unknown*. The structure of B implies that the control inputs are injected directly into m separate compartments. For compartmental systems this assumption is not restrictive since control inputs correspond to control inflows to each individual compartment. The control input $u(\cdot)$ is restricted to the class of *admissible controls* consisting of measurable functions on $\mathbb{R}^m$, or $\overline{\mathbb{R}}_+^m$ if $u(t)$, $t \geq 0$, is constrained to be nonnegative.

In this chapter, we consider two cases for the disturbance signal $d : \mathbb{R}^n \times [0, \infty) \to \mathbb{R}^n$. Namely, in the first case, the disturbance signal is given by

$$d(x(t), t) = -B\Psi^* w(x(t), t), \tag{4.8}$$

where Ψ^* is an *unknown* constant diagonal disturbance weighting matrix given by

$$\Psi^* = \mathrm{diag}[\, \psi_1^*, \ldots, \psi_m^* \,], \quad \psi_i^* > 0, \quad i = 1, 2, \ldots, m, \tag{4.9}$$

and $w(x, t) = [\, w_1(x, t), \ldots, w_m(x, t) \,]^{\mathrm{T}}$ is a *known* disturbance signal satisfying sufficient regularity conditions so that (4.6) has a unique solution forward in time. Fur-

thermore, we assume that for the uncontrolled (i.e., $u(t) \equiv 0$) system (4.6) the disturbance signal $w(x,t)$ is such that for any time $t \in [0, \infty)$ such that $x_i(t) = 0$, $w_i(x(t),t) = 0$. In this case, $x(t) \in \overline{\mathbb{R}}^n_+$ for all $t \geq 0$ and $u(t) \equiv 0$.

In the second case, the disturbance signal $d : \mathbb{R}^n \times [0, \infty) \to \mathbb{R}^n$ is given by

$$d(x(t),t) = J(x(t))w(t), \tag{4.10}$$

where $J : \overline{\mathbb{R}}^n_+ \to \mathbb{R}^{n\times d}$ is an *unknown* bounded continuous function and $w : [0,\infty) \to \mathbb{R}^d$ is an *unknown* continuous function such that $w(\cdot) \in \mathcal{L}_2$. Note that since $J(\cdot)$ is bounded, there exists $\alpha > 0$ such that $\|J(x)\| \leq \alpha$, $x \in \overline{\mathbb{R}}^n_+$, where $\|\cdot\|$ is a matrix norm on $\mathbb{R}^{n\times d}$. Furthermore, since $w(\cdot)$ is continuous on $[0,\infty)$ and $w(\cdot) \in \mathcal{L}_2$, there exists $\beta > 0$ such that $\|w(t)\| \leq \beta$, $t \geq 0$, where $\|\cdot\|$ is a vector norm on $\mathbb{R}^d$. In addition, we assume that $J(x)w(t) \geq\geq 0$ for all $x \in \partial\overline{\mathbb{R}}^n_+$ and $t \geq 0$, where $\partial\overline{\mathbb{R}}^n_+$ denotes the boundary of the nonnegative orthant. This assumption ensures that the uncontrolled (i.e., $u(t) \equiv 0$) system (4.6) remains nonnegative for all $x(0) \in \overline{\mathbb{R}}^n_+$.

Given a desired set point $x_{\mathrm{e}} \in \mathbb{R}^n_+ \backslash \{x_0\}$ our goal is to design a measurable control law $u : [0,\infty) \to \mathbb{R}^m$ (or $u : [0,\infty) \to \overline{\mathbb{R}}^m_+$) guaranteeing partial asymptotic set point stability of the closed-loop system; that is, asymptotic set point stability with respect to part of the closed loop-system state. Since in many applications of nonnegative systems and in particular, compartmental systems, it is often necessary to regulate a subset of the non-negative state variables which usually include a central compartment, here we require that $\lim_{t\to\infty} x_i(t) = x_{\mathrm{d}_i} \geq 0$ for $i = 1, 2, \ldots, m \leq n$, where x_{d_i} is the desired set point for the ith state $x_i(t)$. In addition, we require that the remainder of the state associated with the adaptive controller gains is Lyapunov stable. Finally, we require that $x(t) \in \overline{\mathbb{R}}^n_+$ for all $t \geq 0$.

In certain parts of this presentation we will use the following assumption regarding the existence of an equilibrium point of the undisturbed (i.e., $d(x(t),t) \equiv 0$) dynamical

system (4.6).

Assumption 4.1. For the undisturbed (i.e., $d(x(t), t) \equiv 0$) dynamical system (4.6) and a given desired set point $x_{\mathrm{d}} \in \mathbb{R}^m_+$, there exist nonnegative vectors $x_{\mathrm{u}} \in \mathbb{R}^{n-m}_+$ and $u_{\mathrm{e}} \in \overline{\mathbb{R}}^m_+$ such that (4.4) holds with $x_{\mathrm{e}} \triangleq [\, x_{\mathrm{d}},\ x_{\mathrm{u}} \,]^{\mathrm{T}}$.

It follows from Proposition 4.4 that Assumption 4.1 implies that A is semistable.

4.4. Adaptive Control for Linear Compartmental Uncertain Systems with Exogenous Disturbances

In this section, we consider the problem of characterizing adaptive disturbance rejection feedback control laws for linear compartmental uncertain dynamical systems of the form given by (4.6) with the disturbance $d(x(t), t)$, $t \geq 0$, given by (4.8). Specifically, we consider the controlled uncertain dynamical system given by

$$\dot{x}(t) = Ax(t) + B[u(t) - \Psi^* w(x(t), t)], \quad x(0) = x_0, \quad t \geq 0. \tag{4.11}$$

First, we consider the case where there is no restriction on the sign of the control input $u(t)$, $t \geq 0$.

Theorem 4.2. Consider the linear uncertain dynamical system given by (4.11) where A is essentially nonnegative, B is nonnegative and given by (4.7), and Ψ^* is given by (4.9). Suppose Assumption 4.1 holds and assume that there exists a diagonal matrix $K_{\mathrm{g}} = \mathrm{diag}[\, k_{\mathrm{g}_1},\ \ldots,\ k_{\mathrm{g}_m}]$ such that $A_{\mathrm{s}} \triangleq A + B\tilde{K}_{\mathrm{g}}$ is Hurwitz, where $\tilde{K}_{\mathrm{g}} \triangleq \big[K_{\mathrm{g}},\ 0_{m\times(n-m)}\big]$. Furthermore, let q_i, $\hat{q}_i$, and γ_i, $i = 1, \ldots, m$, be positive constants. Then the adaptive feedback control law

$$u(t) = K(t)(\hat{x}(t) - x_{\mathrm{d}}) + \phi(t) + \Psi(t) w(x(t), t), \quad t \geq 0, \tag{4.12}$$

where $K(t) \triangleq \mathrm{diag}[\,k_1(t),\,\ldots,\,k_m(t)]$, $\hat{x}(t) \triangleq [\,x_1(t),\,\ldots,\,x_m(t)]$, $\phi(t) \in \mathbb{R}^m$, and $\Psi(t) \triangleq \mathrm{diag}[\,\psi_1(t),\,\ldots,\,\psi_m(t)]$, $t \geq 0$, or, equivalently,

$$u_i(t) = k_i(t)(\hat{x}_i(t) - x_{\mathrm{d}_i}) + \phi_i(t) + \psi_i(t)w_i(x(t),t), \quad t \geq 0, \quad i = 1,\,\ldots,\,m, \tag{4.13}$$

with update laws

$$\dot{k}_i(t) = -q_i(x_i(t) - x_{\mathrm{e}_i})^2, \quad k_i(0) \leq 0, \quad t \geq 0, \quad i = 1,\,\ldots,\,m, \tag{4.14}$$

$$\dot{\phi}_i(t) = \begin{cases} 0, & \text{if } \phi_i(t) = 0 \text{ and } x_i(t) - x_{\mathrm{d}_i} \geq 0, \\ -\hat{q}_i(x_i(t) - x_{\mathrm{d}_i}), & \text{otherwise,} \end{cases} \tag{4.15}$$
$$\phi_i(0) \geq 0, \quad t \geq 0, \quad i = 1,\,\ldots,\,m,$$

$$\dot{\psi}_i(t) = \begin{cases} 0, & \text{if } \psi_i(t) = 0 \text{ and } (x_i(t) - x_{\mathrm{d}_i})w_i(x(t),t) \geq 0, \\ -\gamma_i(x_i(t) - x_{\mathrm{d}_i})w_i(x(t),t), & \text{otherwise,} \end{cases} \tag{4.16}$$
$$\psi_i(0) = 0, \quad t \geq 0, \quad i = 1,\,\ldots,\,m,$$

guarantees that the solution $(x(t), K(t), \phi(t), \Psi(t)) \equiv (x_{\mathrm{e}}, K_{\mathrm{g}}, u_{\mathrm{e}}, \Psi^*)$ of the closed-loop system given by (4.11)–(4.16) is Lyapunov stable and $x_i(t) \to x_{\mathrm{d}_i}$, $i = 1,\,\ldots,\,m$, as $t \to \infty$ for all $x_0 \in \overline{\mathbb{R}}^n_+$. Furthermore, $x(t) \geq\geq 0$ for all $x_0 \in \overline{\mathbb{R}}^n_+$ and $t \geq 0$.

Proof. With $u(t)$, $t \geq 0$, given by (4.12), it follows from (4.4) that

$$\dot{x}(t) = A_{\mathrm{s}}(x(t) - x_{\mathrm{e}}) + B(K(t) - K_{\mathrm{g}})(x(t) - x_{\mathrm{e}}) + B(\phi(t) - u_{\mathrm{e}}) + B(\Psi(t) - \Psi^*)w(t),$$
$$x(0) = x_0, \quad t \geq 0. \tag{4.17}$$

Furthermore, since A_{s} is essentially nonnegative and Hurwitz it follows from Theorem 4.1 that there exist a positive diagonal matrix $P \triangleq \mathrm{diag}[\,p_1,\,\ldots,\,p_n\,]$ and a positive-definite matrix $R \in \mathbb{R}^{n\times n}$ such that

$$0 = A_{\mathrm{s}}^{\mathrm{T}}P + PA_{\mathrm{s}} + R. \tag{4.18}$$

To show Lyapunov stability of the closed-loop system (4.11)–(4.16) consider the Lyapunov function candidate

$$V(x,K,\phi,\Psi) = (x-x_{\rm e})^{\rm T}P(x-x_{\rm e}) + {\rm tr}(K-K_{\rm g})^{\rm T}Q^{-1}(K-K_{\rm g}) \\ +(\phi-u_{\rm e})^{\rm T}\hat{Q}^{-1}(\phi-u_{\rm e}) + {\rm tr}(\Psi-\Psi^*)^{\rm T}\Gamma^{-1}(\Psi-\Psi^*), \quad (4.19)$$

where

$$Q \triangleq {\rm diag}\left[\frac{q_1}{p_1b_1},\ldots,\frac{q_m}{p_mb_m}\right], \ \hat{Q} \triangleq {\rm diag}\left[\frac{\hat{q}_1}{p_1b_1},\ldots,\frac{\hat{q}_m}{p_mb_m}\right], \\ \Gamma \triangleq {\rm diag}\left[\frac{\gamma_1}{p_1b_1},\ldots,\frac{\gamma_m}{p_mb_m}\right]. \quad (4.20)$$

Note that $V(x_{\rm e},K_{\rm g},u_{\rm e},\Psi^*) = 0$ and, since P, Q, $\hat{Q}$, and Γ are positive definite, $V(x_{\rm e},K_{\rm g},u_{\rm e},\Psi^*) > 0$ for all $(x,K,\phi,\Psi) \neq (x_{\rm e},K_{\rm e},u_{\rm e},\Psi^*)$. Furthermore, $V(x,K,\phi,\Psi)$ is radially unbounded. Now, letting $x(t)$, $t \geq 0$, denote the solution to (4.17) and using (4.14)–(4.16) it follows that the Lyapunov derivative along the trajectories of the closed-loop system (4.11)–(4.16) is given by

$$\begin{aligned}\dot{V}(x(t),K(t),\phi(t),\Psi(t)) = {} & 2(x(t)-x_{\rm e})^{\rm T}P[A_{\rm s}(x(t)-x_{\rm e}) + B(K(t)-K_{\rm g})(x(t)-x_{\rm e}) \\ & +B(\phi(t)-u_{\rm e}) + B(\Psi(t)-\Psi^*)w(t)] \\ & +2{\rm tr}(K(t)-K_{\rm g})^{\rm T}Q^{-1}\dot{K}(t) + 2(\phi(t)-u_{\rm e})^{\rm T}\hat{Q}^{-1}\dot{\phi}(t) \\ & +2{\rm tr}(\Psi(t)-\Psi^*)^{\rm T}\Gamma^{-1}\dot{\Psi}(t) \\ = {} & -(x(t)-x_{\rm e})^{\rm T}R(x(t)-x_{\rm e}) \\ & +2\sum_{i=1}^{m} p_ib_i(k_i(t)-k_{{\rm g}_i})\left[(x_i(t)-x_{{\rm d}_i})^2 + \frac{1}{q_i}\dot{k}_i(t)\right] \\ & +2\sum_{i=1}^{m} p_ib_i(\phi_i(t)-u_{{\rm e}_i})\left[(x_i(t)-x_{{\rm d}_i}) + \frac{1}{\hat{q}_i}\dot{\phi}_i(t)\right] \\ & +2\sum_{i=1}^{m} p_ib_i(\psi_i(t)-\psi_i^*)\left[(x_i(t)-x_{{\rm d}_i})w_i(x,t) + \frac{1}{\hat{\gamma}_i}\dot{\psi}_i(t)\right].\end{aligned}$$

Next, it follows from (4.14) that, for each $i \in \{1,\ldots,m\}$,

$$p_ib_i(k_i(t)-k_{{\rm g}_i})\left[(x_i(t)-x_{{\rm e}_i})^2 + \frac{1}{q_i}\dot{k}_i(t)\right] = 0, \quad t \geq 0.$$

Using (4.15) it follows that if $\phi_i(t) = 0$ and $x_i(t) - x_{\mathrm{d}_i} \geq 0$, $t \geq 0$, then

$$p_i b_i(\phi_i(t) - u_{\mathrm{e}_i}) \left[(x_i(t) - x_{\mathrm{d}_i}) + \frac{1}{\hat{q}_i}\dot{\phi}(t)\right] = -p_i b_i u_{\mathrm{e}_i}(x_i(t) - x_{\mathrm{d}_i}) \leq 0, \quad t \geq 0,$$

and if $\phi_i(t) \neq 0$ or $x_i(t) - x_{\mathrm{d}_i} < 0$, $t \geq 0$, then

$$p_i b_i(\phi_i(t) - u_{\mathrm{e}_i}) \left[(x_i(t) - x_{\mathrm{d}_i}) + \frac{1}{\hat{q}_i}\dot{\phi}(t)\right] = 0.$$

From (4.16) it follows that if $\psi_i(t) = 0$ and $(x_i(t) - x_{\mathrm{d}_i})w_i(x(t), t) \geq 0$, $t \geq 0$, then

$$p_i b_i(\psi_i(t) - \psi_i^*) \left[(x_i(t) - x_{\mathrm{d}_i})w_i(x, t) + \frac{1}{\hat{\gamma}_i}\dot{\psi}_i(t)\right] = -p_i b_i \psi_i^*(x_i(t) - x_{\mathrm{d}_i})w_i(x, t) \leq 0, \quad t \geq 0,$$

and if $\psi_i(t) \neq 0$, or $(x_i(t) - x_{\mathrm{d}_i})w_i(x(t), t) < 0$, $t \geq 0$, then

$$p_i b_i(\psi_i(t) - \psi_i^*) \left[(x_i(t) - x_{\mathrm{d}_i})w_i(x, t) + \frac{1}{\hat{\gamma}_i}\dot{\psi}_i(t)\right] = 0, \quad t \geq 0.$$

Hence,

$$\dot{V}(x(t), K(t), \phi(t), \Psi(t)) \leq -(x(t) - x_{\mathrm{e}})^{\mathrm{T}} R(x(t) - x_{\mathrm{e}}) \leq 0, \quad t \geq 0,$$

which proves that the solution $(x(t), K(t), \phi(t), \Psi(t)) \equiv (x_{\mathrm{e}}, K_{\mathrm{g}}, u_{\mathrm{e}}, \Psi^*)$ of the closed-loop system given by (4.11)–(4.16) is Lyapunov stable. Moreover, since R is positive definite, it follows from Theorem 2.2 of [23] that $x(t) \to x_{\mathrm{e}}$ as $t \to \infty$.

To show that $x(t) \geq\geq 0$ for all $x_0 \in \overline{\mathbb{R}}_+^n$ and $t \geq 0$ note that the closed-loop system (4.11)–(4.16) is given by

$$\begin{aligned}\dot{x}(t) = {} & (A + B\left[K(t),\, 0_{m\times(n-m)}\right])x(t) - BK(t)x_{\mathrm{d}} + B\phi(t) + B\Psi(t)w(x(t), t) \\ & -B\Psi^* w(x(t), t) \\ = {} & \tilde{A}(t)x(t) + v(t) + h(t) + g(t) + d(x(t), t), \quad x(0) = x_0, \quad t \geq 0, \end{aligned} \tag{4.21}$$

where $\tilde{A}(t) \triangleq A + B\left[K(t),\, 0_{m\times(n-m)}\right]$, $v(t) \triangleq -BK(t)x_{\mathrm{d}}$, $h(t) \triangleq B\phi(t)$, and $g(t) \triangleq B\Psi(t)w(x(t), t)$. Now, since A is essentially nonnegative, B is nonnegative

and diagonal, $K(t)$ is diagonal, and, by (4.14), $k_i(t) \leq 0$, $t \geq 0$, $i = 1, \ldots, m$, it follows that $\tilde{A}(t)$ is essentially nonnegative pointwise-in-time and $v(t) \geq\geq 0$, $t \geq 0$. Next, it follows from (4.15) and (4.16) that $\phi_i(t) \geq 0$, $t \geq 0$, $i = 1, \ldots, m$, and hence, $h(t) \geq\geq 0$, $t \geq 0$. Now, if $g(t) \equiv 0$ and $d(x(t), t) \equiv 0$, then it follows from Proposition 4.5 that $x(t) \geq\geq 0$, $t \geq 0$, for all $x_0 \in \overline{\mathbb{R}}_+^m$.

Finally, we show that the signals $g(\cdot)$ and $d(x(\cdot), \cdot)$ are such that (4.21) remains nonnegative. To see this, assume that for a given time $\hat{t} \in [0, \infty)$, $x(\hat{t}) \in \mathbb{R}_+^n$. In this case, it follows from continuity of solutions with respect to the system initial conditions that, over a sufficiently small interval of time, the nonnegativity of the state of (4.21) is guaranteed irrespective of the sign of the components of $g(\cdot)$ and $d(x(\cdot), \cdot)$. Alternatively, suppose that $x(\hat{t}) \in \partial\overline{\mathbb{R}}_+^n$. In this case, there exists $i \in \{1, \ldots, m\}$ such that $x_i(\hat{t}) = 0$, and hence, by assumption (see the discussion in Section 4.3), $w_i(x(\hat{t}), \hat{t}) = 0$. Hence, $d_i(x(\hat{t}), \hat{t}) = 0$ and $g_i(\hat{t}) = b_i\psi_i(\hat{t})w_i(x(\hat{t}), \hat{t}) = 0$. Thus, the signals $g(\cdot)$ and $d(x(\cdot), \cdot)$ do not destroy the nonnegativity of (4.21). This completes the proof. □

Remark 4.1. In the case where (4.11) is such that $w(x(t), t) \equiv 0$, the controller (4.13) with update laws (4.14)–(4.16) collapses to

$$u_i(t) = k_i(t)(x_i(t) - x_{\mathrm{d}_i}) + \phi_i(t), \quad t \geq 0, \quad i = 1, \ldots, m, \tag{4.22}$$

with update laws (4.14) and (4.15). This is precisely the result given in [53], where an adaptive control framework for nonnegative dynamical systems is developed for the undisturbed case (i.e., $w(x(t), t) \equiv 0$).

Remark 4.2. It is important to note that the adaptive control framework addressed in this section requires that the bounded disturbance $w(x(t), t)$, $t \geq 0$, can be accurately measured even though the disturbance signal $d(x(t), t)$, $t \geq 0$, is an unknown bounded disturbance since $B\Psi^*$ is unknown. Such a disturbance model can,

for example, address sinusoidal disturbances with unknown amplitude and phase. In the next section, we consider the more general problem of $\mathcal{L}_2$ disturbances.

Remark 4.3. Since the dynamical system considered in this section is minimum phase, it is possible, in principle, to stabilize the system by simply employing the controller (4.13) with $\phi_i(t) \equiv 0$ and $\psi_i(t) \equiv 0$, and with a sufficiently high gain $k_i(t)$, $t \geq 0$, $i = 1, \ldots, m$. However, this is a very unsafe strategy when the disturbance $w(x(t), t)$, $t \geq 0$, is not accurately known and unmodeled system dynamics are present. In this case, unsafe high gain levels can excite unmodeled dynamics and drive the system to instability.

Next, we consider the case where the control input is constrained to be nonnegative. In this case, we assume that $w(x(t), t) \geq\geq 0$ for all $x(t) \in \mathbb{R}^n_+$ and $t \geq 0$, and if $x_i(t) = 0$ for some $t \in [0, \infty)$, then $w_i(x(t), t) = 0$.

Theorem 4.3. Consider the linear uncertain dynamical system given by (4.11) where A is Hurwitz and compartmental, B is nonnegative and given by (4.7), and Ψ^* is given by (4.9). Suppose Assumption 4.1 holds. Furthermore, let $\hat{q}_i$ and γ_i, $i = 1, \ldots, m$, be positive constants. Then the adaptive feedback control law

$$u(t) = \phi(t) + \Psi(t)w(x(t), t), \quad t \geq 0, \tag{4.23}$$

where $\phi(t) = [\, \phi_1(t), \ldots, \phi_m(t)]$ and $\Psi(t) = \mathrm{diag}[\, \psi_1(t), \ldots, \psi_m(t)]$, $t \geq 0$, or, equivalently,

$$u_i(t) = \phi_i(t) + \psi_i(t)w_i(x(t), t), \quad t \geq 0, \quad i = 1, \ldots, m, \tag{4.24}$$

with update laws $\phi_i(t)$, $t \geq 0$, and $\psi_i(t)$ given by (4.15) and (4.16), respectively, guarantees that the solution $(x(t), \phi(t), \Psi(t)) \equiv (x_{\mathrm{e}}, u_{\mathrm{e}}, \Psi^*)$ of the closed-loop system given by (4.11), (4.23), and (4.24) is Lyapunov stable and $x_i(t) \to x_{\mathrm{d}_i}$, $i = 1, \ldots, m$,

as $t \to \infty$ for all $x_0 \in \overline{\mathbb{R}}^n_+$. Furthermore, $u(t) \geq\geq 0$, $t \geq 0$, and $x(t) \geq\geq 0$ for all $x_0 \in \overline{\mathbb{R}}^n_+$ and $t \geq 0$.

Proof. The proof is analogous to the proof of the Theorem 4.2 with $K(t) \equiv 0$, and, hence, is omitted. □

Finally, we consider the case where the control input is constrained to be nonnegative and the disturbance signal $d(x(t), t)$ is sign indefinite over a finite-time interval, and nonpositive otherwise.

Theorem 4.4. Consider the linear uncertain dynamical system given by (4.11) where A is Hurwitz and compartmental, B is nonnegative and given by (4.7), and Ψ^* is given by (4.9). Suppose Assumption 4.1 holds and there exists a finite-time $T > 0$ such that $w(x(t), t) \geq\geq 0$ for all $x(t) \in \mathbb{R}^n_+$ and $t \geq T$, and if $x_i(t) = 0$ for some $t \in [0, \infty)$, then $w_i(x(t), t) = 0$. Furthermore, let q_i, $\hat{q}_i$ and γ_i, $i = 1, \ldots, m$, be positive constants. Then the adaptive feedback control law

$$u_i(t) = \max\{0, \hat{u}_i(t)\}, \quad t \geq 0, \quad i = 1, \ldots, m, \tag{4.25}$$

where

$$\hat{u}_i(t) = k_i(t)(x_i(t) - x_{\mathrm{e}_i}) + \phi_i(t) + \psi_i(t) w_i(x(t), t), \quad t \geq 0, \quad i = 1, \ldots, m, \tag{4.26}$$

with update laws $k_i(t)$, $\phi_i(t)$, and $\psi_i(t)$ given by

$$\dot{k}_i(t) = \begin{cases} 0, & \text{if } \hat{u}_i < 0, \\ -q_i(x_i(t) - x_{\mathrm{d}_i})^2, & \text{otherwise,} \end{cases} \tag{4.27}$$

$$k_i(0) \leq 0, \quad t \geq 0, \quad i = 1, \ldots, m,$$

$$\dot{\phi}_i(t) = \begin{cases} 0, & \text{if } \phi_i(t) = 0 \text{ and } x_i(t) - x_{\mathrm{d}_i} \geq 0, \text{ or if } \hat{u}_i(t) < 0 \\ -\hat{q}_i(x_i(t) - x_{\mathrm{d}_i}), & \text{otherwise,} \end{cases} \tag{4.28}$$

$$\phi_i(0) \geq 0, \quad t \geq 0, \quad i = 1, \ldots, m,$$

$$\dot{\psi}_i(t) = \begin{cases} 0, & \text{if } \psi_i(t) = 0 \text{ and } (x_i(t) - x_{\mathrm{d}_i}) w_i(x(t), t) \geq 0, \text{ or if } \hat{u}_i(t) < 0 \\ -\gamma_i (x_i(t) - x_{\mathrm{d}_i}) w_i(x(t), t), & \text{otherwise,} \end{cases}$$

$$\psi_i(0) = 0, \quad t \geq 0, \quad i = 1, \ldots, m, \tag{4.29}$$

guarantees that the solution $(x(t), K(t), \phi(t), \Psi(t)) \equiv (x_{\mathrm{e}}, K_{\mathrm{g}}, u_{\mathrm{e}}, \Psi^*)$, where $K_{\mathrm{g}} = \mathrm{diag}[\, k_{\mathrm{g}_1}, \quad \ldots, k_{\mathrm{g}_m}]$, $k_{\mathrm{g}_i} \leq 0$, $i = 1, \ldots, m$, $\phi(t) \triangleq [\, \phi_1(t), \ldots, \phi_m(t)]^{\mathrm{T}}$, and $\Psi(t) \triangleq \mathrm{diag}[\, \psi_1(t), \ldots, \psi_m(t)]$, of the closed-loop system given by (4.11), (4.25)–(4.29) is Lyapunov stable and $x_i(t) \to x_{\mathrm{d}_i}$, $i = 1, \ldots, m$, as $t \to \infty$ for all $x_0 \in \overline{\mathbb{R}}^n_+$. Furthermore, $u(t) \geq\geq 0$, $t \geq 0$, and $x(t) \geq\geq 0$ for all $x_0 \in \overline{\mathbb{R}}^n_+$ and $t \geq 0$.

Proof. First, note that the update laws (4.27)–(4.29) guarantee that for each $i \in \{1, \ldots, m\}$ and for all $t \geq 0$ the adaptive gain $k_i(t)$ remains nonpositive, and adaptive gains $\phi_i(t)$ and $\psi_i(t)$ remain nonnegative. Next, define $K_u \triangleq \mathrm{diag}[\, k_{u_1}, \ldots, k_{u_m}]$, $\phi_u \triangleq [\, \phi_{u_1}, \ldots, \phi_{u_m}]^{\mathrm{T}}$, and $\Psi_u \triangleq \mathrm{diag}[\, \psi_{u_1}, \ldots, \psi_{u_m}]$, where

$$k_{u_i}(t) = \begin{cases} 0, & \text{if } \hat{u}_i(t) < 0 \\ k_i(t), & \text{otherwise,} \end{cases} \qquad i = 1, \ldots, m, \tag{4.30}$$

$$\phi_{u_i}(t) = \begin{cases} 0, & \text{if } \hat{u}_i(t) < 0 \\ \phi_i(t), & \text{otherwise,} \end{cases} \qquad i = 1, \ldots, m, \tag{4.31}$$

$$\psi_{u_i}(t) = \begin{cases} 0, & \text{if } \hat{u}_i(t) < 0 \\ \psi_i(t), & \text{otherwise.} \end{cases} \qquad i = 1, \ldots, m, \tag{4.32}$$

Now, note that with $u(t)$, $t \geq 0$, given by (4.25), it follows from (4.11) that

$$\dot{x}(t) = A(x(t) - x_{\mathrm{e}}) + BK_u(t)(\hat{x}(t) - x_{\mathrm{d}}) + B(\phi_u(t) - u_{\mathrm{e}}) + B(\Psi_u(t) - \Psi^*) w(x(t), t),$$

$$x(0) = x_0, \quad t \geq 0. \tag{4.33}$$

Furthermore, since A is essentially nonnegative and Hurwitz it follows from Theorem 4.1 that there exist a positive diagonal matrix $P \triangleq \mathrm{diag}[\, p_1, \ldots, p_n\,]$ and a positive-definite matrix $R \in \mathbb{R}^{n \times n}$ such that (4.2) holds.

To show Lyapunov stability of the closed-loop system (4.11), (4.25)–(4.29) consider the Lyapunov function candidate (4.19). Now, letting $x(t)$, $t \geq 0$, denote the solution to (4.33) and using (4.27)–(4.29) it follows that the Lyapunov derivative along the trajectories of the closed-loop system (4.11), (4.25)–(4.29) is given by

$$\begin{aligned}
&\dot{V}(x(t), K(t), \phi(t), \Psi(t)) \\
&\quad = 2(x(t) - x_{\mathrm{e}})^{\mathrm{T}} P[A(x(t) - x_{\mathrm{e}}) + B(K_u(t) - K_{\mathrm{g}})(x(t) - x_{\mathrm{e}}) \\
&\qquad + B(\phi_u(t) - u_{\mathrm{e}}) + B(\Psi_u(t) - \Psi^*)w(t)] \\
&\qquad + 2\mathrm{tr}(K(t) - K_{\mathrm{g}})^{\mathrm{T}} Q^{-1} \dot{K}(t) + 2(\phi(t) - u_{\mathrm{e}})^{\mathrm{T}} \hat{Q}^{-1} \dot{\phi}(t) \\
&\qquad + 2\mathrm{tr}(\Psi(t) - \Psi^*)^{\mathrm{T}} \Gamma^{-1} \dot{\Psi}(t) \\
&\quad = -(x(t) - x_{\mathrm{e}})^{\mathrm{T}} R(x(t) - x_{\mathrm{e}}) \\
&\qquad + 2 \sum_{i=1}^{m} p_i b_i \left[k_{u_i}(t)(x_i(t) - x_{\mathrm{d}_i})^2 + \frac{1}{q_i}(k_i(t) - k_{\mathrm{g}_i}) \dot{k}_i(t) \right] \\
&\qquad + 2 \sum_{i=1}^{m} p_i b_i \left[(\phi_{u_i}(t) - u_{\mathrm{e}_i})(x_i(t) - x_{\mathrm{d}_i}) + \frac{1}{\hat{q}_i}(\phi_i(t) - u_{\mathrm{e}_i}) \dot{\phi}_i(t) \right] \\
&\qquad + 2 \sum_{i=1}^{m} p_i b_i \Big[(\psi_{u_i}(t) - \psi_i^*)(x_i(t) - x_{\mathrm{d}_i}) w_i(x, t) \\
&\qquad + \frac{1}{\hat{\gamma}_i}(\psi_i(t) - \psi_i^*) \dot{\psi}_i(t) \Big]. \qquad (4.34)
\end{aligned}$$

First, consider the case where $w(x(t), t) >> 0$, $t \geq 0$. For each $i \in \{1, \ldots, m\}$ the last three terms in (4.34) give:

(i) If $\hat{u}_i(t) < 0$, $t \geq 0$, then $k_{u_i}(t) = 0$, $\phi_{u_i}(t) = 0$, and $\psi_{u_i}(t) = 0$. Furthermore, since $k_i(t) \leq 0$, $\phi_i(t) \geq 0$, and $\psi_i(t) \geq 0$, for all $t \geq 0$, it follows from (4.26) that if $w(x(t), t) >> 0$, $t \geq 0$, then $\hat{u}_i(t) < 0$, $t \geq 0$, only if $x_i(t) > x_{\mathrm{d}_i}$. Hence, it follows from (4.27)–(4.32) that if $w(x(t), t) >> 0$, $t \geq 0$, then

$$p_i b_i \left[k_{u_i}(t)(x_i(t) - x_{\mathrm{d}_i})^2 + \frac{1}{q_i}(k_i(t) - k_{\mathrm{g}_i}) \dot{k}_i(t) \right] = 0,$$

$$p_i b_i \left[(\phi_{u_i}(t) - u_{\mathrm{e}_i})(x_i(t) - x_{\mathrm{d}_i}) + \frac{1}{\hat{q}_i}(\phi_i(t) - u_{\mathrm{e}_i}) \dot{\phi}_i(t) \right]$$

$$= -p_i b_i u_{\mathrm{e}_i}(x_i(t) - x_{\mathrm{d}_i})$$
$$\leq 0, \tag{4.35}$$

$$p_i b_i \Big[(\psi_{u_i}(t) - \psi_i^*)(x_i(t) - x_{\mathrm{d}_i})w_i(x,t) + \frac{1}{\hat{\gamma}_i}(\psi_i(t) - \psi_i^*)\dot{\psi}_i(t)\Big]$$
$$= -p_i b_i \psi_i^*(x_i(t) - x_{\mathrm{d}_i})w_i(x,t)$$
$$\leq 0. \tag{4.36}$$

(*ii*) Otherwise, if $\hat{u}_i(t) \geq 0$, $t \geq 0$, then $k_{u_i}(t) = k_i(t)$, $\phi_{u_i}(t) = \phi_i(t)$, and $\psi_{u_i}(t) = \psi_i(t)$, and hence,

$$p_i b_i \left[k_{u_i}(t)(x_i(t) - x_{\mathrm{d}_i})^2 + \frac{1}{q_i}(k_i(t) - k_{\mathrm{g}_i})\dot{k}_i(t)\right] = k_{\mathrm{g}_i}(x_i(t) - x_{\mathrm{d}_i})^2 \leq 0, \tag{4.37}$$

$$p_i b_i \left[(\phi_{u_i}(t) - u_{\mathrm{e}_i})(x_i(t) - x_{\mathrm{d}_i}) + \frac{1}{\hat{q}_i}(\phi_i(t) - u_{\mathrm{e}_i})\dot{\phi}_i(t)\right]$$
$$= \begin{cases} -p_i b_i u_{\mathrm{e}_i}(x_i(t) - x_{\mathrm{d}_i}) \leq 0, & \text{if } \phi_i(t) = 0 \text{ and } x_i(t) - x_{\mathrm{d}_i} \geq 0, \\ 0, \text{ otherwise,} \end{cases} \tag{4.38}$$

$$p_i b_i \Big[(\psi_{u_i}(t) - \psi_i^*)(x_i(t) - x_{\mathrm{d}_i})w_i(x,t) + \frac{1}{\hat{\gamma}_i}(\psi_i(t) - \psi_i^*)\dot{\psi}_i(t)\Big]$$
$$= \begin{cases} -p_i b_i \psi_i^*(x_i(t) - x_{\mathrm{d}_i})w_i(x,t) \leq 0, & \text{if } \psi_i(t) = 0 \text{ and } (x_i(t) - x_{\mathrm{d}_i})w(x(t),t) \geq 0, \\ 0, \text{ otherwise.} \end{cases} \tag{4.39}$$

Hence, for all $t > T$ and for $t \leq T$ such that $w(x(t),t) >> 0$,

$$\dot{V}(x(t), K(t), \phi(t), \Psi(t)) \leq -(x(t) - x_{\mathrm{e}})^{\mathrm{T}} R(x(t) - x_{\mathrm{e}}) \leq 0. \tag{4.40}$$

Next, consider the case where for $t \in [0,\, T]$ and $i \in \{1,\, \ldots,\, m\}$, $w_i(x(t),t) < 0$. If $\hat{u}_i(t) \geq 0$, $t \in [0,\, T]$, then (4.37)–(4.39) hold, and hence, (4.40) holds. Alternatively, if $\hat{u}_i(t) < 0$, $t \in [0,\, T]$, then, since $w_i(x(t),t) < 0$, $x_i(t) - x_{\mathrm{d}}(t) \geq 0$ does not necessarily hold, and hence, (4.35) and (4.36) do not necessarily hold. Now, note that if $\hat{u}_i(t) < 0$, $t \in [0,\, T]$, then $u_i(t) = 0$, and hence, the disturbed system (4.33) is uncontrolled.

Furthermore, if $\hat{u}_i(t) < 0$, $t \in [0, T]$, then $k_{u_i}(t) = 0$, $\phi_{u_i}(t) = 0$, and $\psi_{u_i}(t) = 0$, and hence, the Lyapunov derivative (4.34) along the trajectories of the closed-loop system (4.11), (4.25)–(4.29) can be nonnegative over the finite-time interval $[0, T]$. Since A is Hurwitz and the continuous bounded disturbance signal can take nonnegative values over the time interval $[0, T]$, the trajectory of the system (4.11) remains bounded on the time interval $[0, T]$. Furthermore, since for all $t \geq T$ (4.40) holds, it follows that there exists an increasing unbounded sequence $\{t_n\}_{n=0}^{\infty}$, with $t_0 = 0$, such that $0 < t_{n+1} - t_n \leq \hat{T}$, $\hat{T} > 0$, $n = 0, 1, \ldots$, and $V(\tilde{x}(t_{n+1})) - V(\tilde{x}(t_n)) \leq 0$, where $\tilde{x} = [x^{\mathrm{T}}, \mathrm{vec}^{\mathrm{T}}(K), \phi^{\mathrm{T}}, \mathrm{vec}^{\mathrm{T}}(\Psi)]$ and $\mathrm{vec}(\cdot)$ denotes the column stacking operator. In addition, for all $t \geq 0$, $V(\tilde{x}(t))$ satisfies $\alpha(\|\tilde{x}(t)\|) \leq V(\tilde{x}(t)) \leq \beta(\|\tilde{x}(t)\|)$, where $\alpha(\cdot)$ and $\beta(\cdot)$ are class $\mathcal{K}$ functions defined on $[0, \epsilon)$ for all $\epsilon > 0$. Hence, by Theorem 1 of [2], the solution $(x(t), K(t), \phi(t), \Psi(t)) \equiv (x_{\mathrm{e}}, K_{\mathrm{g}}, u_{\mathrm{e}}, \Psi^*)$ of the closed-loop system given by (4.11) and (4.25)–(4.29) is Lyapunov stable. Moreover, since R is positive definite, it follows from Theorem 1 of [2] using similar arguments as in Theorem 2.2 of [23] that $x(t) \to x_{\mathrm{e}}$ as $t \to \infty$. Finally, $u(t) \geq\geq 0$, $t \geq 0$, is a restatement of (4.25). The nonnegativity of $x(t)$, $t \geq 0$, trivially follows from the fact that A is essentially nonnegative, the control input is nonnegative, and disturbance signal is such that nonnegativity is preserved. □

Example 4.1. As an illustrative numerical example for the proposed disturbance rejection adaptive controller given by Theorem 4.2, consider the uncertain compartmental dynamical system given by (4.11) with

$$A = \begin{bmatrix} -1 & 1 \\ 1 & -1 \end{bmatrix}, \quad B = \begin{bmatrix} 1 & 0 \\ 0 & 0.4 \end{bmatrix}, \quad \Psi^* = \begin{bmatrix} 0.1 & 0 \\ 0 & 0.2 \end{bmatrix},$$

and initial condition $x_0 = [0.5, 0.75]^{\mathrm{T}}$. Here, the disturbance vector is given by $w(x(t), t) = [\sin(x_1(t)\omega_1 t), \quad 1 - \cos(x_2(t)\omega_2 t)]^{\mathrm{T}}$, where $\omega_1 = 1$ rad/sec and $\omega_2 = 5$ rad/sec, and $x_{\mathrm{e}} = [1, 1]^{\mathrm{T}}$. For the given A, B, and x_{e}, u_{e} satisfying (4.4) is $u_{\mathrm{e}} = [0, 0]^{\mathrm{T}}$.

Here, we consider the control law given by (4.12)–(4.16) with $q_1 = q_2 = 3$, $k_1(0) = k_2(0) = 0$, $\hat{q}_1 = \hat{q}_2 = 1$, $\phi_1(0) = \phi_2(0) = 0.01$, $\gamma_1 = \gamma_2 = 7$, and $\psi_1(0) = \psi_2(0) = 0.01$. Figure 4.1 shows the controlled system trajectories for the cases where $\Psi(t)$, $t \geq 0$, is given by (4.16) and $\Psi(t) \equiv 0$, $t \geq 0$. Figure 4.2 shows the control input and disturbance signal time histories.

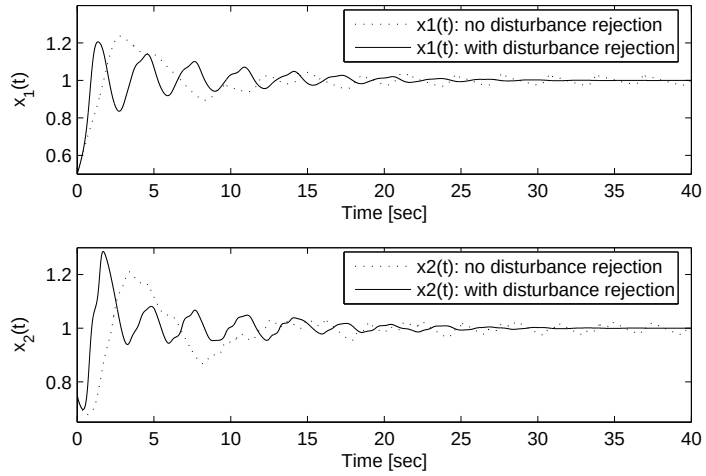

Figure 4.1: System trajectories with and without ($\Psi(t) \equiv 0$) disturbance rejection

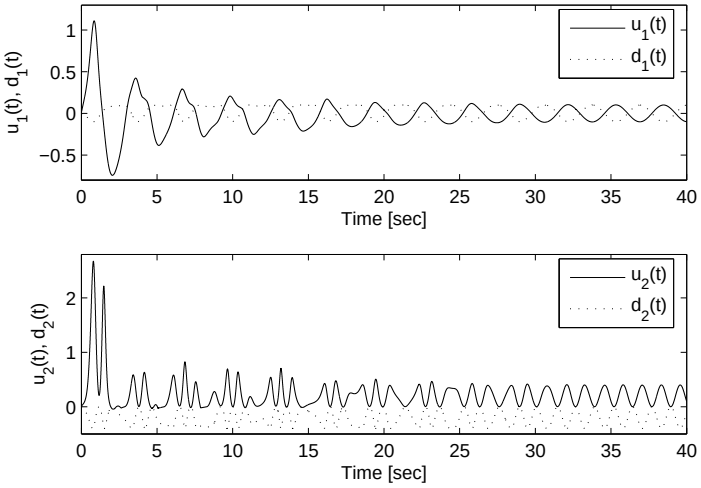

Figure 4.2: Control input and disturbance signal

4.5. Adaptive Control for Linear Compartmental Dynamical Systems with $\mathcal{L}_2$ Disturbances

In this section, we consider the problem for characterizing disturbance rejection control laws for linear compartmental dynamical systems with $\mathcal{L}_2$ exogenous disturbances. Specifically, we consider the controlled system (4.6) with disturbance $d(x(t), t)$ given by (4.10) so that

$$\dot{x}(t) = Ax(t) + Bu(t) + J(x(t))w(t), \quad x(0) = x_0, \quad t \geq 0. \tag{4.41}$$

Define the set $\mathcal{S}(x_{\mathrm{e}}) \triangleq \{y \in \mathbb{R}^n : y = x - x_{\mathrm{e}},\ x \in \overline{\mathbb{R}}_+^n\}$. Next, we partition the nonnegative orthant $\overline{\mathbb{R}}_+^n$ into 2^n non-intersecting open orthants $\mathcal{S}_1(x_{\mathrm{e}}), \ldots, \mathcal{S}_{2^n}(x_{\mathrm{e}})$, where $\mathcal{S}_q(x_{\mathrm{e}}) \subset \mathcal{S}(x_{\mathrm{e}}),\ q = 1, \ldots, 2^n$, such that in each of the orthants $\mathcal{S}_q(x_{\mathrm{e}})$, every ith component of any vector $y \in \mathcal{S}_q(x_{\mathrm{e}})$ is either strictly positive or strictly negative. Furthermore, define

$$\mathcal{S}_0(x_{\mathrm{e}}) \triangleq \{y \in \mathcal{S}(x_{\mathrm{e}}) : \text{ there exists } i \in \{1, \ldots, n\} : y_i = 0\}. \tag{4.42}$$

Clearly, $\mathcal{S}(x_{\mathrm{e}}) = \mathcal{S}_0(x_{\mathrm{e}}) \cup \mathcal{S}_1(x_{\mathrm{e}}) \cup \cdots \cup \mathcal{S}_{2^n}(x_{\mathrm{e}})$ and for all $i, j = 1, \ldots, 2^n,\ i \neq j,\ S_j(x_{\mathrm{e}}) \cap \mathcal{S}_i(x_{\mathrm{e}}) = \varnothing$ and $\mathcal{S}_0(x_{\mathrm{e}}) \cap \mathcal{S}_i(x_{\mathrm{e}}) = \varnothing$.

Next, define the function $V_{\mathrm{s}} : \mathcal{S}(x_{\mathrm{e}}) \to \overline{\mathbb{R}}_+$ by $V_{\mathrm{s}}(y) = \|y\|_1$, where $\|\cdot\|_1$ denotes the absolute sum norm. Note that $V_{\mathrm{s}}(\cdot)$ is continuous everywhere in $\mathcal{S}(x_{\mathrm{e}})$ and $V_{\mathrm{s}}(y) = 0$ if and only if $y = 0$, and $V_{\mathrm{s}}(y) > 0$ for all $y \neq 0$. Furthermore, note that for every $y \in \mathcal{S}_q(x_{\mathrm{e}}),\ q = 1, \ldots, 2^n$, $V_{\mathrm{s}}(\cdot)$ is continuously differentiable, whereas for every $y \in \mathcal{S}_0(x_{\mathrm{e}})$, $V_{\mathrm{s}}(\cdot)$ is continuous, but not continuously differentiable.

Theorem 4.5. Consider the linear uncertain dynamical system given by (4.41) where A is compartmental and $\mathbf{e}^{\mathrm{T}}A << 0$, B is nonnegative and given by (4.7), $J : \overline{\mathbb{R}}_+^n \to \mathbb{R}^{n \times d}$ is continuous and bounded on $\overline{\mathbb{R}}_+^n$, and $w(\cdot) \in \mathcal{L}_2$. Then the adaptive

control law $u(t) = [u_1(t), \ldots, u_m(t)]^{\mathrm{T}}$, with $u_i(t)$, $t \geq 0$, $i = 1, \ldots, m$, satisfying

$$\dot{u}_i(t) = \begin{cases} 0, & \text{if } y_i(t) = x_i(t) - x_{\mathrm{d}_i} \geq 0 \text{ and } u_i(t) = 0, \\ -\frac{1}{2}, & \text{if } y_i(t) \geq 0 \text{ and } u_i(t) \neq 0, \\ \frac{1}{2}, & \text{otherwise.} \end{cases} \tag{4.43}$$

$$u_i(0) \geq 0, \quad t \geq 0, \quad i = 1, \ldots, m,$$

guarantees that the solution $(x(t), u(t)) \equiv (x_{\mathrm{e}}, u_{\mathrm{e}})$ of the undisturbed $(J(x(t))w(t) \equiv 0)$ closed-loop system (4.41) and (4.43) is Lyapunov stable, and $x(t) \to x_{\mathrm{e}}$ as $t \to \infty$ for all $x_0 \in \overline{\mathbb{R}}_+^n$. Moreover, the solution $x(t)$, $t \geq 0$, to the disturbed closed-loop system (4.41) and (4.43) satisfies the non-expansivity constraint

$$\sum_{j=1}^{n} |\gamma_j| \int_0^t |y_j(\sigma)| \mathrm{d}\sigma \leq \frac{\alpha\sqrt{n}}{\beta} \int_0^t w^{\mathrm{T}}(\sigma) w(\sigma) \mathrm{d}\sigma + V(x_0, u(0)), \tag{4.44}$$

where

$$V(x, u) = V_{\mathrm{s}}(x - x_{\mathrm{e}}) + (u - u_{\mathrm{e}})^{\mathrm{T}} \Gamma^{-1} (u - u_{\mathrm{e}}), \tag{4.45}$$

$\gamma_j = \sum_{i=1}^{n} p_{q_i} A_{(i,j)}$ and $p_{q_i} \pm 1$, $j = 1, \ldots, n$, $\Gamma^{-1} = \mathrm{diag}[\, b_1, \ldots, b_m \,]$ is positive definite, $y(t) \triangleq x(t) - x_{\mathrm{e}}$, and $\alpha, \beta > 0$ are as defined in Section 4.3. Furthermore, $u(t) \geq\geq 0$, $t \geq 0$, and $x(t) \geq\geq 0$ for all $x_0 \in \overline{\mathbb{R}}_+^n$ and $t \geq 0$.

Proof. First, note that even though the update law given by (4.43) is not continuous, the adaptive control $u_i(t)$, $t \geq 0$, $i = 1, \ldots, m$, is continuous. Hence, for each $i \in \{1, \ldots, m\}$, a function $u_i : \mathcal{I}_{u_i(0)} \to \mathbb{R}$ is a solution to (4.43) on the interval $\mathcal{I}_{u_i(0)} \subseteq \mathbb{R}$ with initial condition $u_i(0)$ if $u_i(\cdot)$ is continuous and $u_i(t)$ satisfies (4.43) for all $t \in \mathcal{I}_{u_i(0)}$. Next, note that the system dynamics (4.41) can be rewritten as

$$\dot{x}(t) = A(x(t) - x_{\mathrm{e}}) + B(u(t) - u_{\mathrm{e}}) + J(x(t))w(t), \quad x(0) = x_0, \quad t \geq 0. \tag{4.46}$$

Consider the Lyapunov function candidate for the closed-loop system (4.46) and (4.43) given by (4.45) and note that $V(x, u) \geq 0$ for all x and u, and $V(x, u) = 0$ if and only

if $x = x_{\rm e}$ and $u = u_{\rm e}$. Equation (4.45) can be written as

$$V(x,u) = V_{\rm s}(y) + (u-u_{\rm e})^{\rm T}\Gamma^{-1}(u-u_{\rm e}). \tag{4.47}$$

Now, suppose that at some time $t \in [0,\infty)$, $y(t) = x(t) - x_{\rm e} \notin \mathcal{S}_0(x_{\rm e})$. In this case, there exists an index $q \in \{1,\ldots,2^n\}$ such that $y(t) \in \mathcal{S}_q(x_{\rm e})$, and hence, (4.47) is continuously differentiable for every $y \in \mathcal{S}_q(x_{\rm e})$. Next, for every set $\mathcal{S}_q(x_{\rm e})$ we associate a single vector p_q consisting of the components ± 1 defined as $p_q \triangleq \mathrm{sgn}(y),\ y \in S_q(x_{\rm e})$, where the $\mathrm{sgn}(\cdot)$ operator is taken componentwise and is defined as $\mathrm{sgn}(\mu) \triangleq \frac{\mu}{|\mu|},\ \mu \neq 0$, and $\mathrm{sgn}(0) \triangleq 0$.

Now, rewriting (4.47) as $V(x,u) = p_q^{\rm T}y + (u-u_{\rm e})^{\rm T}\Gamma^{-1}(u-u_{\rm e})$, the derivative of $V(x,u)$ along the trajectories of closed-loop system (4.46) and (4.43) is given by

$$\begin{aligned}\dot{V}(x(t),u(t)) &= p_q^{\rm T}Ay(t) + p_q^{\rm T}B(u(t)-u_{\rm e}) + p_q^{\rm T}J(y(t)+x_{\rm e})w(t) + 2(u-u_{\rm e})^{\rm T}\Gamma^{-1}\dot{u}(t)\\ &= p_q^{\rm T}Ay(t) + p_q^{\rm T}J(y(t)+x_{\rm e})w(t) + \sum_{i=1}^{m} b_i(u_i(t)-u_{{\rm e}_i})(p_{q_i} + 2\dot{u}_i(t)) \end{aligned} \tag{4.48}$$

Note that $p_q^{\rm T}Ay$ can be written as $p_q^{\rm T}Ay = \gamma_1 y_1 + \ldots \gamma_n y_n$, where $\gamma_j \triangleq \sum_{i=1}^{n} p_{q_i}A_{(i,j)}$ and p_q are elementary vectors consisting of the components ± 1. If $y_j > 0$, then $p_{q_j} = 1$ and, since $\mathbf{e}^{\rm T}A << 0$, it follows that $\gamma_j < 0$, and hence, $\gamma_j y_j < 0$. Alternatively, if $y_j < 0$, then using identical arguments $p_{q_j} = -1$ and $\gamma_j > 0$, which yields $\gamma_j y_j < 0$. Thus, $\gamma_j y_j = -|\gamma_j||y_j|$, and hence,

$$p_q^{\rm T}Ay(t) \leq \sum_{j=1}^{n} -|\gamma_j||y_j(t)|, \quad t \geq 0. \tag{4.49}$$

Furthermore, note that

$$p_q^{\rm T}J(y(t)+x_{\rm e})w(t) \leq \frac{\alpha\sqrt{n}}{\beta}w^{\rm T}(t)w(t), \quad t \geq 0. \tag{4.50}$$

Next, for each $i \in \{1,\ldots,m\}$ and $\dot{u}_i(t)$, $t \geq 0$, given by (4.43), the last term of (4.48) gives:

(i) If $y_i > 0$ or, equivalently, $p_{q_i} = 1$, and $u_i(t) = 0$, $t \geq 0$, then $\dot{u}_i(t) = 0$, $t \geq 0$, and

$$b_i(u_i(t) - u_{\mathrm{e}_i})(p_{q_i} + 2\dot{u}_i(t)) = -b_i u_{\mathrm{e}_i} \leq 0, \quad t \geq 0.$$

(ii) If $y_i > 0$ and $u_i(t) \neq 0$, $t \geq 0$, then $\dot{u}_i(t) = -\frac{1}{2}$, $t \geq 0$, and

$$b_i(u_i(t) - u_{\mathrm{e}_i})(p_{q_i} + 2\dot{u}_i(t)) = 0, \quad t \geq 0.$$

(iii) If $y_i < 0$, or, equivalently, $p_{q_i} = -1$, then $\dot{u}_i(t) = \frac{1}{2}$, $t \geq 0$, and

$$b_i(u_i(t) - u_{\mathrm{e}_i})(p_{q_i} + 2\dot{u}_i(t)) = 0, \quad t \geq 0.$$

Hence,

$$\sum_{i=1}^{m} b_i(u_i(t) - u_{\mathrm{e}_i})(p_{q_i} + 2\dot{u}_i(t)) \leq 0, \quad t \geq 0.$$

Now, using (4.49) and (4.50), it follows that

$$\dot{V}(x, u) \leq \sum_{j=1}^{n} -|\gamma_j||y_j| + \frac{\alpha\sqrt{n}}{\beta} w^{\mathrm{T}} w, \quad t \geq 0. \tag{4.51}$$

Since $\mathcal{S}_q(x_{\mathrm{e}})$ is open, it follows from continuity of the system trajectories that there exists a time interval $[t, T)$, $T > t$, such that $y(\sigma) = x(\sigma) - x_{\mathrm{e}} \in \mathcal{S}_q(x_{\mathrm{e}})$ for all $\sigma \in [t, T)$. Integrating (4.51) over $\sigma \in [t, T)$ yields

$$V(x(T), u(T)) \leq \frac{\alpha\sqrt{n}}{\beta} \int_t^T w^{\mathrm{T}}(\sigma) w(\sigma) \mathrm{d}\sigma - \sum_{j=1}^{n} |\gamma_j| \int_t^T |y_j(\sigma)| \mathrm{d}\sigma + V(x(t), u(t)).$$

Noting that $V(x(T), u(T)) \geq 0$ for all possible $x(T)$ and $u(T)$ it follows that

$$\sum_{j=1}^{n} |\gamma_j| \int_t^T |y_j(\sigma)| \mathrm{d}\sigma \leq \frac{\alpha\sqrt{n}}{\beta} \int_t^T w^{\mathrm{T}}(\sigma) w(\sigma) \mathrm{d}\sigma + V(x(t), u(t)), \tag{4.52}$$

where $w(\cdot) \in \mathcal{L}_2$. Now, since $|\gamma_i| > 0$, the nonnegative expression on the left-hand side of the inequality (4.52) is zero only if $y_i = 0$ for all $i = 1, \ldots, n$.

Next, suppose that on an arbitrary time interval $[t, T)$, $T > 0$, $y(\sigma) \in \mathcal{S}_0(x_{\mathrm{e}})$ for all $\sigma \in [t, T)$, $y(\sigma) \neq 0$, and all $y_i(\sigma)$ remain either strictly positive, strictly negative, or

zero. In this case, there exists a set of indices $\mathcal{I} = \{i_1, \ldots, i_k\}$ such that for all $j \in \mathcal{I}$, $y_j(\sigma) \equiv 0$. Now, it follows from (4.43) that $u_j(t)$, $j \in \{1, \ldots, m\} \cap \mathcal{I}$, remains bounded since it either remains constant, or decreases and is always nonnegative. Since for all $j \in \mathcal{I}$ and $\sigma \in [t, T)$, $x_j(\sigma) \equiv x_{\mathrm{e}_j}$, it follows that $\dot{x}_j(\sigma) \equiv 0$. Now, to examine the stability of the closed-loop system (4.41) and (4.43), we can consider a reduced dynamical system obtained from (4.46) by deleting the equations corresponding to $\dot{x}_j$, $j \in \mathcal{I}$, since these states are constant, and hence, do not affect the non-expansivity constraint (4.52).

To see this, consider a Lyapunov function candidate having the same form as (4.45) with the states x_j and control inputs u_j, where $j \in \mathcal{I}$, deleted. Specifically, consider the reduced vectors y_{r} and u_{r} with components y_i and u_j, respectively, where $i \in \{1, \ldots, n\} \backslash \mathcal{I}$ and $j \in \{1, \ldots, m\} \backslash \mathcal{I}$. In this case, the Lyapunov function candidate is given by

$$V(y_{\mathrm{r}}, u_{\mathrm{r}}) = V_{\mathrm{s}}(y_{\mathrm{r}}) + (u_{\mathrm{r}} - u_{\mathrm{e}_{\mathrm{r}}})^{\mathrm{T}} \Gamma_{\mathrm{r}}^{-1} (u_{\mathrm{r}} - u_{\mathrm{e}_{\mathrm{r}}}), \tag{4.53}$$

where $\Gamma_{\mathrm{r}}^{-1} = \mathrm{diag}[\, b_{j_1}, \ldots, b_{j_k}\,]$ and $j_1, j_2, \ldots, j_k \in \{1, \ldots, m\} \backslash \mathcal{I}$. Next, repeating the analysis above, it can be shown that

$$\sum_{j \in \{1, 2, \ldots, n\} \backslash \mathcal{I}} |\gamma_j| \int_t^T |y_j(\sigma)| \mathrm{d}\sigma \leq \frac{\alpha \sqrt{n}}{\beta} \int_t^T \sum_{j \in \{1, 2, \ldots, n\} \backslash \mathcal{I}} w_j^2(\sigma) \mathrm{d}\sigma + V(y_{\mathrm{r}}(t), u_{\mathrm{r}}(t)). \tag{4.54}$$

Now, adding $\sum_{j \in \mathcal{I}} |\gamma_j| \int_t^T |y_j(\sigma)| \mathrm{d}\sigma = 0$ to the left-hand side of the inequality (4.54), and the nonnegative term $\frac{\alpha \sqrt{n}}{\beta} \int_t^T \sum_{j \in \mathcal{I}} w_j^2(\sigma) \mathrm{d}\sigma$ to the right-hand side of the inequality (4.54), inequality (4.54) still holds and has the same form as inequality (4.52). Hence, inequality (4.52) holds on the time interval $[0, t)$ for all $t > 0$, that is,

$$\sum_{j=1}^{n} |\gamma_j| \int_0^t |y_j(\sigma)| \mathrm{d}\sigma \leq \frac{\alpha \sqrt{n}}{\beta} \int_0^t w^{\mathrm{T}}(\sigma) w(\sigma) \mathrm{d}\sigma + V(x_0, u(0)), \tag{4.55}$$

where $w(\cdot) \in \mathcal{L}_2$. Now, it follows from (4.51) that the solution $(x(t), u(t)) \equiv (x_{\mathrm{e}}, u_{\mathrm{e}})$ of the undisturbed ($J(x(t))w(t) \equiv 0$) closed-loop system (4.41) and (4.43) is Lyapunov

stable. Furthermore, by Theorem 4.4 of [80], $y(t) = x(t) - x_{\mathrm{e}} \to 0$ as $t \to \infty$ for all $x_0 \in \overline{\mathbb{R}}^n_+$.

Finally, note that, since, by assumption, $J(x)w(t) \geq\geq 0$, $x \in \partial\overline{\mathbb{R}}^n_+$ and $t \geq 0$, and the control inputs $u_i(t)$, $t \geq 0$, defined by (4.43) are nonnegative, $u(t) \geq\geq 0$, $t \geq 0$, and hence, the trajectory of the system (4.41) remains in the nonnegative orthant. This completes the proof. □

Remark 4.4. It is important to note that the adaptive feedback control law, $u(t)$, $t \geq 0$, characterized by (4.43) is continuous, but not continuously differentiable. Namely, even though for each $i \in \{1, \ldots, m\}$, $\dot{u}_i(\cdot)$ is continuous on $\overline{\mathbb{R}}^n_+ \setminus \mathcal{S}(x_{\mathrm{e}})$ and discontinuous on $\mathcal{S}(x_{\mathrm{e}})$, $u_i(\cdot)$ is continuous on $\overline{\mathbb{R}}^n_+$. Hence, the closed-loop system (4.46) generates a continuous closed-loop vector field.

Next, we present a different control law for the disturbance rejection problem considered in this section. The following assumption is needed for the next result

Assumption 4.2. Consider the controlled system (4.41) and let $\|\cdot\| : \mathbb{R}^{n\times d} \to \mathbb{R}$. Assume $J(x)$, $x \in \overline{\mathbb{R}}^n_+$ in (4.41) is such that $\|J(x)\| \leq \alpha$, $x \in \overline{\mathbb{R}}^n_+$, where $\alpha < \frac{\lambda_{\min}(R)}{\|P\|}$ and P and R satisfy (4.2).

Theorem 4.6. Consider the linear uncertain dynamical system given by (4.41) where A is Hurwitz and compartmental, B is nonnegative and given by (4.7), $J : \overline{\mathbb{R}}^n \to \mathbb{R}^{n\times d}$ is continuous and bounded on $\overline{\mathbb{R}}^n$, and $w(\cdot) \in \mathcal{L}_2$. Suppose Assumption 4.2 holds. Then the control law $u(t) = [u_1(t), \ldots, u_m(t)]^{\mathrm{T}}$, with $u_i(t)$, $t \geq 0$, $i = 1, \ldots, m$, satisfying

$$\dot{u}_i(t) = \begin{cases} 0, & \text{if } u_i(t) = 0 \text{ and } y_i(t) \triangleq x_i(t) - x_{\mathrm{d}_i} \geq 0, \\ -\gamma_i y_i(t), & \text{otherwise,} \end{cases} \tag{4.56}$$

$$u_i(0) \geq 0, \quad \gamma_i > 0, \quad t \geq 0, \quad i = 1, \ldots, m,$$

guarantees that the solution $(x(t), u(t)) \equiv (x_{\rm e}, u_{\rm e})$ of the undisturbed ($J(x(t))w(t) \equiv 0$) closed-loop system (4.41) and (4.56) is Lyapunov stable and $x_i(t) \to x_{{\rm d}_i}$, $i = 1, \ldots, m$, as $t \to \infty$ for all $x_0 \in \overline{\mathbb{R}}_+^n$. Moreover, the solution $x(t)$, $t \geq 0$, to the disturbed closed-loop system (4.41) and (4.56) satisfies the non-expansivity constraint

$$\gamma \int_0^t (x(\sigma) - x_{\rm e})^{\rm T}(x(\sigma) - x_{\rm e}){\rm d}\sigma \leq \frac{1}{2}\int_0^t w^{\rm T}(\sigma)w(\sigma){\rm d}\sigma + C,\ \gamma > 0,\ C \geq 0,\ t \geq 0. \tag{4.57}$$

Furthermore, $u(t) \geq\geq 0$, $t \geq 0$, and $x(t) \geq\geq 0$ for all $x_0 \in \overline{\mathbb{R}}_+^n$ and $t \geq 0$.

Proof. Since A is Hurwitz it follows from Theorem 4.1 that there exist a positive diagonal matrix P and a positive-definite matrix $R \in \mathbb{R}^{n\times n}$ satisfying (4.2). Now, consider the Lyapunov function candidate

$$V(x, u) = (x - x_{\rm e})^{\rm T}P(x - x_{\rm e}) + (u - u_{\rm e})^{\rm T}\Gamma^{-1}(u - u_{\rm e}), \tag{4.58}$$

where $\Gamma^{-1} = {\rm diag}\left[\frac{b_1}{\gamma_1}, \ldots, \frac{b_m}{\gamma_m}\right]$. Note that $V(x, u)$ is nonnegative for all x and u, and $V(x, u) = 0$ if and only if $x = x_{\rm e}$ and $u = u_{\rm e}$. The Lyapunov derivative along the trajectories of the closed-loop system (4.41) and (4.56) is given by

$$\begin{aligned}\dot{V}(x(t), u(t)) =\ & 2(x(t) - x_{\rm e})^{\rm T}PA(x(t) - x_{\rm e}) + 2(x(t) - x_{\rm e})^{\rm T}PB(u(t) - u_{\rm e})\\ & +2(x(t) - x_{\rm e})^{\rm T}PJ(x(t))w(t)) + 2(u(t) - u_{\rm e})^{\rm T}\Gamma^{-1}\dot{u}(t)\\ =\ & -(x(t) - x_{\rm e})^{\rm T}R(x(t) - x_{\rm e}) + 2(x(t) - x_{\rm e})^{\rm T}PJ(x(t))w(t)\\ & +2\sum_{j=1}^{m} p_i b_i (u_i(t) - u_{\rm e})\left(y_i(t) + \frac{1}{\gamma_i}\dot{u}_i(t)\right), \quad t \geq 0. \end{aligned} \tag{4.59}$$

Now, for each $i \in \{1, \ldots, m\}$ and for the two cases given in (4.56) the last term on the right-hand side of (4.59) gives:

(i) If $u_i(t) = 0$ and $y_i(t) \geq 0$, $t \geq 0$, then $\dot{u}_i(t) = 0$, $t \geq 0$, and hence,

$$p_i b_i (u_i(t) - u_{\rm e})\left(y_i(t) + \frac{1}{\gamma_i}\dot{u}_i(t)\right) = -p_i b_i u_{\rm e} y_i(t) \leq 0, \quad t \geq 0.$$

(ii) Otherwise, $\dot{u}_i(t) = -\gamma_i y_i(t)$, and hence,

$$p_i b_i (u_i(t) - u_{\mathrm{e}}) \left(y_i(t) + \frac{1}{\gamma_i} \dot{u}_i(t) \right) = 0, \quad t \geq 0.$$

Thus, it follows that

$$\begin{aligned}
\dot{V}(x(t), u(t)) &\leq -(x(t) - x_{\mathrm{e}})^{\mathrm{T}} R (x(t) - x_{\mathrm{e}}) + 2(x(t) - x_{\mathrm{e}})^{\mathrm{T}} P J(x(t)) w(t) \\
&\leq -(x(t) - x_{\mathrm{e}})^{\mathrm{T}} R (x(t) - x_{\mathrm{e}}) + \alpha \|P\| \|x(t) - x_{\mathrm{e}}\|^2 + \frac{1}{2} \|w(t)\|^2 \\
&\leq (-\lambda_{\min}(R) + \alpha \|P\|) \|x(t) - x_{\mathrm{e}}\|^2 + \frac{1}{2} w^{\mathrm{T}}(t) w(t) \\
&\leq -\gamma \|x(t) - x_{\mathrm{e}}\|^2 + \frac{1}{2} w^{\mathrm{T}}(t) w(t), \quad t \geq 0,
\end{aligned}$$

where, by Assumption 4.2, $\gamma \triangleq \lambda_{\min}(R) - \alpha \|P\| > 0$. Hence,

$$\dot{V}(x(t), u(t)) \leq -\gamma \|x(t) - x_{\mathrm{e}}\|^2 + w^{\mathrm{T}}(t) w(t), \quad t \geq 0. \tag{4.60}$$

Integrating (4.60) over the time interval $[0, t)$, $t \geq 0$, yields

$$V(x(t), u(t)) \leq \frac{1}{2} \int_0^t w^{\mathrm{T}}(\sigma) w(\sigma) \mathrm{d}\sigma - \gamma \int_0^t (x(\sigma) - x_{\mathrm{e}})^{\mathrm{T}} (x(\sigma) - x_{\mathrm{e}}) \mathrm{d}\sigma + V(x_0, u(0)).$$

Noting that $V(x(t), u(t)) \geq 0$ for all possible $x(t)$ and $u(t)$ it follows that

$$\gamma \int_0^t (x(\sigma) - x_{\mathrm{e}})^{\mathrm{T}} (x(\sigma) - x_{\mathrm{e}}) \mathrm{d}\sigma \leq \frac{1}{2} \int_0^t w^{\mathrm{T}}(\sigma) w(\sigma) \mathrm{d}\sigma + V(x_0, u(0)), \quad \gamma > 0, \tag{4.61}$$

where $w(\cdot) \in \mathcal{L}_2$.

Finally, it follows from (4.60) that the solution $(x(t), u(t)) \equiv (x_{\mathrm{e}}, u_{\mathrm{e}})$ of the undisturbed ($J(x(t))w(t) \equiv 0$) closed-loop system (4.41) and (4.56) is Lyapunov stable. Furthermore, by Theorem 4.4 of [80], $x(t) - x_{\mathrm{e}} \to 0$ as $t \to \infty$ for all $x_0 \in \overline{\mathbb{R}}_+^n$. Now, the nonnegativity of the dynamical system (4.41) follows trivially by noting that control input $u(t)$ defined by (4.56) is nonnegative and $J(x)w(t) \geq\geq 0$ for all $x \in \partial\overline{\mathbb{R}}_+^n$ and $t \geq 0$. □

Example 4.2. In this example, we consider the adaptive controller given by (4.43). Specifically, consider the dynamical system given by (4.41) with

$$A = \begin{bmatrix} -1.5 & 2.0 & 1.5 \\ 0.5 & -3 & 0.9 \\ 0.75 & 0.5 & -2.5 \end{bmatrix}, \quad B = \begin{bmatrix} 0.5 & 0 & 0 \\ 0 & 0.33 & 0 \\ 0 & 0 & 0.2 \end{bmatrix},$$

$$J(x) = \begin{bmatrix} 0.001 & 0.02 & 0.003 \\ 0.012 & 0.001 & 0.032 \\ 0.022 & 0.003 & 0.007 \end{bmatrix}, \tag{4.62}$$

and initial condition $x_0 = [0.5,\, 2,\, 3]^{\mathrm{T}}$. Here, the disturbance vector is given by $w(x(t), t) = [e^{-\lambda_1 t}\sin(x_1(t)\omega_1 t), \quad e^{-\lambda_2 t}(1+\cos(\omega_2 t)]^{\mathrm{T}}), \quad e^{-\lambda_3 t}(1+\sin(\omega_3 t))]^{\mathrm{T}}$, where $\omega_1 = 1$ rad/sec, $\omega_2 = 2$ rad/sec, $\omega_3 = 3$ rad/sec, $\lambda_1 = 0.01$, $\lambda_2 = 0.02$, and $\lambda_3 = 0.03$. The desired set-point is $x_{\mathrm{e}} = [2.5,\, 1,\, 1]^{\mathrm{T}}$. For the given A, B, and x_{e}, u_{e} satisfying (4.4) is $u_{\mathrm{e}} = [0.5,\, 2.55,\, 0.625]^{\mathrm{T}}$. Here, we consider the control law given by (4.43) with $u_1(0) = u_2(0) = u_3(0) = 0$. The controlled and uncontrolled system trajectories are shown in Figure 4.3. The control input and disturbance signal are shown in Figure 4.4. Note that the proposed controller achieves disturbance rejection and the trajectory of the system converges to the desired set-point.

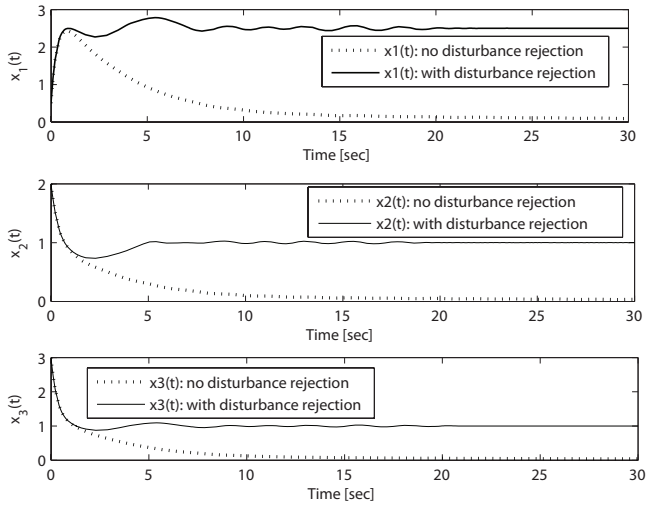

Figure 4.3: System trajectories with and without disturbance rejection

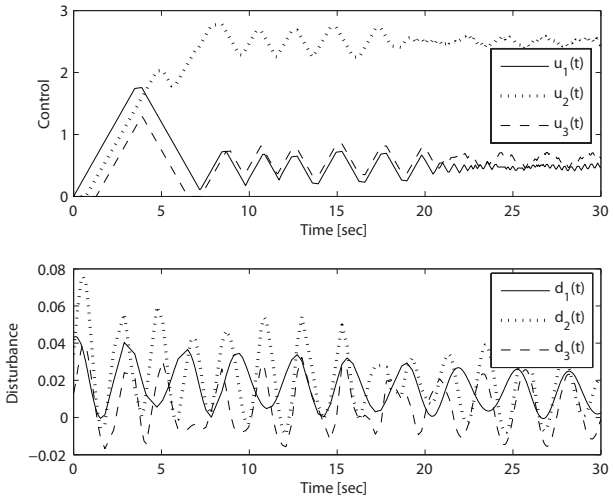

Figure 4.4: Control input and disturbance signal

Example 4.3. In this example, we consider the adaptive controller given by (4.56). Specifically, consider the dynamical system (4.41) with the same parameters and disturbance signal as in Example 4.2, and A given by

$$A = \begin{bmatrix} -1.5 & 2.0 & 1.5 \\ 0.5 & -3 & 1 \\ 0.75 & 0.5 & -2.5 \end{bmatrix}.$$

For the given A, B, and $x_{\mathrm{e}} = [2.5,\ 1,\ 1]^{\mathrm{T}}$, u_{e} satisfying (4.4) is $u_{\mathrm{e}} = [0.5,\ 2.25,\ 0.625]^{\mathrm{T}}$. Here, we consider the controller given by (4.56) with $\gamma_1 = \gamma_2 = \gamma_3 = 2$ and $u_1(0) = u_2(0) = u_3(0) = 0.01$. Figure 4.5 shows the controlled and uncontrolled system trajectories and Figure 4.6 shows the control input and disturbance versus time. Since the disturbance signal is an $\mathcal{L}_2$ signal and A is Hurwitz, the states of the uncontrolled system ($u(t) \equiv 0$) converge to zero. Alternatively, the controlled system with the adaptive disturbance rejection controller given by (4.56) guarantees that the system trajectories converge to the desired set-point.

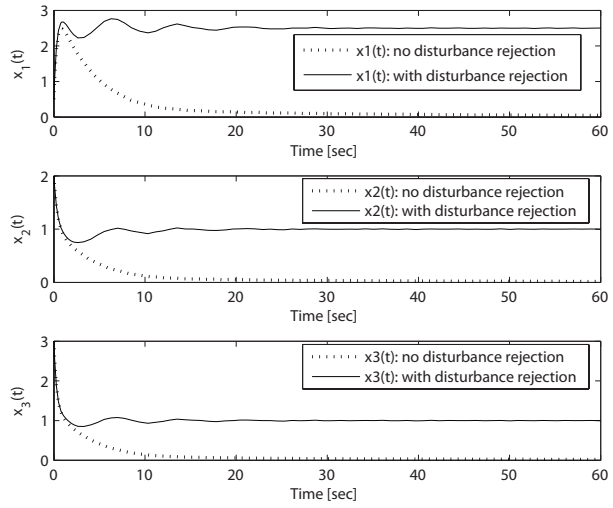

Figure 4.5: System trajectories with and without disturbance rejection

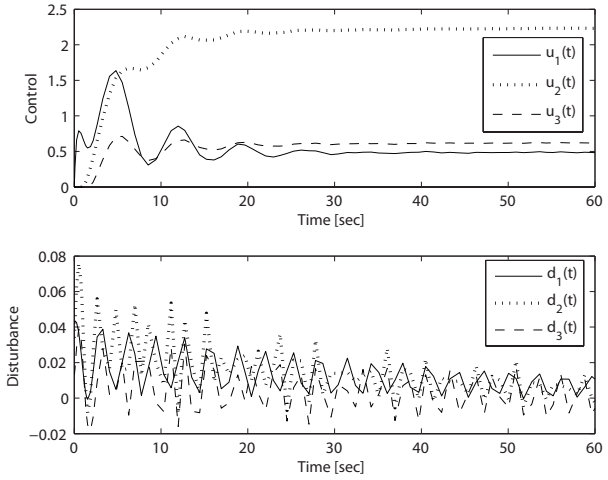

Figure 4.6: Control input and disturbance signal

4.6. Adaptive Control for Automated Anesthesia with Hemorrhage and Hemodilution Effects

Almost all anesthetics are *myocardial* depressants, that is, they decrease the contractility of the heart and lower *cardiac output* (i.e., the volume of blood pumped by the heart per unit time). Decreased cardiac output can decrease the rate of transfer

of drug from the intravascular volume to peripheral tissues, resulting in an increase in plasma concentration. This can lead to overdosing which, at the very least, can delay recovery from anesthesia and, in the worst case, can result in respiratory and cardiovascular collapse. Alternatively, underdosing can cause psychological trauma from awareness and pain during surgery.

Control of drug effect is clinically important since overdosing or underdosing incur risk for the patient. To illustrate the adaptive disturbance rejection control framework developed in Section 4.4 of this presentation for general anesthesia we consider a hypothetical model for the intravenous anesthetic propofol. The pharmacokinetics of propofol are described by the three-compartment model [53, 96] shown in Figure 4.7, where x_1 denotes the mass of drug in the central compartment, which is the site of drug administration and is identified with tissues whose drug concentration equilibrates, within the assumptions of the model, instantaneously with the site of drug administration. This implies tissues with high ratios of blood flow to tissue mass, such as those found in the myocardium, brain, etc., although compartment models do not strictly equate the compartment with any specific organ. The remainder of the drug in the body is assumed to reside in two peripheral compartments, corresponding to tissues with progressively slower drug equilibration with the site of administration. The masses in these compartments are denoted by x_2 and x_3, respectively. These compartments receive less than 20% of the cardiac output. It should be noted that pharmacokinetic compartmental models may utilize any number of compartments and the decision about model complexity depends largely on the resolution of concentration measurements as a function of time. The three-compartment model shown in Figure 4.7 has been found to be effective for describing the disposition of propofol after intravenous injection [96].

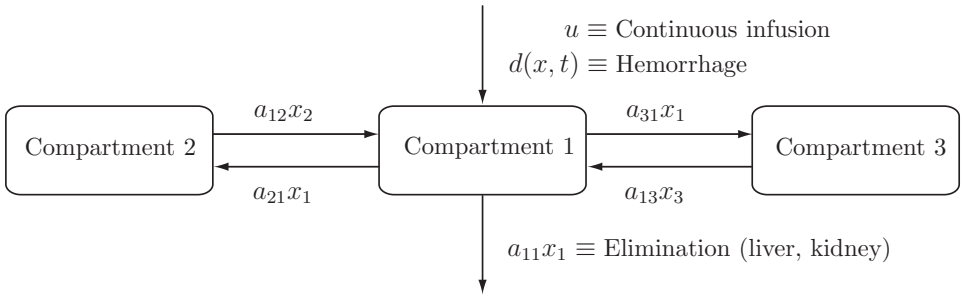

Figure 4.7: Three-compartment mammillary model for disposition of propofol

A mass balance for the whole compartmental system yields

$$\dot{x}_1(t) = -(a_{11} + a_{21} + a_{31})x_1(t) + a_{12}x_2(t) + a_{13}x_3(t) + u(t) + d(x(t), t),$$
$$x_1(0) = x_{10}, \quad t \geq 0, \tag{4.63}$$

$$\dot{x}_2(t) = a_{21}x_1(t) - a_{12}x_2(t), \quad x_2(0) = x_{20}, \tag{4.64}$$

$$\dot{x}_3(t) = a_{31}x_1(t) - a_{13}x_3(t), \quad x_3(0) = x_{30}, \tag{4.65}$$

where $x_1(t)$, $x_2(t)$, $x_3(t)$, $t \geq 0$, are the masses in grams of propofol in the central compartment and compartments 2 and 3, respectively, $u(t)$, $t \geq 0$, is the infusion rate in grams/min of the anesthetic drug propofol into the central compartment, $d(x(t), t)$ is an exogenuous disturbance signal in grams/min which has been included to model the effect of hemorrhage on the dynamics of the mass of propofol in the central compartment, $a_{ij} > 0$, $i \neq j$, $i, j = 1, 2, 3$, are the rate constants in min^{-1} for drug transfer between compartments, and $a_{11} > 0$ is the rate constant in min^{-1} of drug metabolism and elimination (metabolism typically occurs in the liver) from the central compartment.

Even though the transfer and loss coefficients are positive, they are uncertain due to patient gender, weight, pre-existing disease, age, and concomitant medication. Hence, adaptive control for propofol set-point regulation can significantly improve the outcome for drug administration over manual (open-loop) control. It has been reported in [142] that a 2.5–6 μg/ml blood concentration level of propofol is required

during the maintenance stage in general anesthesia depending on patient fitness and extent of surgical stimulation. Hence, continuous infusion control is required for maintaining this desired level of anesthesia. Here, we assume that the transfer and loss coefficients a_{11}, a_{12}, a_{21}, a_{13}, and a_{31} are unknown and our objective is to regulate the propofol concentration level of the central compartment to the desired level of 3.4 μg/ml in the face of system uncertainty and system disturbances due to hemorrhage.

Next, note that (4.63)–(4.65) can be written in state space form (4.6) with $x = [x_1, x_2, x_3]^{\mathrm{T}}$,

$$A = \begin{bmatrix} -(a_{11}+a_{21}+a_{31}) & a_{12} & a_{13} \\ a_{21} & -a_{12} & 0 \\ a_{31} & 0 & -a_{13} \end{bmatrix}, \; B = \begin{bmatrix} 1 \\ 0 \\ 0 \end{bmatrix}, \; d(x,t) = \begin{bmatrix} -\psi^* w(x,t) \\ 0 \\ 0 \end{bmatrix},$$

where ψ^* is an *unknown* positive constant and the function $w(x,t)$ represents blood loss due to hemorrhage. A model for the effect of hemorrhage on the dynamics of the mass of propofol in the central compartment is developed below. Even though propofol concentration levels in the blood plasma will lead to the desired depth of anesthesia, they cannot be measured in *real-time* during surgery. Furthermore, we are more interested in drug *effect* (depth of hypnosis) rather than drug *concentration*. Hence, we consider a realistic model involving pharmacokinetics (drug concentration as a function of time) and pharmacodynamics (drug effect as a function of concentration) for control of anesthesia. Specifically, we use an electroencephalogram (EEG) signal as a measure of the hypnotic effect of propofol on the brain [123]. Since electroencephalography provides real-time monitoring of the central nervous system activity, it can be used to quantify levels of consciousness and hence is amenable for feedback (closed-loop) control in general anesthesia. Furthermore, we use the Bispectral Index (BIS), an EEG indicator, as a measure of hypnotic effect [99]. This index quantifies the nonlinear relationships between the component frequencies in the

electroencephalogram, as well as analyzing their phase and amplitude.

The BIS signal is related to drug concentration by the empirical relationship

$$\mathrm{BIS}(c_{\mathrm{eff}}) = \mathrm{BIS}_0 \left(1 - \frac{c_{\mathrm{eff}}^{\gamma}}{c_{\mathrm{eff}}^{\gamma} + \mathrm{EC}_{50}^{\gamma}}\right), \tag{4.66}$$

where BIS_0 denotes the base line (awake state) value and, by convention, is typically assigned a value of 100, c_{eff} is the propofol concentration in grams/liter in the effect site compartment (brain), EC_{50} is the concentration at half maximal effect and represents the patient's sensitivity to the drug, and γ determines the degree of nonlinearity in (4.66). Here, the effect-site compartment is introduced to account for finite equilibration time between the central compartment concentration and the central nervous system concentration [115].

The effect-site compartment concentration is related to the concentration in the central compartment by the first-order model [115]

$$\dot{c}_{\mathrm{eff}}(t) = a_{\mathrm{eff}}(x_1(t)/V_{\mathrm{c}} - c_{\mathrm{eff}}(t)), \quad c_{\mathrm{eff}}(0) = x_1(0)/V_{\mathrm{c}}, \quad t \geq 0, \tag{4.67}$$

where a_{eff} in min^{-1} is an unknown positive time constant and V_{c} is the volume in liters of the central compartment. As noted in [94], V_{c} can be approximately calculated by $V_{\mathrm{c}} = (0.159\,\mathrm{l/kg})(M\,\mathrm{kg})$, where M is the mass in kilograms of the patient, and a_{eff} is obtained as $a_{\mathrm{eff}} = 0.693/2.2\ \mathrm{min} = 0.3150\ \mathrm{min}^{-1}$, where 2.2 min is the half-time k_{e0} value reported in [130]. In reality, the effect-site compartment equilibrates with the central compartment in a matter of a few minutes. However, in the case of significant blood loss, this equilibration can be slowed down. The parameters a_{eff}, EC_{50} and γ are determined by data fitting and vary from patient to patient. BIS index values of 0 and 100 correspond, respectively, to an *isoelectric* EEG signal (no cerebral electrical activity) and an EEG signal of a fully conscious patient; the range between 40 and 60 indicates a moderate hypnotic state [39].

In the following numerical simulation we set $\mathrm{EC}_{50} = 3.4$ μg/ml, $\gamma = 3$, and $\mathrm{BIS}_0 = 100$, so that the BIS signal is shown in Figure 4.8. The values for the pharmacodynamic parameters (EC_{50}, γ) are within the typical range of those observed for ligand-receptor binding [33, 78]. The target (desired) BIS value, $\mathrm{BIS}_{\mathrm{target}}$, is set at 50. In this case, the linearized BIS function about the target BIS value is given by

$$\begin{aligned}\mathrm{BIS}(c_{\mathrm{eff}}) &\simeq \mathrm{BIS}(\mathrm{EC}_{50}) - \mathrm{BIS}_0 \cdot \mathrm{EC}_{50}^{\gamma} \cdot \left.\frac{\gamma c_{\mathrm{eff}}^{\gamma-1}}{(c_{\mathrm{eff}}^{\gamma} + \mathrm{EC}_{50}^{\gamma})^2}\right|_{c_{\mathrm{eff}}=\mathrm{EC}_{50}} \cdot (c_{\mathrm{eff}} - \mathrm{EC}_{50}) \\ &= b_{\mathrm{BIS}} + k_{\mathrm{BIS}} \cdot c_{\mathrm{eff}}, \end{aligned} \tag{4.68}$$

where $b_{\mathrm{BIS}} = 125$ and $k_{\mathrm{BIS}} = -22.06$ ml/μg.

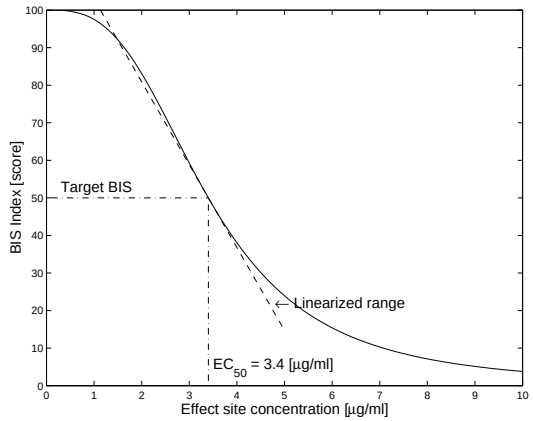

Figure 4.8: BIS index versus effect site concentration

During surgery hemorrhage and *hemodilution* (i.e., increase in fluid content of blood resulting in reduced concentration of red blood cells in the blood) often take place which can affect the concentration of a drug in the blood, and hence, the level of patient sedation [79]. Hence, it is of paramount importance that the adaptive controller is able to compensate for the effects of hemorrhage and hemodilution. In particular, during hemorrhage when perfusion pressure falls, perfusion of certain regions (e.g., brain and heart) takes precedence over perfusion of other regions, and blood flow to these other regions is significantly slowed down. Such an effect can be modeled by decreasing the transfer coefficients between compartments, as well as

adding an exogenous disturbance to the baseline pharmacokinetic system to account for the effect of hemorrhage on the dynamics of the mass of propofol in the central compartment. The system equations (4.63)–(4.65) then take the form of (4.6).

To develop a disturbance model for hemorrhage and hemodilution on the dynamics of the mass of propofol, we assume that the bleeding is arterial and the size of the holes in the bleeding vessels remain constant during the period of hemorrhaging. Assuming that blood loss occurs only through the central compartment, we model the disturbance signal (4.8) as $d(x(t),t) = [\beta c(t) BL(x_1(t),t), 0, 0]^{\mathrm{T}}$, where β is a dimensionless unknown positive constant coefficient, $c(t) = x_1(t)/V_{\mathrm{c}}(t)$ is the concentration of propofol in the central compartment in grams/liter, and $BL(x_1(t),t)$ is the rate of blood loss in liters/min.

Using [77], we model blood loss rate as

$$BL(x_1(t),t) = \frac{BL_0}{MAP_0}\sigma(t) MAP(x_1(t),t), \quad t \geq 0, \tag{4.69}$$

where BL_0 is the initial rate of blood loss, MAP_0 is the initial mean arterial pressure, $MAP(x_1(t),t)$ is the mean arterial pressure at time $t \geq 0$, and $\sigma : [0, \infty) \to \{0, 1\}$ is a piecewise switching function describing a particular hemorrhage scenario, including hemorrhage start and stop times. Note that the blood pressure is a function of propofol mass in the central compartment. Using the linear approximation of the BIS index given by (4.68), the disturbance signal can be rewritten in the form $d(x(t),t) = [\psi^* w(x(t),t), 0, 0]^{\mathrm{T}}$, where $\psi^* = \beta \frac{BL_0}{k_{\mathrm{BIS}}}$ is an unknown parameter and $w(x(t),t) = \sigma(t)\frac{MAP(x_1(t),t)}{MAP_0}(\mathrm{BIS}(t) - b_{\mathrm{BIS}})$. In the numerical simulation the dimensionless parameter β is set to 8.25, BL_0 is 0.216 liter/min, and $MAP_0 = 80$ mm Hg.

In order to proceed we need to develop a model for the relationships between blood pressure, blood volume, and propofol concentration. By definition (of vascular

resistance), mean arterial blood pressure is given by [6]

$$MAP(x_1(t),t) = CO(x_1(t),t) \times SVR(x_1(t),t) + CVP(t), \quad t \geq 0, \tag{4.70}$$

where $CO(x_1(t),t)$ is cardiac output (the volume of blood the heart pumps per minute), $SVR(x_1(t),t)$ is systemic vascular resistance (an index of arteriolar compliance or constriction throughout the body), and $CVP(t)$ is central venous pressure (the venous pressure of the right atrium of the heart). Since $CVP(\cdot)$ is usually an order of magnitude less than mean arterial pressure, (4.70) can be approximated as

$$MAP(x_1(t),t) = CO(x_1(t),t) \times SVR(x_1(t),t), \quad t \geq 0. \tag{4.71}$$

Since cardiac output is equal to the product of heart rate HR and stroke volume SV (the volume of blood pumped per heart beat) it follows that

$$MAP(x_1(t),t) = HR(x_1(t),t) \times SV(x_1(t),t) \times SVR(x_1(t),t), \quad t \geq 0. \tag{4.72}$$

If the contractile strength of the heart were to remain constant during hemorrhage, to a first order approximation, stroke volume can be modeled as

$$SV(x_1(t),t) = (SV_0 \times BV(t))/BV_0, \quad t \geq 0, \tag{4.73}$$

where SV_0 is the baseline stroke volume, $BV(t)$ is the blood volume during hemorrhage, and BV_0 is the baseline blood volume.

Using (4.72) and (4.73) it follows that mean arterial pressure is proportional to blood volume. However, there are physiological compensatory mechanisms that act to maintain blood pressure in the face of hemorrhage. The autonomic nervous system responds to blood loss with an increase in sympathetic nervous tone leading to an increase in both heart rate and systematic vascular resistance, and also the contractile strength of the heart. In otherwise healthy conscious individuals, these mechanisms are so effective that blood pressure can be maintained even after significant blood loss.

However, in the anesthetized individual, the situation is more complex as anesthetic agents, including propofol, blunt these compensatory mechanisms. Thus, for our simulation we must consider the relationship between blood loss and blood pressure to be a spectrum with two extremes; namely, ranging from completely effective compensatory mechanisms with the blood pressure maintained at baseline levels despite blood loss, to completely blunted compensatory mechanisms in which blood pressure is proportional to the blood volume. To our knowledge, this relationship has never undergone mathematical modeling.

Given its nearly ubiquitous value for modeling biological phenomena, we believe that using a modified Hill equation is a plausible approach for modeling the relationship between blood pressure, blood volume, and propofol concentration. Specifically, for our simulations we assume that

$$MAP(x_1(t),t) = MAP_0 - \left[MAP_0 - \frac{MAP_0}{BV_0}BV(t)\right] \times \frac{c^\alpha(t)}{c^\alpha(t) + C_{50}^\alpha}, \quad t \geq 0, \quad (4.74)$$

where $c(t)$ is propofol concentration in the central compartment, C_{50} is an empirical constant which defines the midpoint of the relationship between propofol concentration and the blunting of compensatory mechanisms for the maintenance of blood pressure, and α is an empirical constant that describes the steepness of this relationship. Note that if C_{50} is zero, compensatory mechanisms are totally ineffective and mean arterial pressure is proportional to blood volume, while if C_{50} is large, blood pressure is largely maintained despite hemorrhage. We emphasize that this is a hypothetical relationship which we postulate in order to proceed with simulations. While the relationship is hypothetical, it is biologically plausible and by appropriate choices of the empirical constants C_{50} and α, the spectrum of relationship between blood pressure, blood loss, and propofol concentration may be explored. In order to account for the two extremes between blood pressure being proportional to blood volume and blood pressure maintained at baseline levels despite blood loss, we have performed

simulations using multiple values of C_{50} and α with C_{50} ranging from 0.5 to 10 in increments of 0.1 and α ranging from 2 to 8 in increments of 0.5. Our numerical study showed imperceptible differences indicating that the proposed disturbance rejection algorithm is very robust. In the simulation shown below we set $C_{50} = 2\mu$g/ml and $\alpha = 3$. Finally, we note that in actual surgery the mean arterial pressure is measured and does not need to be modeled.

The dynamic behavior of the blood volume components involving the red blood cell volume $y_1(t)$ and the plasma volume $y_2(t)$ can be described by [77]

$$\dot{y}_1(t) = r(t) - y_1(t)BL(x_1(t), t)/BV(t), \quad y_1(0) = y_{10}, \quad t \geq 0 \tag{4.75}$$

$$\dot{y}_2(t) = CL(t) + CR(t) + TRANS(t) - y_2(t)BL(x_1(t), t)/BV(t), \quad y_2(0) = y_{20}, \tag{4.76}$$

where $r(t)$ is the packed red blood cell infusion rate, $CL(t)$ is the colloid infusion rate, $CR(t)$ is the crystalloid infusion rate, and $TRANS(t)$ represents the effect of the Starling's transcapillary refill [77], $BL(x_1(t), t)$ is the rate of blood loss in liters/min, and $BV(t)$ is the blood volume in the central compartment, which can be approximated by

$$BV(t) = y_1(t) + y_2(t), \quad t \geq 0. \tag{4.77}$$

For our simulation we assume that the initial blood volume BV_0 is 5 liters. The initial red blood cell volume y_{10} is assumed to be 45% of BV_0 and the initial plasma volume y_{20} is 55% of BV_0. The time histories of the blood loss rate, as well as the red blood cell and crystalloid infusion rates, and the Starling's transcapillary refill rate are shown in Figure 4.9. In the simulation we assume that the colloid infusion rate is zero. For the chosen parameters, the dynamics of blood volume $BV(t)$, as well as *hematocrit*, that is, the proportion of red blood cell volume to the total blood volume, and mean arterial pressure $MAP(x_1(t), t)$ are shown in Figure 4.10.

During actual surgery neither the mass of propofol $x_1(t)$ nor the concentration of propofol $c(t)$ in the central compartment can be measured in real time. Moreover, due to hemorrhage and hemodilution, the blood volume, and hence, the volume of the central compartment are not constant. As a result, the desired mass x_{d} of propofol in the central compartment is not a fixed set-point but rather a bounded unknown function of time. This makes the automated anesthesia control problem with hemorrhage and hemodilution effects more challenging than the automated anesthesia problem without modeling these effects [53]. However, using the BIS signal it is possible to achieve the desired level of hypnotic state. In particular, using the linearized BIS given by (4.68), and assuming that the concentrations of propofol in the effect site and central compartment are equal, it follows that

$$\mathrm{BIS}(c_{\mathrm{eff}}) - \mathrm{BIS}_{\mathrm{target}} \simeq k_{\mathrm{BIS}}(c(t) - c_{\mathrm{target}}) = \frac{k_{\mathrm{BIS}}}{V_{\mathrm{c}}(t)}(x_1(t) - x_{\mathrm{d}_1}(t)), \tag{4.78}$$

where the volume of the central compartment $V_{\mathrm{c}}(t)$ and the desired level of mass of propofol in the central compartment $x_{\mathrm{d}_1}(t)$ are bounded. Hence, the difference between the BIS index and target value of BIS index is approximately equal to the difference between the mass of propofol in the central compartment and its desired level multiplied by the bounded time-varying negative gain $\frac{k_{\mathrm{BIS}}}{V_{\mathrm{c}}(t)}$.

In light of the above discussion we use the controller architecture of Theorem 4.4 with $i = 1$, $x_1(t) - x_{\mathrm{d}_1} = \mathrm{BIS}_{\mathrm{target}} - \mathrm{BIS}(c_{\mathrm{eff}}(t))$, $q_1 = q$, $\hat{q}_1 = q_{\mathrm{BIS}_1}$, $\gamma_1 = q_{\mathrm{BIS}_2}$, where $q = 2.0 \times 10^{-8}$ g/min^2, $\hat{q}_{\mathrm{BIS}_1} = 1.0 \times 10^{-5}$ g/min^2, $\hat{q}_{\mathrm{BIS}_2} = 4.0 \times 10^{-3}$ g/min^2, $k(0) = 0$, $\phi(0) = 0.01$ g/min^{-1}, and $\psi(0) = 0$, for maintaining a desired constant level of depth of anesthesia while accounting for hemorrhage and hemodilution. It is important to note that during actual surgery the BIS signal is obtained directly from the EEG and not (4.66). Furthermore, since our adaptive controller only requires the error signal $\mathrm{BIS}(t) - \mathrm{BIS}_{\mathrm{target}}$ over the linearized range of (4.66), we do not require knowledge of the slope of the linearized equation (4.68), nor do we require knowledge

of the parameters γ and EC_{50}.

To numerically illustrate the efficacy of the proposed adaptive control law, we use the average set of pharmacokinetic parameters given in [42] for 29 patients. Specifically, we assume $M = 70$ kg, $a_{11} = 0.152$ min^{-1}, $a_{21} = 0.207$ min^{-1}, $a_{12} = 0.092$ min^{-1}, $a_{31} = 0.040$ min^{-1}, and $a_{13} = 0.0048$ min^{-1} [42]. Figures 4.11 and 4.12 show the central compartment and effect-site concentrations versus time, and the control, disturbance, and BIS signal versus time. Note that the effect site compartment equilibrates with the central compartment in a matter of several minutes. In addition, note that when the adaptive controller does not account for hemorrhage and hemodilution the BIS index drops dangerously low into the low 20's increasing the possibility of patient respiratory and cardiovascular collapse.

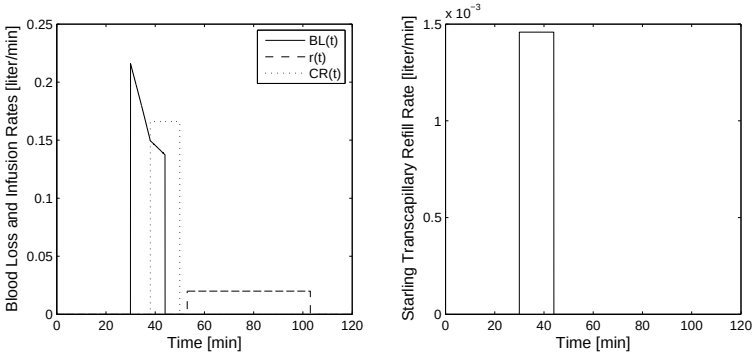

Figure 4.9: Blood loss rate, infusion rates and transcapillary refill rate versus time

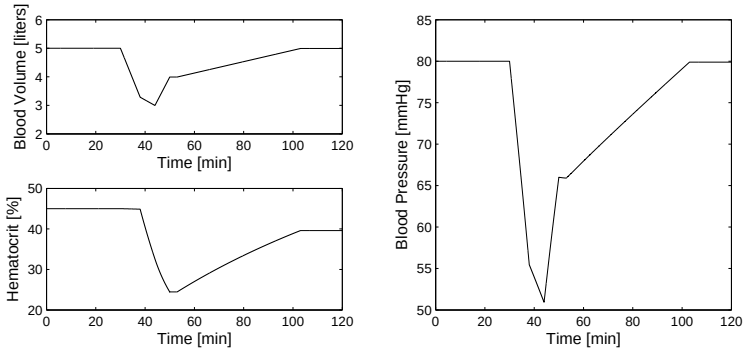

Figure 4.10: Blood volume, hematocrit, and mean arterial pressure versus time

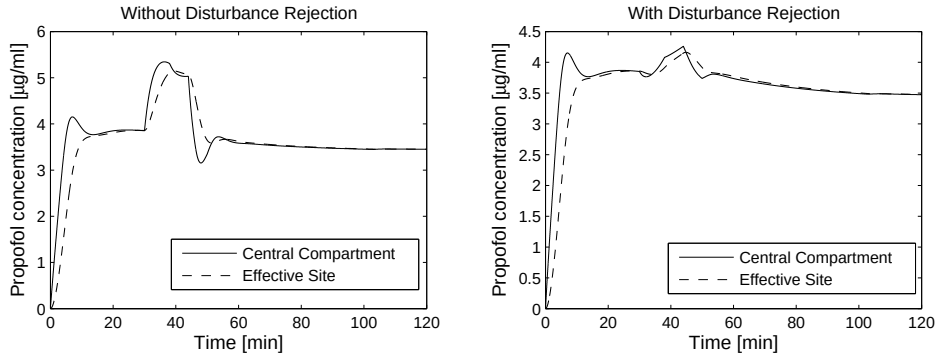

Figure 4.11: Concentration of propofol with and without disturbance rejection

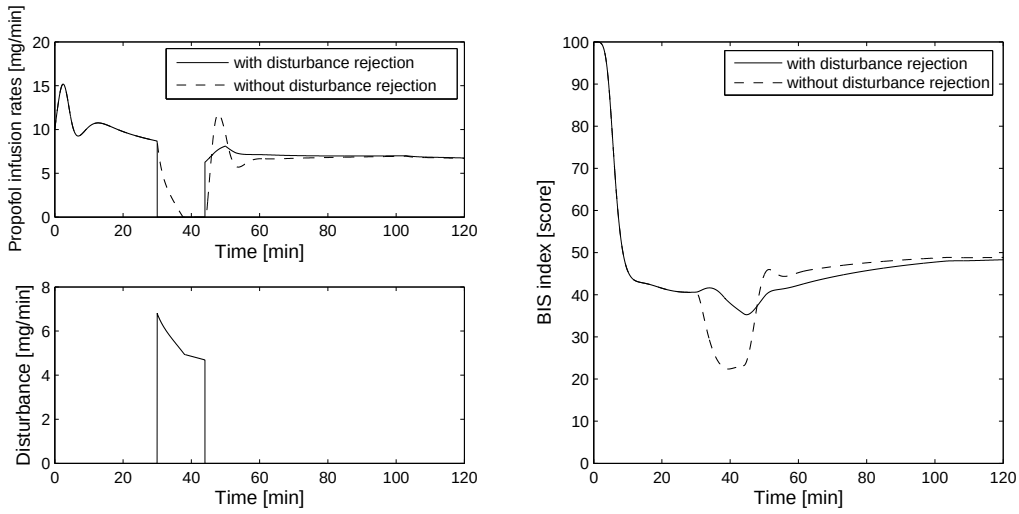

Figure 4.12: Control signal (infusion rate), system disturbance, and BIS index versus time

Chapter 5

Neuroadaptive Output Feedback Control for Automated Anesthesia with Noisy EEG Measurements

5.1. Introduction

The dosing of most drugs is a process of empirical administration of a low dose with observation of the biological effect and subsequent adjustment of the dose in the hopes of achieving the desired effect. This is true of anesthetic drugs, just as it is of chronically administered medications (for example, anti-hypertensive agents). In the acute environment of the operating room and intensive care unit (ICU), this can result in inefficient, and possibly even dangerous, titration of drug to the desired effect. There has been a long interest in use of the electroencephalograph (EEG) as an objective, quantitative measure of consciousness that could be used as a performance variable for closed-loop control of anesthesia [110]. Ever since the pioneering work of Bickford [16], it has been known that the EEG changes with the induction of anesthesia. Processed electroencephalogram algorithms have been extensively investigated as monitors of the level of consciousness in patients requiring surgical anesthesia [11, 16, 118, 119, 122]. However, the EEG is a complex of multiple time series and in earlier work it was difficult to identify one single aspect of the EEG signal that correlated with the clinical signs of anesthesia.

Subsequent to this early research there has been substantial progress in the development of processed EEG monitors that analyze the raw data to extract a single measure of the depth of anesthesia. The best known of these monitors is the bispectral or BIS monitor, which calculates a single composite EEG measure that is well correlated with the depth of anesthesia [41, 110, 120]. The BIS signal ranges from 0 (no cerebral electrical activity) to 100 (the normal awake state). Available evidence indicates that a BIS signal less than 55 is associated with lack of consciousness. While BIS monitoring has proven useful in the operating room environment, there have been inconsistencies reported and attempts to extend BIS monitoring for the evaluation of sedation outside of the operating room have been unsuccessful [107]. One of the key reasons for this is due to the fact that the signal-averaging algorithm within the BIS monitor ignores signal noise, and when there is excessive noise, the BIS monitor does not generate a signal.

It is widely appreciated that BIS monitoring, or for that matter, any EEG monitoring, can be fraught with error because of the potential for outside interference to produce an unfavorable signal-to-noise ratio yielding spurious results. Nonphysiologic artifactual signals may be generated from sources external to the patient that include lights, electric cautery devices, ventilators, pacemakers, patient warming systems, and electrical noise related to the many different kinds of monitors normally found in an operating room or ICU. Physiologic movements such as eye movements, myogenic activity, perspiration, and ventilation can produce artifactual increases in the BIS score. In particular, it is apparent that electromyographic (EMG) activity can spuriously increase the BIS score [75]. The co-administration of neuromuscular blockade eliminates artifacts from muscle movement, which can be superimposed on the BIS score; and this undoubtedly contributes to the widespread use and value of the BIS device during surgery. However, to extend this technology outside of the

operating room, or for that matter, to nonparalyzed patients in the operating room, further refinements are needed. In addition, if the BIS signal is to be used to quantify levels of consciousness for feedback control in general anesthesia, then the observation noise needs to be accounted for in the control system design process.

The challenge to the use of the BIS signal for closed-loop control of anesthesia is that the relationships between drug dose and tissue concentration (pharmacokinetics) and between tissue concentration and physiological effect (pharmacodynamics) is highly variable between individuals. In addition, observation noise in the BIS signal results in feedback measurement signals with high signal-to-noise ratios that need to be accounted for in the control algorithm. Adaptive feedback controllers seem particularly promising given this interpatient variability as well as BIS signal variation due to noise. In previous work, we have used nonnegative and compartmental dynamical systems theory to develop adaptive and neuroadaptive controllers for controlling the depth of anesthesia [46, 53, 54].

One of our initial efforts was the development of a direct adaptive control framework for uncertain nonlinear nonnegative and compartmental systems with nonnegative control inputs [53,54]. This framework is Lyapunov-based and guarantees partial asymptotic set-point regulation, that is, asymptotic setpoint stability with respect to part of the closed-loop system states associated with the physiological state variables. In addition, the adaptive controllers, which are constructed without requiring knowledge of the pharmacokinetic and pharmacodynamic parameters, provide a nonnegative control input for stabilization with respect to a given setpoint in the nonnegative orthant. Subsequently, we also developed a neuroadaptive output feedback control framework for uncertain nonlinear nonnegative and compartmental systems with nonnegative control inputs [46, 59]. This framework is also Lyapunov-based and guarantees ultimate boundedness of the error signals corresponding to the physical

system states in the face of interpatient pharmacokinetic and pharmacodynamic variability.

In a recent paper [8] the authors presented numerical and clinical results that compares and contrasts our adaptive control algorithm with our neural network adaptive control algorithm for controlling the depth of anesthesia in the operating theater during surgery. Specifically eleven clinical trials were performed with our adaptive control algorithm [54] and seven clinical trials were performed with our neural network algorithm [46] at the Northeast Georgia Medical Center in Gainesville, Georgia. The proposed automated anesthesia controllers demonstrated excellent regulation of unconsciousness and allowed for a safe and effective administration of the anesthetic agent propofol. However, the adaptive and neuroadaptive controllers presented in [8] did not account for measurement noise in the EEG signal. Clinical testing has clearly demonstrated the need for developing adaptive and neuroadaptive controllers that can address system measurement noise [8].

In this chapter, we extend the neuroadaptive controller framework developed in [46, 59] to address measurement noise in the BIS signal. Specifically, we develop an output feedback neural network adaptive controller that operates over a tapped delay line (TDL) of available input and filtered output measurements. The neuroadaptive laws for the neural network weights are constructed using a linear observer for the nominal normal form error system dynamics. The proposed framework is Lyapunov-based and guarantees ultimate boundness of the error signals. In addition, the nonnegative neuroadaptive controller guarantees that the physiological system states remain in the nonnegative orthant of the state space. Finally, we present numerical and clinical results for controlling the depth of anesthesia in the operating theater during surgery. The proposed automated anesthesia neuroadaptive controller demonstrates excellent regulation of unconsciousness and allows for a safe

and effective administration of the anesthetic agent propofol in the face of noisy EEG measurements.

5.2. Notation and Mathematical Preliminaries

In this section, we introduce notation, several definitions, and some key results concerning nonlinear nonnegative dynamical systems [13, 47] that are necessary for developing the main results of this chapter. The following definition introduces the notion of essentially nonnegative and compartmental vector fields [47].

Definition 5.1. Let $f = [f_1, \cdots, f_n]^{\mathrm{T}} : \mathcal{D} \subseteq \overline{\mathbb{R}}_+^n \to \mathbb{R}^n$. Then f is *essentially nonnegative* if $f_i(x) \geq 0$, for all $i = 1, \ldots, n$, and $x \in \overline{\mathbb{R}}_+^n$ such that $x_i = 0$, where x_i denotes the ith component of x. f is *compartmental* if f is essentially nonnegative and $\mathbf{e}^{\mathrm{T}} f(x) \leq 0$, $x \in \overline{\mathbb{R}}_+^n$.

Note that if $f(x) = Ax$, where $A \in \mathbb{R}^{n \times n}$, then f is essentially nonnegative if and only if A is essentially nonnegative, that is, $A_{(i,j)} \geq 0$, $i, j = 1, ..., n$, $i \neq j$, where $A_{(i,j)}$ denotes the (i, j)th entry of A.

In this chapter, we consider controlled nonlinear dynamical systems of the form

$$\dot{x}(t) = f(x(t)) + G(x(t))u(t), \ x(0) = x_0, \ t \geq 0, \tag{5.1}$$

where $x(t) \in \mathbb{R}^n$, $t \geq 0$, $u(t) \in \mathbb{R}^m$, $t \geq 0$, $f : \mathbb{R}^n \to \mathbb{R}^n$ is locally Lipschitz continuous and satisfies $f(0) = 0$, $G : \mathbb{R}^n \to \mathbb{R}^{n \times m}$ is continuous, and $u : [0, \infty) \to \mathbb{R}^m$ is piecewise continuous.

The following definition and proposition are needed for the main results of this chapter.

Definition 5.2. The nonlinear dynamical system given by (5.1) is *nonnegative*

if for every $x(0) \in \overline{\mathbb{R}}_+^n$ and $u(t) \geq\geq 0$, $t \geq 0$, the solution $x(t)$, $t \geq 0$, to (5.1) is nonnegative.

Proposition 5.1 [47]. The nonlinear dynamical system given by (5.1) is nonnegative if $f : \mathbb{R}^n \to \mathbb{R}^n$ is essentially nonnegative and $G(x) \geq\geq 0$, $x \in \overline{\mathbb{R}}_+^n$.

It follows from Proposition 5.1 that if $f(\cdot)$ is essentially nonnegative, then a nonnegative input signal $G(x(t))u(t)$, $t \geq 0$, is sufficient to guarantee the nonnegativity of the state of (5.1).

5.3. Neuroadaptive Output Feedback Control for Nonlinear Nonnegative Uncertain Systems

In this section, we consider the problem of characterizing neuroadaptive dynamic output feedback control laws for nonlinear nonnegative and compartmental uncertain dynamical systems to achieve *set-point* regulation in the nonnegative orthant. Specifically, consider the controlled square (i.e., the number of inputs is equal to the number of outputs) nonlinear uncertain dynamical system $\mathcal{G}$ given by

$$\dot{x}(t) = f(x(t)) + G(x(t))u(t), \ x(0) = x_0, \ t \geq 0, \tag{5.2}$$

$$y(t) = h(x(t)), \tag{5.3}$$

$$y_{\mathrm{n}}(t) = y(t) + n(t), \tag{5.4}$$

where $x(t) \in \mathbb{R}^n$, $t \geq 0$, is the state vector, $u(t) \in \mathbb{R}^m$, $t \geq 0$, is the control input, $y(t) \in \mathbb{R}^m$, $t \geq 0$, is the system output, $y_{\mathrm{n}}(t) \in \mathbb{R}^m$, $t \geq 0$, is the noisy system output, $n(t) \in \mathbb{R}^m$, $t \geq 0$, is a noise signal such that $\|n(t)\| \leq n^* < \infty$ for all $t \geq 0$, $f : \mathbb{R}^n \to \mathbb{R}^n$ is essentially nonnegative but otherwise unknown, $G : \mathbb{R}^n \to \mathbb{R}^{n \times m}$ is an unknown nonnegative input matrix function, and $h : \mathbb{R}^n \to \mathbb{R}^m$ is a nonnegative output function. We assume that $f(\cdot)$, $G(\cdot)$, and $h(\cdot)$ are smooth (at

least C^n mappings) and the control input $u(\cdot)$ in (5.2) is restricted to the class of *admissible controls* consisting of measurable functions such that $u(t) \in \mathbb{R}^m$, $t \geq 0$. Furthermore, we assume that the distribution spanned by the vector fields composed by the column vectors of $G(x)$, $x \in \mathbb{R}^n$, has a constant dimension and is involutive in a neighborhood of the equilibrium point of (5.2).

As discussed in Section 5.1, control (source) inputs of drug delivery systems for physiological and pharmacological processes are usually constrained to be nonnegative as are the system states. Hence, in this chapter we develop neuroadaptive dynamic output feedback control laws for nonnegative systems with nonnegative control inputs. Specifically, for a given desired set point $y_{\mathrm{d}} \in \overline{\mathbb{R}}_+^m$ and for a given $\varepsilon > 0$, our aim is to design a nonnegative control input $u(t)$, $t \geq 0$, predicated on the system measurement $y_{\mathrm{n}}(t)$, $t \geq 0$, such that $\|y(t) - y_{\mathrm{d}}\| < \varepsilon$ for all $t \geq T$, where $T \in [0, \infty)$, and $x(t) \geq\geq 0$, $t \geq 0$, for all $x_0 \in \overline{\mathbb{R}}_+^n$.

In this chapter, we assume that for the nonlinear dynamical system (5.2) and (5.3), the conditions for the existence of a globally defined diffeomorphism transforming (5.2) and (5.3) into a normal form [18, 67] are satisfied. Specifically, we assume that there exist a global diffeomorphism $\mathcal{T} : \mathbb{R}^n \to \mathbb{R}^n$ and C^n functions $f_\xi : \mathbb{R}^r \times \mathbb{R}^{n-r} \to \mathbb{R}^r$ and $f_z : \mathbb{R}^r \times \mathbb{R}^{n-r} \to \mathbb{R}^{n-r}$ such that, in the coordinates $\left[\xi^{\mathrm{T}},\ z^{\mathrm{T}}\right]^{\mathrm{T}} \triangleq \mathcal{T}(x)$, where $\xi \triangleq [y_1, \dot{y}_1, \cdots, y_1^{(r_1-2)}, \cdots, y_m, \dot{y}_m, \cdots, y_m^{(r_m-2)};\ y_1^{(r_1-1)}, \cdots, y_m^{(r_m-1)}] \in \mathbb{R}^r$, $y_i^{(r_i)}$ denotes the r_ith derivative of y_i, r_i denotes the relative degree of $\mathcal{G}$ with respect to the output y_i, $z \in \mathbb{R}^{n-r}$, and $r \triangleq r_1 + \cdots + r_m$ is the (vector) relative degree of $\mathcal{G}$, the nonlinear dynamical system $\mathcal{G}$ given by (5.2)–(5.4) is equivalent to

$$\dot{\xi}(t) = f_\xi(\xi(t), z(t)) + G_\xi(\xi(t), z(t))u(t), \quad \xi(0) = \xi_0, \quad t \geq 0, \tag{5.5}$$

$$\dot{z}(t) = f_z(\xi(t), z(t)), \quad z(0) = z_0, \tag{5.6}$$

$$y(t) = C\xi(t), \tag{5.7}$$

$$y_{\mathrm{n}}(t) = C\xi(t) + n(t), \tag{5.8}$$

where $\xi(t) \in \mathbb{R}^r$, $t \geq 0$, $z(t) \in \mathbb{R}^{n-r}$, $t \geq 0$,

$$f_\xi(\xi, z) = A\xi + \tilde{f}_{\mathrm{u}}(\xi, z),\ G_\xi(\xi, z) = \left[\begin{array}{c} 0_{(r-m)\times m} \\ \hat{G}(\tilde{x}) \end{array} \right], \tag{5.9}$$

$$A = \left[\begin{array}{c} A_0 \\ \hat{A} \end{array} \right], \quad \tilde{f}_{\mathrm{u}}(\xi, z) = \left[\begin{array}{c} 0_{(r-m)\times 1} \\ f_{\mathrm{u}}(\tilde{x}) \end{array} \right], \tag{5.10}$$

$\tilde{x} \triangleq [\xi^{\mathrm{T}}, z^{\mathrm{T}}]^{\mathrm{T}}$, $A_0 \in \mathbb{R}^{(r-m)\times r}$ is a known matrix of zeros and ones capturing the multivariable observable canonical form representation [24], $\hat{A} \in \mathbb{R}^{m\times r}$ is such that A is asymptotically stable, $f_{\mathrm{u}} : \mathbb{R}^n \to \mathbb{R}^m$ is an unknown function, $C \in \mathbb{R}^{m\times r}$ is a known matrix of zeros and ones capturing the system output, and $\hat{G} : \mathbb{R}^n \to \mathbb{R}^{m\times m}$ is an unknown matrix function such that $\det \hat{G}(\tilde{x}) \neq 0$, $\tilde{x} \in \mathbb{R}^n$. Furthermore, we assume that for a given $y_{\mathrm{d}} \in \overline{\mathbb{R}}_+^m$ there exist $z_{\mathrm{e}} \in \mathbb{R}^{n-r}$ and $u_{\mathrm{e}} \in \overline{\mathbb{R}}_+^m$ such that $x_{\mathrm{e}} \triangleq \mathcal{T}^{-1}(\tilde{x}_{\mathrm{e}}) \geq\geq 0$ and

$$0 = f_\xi(\xi_{\mathrm{e}}, z_{\mathrm{e}}) + G_\xi(\xi_{\mathrm{e}}, z_{\mathrm{e}})u_{\mathrm{e}}, \tag{5.11}$$

$$0 = f_z(\xi_{\mathrm{e}}, z_{\mathrm{e}}), \tag{5.12}$$

where $\tilde{x}_{\mathrm{e}} \triangleq [\xi_{\mathrm{e}}^{\mathrm{T}}, z_{\mathrm{e}}^{\mathrm{T}}]^{\mathrm{T}}$ and ξ_{e} is given with $y_i = y_{\mathrm{d}i}$, $i = 1, \ldots, m$, and $\dot{y}_i = \cdots = y_i^{(r_i-1)} = 0$, $i = 1, \ldots, m$. As we see in Section 5.4, the aforementioned assumptions are automatically satisfied for our clinical compartmental model.

To ensure that for a bounded state $\xi(t)$, $t \geq 0$, the dynamics given by (5.6) are bounded, we assume that (5.6) is input-to-state stable at $z(t) \equiv z_{\mathrm{e}}$ with $\xi(t) - \xi_{\mathrm{e}}$ viewed as the input; that is, there exist a class $\mathcal{KL}$ function $\eta(\cdot, \cdot)$ and a class $\mathcal{K}$ function $\gamma(\cdot)$ such that

$$\|z(t) - z_{\mathrm{e}}\| \leq \eta(\|z_0 - z_{\mathrm{e}}\|, t) + \gamma\left(\sup_{0\leq\tau\leq t} \|\xi(\tau) - \xi_{\mathrm{e}}\| \right), \tag{5.13}$$

where $\|\cdot\|$ denotes the Euclidean vector norm. Unless otherwise stated, henceforth we use $\|\cdot\|$ to denote the Euclidean vector norm. Note that $(\xi_{\mathrm{e}}, z_{\mathrm{e}}) \in \mathbb{R}^r \times \mathbb{R}^{n-r}$ is

an equilibrium point of (5.5) and (5.6) if and only if there exists $u_{\mathrm{e}} \in \overline{\mathbb{R}}_{+}^{m}$ such that (5.11) and (5.12) hold.

Finally, we assume that the functions $f_{\mathrm{u}}(\mathcal{T}(x)) - f_{\mathrm{u}}(\mathcal{T}(x_{\mathrm{e}})) - \hat{G}(\mathcal{T}(x_{\mathrm{e}}))u_{\mathrm{e}}$ and $\hat{G}(\mathcal{T}(x)) - \hat{B}$, where $\hat{B} \in \mathbb{R}^{m \times m}$, can be approximated over a compact set $\mathcal{D}_{\mathrm{c}} \subset \overline{\mathbb{R}}_{+}^{n}$ by a linear in the parameters neural network up to a desired accuracy. In this case, there exist $\varepsilon_1 : \mathbb{R}^n \to \mathbb{R}^m$ and $\varepsilon_2 : \mathbb{R}^n \to \mathbb{R}^{m \times m}$ such that $\|\varepsilon_1(x)\| < \varepsilon_1^*$ and $\|\varepsilon_2(x)\|_{\mathrm{F}} < \varepsilon_2^*$, $x \in \mathcal{D}_{\mathrm{c}}$, where $\varepsilon_1^* > 0$ and $\varepsilon_2^* > 0$, and

$$f_{\mathrm{u}}(\mathcal{T}(x)) - f_{\mathrm{u}}(\mathcal{T}(x_{\mathrm{e}})) - \hat{G}(\mathcal{T}(x_{\mathrm{e}}))u_{\mathrm{e}} = W_1^{\mathrm{T}}\hat{\sigma}_1(x) + \varepsilon_1(x), \tag{5.14}$$

$$\hat{G}(\mathcal{T}(x)) - \hat{B} = W_2^{\mathrm{T}}[I_m \otimes \hat{\sigma}_2(x)] + \varepsilon_2(x), \tag{5.15}$$

where $x \in \mathcal{D}_{\mathrm{c}}$, $W_1 \in \mathbb{R}^{s_1 \times m}$ and $W_2 \in \mathbb{R}^{ms_2 \times m}$ are optimal *unknown* (constant) weights that minimize the approximation errors over $\mathcal{D}_{\mathrm{c}}$, $\hat{\sigma}_1 : \mathbb{R}^n \to \mathbb{R}^{s_1}$ and $\hat{\sigma}_2 : \mathbb{R}^n \to \mathbb{R}^{s_2}$ are basis functions such that each component of $\hat{\sigma}_1(\cdot)$ and $\hat{\sigma}_2(\cdot)$ takes values between 0 and 1, and $\varepsilon_1(\cdot)$ and $\varepsilon_2(\cdot)$ are the modeling errors, and "$\otimes$" denotes Kronecker product. Note that $s_1 + s_2$ denotes the total number of basis functions or, equivalently, the number of nodes of the neural network.

Since $f_{\mathrm{u}}(\cdot)$ and $\hat{G}(\cdot)$ are continuous, we can choose $\hat{\sigma}_1(\cdot)$ and $\hat{\sigma}_2(\cdot)$ from a linear space $\mathcal{X}$ of continuous functions that forms an algebra and separates points in $\mathcal{D}_{\mathrm{c}}$. In this case, it follows from the Stone-Weierstrass theorem [111, p. 212] that $\mathcal{X}$ is a dense subset of the set of continuous functions on $\mathcal{D}_{\mathrm{c}}$. Now, as is the case in the standard neuroadaptive control literature [92], we can construct the signal $u_{\mathrm{ad}} = F(\hat{W}_1, \hat{W}_2, \hat{\sigma}_1(x), \hat{\sigma}_2(x))$, where $F : \mathbb{R}^{s_1 \times m} \times \mathbb{R}^{ms_2 \times m} \times \mathbb{R}^{s_1} \times \mathbb{R}^{s_2} \to \mathbb{R}^m$, involving the estimates of the optimal weights and basis functions as our adaptive control signal. It is important to note here that we assume that we know both the structure and the size of the approximator. This is a standard assumption in the neural network adaptive control literature. In online neural network training, the size and the structure of

the optimal approximator are not known and are often chosen by the rule that the larger the size of the neural network and the richer the distribution class of the basis functions over a compact domain, the tighter the resulting approximation error bounds ε_1^* and ε_2^*. This goes back to the Stone-Weierstrass theorem which only provides an existence result without any constructive guidelines.

Since the actual measurement $y_{\rm n}(t)$, $t \geq 0$, is noisy with $n(t)$, $t \geq 0$, representing a high-frequency noise signal, we use a filtered version of $y_{\rm n}(t)$, $t \geq 0$, in the control input $u(t)$, $t \geq 0$. Specifically, we design an asymptotically stable low-pass filter of the form

$$\dot{x}_{\rm f}(t) = A_{\rm f} x_{\rm f}(t) + B_{\rm f} y_{\rm n}(t), \quad x_{\rm f}(0) = x_{\rm f_0}, \quad t \geq 0, \tag{5.16}$$

$$y_{\rm f}(t) = C_{\rm f} x_{\rm f}(t), \tag{5.17}$$

where $A_{\rm f} \in \mathbb{R}^{n_{\rm f} \times n_{\rm f}}$ is Hurwitz and $B_{\rm f} \in \mathbb{R}^{n_{\rm f} \times m}$ and $C_{\rm f} \in \mathbb{R}^{m \times n_{\rm f}}$ are such that $\lim_{\omega \to \infty} |G_{(i,j)}(\jmath\omega)| = 0$, $i, j = 1, \ldots, m$, where $G_{(i,j)}(s)$ denotes the (i,j)th entry of the transfer function $G(s) \triangleq C_{\rm f}(sI_{n_{\rm f}} - A_{\rm f})^{-1} B_{\rm f}$. Here, we choose the matrices $A_{\rm f}$, $B_{\rm f}$, and $C_{\rm f}$ such that $C_{\rm f} A_{\rm f}^{-1} B_{\rm f} = -I_m$. In this case, for every $y_{\rm d} \in \overline{\mathbb{R}}_+^m$, there exists $x_{\rm f_e} \in \mathbb{R}^{n_{\rm f}}$ such that

$$0 = A_{\rm f} x_{\rm f_e} + B_{\rm f} y_{\rm d}, \tag{5.18}$$

$$y_{\rm d} = C_{\rm f} x_{\rm f_e}. \tag{5.19}$$

Note that since $A_{\rm f}$ is Hurwitz there exist positive-definite matrices $\hat{P} \in \mathbb{R}^{n_{\rm f} \times n_{\rm f}}$ and $\hat{R} \in \mathbb{R}^{n_{\rm f} \times n_{\rm f}}$ such that

$$0 = A_{\rm f}^{\rm T} \hat{P} + \hat{P} A_{\rm f} + \hat{R}. \tag{5.20}$$

In order to develop an *output* feedback neural network, we use the recent approach developed in [87] for reconstructing the system states via the system delayed inputs and filtered outputs. Specifically, we use a *memory unit* as a particular form of

a tapped delay line that takes a scalar time series input and provides an $(2mn - r)$-dimensional vector output consisting of the present values of the system filtered outputs and system inputs, and their $2(n-1)m - r$ delayed values given by

$$\begin{aligned}\zeta(t) \triangleq [&y_{\mathrm{f}_1}(t), y_{\mathrm{f}_1}(t-d), \ldots, y_{\mathrm{f}_1}(t-(n-1)d), \ldots, y_{\mathrm{f}_m}(t), y_{\mathrm{f}_m}(t-d), \ldots,\\ &y_{\mathrm{f}_m}(t-(n-1)d); u_1(t), u_1(t-d), \ldots, u_1(t-(n-r_1-1)d), \ldots,\\ &u_m(t), u_m(t-d), \ldots, u_m(t-(n-r_m-1)d)]^{\mathrm{T}}, \quad t \geq 0, \end{aligned} \tag{5.21}$$

where $d > 0$.

For the statement of our main result, define the projection operator $\mathrm{Proj}(\tilde{W}, Y)$ given by

$$\mathrm{Proj}(\tilde{W}, Y) \triangleq \begin{cases} Y, & \text{if } \mu(\tilde{W}) < 0, \\ Y, & \text{if } \mu(\tilde{W}) \geq 0 \text{ and } \mu'(\tilde{W})Y \leq 0, \\ Y - \frac{\mu' T(\tilde{W}) \mu'(\tilde{W}) Y}{\mu'(\tilde{W}) \mu' T(\tilde{W})} \mu(\tilde{W}), & \text{otherwise,} \end{cases}$$

where $\tilde{W} \in \mathbb{R}^{s \times m}$, $Y \in \mathbb{R}^{n \times m}$, $\mu(\tilde{W}) \triangleq \frac{\mathrm{tr}\, \tilde{W}^{\mathrm{T}} \tilde{W} - \tilde{w}_{\max}^2}{\varepsilon_{\tilde{W}}}$, $\tilde{w}_{\max} \in \mathbb{R}$ is the norm bound imposed on $\tilde{W}$, and $\varepsilon_{\tilde{W}} > 0$. Note that for a given matrix $\tilde{W} \in \mathbb{R}^{s \times m}$ and $Y \in \mathbb{R}^{n \times m}$, it follows that

$$\begin{aligned} &\mathrm{tr}[(\tilde{W} - W)^{\mathrm{T}}(\mathrm{Proj}(\tilde{W}, Y) - Y)] \\ &= \sum_{i=1}^{n} [\mathrm{col}_i(\tilde{W} - W)]^{\mathrm{T}} [\mathrm{Proj}(\mathrm{col}_i(\tilde{W}), \mathrm{col}_i(Y)) - \mathrm{col}_i(Y)] \\ &\leq 0, \end{aligned} \tag{5.22}$$

where $\mathrm{col}_i(X)$ denotes the ith column of the matrix X.

Assumption 5.1. For a given $y_{\mathrm{d}} \in \overline{\mathbb{R}}_+^m$ assume there exist nonnegative vectors $x_{\mathrm{e}} \in \overline{\mathbb{R}}_+^n$ and $u_{\mathrm{e}} \in \overline{\mathbb{R}}_+^m$ such that

$$0 = f(x_{\mathrm{e}}) + G(x_{\mathrm{e}}) u_{\mathrm{e}}, \tag{5.23}$$

$$y_{\mathrm{d}} = h(x_{\mathrm{e}}). \tag{5.24}$$

Furthermore, assume that the equilibrium point x_{e} of (5.2) is globally asymptotically stable and nonnegative with $u(t) \equiv u_{\mathrm{e}}$. Finally, assume that there exists a global diffeomorphism $\mathcal{T} : \mathbb{R}^n \to \mathbb{R}^n$ such that $\mathcal{G}$ can be transformed into the normal form given by (5.5) and (5.6), and (5.6) is input-to-state stable at z_{e} with $\xi(t) - \xi_{\mathrm{e}}$ viewed as the input.

Consider the neuroadaptive output feedback control law given by

$$u(t) = \begin{cases} \hat{u}(t), & \text{if } \hat{u}(t) \geq\geq 0, \\ 0, & \text{otherwise,} \end{cases} \tag{5.25}$$

where

$$\hat{u}(t) = -\left(\hat{B} + \hat{W}_2^{\mathrm{T}}(t)[I_m \otimes \sigma_2(\zeta(t))]\right)^{-1} \hat{W}_1^{\mathrm{T}}(t)\sigma_1(\zeta(t)), \tag{5.26}$$

$\hat{B} \in \mathbb{R}^{m \times m}$ is nonsingular, $\zeta(t)$, $t \geq 0$, is given by (5.21), $\sigma_1 : \mathbb{R}^n \to \mathbb{R}^{s_1}$ and $\sigma_2 : \mathbb{R}^n \to \mathbb{R}^{s_2}$ are basis functions such that each component of $\sigma_1(\cdot)$ and $\sigma_2(\cdot)$ takes values between 0 and 1, $\hat{W}_1(t) \in \mathbb{R}^{s_1 \times m}$, $t \geq 0$, and $\hat{W}_2(t) \in \mathbb{R}^{ms_2 \times m}$, $t \geq 0$. Here, the update laws satisfy

$$\dot{\hat{W}}_1(t) = Q_1 \mathrm{Proj}[\hat{W}_1(t), -\sigma_1(\zeta(t))\xi_{\mathrm{c}}^{\mathrm{T}}(t)\tilde{P}B_0], \quad \hat{W}_1(0) = \hat{W}_{10}, \quad t \geq 0, \tag{5.27}$$

$$\dot{\hat{W}}_2(t) = Q_2 \mathrm{Proj}[\hat{W}_2(t), -[I_m \otimes \sigma_2(\zeta(t))]u(t)\xi_{\mathrm{c}}^{\mathrm{T}}(t)\tilde{P}B_0], \quad \hat{W}_2(0) = \hat{W}_{20}, \tag{5.28}$$

where $Q_1 \in \mathbb{R}^{s_1 \times s_1}$ and $Q_2 \in \mathbb{R}^{ms_2 \times ms_2}$ are positive definite matrices, $\tilde{P} \in \mathbb{R}^{r \times r}$ is a positive-definite solution of the Lyapunov equation

$$0 = (A - LC)^{\mathrm{T}}\tilde{P} + \tilde{P}(A - LC) + \tilde{R}, \tag{5.29}$$

where $\tilde{R} > 0$, and $\xi_{\mathrm{c}}(t)$, $t \geq 0$, is the solution to the estimator dynamics

$$\dot{\xi}_{\mathrm{c}}(t) = A\xi_{\mathrm{c}}(t) + L(y_{\mathrm{f}}(t) - y_{\mathrm{c}}(t) - y_{\mathrm{d}}), \quad \xi_{\mathrm{c}}(0) = \xi_{\mathrm{c}0}, \quad t \geq 0, \tag{5.30}$$

$$y_{\mathrm{c}}(t) = C\xi_{\mathrm{c}}(t), \tag{5.31}$$

where $\xi_{\mathrm{c}}(t) \in \mathbb{R}^r$, $t \geq 0$, $A \in \mathbb{R}^{r \times r}$ is given by (5.10), $L \in \mathbb{R}^{r \times m}$ is such that $A - LC$ is Hurwitz, $y_{\mathrm{f}}(t)$, $t \geq 0$, is the output of the filter (5.16) and (5.17), and

$B_0 \triangleq [0_{m\times(r-m)}, I_m]^{\mathrm{T}}$. For the statement of the next result recall the definition of ultimate boundedness given in [48, p. 241].

Theorem 5.1. Consider the nonlinear uncertain dynamical system $\mathcal{G}$ given by (5.2) and (5.3) with $u(t)$, $t \geq 0$, given by (5.25). Assume Assumption 5.1 holds, $\lambda_{\min}(RP^{-1}) > 1$, $\lambda_{\min}(\tilde{R}\tilde{P}^{-1}) > 1$, and $\lambda_{\min}(\hat{R}) > \|\hat{P}B_{\mathrm{f}}CP^{-1/2}\|$, where $\hat{P} \in \mathbb{R}^{n_{\mathrm{f}}\times n_{\mathrm{f}}}$, $\tilde{P} \in \mathbb{R}^{r\times r}$, and $P \in \mathbb{R}^{r\times r}$ are the positive-definite solutions of the Lyapunov equations (5.20), (5.29), and

$$0 = A^{\mathrm{T}}P + PA + R, \tag{5.32}$$

where $R > 0$. Then there exists a compact positively invariant set $\mathcal{D}_\alpha \subset \mathbb{R}^n \times \mathbb{R}^r \times \mathbb{R}^{s_1\times m} \times \mathbb{R}^{ms_2\times m} \times \mathbb{R}^{n_{\mathrm{f}}}$ such that $(x_{\mathrm{e}}, 0, W_1, W_2, x_{\mathrm{f_e}}) \in \mathcal{D}_\alpha$, where $W_1 \in \mathbb{R}^{s_1\times m}$ and $W_2 \in \mathbb{R}^{ms_2\times m}$, and the solution $(x(t), \xi_{\mathrm{c}}(t), \hat{W}_1(t), \hat{W}_2(t), x_{\mathrm{f}}(t))$, $t \geq 0$, of the closed-loop system given by (5.2), (5.16), (5.17), (5.25), (5.27), (5.28), (5.30), and (5.31) is ultimately bounded for all $(x(0), \xi_{\mathrm{c}}(0), \hat{W}_1(0), \hat{W}_2(0), x_{\mathrm{f}}(0)) \in \mathcal{D}_\alpha$ with ultimate bound $\|y(t) - y_{\mathrm{d}}\|^2 < \varepsilon$, $t \geq T$, where

$$\begin{aligned}
\varepsilon > \Big[&(\nu^{\frac{1}{2}}(\lambda_{\min}(RP^{-1}) - 1)^{-\frac{1}{2}} + \alpha_1)^2 + (\nu^{\frac{1}{2}}\lambda_{\min}^{-\frac{1}{2}}(\tilde{R}\tilde{P}^{-1}) + \alpha_2)^2 \\
&+(\nu^{\frac{1}{2}}(\lambda_{\min}(\hat{R}) - \|\hat{P}B_{\mathrm{f}}CP^{-1/2}\|)^{-\frac{1}{2}} + \alpha_3)^2 + \lambda_{\max}(Q_1^{-1})\hat{w}_{1\max}^2 \\
&+\lambda_{\max}(Q_2^{-1})\hat{w}_{2\max}^2\Big]^{\frac{1}{2}},
\end{aligned} \tag{5.33}$$

$$\begin{aligned}
\nu \triangleq\ &(\lambda_{\min}(RP^{-1}) - 1)\alpha_1^2 + \lambda_{\min}(\tilde{R}\tilde{P}^{-1})\alpha_2^2 + \Big(\lambda_{\min}(\hat{R}) - \|\hat{P}B_{\mathrm{f}}CP^{-1/2}\|\Big)\alpha_3^2, \\
&+ \Big(\lambda_{\min}(\hat{R}) - \|\hat{P}B_{\mathrm{f}}CP^{-1/2}\|\Big)\alpha_3^2,
\end{aligned} \tag{5.34}$$

$$\begin{aligned}
\alpha_1 \triangleq\ &\Big(\|P^{-1/2}(P + \tilde{P})B_0\|[\sqrt{s_1}\hat{w}_{1\max} + \sqrt{ms_2}\hat{w}_{2\max}u^*] + (2\sqrt{s_1}\hat{w}_{1\max} \\
&+\sqrt{ms_2}\hat{w}_{2\max}u^* + \varepsilon_1^* + \varepsilon_2^*u^*)\|P^{1/2}B_0\|\Big)(\lambda_{\min}(RP^{-1}) - 1)^{-1},
\end{aligned} \tag{5.35}$$

$$\alpha_2 \triangleq \lambda_{\min}^{-1}(\tilde{R}\tilde{P}^{-1})\Big[2\sqrt{s_1}\hat{w}_{1\max} + \sqrt{ms_2}\hat{w}_{2\max}u^* + (\varepsilon_1^* + \varepsilon_2^*u^*)\Big]\|\tilde{P}^{1/2}B_0\|, \tag{5.36}$$

$$\alpha_3 \triangleq n^*\|\hat{P}B_{\mathrm{f}}\|\Big(\lambda_{\min}(\hat{R}) - \|\hat{P}B_{\mathrm{f}}CP^{-1/2}\|\Big)^{-1}, \tag{5.37}$$

$u^* \triangleq \sup_{t\geq 0}\|u(t)\|$, $\hat{w}_{i\max}$, $i = 1, 2$, are norm bounds imposed on $\hat{W}_i$, and $\tilde{P} \in \mathbb{R}^{r\times r}$ is

the positive-definite solution of the Lyapunov equations (5.29). Furthermore, $u(t) \geq\geq 0$, $t \geq 0$, and $x(t) \geq\geq 0$, $t \geq 0$, for all $x_0 \in \overline{\mathbb{R}}_+^n$.

Proof. First, define

$$\hat{W}_{1u}(t) \triangleq \begin{cases} \hat{W}_1(t), & \text{if } \hat{u}(t) \geq\geq 0, \\ 0, & \text{otherwise.} \end{cases} \tag{5.38}$$

Next, defining $e_\xi(t) \triangleq \xi(t) - \xi_{\mathrm{e}}$, $e_z(t) \triangleq z(t) - z_{\mathrm{e}}$, $\tilde{\xi}(t) \triangleq \xi_{\mathrm{c}}(t) - e_\xi(t)$, and $\tilde{x}_{\mathrm{f}}(t) \triangleq x_{\mathrm{f}}(t) - x_{\mathrm{f_e}}$, and using (5.5)–(5.12), (5.14), (5.15), and (5.25) it follows from (5.5), (5.6), (5.30), and (5.16)–(5.19) that

$$\begin{aligned}
\dot{e}_\xi(t) = {} & Ae_\xi(t) + A\xi_{\mathrm{e}} + \tilde{f}_{\mathrm{u}}(\xi(t), z(t)) + G_\xi(\xi(t), z(t))u(t) \\
= {} & Ae_\xi(t) + B_0[f_{\mathrm{u}}(\mathcal{T}(x(t))) - f_{\mathrm{u}}(\mathcal{T}(x_{\mathrm{e}})) - \hat{G}(\mathcal{T}(x_{\mathrm{e}}))u_{\mathrm{e}}] + B_0\hat{G}(\mathcal{T}(x(t)))u(t) \\
& + B_0\left(\hat{B} + \hat{W}_2^{\mathrm{T}}(t)[I_m \otimes \sigma_2(\zeta(t))]\right) \\
& \cdot \left(-u(t) - \left(\hat{B} + \hat{W}_2^{\mathrm{T}}(t)[I_m \otimes \sigma_2(\zeta(t))]\right)^{-1} \hat{W}_{1u}^{\mathrm{T}}(t)\sigma_1(\zeta(t))\right) \\
= {} & Ae_\xi(t) + B_0[W_1^{\mathrm{T}}\hat{\sigma}_1(x(t)) + \varepsilon_1(x(t))] + B_0\left(W_2^{\mathrm{T}}[I_m \otimes \hat{\sigma}_2(x(t))] + \varepsilon_2(x(t))\right)u(t) \\
& - B_0\hat{W}_2^{\mathrm{T}}(t)[I_m \otimes \sigma_2(\zeta(t))]u(t) - B_0\hat{W}_{1u}^{\mathrm{T}}(t)\sigma_1(\zeta(t)) \\
= {} & Ae_\xi(t) + B_0[W_1^{\mathrm{T}}\hat{\sigma}_1(x(t)) - W_1^{\mathrm{T}}\sigma_1(\zeta(t)) + W_1^{\mathrm{T}}\sigma_1(\zeta(t)) + \varepsilon_1(x(t))] \\
& + B_0\left(W_2^{\mathrm{T}}[I_m \otimes \hat{\sigma}_2(x(t))] - W_2^{\mathrm{T}}[I_m \otimes \sigma_2(\zeta(t))] + W_2^{\mathrm{T}}[I_m \otimes \sigma_2(\zeta(t))]\right. \\
& \left. + \varepsilon_2(x(t))\right)u(t) - B_0\hat{W}_2^{\mathrm{T}}(t)[I_m \otimes \sigma_2(\zeta(t))]u(t) - B_0\hat{W}_{1u}^{\mathrm{T}}(t)\sigma_1(\zeta(t)) \\
= {} & Ae_\xi(t) - B_0\tilde{W}_1^{\mathrm{T}}(t)\sigma_1(\zeta(t)) - B_0\tilde{W}_2^{\mathrm{T}}(t)[I_m \otimes \sigma_2(\zeta(t))]u(t) \\
& + B_0(\hat{W}_1(t) - \hat{W}_{1u}(t))^{\mathrm{T}}\sigma_1(\zeta(t)) + B_0\varepsilon_1(x(t)) + B_0\varepsilon_2(x(t))u(t) \\
& + B_0W_1^{\mathrm{T}}[\hat{\sigma}_1(x(t)) - \sigma_1(\zeta(t))] + B_0W_2^{\mathrm{T}}\left[I_m \otimes (\hat{\sigma}_2(x(t)) - \sigma_2(\zeta(t)))\right]u(t), \\
& \qquad\qquad e_\xi(0) = \xi_0 - \xi_{\mathrm{e}}, \quad t \geq 0,
\end{aligned} \tag{5.39}$$

$$\dot{e}_z(t) = \tilde{f}_z(e_\xi(t), e_z(t)), \quad e_z(0) = z_0 - z_{\mathrm{e}}, \tag{5.40}$$

and

$$\dot{\tilde{\xi}}(t) = \dot{\xi}_{\mathrm{c}}(t) - \dot{e}_\xi(t)$$

$$
\begin{aligned}
&= \tilde{A}\tilde{\xi}(t) + B_0\tilde{W}_1^{\mathrm{T}}(t)\sigma_1(\zeta(t)) + B_0\tilde{W}_2^{\mathrm{T}}(t)[I_m \otimes \sigma_2(\zeta(t))]u(t) \\
&\quad -B_0(\hat{W}_1(t) - \hat{W}_{1u}(t))^{\mathrm{T}}\sigma_1(\zeta(t)) - B_0\varepsilon_1(x(t)) + B_0\varepsilon_2(x(t))u(t) \\
&\quad -B_0W_1^{\mathrm{T}}[\hat{\sigma}_1(x(t)) - \sigma_1(\zeta(t))] - B_0W_2^{\mathrm{T}}\left[I_m \otimes (\hat{\sigma}_2(x(t)) - \sigma_2(\zeta(t)))\right]u(t) \\
&\quad +LC_{\mathrm{f}}\tilde{x}_{\mathrm{f}}(t) - LCe_\xi(t), \qquad\qquad \tilde{\xi}(0) = \xi_{\mathrm{c}0} - \xi_0 + \xi_{\mathrm{e}}, \qquad (5.41)
\end{aligned}
$$

where $\tilde{A} \triangleq A - LC$, $\tilde{f}_z(e_\xi, e_z) \triangleq f_z(e_\xi + x_{\mathrm{e}}, e_z + z_{\mathrm{e}})$, $\tilde{W}_i(t) \triangleq \hat{W}_i(t) - W_i$, $i = 1, 2$, and $\hat{\sigma}_1 : \mathbb{R}^n \to \mathbb{R}^{s_1}$ and $\hat{\sigma}_2 : \mathbb{R}^n \to \mathbb{R}^{s_2}$ are such that each component of $\hat{\sigma}_1(\cdot)$ and $\hat{\sigma}_2(\cdot)$ takes values between 0 and 1.

To show ultimate boundedness of the closed-loop system (5.27), (5.28), (5.39)–(5.41), consider the Lyapunov-like function

$$
V(e_\xi, e_z, \tilde{\xi}, \tilde{W}_1, \tilde{W}_2, \tilde{x}_{\mathrm{f}}) = e_\xi^{\mathrm{T}}Pe_\xi + \tilde{\xi}^{\mathrm{T}}\tilde{P}\tilde{\xi} + \operatorname{tr}\tilde{W}_1Q_1^{-1}\tilde{W}_1^{\mathrm{T}} + \operatorname{tr}\tilde{W}_2Q_2^{-1}\tilde{W}_2^{\mathrm{T}} + \tilde{x}_{\mathrm{f}}^{\mathrm{T}}\hat{P}\tilde{x}_{\mathrm{f}}, \qquad (5.42)
$$

where $P > 0$, $\tilde{P} > 0$, and $\hat{P}$ satisfy (5.29), (5.32), and (5.20) respectively. Note that (5.42) satisfies $\alpha(\|x_1\|) \leq V(x_1, x_2) \leq \beta(\|x_1\|)$ with $x_1 = [e_\xi^{\mathrm{T}}, \tilde{\xi}^{\mathrm{T}}, (\operatorname{vec}\hat{W}_1)^{\mathrm{T}}, (\operatorname{vec}\hat{W}_2)^{\mathrm{T}}, \tilde{x}_{\mathrm{f}}^{\mathrm{T}}]^{\mathrm{T}}$, $x_2 = e_z$, $\alpha(\|x_1\|) = \beta(\|x_1\|) = \|x_1\|^2$, where $\|x_1\|^2 \triangleq e_\xi^{\mathrm{T}}Pe_\xi + \tilde{\xi}^{\mathrm{T}}\tilde{P}\tilde{\xi} + \operatorname{tr}\tilde{W}_1Q_1^{-1}\tilde{W}_1^{\mathrm{T}} + \operatorname{tr}\tilde{W}_2Q_2^{-1}\tilde{W}_2^{\mathrm{T}} + \tilde{x}_{\mathrm{f}}^{\mathrm{T}}\hat{P}\tilde{x}_{\mathrm{f}}$ and $\operatorname{vec}(\cdot)$ denotes the column stacking operator. Furthermore, $\alpha(\cdot)$ and $\beta(\cdot)$ are class $\mathcal{K}_\infty$ functions. Using (5.18), (5.19) and (5.4), the filter dynamics given by (5.16) and (5.17) can be rewritten as

$$
\begin{aligned}
\dot{\tilde{x}}_{\mathrm{f}}(t) &= A_{\mathrm{f}}\tilde{x}_{\mathrm{f}}(t) + B_{\mathrm{f}}(y(t) + n(t) - y_{\mathrm{d}}),\ \tilde{x}_{\mathrm{f}}(0) = x_{\mathrm{f}_0} - x_{\mathrm{f}_e}, \quad t \geq 0, \qquad (5.43) \\
y_{\mathrm{f}}(t) &= C_{\mathrm{f}}\tilde{x}_{\mathrm{f}}(t) + y_{\mathrm{d}}, \qquad (5.44)
\end{aligned}
$$

Now, letting $e_\xi(t)$, $\xi_{\mathrm{c}}(t)$, and $\tilde{x}_{\mathrm{f}}(t)$, $t \geq 0$, denote the solution to (5.39), (5.30), and (5.43), respectively, and using (5.14), (5.15), (5.22), (5.27), and (5.28), it follows that the time derivative of $V(e_\xi, e_z, \tilde{\xi}, \tilde{W}_1, \tilde{W}_2, \tilde{x}_{\mathrm{f}})$ along the closed-loop system trajectories is given by

$$
\dot{V}(e_\xi(t), e_z(t), \tilde{\xi}(t), \tilde{W}_1(t), \tilde{W}_2(t), \tilde{x}_{\mathrm{f}}(t))
$$

$$
\begin{aligned}
=\ & 2e_\xi^{\mathrm{T}}(t)P\Big[Ae_\xi(t) - B_0\tilde{W}_1^{\mathrm{T}}(t)\sigma_1(\zeta(t)) - B_0\tilde{W}_2^{\mathrm{T}}(t)[I_m \otimes \sigma_2(\zeta(t))]u(t) \\
& + B_0(\hat{W}_1(t) - \hat{W}_{1u}(t))^{\mathrm{T}}\sigma_1(\zeta(t)) + B_0\varepsilon_1(x(t)) + B_0\varepsilon_2(x(t))u(t) \\
& + B_0W_1^{\mathrm{T}}[\hat{\sigma}_1(x(t)) - \sigma_1(\zeta(t))] + B_0W_2^{\mathrm{T}}\left[I_m \otimes (\hat{\sigma}_2(x(t)) - \sigma_2(\zeta(t)))\right]u(t)\Big] \\
& + 2\tilde{\xi}^{\mathrm{T}}(t)\tilde{P}\Big[\tilde{A}\tilde{\xi}(t) + B_0\tilde{W}_1^{\mathrm{T}}(t)\sigma_1(\zeta(t)) + B_0\tilde{W}_2^{\mathrm{T}}(t)[I_m \otimes \sigma_2(\zeta(t))]u(t) \\
& - B_0(\hat{W}_1(t) - \hat{W}_{1u}(t))^{\mathrm{T}}\sigma_1(\zeta(t)) - B_0\varepsilon_1(x(t)) + B_0\varepsilon_2(x(t))u(t) \\
& - B_0W_1^{\mathrm{T}}[\hat{\sigma}_1(x(t)) - \sigma_1(\zeta(t))] - B_0W_2^{\mathrm{T}}\left[I_m \otimes (\hat{\sigma}_2(x(t)) - \sigma_2(\zeta(t)))\right]u(t)\Big] \\
& + 2\mathrm{tr}\,\tilde{W}_1^{\mathrm{T}}(t)Q_1^{-1}\dot{\hat{W}}_1(t) + 2\mathrm{tr}\,\tilde{W}_2^{\mathrm{T}}(t)Q_2^{-1}\dot{\hat{W}}_2(t) + 2\tilde{x}_{\mathrm{f}}^{\mathrm{T}}(t)\hat{P}\Big[A_{\mathrm{f}}\tilde{x}_{\mathrm{f}}(t) + B_{\mathrm{f}}(y(t) \\
& + n(t) - y_{\mathrm{d}})\Big] \\
=\ & -e_\xi^{\mathrm{T}}(t)Re_\xi(t) - \tilde{\xi}^{\mathrm{T}}(t)\tilde{R}\tilde{\xi}(t) - \tilde{x}_{\mathrm{f}}^{\mathrm{T}}(t)\hat{R}\tilde{x}_{\mathrm{f}}(t) - 2e_\xi^{\mathrm{T}}(t)PB_0\tilde{W}_1^{\mathrm{T}}(t)\sigma_1(\zeta(t)) \\
& - 2e_\xi^{\mathrm{T}}(t)PB_0\tilde{W}_2^{\mathrm{T}}(t)[I_m \otimes \sigma_2(\zeta(t))]u(t) + 2e_\xi^{\mathrm{T}}(t)PB_0(\hat{W}_1(t) - \hat{W}_{1u}(t))^{\mathrm{T}}\sigma_1(\zeta(t)) \\
& + 2e_\xi^{\mathrm{T}}(t)PB_0(\varepsilon_1(x(t)) + \varepsilon_2(x(t))u(t)) \\
& + 2e_\xi^{\mathrm{T}}(t)PB_0\left(W_1^{\mathrm{T}}[\hat{\sigma}_1(x(t)) - \sigma_1(\zeta(t))] + W_2^{\mathrm{T}}\left[I_m \otimes (\hat{\sigma}_2(x(t)) - \sigma_2(\zeta(t)))\right]u(t)\right) \\
& + 2\tilde{\xi}^{\mathrm{T}}(t)\tilde{P}B_0\tilde{W}_1^{\mathrm{T}}(t)\sigma_1(\zeta(t)) + 2\tilde{\xi}^{\mathrm{T}}(t)\tilde{P}B_0\tilde{W}_2^{\mathrm{T}}(t)[I_m \otimes \sigma_2(\zeta(t))]u(t) \\
& - 2\tilde{\xi}^{\mathrm{T}}(t)\tilde{P}B_0(\hat{W}_1(t) - \hat{W}_{1u}(t))^{\mathrm{T}}\sigma_1(\zeta(t)) - 2\tilde{\xi}^{\mathrm{T}}(t)\tilde{P}B_0(\varepsilon_1(x(t)) + \varepsilon_2(x(t))u(t)) \\
& - 2\tilde{\xi}^{\mathrm{T}}(t)\tilde{P}B_0\left(W_1^{\mathrm{T}}[\hat{\sigma}_1(x(t)) - \sigma_1(\zeta(t))] + W_2^{\mathrm{T}}\left[I_m \otimes (\hat{\sigma}_2(x(t)) - \sigma_2(\zeta(t)))\right]u(t)\right) \\
& + 2\mathrm{tr}\,\tilde{W}_1^{\mathrm{T}}(t)\mathrm{Proj}(\hat{W}_1(t), -\sigma_1(\zeta(t))\xi_{\mathrm{c}}^{\mathrm{T}}(t)\tilde{P}B_0) \\
& + 2\mathrm{tr}\,\tilde{W}_2^{\mathrm{T}}(t)\mathrm{Proj}(\hat{W}_2(t), -[I_m \otimes \sigma_2(\zeta(t))]u(t)\xi_{\mathrm{c}}^{\mathrm{T}}(t)\tilde{P}B_0) + 2\tilde{x}_{\mathrm{f}}^{\mathrm{T}}\hat{P}B_{\mathrm{f}}Ce_\xi(t) \\
& + 2\tilde{x}_{\mathrm{f}}^{\mathrm{T}}\hat{P}B_{\mathrm{f}}n(t) \\
\leq\ & -(\lambda_{\min}(RP^{-1}) - 1)\|P^{1/2}e_\xi(t)\|^2 - \lambda_{\min}(\tilde{R}\tilde{P}^{-1})\|\tilde{P}^{1/2}\tilde{\xi}(t)\|^2 \\
& - 2e_\xi^{\mathrm{T}}(t)(P + \tilde{P})B_0\tilde{W}_1^{\mathrm{T}}(t)\sigma_1(\zeta(t)) - 2e_\xi^{\mathrm{T}}(t)(P + \tilde{P})B_0\tilde{W}_2^{\mathrm{T}}(t)[I_m \otimes \sigma_2(\zeta(t))]u(t) \\
& + 2e_\xi^{\mathrm{T}}(t)PB_0(\varepsilon_1(x(t)) + \varepsilon_2(x(t))u(t)) - \left(\lambda_{\min}(\hat{R}) - \|\hat{P}B_{\mathrm{f}}CP^{-1/2}\|\right)\|\tilde{x}_{\mathrm{f}}(t)\|^2 \\
& + 2e_\xi^{\mathrm{T}}(t)PB_0\left(W_1^{\mathrm{T}}[\hat{\sigma}_1(x(t)) - \sigma_1(\zeta(t))] + W_2^{\mathrm{T}}\left[I_m \otimes (\hat{\sigma}_2(x(t)) - \sigma_2(\zeta(t)))\right]u(t)\right) \\
& - 2\tilde{\xi}^{\mathrm{T}}(t)\tilde{P}B_0(\varepsilon_1(x(t)) + \varepsilon_2(x(t))u(t)) + 2\|\tilde{x}_{\mathrm{f}}(t)\|\|\hat{P}B_{\mathrm{f}}\|n^* \\
& - 2\tilde{\xi}^{\mathrm{T}}(t)\tilde{P}B_0\left(W_1^{\mathrm{T}}[\hat{\sigma}_1(x(t)) - \sigma_1(\zeta(t))] + W_2^{\mathrm{T}}\left[I_m \otimes (\hat{\sigma}_2(x(t)) - \sigma_2(\zeta(t)))\right]u(t)\right)
\end{aligned}
$$

$$
\begin{aligned}
&+2(e_\xi^{\mathrm{T}}(t)P-\tilde{\xi}^{\mathrm{T}}(t)\tilde{P})B_0(\hat{W}_1(t)-\hat{W}_{1u}(t))^{\mathrm{T}}\sigma_1(\zeta(t))\\
&+2\mathrm{tr}\,\tilde{W}_1^{\mathrm{T}}(t)\left[\mathrm{Proj}(\hat{W}_1(t),-\sigma_1(\zeta(t))\xi_{\mathrm{c}}^{\mathrm{T}}(t)\tilde{P}B_0)+\sigma_1(\zeta(t))\xi_{\mathrm{c}}^{\mathrm{T}}(t)\tilde{P}B_0\right]\\
&+2\mathrm{tr}\,\tilde{W}_2^{\mathrm{T}}(t)\left[\mathrm{Proj}(\hat{W}_2(t),-[I_m\otimes\sigma_2(\zeta(t))]u(t)\xi_{\mathrm{c}}^{\mathrm{T}}(t)\tilde{P}B_0)\right.\\
&\left.+[I_m\otimes\sigma_2(\zeta(t))]u(t)\xi_{\mathrm{c}}^{\mathrm{T}}(t)\tilde{P}B_0\right]\\
\leq\ &-(\lambda_{\min}(RP^{-1})-1)\|P^{1/2}e_\xi(t)\|^2-\lambda_{\min}(\tilde{R}\tilde{P}^{-1})\|\tilde{P}^{1/2}\tilde{\xi}(t)\|^2\\
&-2e_\xi^{\mathrm{T}}(t)(P+\tilde{P})B_0\tilde{W}_1^{\mathrm{T}}(t)\sigma_1(\zeta(t))-2e_\xi^{\mathrm{T}}(t)(P+\tilde{P})B_0\tilde{W}_2^{\mathrm{T}}(t)[I_m\otimes\sigma_2(\zeta(t))]u(t)\\
&+2e_\xi^{\mathrm{T}}(t)PB_0(\varepsilon_1(x(t))+\varepsilon_2(x(t))u(t))-\left(\lambda_{\min}(\hat{R})-\|\hat{P}B_{\mathrm{f}}CP^{-1/2}\|\right)\|\tilde{x}_{\mathrm{f}}(t)\|^2\\
&+2e_\xi^{\mathrm{T}}(t)PB_0\left(W_1^{\mathrm{T}}[\hat{\sigma}_1(x(t))-\sigma_1(\zeta(t))]+W_2^{\mathrm{T}}\left[I_m\otimes(\hat{\sigma}_2(x(t))-\sigma_2(\zeta(t)))\right]u(t)\right)\\
&-2\tilde{\xi}^{\mathrm{T}}(t)\tilde{P}B_0(\varepsilon_1(x(t))+\varepsilon_2(x(t))u(t))+2\|\tilde{x}_{\mathrm{f}}(t)\|\|\hat{P}B_{\mathrm{f}}\|n^*\\
&-2\tilde{\xi}^{\mathrm{T}}(t)\tilde{P}B_0\left(W_1^{\mathrm{T}}[\hat{\sigma}_1(x(t))-\sigma_1(\zeta(t))]+W_2^{\mathrm{T}}\left[I_m\otimes(\hat{\sigma}_2(x(t))-\sigma_2(\zeta(t)))\right]u(t)\right)\\
&+2(e_\xi^{\mathrm{T}}(t)P-\tilde{\xi}^{\mathrm{T}}(t)\tilde{P})B_0(\hat{W}_1(t)-\hat{W}_{1u}(t))^{\mathrm{T}}\sigma_1(\zeta(t)).
\end{aligned}
\tag{5.45}
$$

For the two cases given in (5.38), the last term on the right-hand side of (5.45) gives:

i) If $\hat{u}(t)\geq\geq 0$, $t\geq 0$, then $\hat{W}_{1u}(t)=\hat{W}_1(t)$, and hence,

$$
2(e_\xi^{\mathrm{T}}(t)P-\tilde{\xi}^{\mathrm{T}}(t)\tilde{P})B_0(\hat{W}_1(t)-\hat{W}_{1u}(t))^{\mathrm{T}}\sigma_1(\zeta(t))=0.
$$

ii) Otherwise, $\hat{W}_{1u}(t)=0$, and hence, for $t\geq 0$,

$$
\begin{aligned}
&2(e_\xi^{\mathrm{T}}(t)P-\tilde{\xi}^{\mathrm{T}}(t)\tilde{P})B_0(\hat{W}_1(t)-\hat{W}_{1u}(t))^{\mathrm{T}}\sigma_1(\zeta(t))\\
&\quad=\ 2(e_\xi^{\mathrm{T}}(t)P-\tilde{\xi}^{\mathrm{T}}(t)\tilde{P})B_0\hat{W}_1^{\mathrm{T}}(t)\sigma_1(\zeta(t))\\
&\quad\leq\ 2\sqrt{s_1}\hat{w}_{1\max}\|P^{1/2}B_0\|\|P^{1/2}e_\xi(t)\|+2\sqrt{s_1}\hat{w}_{1\max}\|\tilde{P}^{1/2}B_0\|\|\tilde{P}^{1/2}\tilde{\xi}(t)\|.
\end{aligned}
$$

Hence, it follows from (5.45) that in either case

$$
\begin{aligned}
&\dot{V}(e_\xi(t),e_z(t),\tilde{\xi}(t),\tilde{W}_1(t),\tilde{W}_2(t),\tilde{x}_{\mathrm{f}}(t))\\
&\leq\ -(\lambda_{\min}(RP^{-1})-1)\|P^{1/2}e_\xi(t)\|^2-\lambda_{\min}(\tilde{R}\tilde{P}^{-1})\|\tilde{P}^{1/2}\tilde{\xi}(t)\|^2
\end{aligned}
$$

$$
\begin{aligned}
&+2\sqrt{s_1}\hat{w}_{1\max}\|P^{-1/2}(P+\tilde{P})B_0\|\|P^{1/2}e_\xi(t)\| - \left(\lambda_{\min}(\hat{R}) - \|\hat{P}B_{\mathrm{f}}CP^{-1/2}\|\right)\|\tilde{x}_{\mathrm{f}}(t)\|^2\\
&+2\sqrt{ms_2}\hat{w}_{2\max}u^*\|P^{-1/2}(P+\tilde{P})B_0\|\|P^{1/2}e_\xi(t)\|\\
&+2(\varepsilon_1^*+\varepsilon_2^*u^*)\|P^{1/2}B_0\|\|P^{1/2}e_\xi(t)\| + 2\|\tilde{x}_{\mathrm{f}}(t)\|\|\hat{P}B_{\mathrm{f}}\|n^*\\
&+2(\sqrt{s_1}\hat{w}_{1\max}+\sqrt{ms_2}\hat{w}_{2\max}u^*)\|P^{1/2}B_0\|\|P^{1/2}e_\xi(t)\|\\
&+2(\sqrt{s_1}\hat{w}_{1\max}+\sqrt{ms_2}\hat{w}_{2\max}u^*)\|\tilde{P}^{1/2}B_0\|\|\tilde{P}^{1/2}\tilde{\xi}(t)\|\\
&+2(\varepsilon_1^*+\varepsilon_2^*u^*)\|\tilde{P}^{1/2}B_0\|\|\tilde{P}^{1/2}\tilde{\xi}(t)\| + 2\sqrt{s_1}\hat{w}_{1\max}\|P^{1/2}B_0\|\|P^{1/2}e_\xi(t)\|\\
&+2\sqrt{s_1}\hat{w}_{1\max}\|\tilde{P}^{1/2}B_0\|\|\tilde{P}^{1/2}\tilde{\xi}(t)\|\\
=\ &-(\lambda_{\min}(RP^{-1})-1)(\|P^{1/2}e_\xi(t)\|-\alpha_1)^2 - \lambda_{\min}(\tilde{R}\tilde{P}^{-1})(\|\tilde{P}^{1/2}\tilde{\xi}(t)\|-\alpha_2)^2\\
&-\left(\lambda_{\min}(\hat{R}) - \|\hat{P}B_{\mathrm{f}}CP^{-1/2}\|\right)(\|\tilde{x}_{\mathrm{f}}(t)\|-\alpha_3)^2 + \nu, \qquad (5.46)
\end{aligned}
$$

where ν, α_1, α_2, and α_3 are given by (5.34), (5.35), (5.36), and (5.37), respectively. Now, for

$$
\|P^{1/2}e_\xi\| \geq \alpha_{e_\xi} \triangleq \sqrt{\frac{\nu}{\lambda_{\min}(RP^{-1})-1}} + \alpha_1, \qquad (5.47)
$$

or

$$
\|\tilde{P}^{1/2}\tilde{\xi}\| \geq \alpha_{\tilde{\xi}} \triangleq \sqrt{\frac{\nu}{\lambda_{\min}(\tilde{R}\tilde{P}^{-1})}} + \alpha_2, \qquad (5.48)
$$

or

$$
\|\tilde{x}_{\mathrm{f}}\| \geq \alpha_{\tilde{x}_{\mathrm{f}}} \triangleq \sqrt{\frac{\nu}{\lambda_{\min}(\hat{R}) - \|\hat{P}B_{\mathrm{f}}CP^{-1/2}\|}} + \alpha_3, \qquad (5.49)
$$

it follows that $\dot{V}(e_\xi(t), e_z(t), \tilde{\xi}(t), \tilde{W}_1(t), \tilde{W}_2(t), \tilde{x}_{\mathrm{f}}(t)) \leq 0$ for all $t \geq 0$, that is, $\dot{V}(e_\xi(t), e_z(t), \tilde{\xi}(t), \tilde{W}_1(t), \tilde{W}_2(t), \tilde{x}_{\mathrm{f}}(t)) \leq 0$ for all $(e_\xi(t), e_z(t), \tilde{\xi}(t), \tilde{W}_1(t), \tilde{W}_2(t), \tilde{x}_{\mathrm{f}}(t)) \in \tilde{\mathcal{D}}_{\mathrm{e}} \backslash \tilde{\mathcal{D}}_{\mathrm{r}}$ and $t \geq 0$, where

$$
\tilde{\mathcal{D}}_{\mathrm{e}} \triangleq \left\{(e_\xi, e_z, \tilde{\xi}, \tilde{W}_1, \tilde{W}_2, \tilde{x}_{\mathrm{f}}) \in \mathbb{R}^m \times \mathbb{R}^{n-m} \times \mathbb{R}^r \times \mathbb{R}^{s_1 \times m} \times \mathbb{R}^{ms_2 \times m} \times \mathbb{R}^{n_{\mathrm{f}}} : x \in \mathcal{D}_{\mathrm{c}}\right\}, \qquad (5.50)
$$

$$
\begin{aligned}
\tilde{\mathcal{D}}_{\mathrm{r}} \triangleq \Big\{&(e_\xi, e_z, \tilde{\xi}, \tilde{W}_1, \tilde{W}_2, \tilde{x}_{\mathrm{f}}) \in \mathbb{R}^m \times \mathbb{R}^{n-m} \times \mathbb{R}^r \times \mathbb{R}^{s_1 \times m} \times \mathbb{R}^{ms_2 \times m} \times \mathbb{R}^{n_{\mathrm{f}}}\\
&: \|P^{1/2}e_\xi\| \leq \alpha_{e_\xi},\ \|\tilde{P}^{1/2}\tilde{\xi}\| \leq \alpha_{\tilde{\xi}},\ \|x_{\mathrm{f}}\| \leq \alpha_{\tilde{x}_{\mathrm{f}}}\Big\}. \qquad (5.51)
\end{aligned}
$$

Next, define

$$\tilde{\mathcal{D}}_\alpha \triangleq \Big\{(e_\xi, e_z, \tilde{\xi}, \tilde{W}_1, \tilde{W}_2, \tilde{x}_{\mathrm{f}}) \in \mathbb{R}^m \times \mathbb{R}^{n-m} \times \mathbb{R}^r \times \mathbb{R}^{s_1 \times m} \times \mathbb{R}^{ms_2 \times m} \times \mathbb{R}^{n_{\mathrm{f}}} : V(e_\xi, e_z, \tilde{\xi}, \tilde{W}_1, \tilde{W}_2, \tilde{x}_{\mathrm{f}}) \leq \alpha\Big\}, \tag{5.52}$$

where α is the maximum value such that $\tilde{\mathcal{D}}_\alpha \subseteq \tilde{\mathcal{D}}_{\mathrm{e}}$, and define

$$\tilde{\mathcal{D}}_\eta \triangleq \Big\{(e_\xi, e_z, \tilde{\xi}, \tilde{W}_1, \tilde{W}_2, \tilde{x}_{\mathrm{f}}) \in \mathbb{R}^m \times \mathbb{R}^{n-m} \times \mathbb{R}^r \times \mathbb{R}^{s_1 \times m} \times \mathbb{R}^{ms_2 \times m} \times \mathbb{R}^{n_{\mathrm{f}}} : V(e_\xi, e_z, \tilde{\xi}, \tilde{W}_1, \tilde{W}_2, \tilde{x}_{\mathrm{f}}) \leq \eta\Big\}, \tag{5.53}$$

where

$$\eta > \beta(\mu) = \mu = \alpha_{e_\xi}^2 + \alpha_{\tilde{\xi}}^2 + \alpha_{\tilde{x}_{\mathrm{f}}}^2 + \lambda_{\max}(Q_1^{-1})\hat{w}_{1\max}^2 + \lambda_{\max}(Q_2^{-1})\hat{w}_{2\max}^2. \tag{5.54}$$

To show ultimate boundedness of the closed-loop system (5.27), (5.28), and (5.39)–(5.41) assume[3] that $\tilde{\mathcal{D}}_\eta \subset \tilde{\mathcal{D}}_\alpha$. Now, since $\dot{V}(e_\xi, e_z, \tilde{\xi}, \tilde{W}_1, \tilde{W}_2, \tilde{x}_{\mathrm{f}}) \leq 0$ for all $(e_\xi, e_z, \tilde{\xi}, \tilde{W}_1, \tilde{W}_2, \tilde{x}_{\mathrm{f}}) \in \tilde{\mathcal{D}}_{\mathrm{e}} \backslash \tilde{\mathcal{D}}_{\mathrm{r}}$ and $\tilde{\mathcal{D}}_{\mathrm{r}} \subset \tilde{\mathcal{D}}_\alpha$, it follows that $\tilde{\mathcal{D}}_\alpha$ is positively invariant. Hence, if $(e_\xi(0), e_z(0), \tilde{\xi}(0), \tilde{W}_1(0), \tilde{W}_2(0), \tilde{x}_{\mathrm{f}}(0)) \in \tilde{\mathcal{D}}_\alpha$, then it follows from Theorem 4.14 of [48] that the solution $(e_\xi(t), e_z(t), \tilde{\xi}(t), \hat{W}_1(t), \hat{W}_2(t))$, $t \geq 0$, to (5.27), (5.28), (5.39)–(5.41) is ultimately bounded with respect to $(e_\xi, \tilde{\xi}, \tilde{W}_1, \tilde{W}_2, \tilde{x}_{\mathrm{f}})$ uniformly in $e_z(0)$ with ultimate bound given by $\varepsilon = \alpha^{-1}(\eta) = \sqrt{\eta}$, which yields (5.33). In addition, since (5.40) is input-to-state stable with e_ξ viewed as the input, it follows from Proposition 4.4 of [48] that the solution $e_z(t)$, $t \geq 0$, to (5.40) is also ultimately bounded.

Next, it follows from Theorem 1 of [128] that there exist a continuously differentiable, radially unbounded, positive-definite function $V_z : \mathbb{R}^{n_z} \to \mathbb{R}$ and class $\mathcal{K}$ functions $\gamma_1(\cdot)$ and $\gamma_2(\cdot)$ such that

$$V_z'(e_z)\tilde{f}_z(e_\xi, e_z) \leq -\gamma_1(\|e_z\|), \quad \|e_z\| \geq \gamma_2(\|e_\xi\|). \tag{5.55}$$

[3]This assumption ensures that in the error space $\tilde{\mathcal{D}}_{\mathrm{e}}$ there exists at least one Lyapunov level set $\tilde{\mathcal{D}}_\eta \subset \tilde{\mathcal{D}}_\alpha$. Equivalently, imposing bounds on the adaptation gains ensures $\tilde{\mathcal{D}}_\eta \subset \tilde{\mathcal{D}}_\alpha$ [61]. In the case where the neural network approximation holds in $\mathbb{R}^n$ with delayed values, this assumption is automatically satisfied.

Since the upper bound for $\|e_\xi\|^2$ is given by η, it follows that the set given by

$$\mathcal{D}_z \triangleq \left\{ z \in \mathbb{R}^{n-r} : V_z(z - z_{\mathrm{e}}) \leq \max_{\|z - z_{\mathrm{e}}\| = \gamma_2\left(\sqrt{\eta}\right)} V_z(z - z_{\mathrm{e}}) \right\} \tag{5.56}$$

is also positively invariant. Now, since $\tilde{\mathcal{D}}_\alpha$ and $\mathcal{D}_z$ are positively invariant, it follows that

$$\begin{aligned} \mathcal{D}_\alpha \triangleq \Big\{ & (x, \tilde{\xi}, \tilde{W}_1, \tilde{W}_2, \tilde{x}_{\mathrm{f}}) \in \mathbb{R}^n \times \mathbb{R}^r \times \mathbb{R}^{s_1 \times m} \times \mathbb{R}^{ms_2 \times m} \times \mathbb{R}^{n_{\mathrm{f}}} \\ & : V(\xi - y_{\mathrm{d}}, z - e_z, \tilde{\xi}, \hat{W}_1 - W_1, \hat{W}_2 - W_2, x_{\mathrm{f}} - x_{\mathrm{f_e}}) \leq \alpha \Big\} \end{aligned} \tag{5.57}$$

is also positively invariant. In addition, since (5.27), (5.28), (5.39)–(5.41), and (5.43) is ultimately bounded with respect to $(e_\xi, \tilde{\xi}, \tilde{W}_1, \tilde{W}_2, \tilde{x}_{\mathrm{f}})$ and (5.40) is input-to-state stable with e_ξ viewed as the input, it follows from Proposition 4.4 of [48] that the solution $(e_\xi(t), e_z(t), \tilde{\xi}(t), \tilde{W}_1(t), \tilde{W}_2(t), \tilde{x}_{\mathrm{f}}(t))$, $t \geq 0$, of the closed-loop system (5.27), (5.28), (5.39)–(5.41), and (5.43) is ultimately bounded for all $(e_\xi(0), e_z(0), \tilde{\xi}(0), \tilde{W}_1(0), \tilde{W}_2(0), \tilde{x}_{\mathrm{f}}(0)) \in \tilde{\mathcal{D}}_\alpha$.

Finally, $u(t) \geq\geq 0$, $t \geq 0$, is a restatement of (5.25). Now, since $G(x(t)) \geq\geq 0$, $t \geq 0$, and $u(t) \geq\geq 0$, $t \geq 0$, it follows from Proposition 5.1 that $x(t) \geq\geq 0$, $t \geq 0$, for all $x_0 \in \overline{\mathbb{R}}^n_+$. □

Remark 5.1. If in Theorem 5.1 $\lambda_{\min}(RP^{-1}) > 1$ is not satisfied for a given A, we can modify (5.9) as $f_\xi(\xi, z) = \bar{A}\xi + \bar{f}_{\mathrm{u}}(\xi, z)$, where $\bar{f}_{\mathrm{u}}(\xi, z) = \tilde{f}_{\mathrm{u}}(\xi, z) + (A - \bar{A})\xi$ and $\bar{A}$ is such that $\lambda_{\min}(\bar{R}\bar{P}^{-1}) > 1$, where

$$0 = \bar{A}^{\mathrm{T}}\bar{P} + \bar{P}\bar{A} + \bar{R}.$$

For example, with $\bar{A} = -\alpha I_n$, where $\alpha > \frac{1}{2}$, $\lambda_{\min}(\bar{R}\bar{P}^{-1}) > 1$ is guaranteed. In this case, Theorem 5.1 holds with A replaced by $\bar{A}$. In addition, by properly choosing L we can ensure that $\lambda_{\min}(\tilde{R}\tilde{P}^{-1}) > 1$. Finally, choosing B_{f} small enough and independent of $\hat{R}$, $\hat{P}$, C, and P, $\lambda_{\min}(\hat{R}) > \|\hat{P}B_{\mathrm{f}}CP^{-\frac{1}{2}}\|$ can also be guaranteed.

Remark 5.2. The domain of attraction $\mathcal{D}_\alpha$ in Theorem 5.1 is given by (5.57) and is characterized by the Lyapunov-like function (5.42) that guarantees ultimate boundedness for the closed-loop system.

A block diagram showing the neuroadaptive control architecture given in Theorem 5.1 is shown in Figure 5.1. It is important to note that the existence of a global neural network approximator for an uncertain nonlinear map using the system filtered outputs and inputs, and its delayed values cannot in general be established. In the proof of Theorem 5.1, as is common in the neural network literature, we assume that for a given arbitrarily large compact set $\mathcal{D}_{\mathrm{c}} \subset \mathbb{R}^n$, there exists an approximator for the unknown nonlinear map up to a desired accuracy. This assumption ensures that in the error space $\tilde{\mathcal{D}}_{\mathrm{e}}$, there exists at least one Lyapunov level set such that the set inclusions invoked in the proof of Theorem 5.1 are satisfied. In the case where $f_{\mathrm{u}}(\cdot)$ and $\hat{G}(\cdot)$ are continuous on $\mathbb{R}^n$, it follows from the Stone-Weierstrass theorem that $f_{\mathrm{u}}(\cdot)$ and $\hat{G}(\cdot)$ can be approximated over an arbitrarily large compact set $\mathcal{D}_{\mathrm{c}}$ in the sense of (5.14) and (5.15). Finally, we note that since the norm of $\hat{W}_2(t)$ is bounded it is always possible to choose $\hat{B}$ so that $(\hat{B} + \hat{W}_2^{\mathrm{T}}(t)[I_m \otimes \sigma_2(\zeta(t))])^{-1}$ exists and is bounded for all $t \geq 0$ so that there exists $u^* > 0$ such that $u^* \geq \|u(t)\|$, $t \geq 0$. This follows from the fact that for any two square matrices A and B, $\det(A + B) \neq 0$ if and only if there exists $\alpha > 0$ such that $\sigma_{\min}(A) > \alpha$ and $\sigma_{\max}(B) \leq \alpha$, where $\sigma_{\min}(\cdot)$ and $\sigma_{\max}(\cdot)$ denote the minimum and maximum singular value, respectively.

Implementing the neuroadaptive controller (5.26) requires a fixed-point iteration at each integration step, that is, the controller contains an algebraic constraint on u. For each choice of $\sigma_1(\cdot)$ and $\sigma_2(\cdot)$ this equation must be examined for solvability in terms of u. It is more practical to avoid this iteration by using one-step delayed values of u in calculating $\hat{u}$. Implementations using both approaches result in imperceptible differences in our numerical studies.

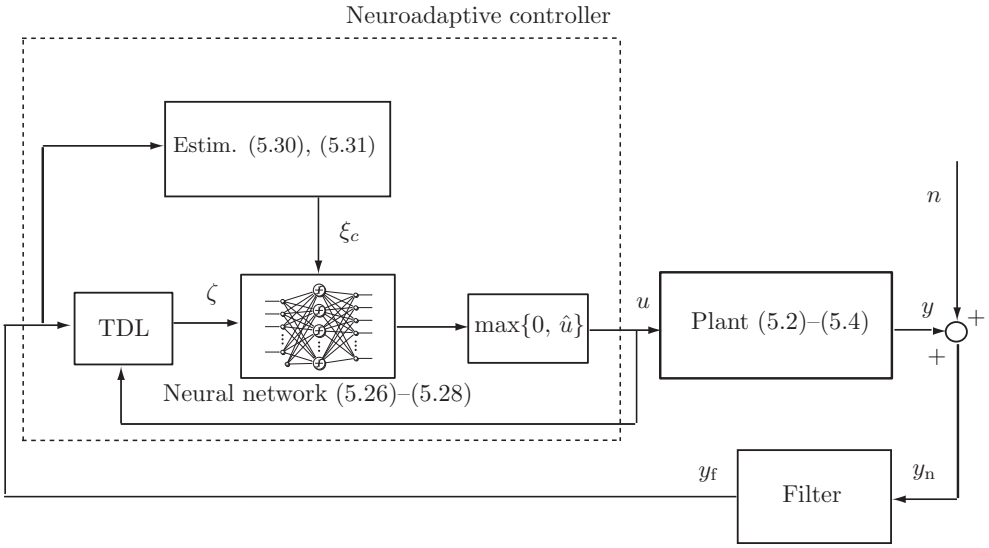

Figure 5.1: Block diagram of the closed-loop system.

In Theorem 5.1 we assumed that the equilibrium point x_e of (5.2) is globally asymptotically stable with $u(t) \equiv u_e$. In general, however, unlike linear nonnegative systems with asymptotically stable plant dynamics, a given set point $x_e \in \mathbb{R}^n_+$ for the nonlinear nonnegative dynamical system (5.2) may not be asymptotically stablizable with a constant control $u(t) \equiv u_e \in \overline{\mathbb{R}}^m_+$. However, if $f(x)$ is homogeneous, cooperative, that is, the Jacobian matrix $\frac{\partial f(x)}{\partial x}$ is essentially nonnegative for all $x \in \overline{\mathbb{R}}^n_+$, the Jacobian matrix $\frac{\partial f(x)}{\partial x}$ is irreducible for all $x \in \overline{\mathbb{R}}^n_+$ [13], and the zero solution $x(t) \equiv 0$ of the undisturbed ($u(t) \equiv 0$) system (5.2) is globally asymptotically stable, then the set point $x_e \in \mathbb{R}^n_+$ satisfying (5.11) and (5.12) is a unique equilibrium point with $u(t) \equiv u_e$ and is also asymptotically stable for all $x_0 \in \overline{\mathbb{R}}^n_+$ [29, 30]. This implies that the solution $x(t) \equiv x_e$ to (5.2) with $u(t) \equiv u_e$ is asymptotically stable for all $x_0 \in \overline{\mathbb{R}}^n_+$.

5.4. Neuroadaptive Output Feedback Control for General Anesthesia

Almost all anesthetics are *myocardial* depressants, that is, they decrease the contractility of the heart and lower *cardiac output* (i.e., the volume of blood pumped

by the heart per unit time). As a consequence, decreased cardiac output slows down redistribution kinetics, that is, the transfer of blood from the central compartment (heart, brain, kidney, and liver) to the peripheral compartments (muscle and fat). In addition, decreased cardiac output could increase drug concentrations in the central compartment, causing even more myocardial depression and further decrease in cardiac output. This instability can lead to overdosing that, at the very least, can delay recovery from anesthesia and, in the worst case, can result in respiratory and cardiovascular collapse. Alternatively, underdosing can result in patients psychologically traumatized by pain and awareness during surgery. Thus, control of drug effect is clinically important since overdosing or underdosing incur risk for the patient.

To illustrate the application of the neuroadaptive control framework presented in Section 5.3 for general anesthesia we develop a model for the intravenous anesthetic propofol. The pharmacokinetics of propofol are described by the three compartment model [54, 96] shown in Figure 5.2, where x_1 denotes the mass of drug in the central compartment, which is the site for drug administration and is generally thought to be comprised of the *intravascular blood* volume (blood within arteries and veins) as well as *highly perfused* organs (organs with high ratios of blood flow to weight) such as the heart, brain, kidney, and liver. These organs receive a large fraction of the cardiac output. The remainder of the drug in the body is assumed to reside in two peripheral compartments, one identified with muscle and one with fat; the masses in these compartments are denoted by x_2 and x_3, respectively. These compartments receive less than 20% of the cardiac output.

A mass balance of the three-state compartmental model yields

$$\begin{aligned}\dot{x}_1(t) = &-[a_{11}(c(t)) + a_{21}(c(t)) + a_{31}(c(t))]x_1(t) + a_{12}(c(t))x_2(t) \\ &+a_{13}(c(t))x_3(t) + u(t), \quad x_1(0) = x_{10}, \quad t \geq 0,\end{aligned} \tag{5.58}$$

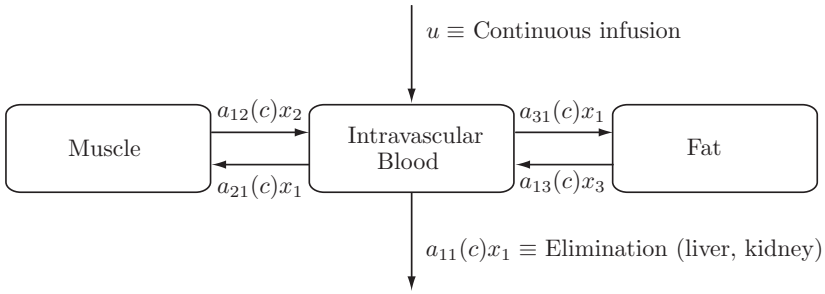

Figure 5.2: Pharmacokinetic model for drug distribution during anesthesia.

$$\dot{x}_2(t) = a_{21}(c(t))x_1(t) - a_{12}(c(t))x_2(t), \quad x_2(0) = x_{20}, \tag{5.59}$$

$$\dot{x}_3(t) = a_{31}(c(t))x_1(t) - a_{13}(c(t))x_3(t), \quad x_3(0) = x_{30}, \tag{5.60}$$

where $c(t) = x_1(t)/V_{\mathrm{c}}$, V_{c} is the volume of the central compartment (about 15 l for a 70 kg patient), $a_{ij}(c)$, $i \neq j$, is the rate of transfer of drug from the jth compartment to the ith compartment, $a_{11}(c)$ is the rate of drug metabolism and elimination (metabolism typically occurs in the liver), and $u(t)$, $t \geq 0$, is the infusion rate of the anesthetic drug propofol into the central compartment. The transfer coefficients are assumed to be functions of the drug concentration c since it is well known that the pharmacokinetics of propofol are influenced by cardiac output [134] and, in turn, cardiac output is influenced by propofol plasma concentrations, both due to *venodilation* (pooling of blood in dilated vains) [101] and myocardial depression [68]. Finally, it is important to note that the compartmental model (5.58)–(5.60) is already in the normal form basis (5.5)–(5.7), and hence, there is no need to construct a global diffeomorphism to transform (5.58)–(5.60) into the form of (5.5)–(5.7).

Experimental data indicate that the transfer coefficients $a_{ij}(\cdot)$ are nonincreasing functions of the propofol concentration [68, 101]. The most widely used empirical models for pharmacodynamic concentration-effect relationships are modifications of the Hill equation [60]. Applying this almost ubiquitous empirical model to the rela-

tionship between transfer coefficients implies that

$$a_{ij}(c) = A_{ij}Q_{ij}(c), \quad Q_{ij}(c) = Q_0 \mathrm{C}_{50,ij}^{\alpha_{ij}}/(\mathrm{C}_{50,ij}^{\alpha_{ij}} + c^{\alpha_{ij}}),$$

where, for $i, j \in \{1, 2, 3\}$, $i \neq j$, $\mathrm{C}_{50,ij}$ is the drug concentration associated with a 50% decrease in the transfer coefficient, α_{ij} is a parameter that determines the steepness of the concentration-effect relationship, and A_{ij} are positive constants. Note that both pharmacokinetic parameters are functions of i and j, that is, there are distinct Hill equations for each transfer coefficient. Furthermore, since for many drugs the rate of metabolism $a_{11}(c)$ is proportional to the rate of transport of drug to the liver we assume that $a_{11}(c)$ is also proportional to the cardiac output so that $a_{11}(c) = A_{11}Q_{11}(c)$.

To illustrate the neuroadaptive control of propofol, we assume that $\mathrm{C}_{50,ij}$ and α_{ij} are independent of i and j. Also, since decreases in cardiac output are observed at clinically-utilized propofol concentrations we arbitrarily assign C_{50} a value of 4 μg/ml since this value is in the mid-range of clinically utilized values. We also assign α a value of 3 [78]. This value is within the typical range of those observed for ligand-receptor binding (see the discussion in [33]). The nonnegative transfer and loss coefficients A_{12}, A_{21}, A_{13}, A_{31}, and A_{11}, and the parameters $\alpha > 1$, $\mathrm{C}_{50} > 0$, and $Q_0 > 0$, are uncertain due to patient gender, weight, pre-existing disease, age, and concomitant medication. Hence, the need for adaptive control to regulate intravenous anesthetics during surgery is essential.

Even though propofol concentration levels in the blood plasma will lead to the desired depth of anesthesia, they cannot be measured in real-time during surgery. Furthermore, we are more interested in drug *effect* (depth of hypnosis) rather than drug *concentration*. Hence, we consider a model involving pharmacokinetics (drug concentration as a function of time) and pharmacodynamics (drug effect as a function of

concentration) for controlling consciousness. Specifically, we use an electroencephalogram (EEG) signal as a measure of hypnotic drug effect of anesthetic compounds on the brain [41, 99, 123]. Since electroencephalography provides real-time monitoring of the central nervous system activity, it can be used to quantify levels of consciousness, and hence, is amenable for feedback control in general anesthesia.

As discussed in the introduction, the Bispectral Index (BIS), an EEG indicator, has been proposed as a measure of hypnotic effect. This index quantifies the nonlinear relationships between the component frequencies in the electroencephalogram, as well as analyzing their phase and amplitude. The BIS signal is related to drug concentration by the empirical relationship

$$\mathrm{BIS_n}(c_{\mathrm{eff}}(t)) = \mathrm{BIS_0}\left(1 - \frac{c_{\mathrm{eff}}^{\gamma}(t)}{c_{\mathrm{eff}}^{\gamma}(t) + \mathrm{EC}_{50}^{\gamma}}\right) + n(t), \tag{5.61}$$

where $\mathrm{BIS_0}$ denotes the baseline (awake state) value and, by convention, is typically assigned a value of 100, c_{eff} is the propofol concentration in μg/ml in the effect-site compartment (brain), EC_{50} is the concentration at half maximal effect and represents the patient's sensitivity to the drug, γ determines the degree of nonlinearity in (5.61), and n is a high-frequency observation noise signal. Here, the effect-site compartment is introduced to account for finite equilibration time between the central compartment concentration and the central nervous system concentration [115].

The effect-site compartment concentration is related to the concentration in the central compartment by the first-order model ([115])

$$\dot{c}_{\mathrm{eff}}(t) = a_{\mathrm{eff}}(c(t) - c_{\mathrm{eff}}(t)), \quad c_{\mathrm{eff}}(0) = c(0), \quad t \geq 0, \tag{5.62}$$

where a_{eff} in min^{-1} is an unknown positive time constant. In reality, the effect-site compartment equilibrates with the central compartment in a matter of a few minutes. The parameters a_{eff}, EC_{50}, and γ are determined by data fitting and vary from patient to patient. BIS index values of 0 and 100 correspond, respectively, to an *isoelectric*

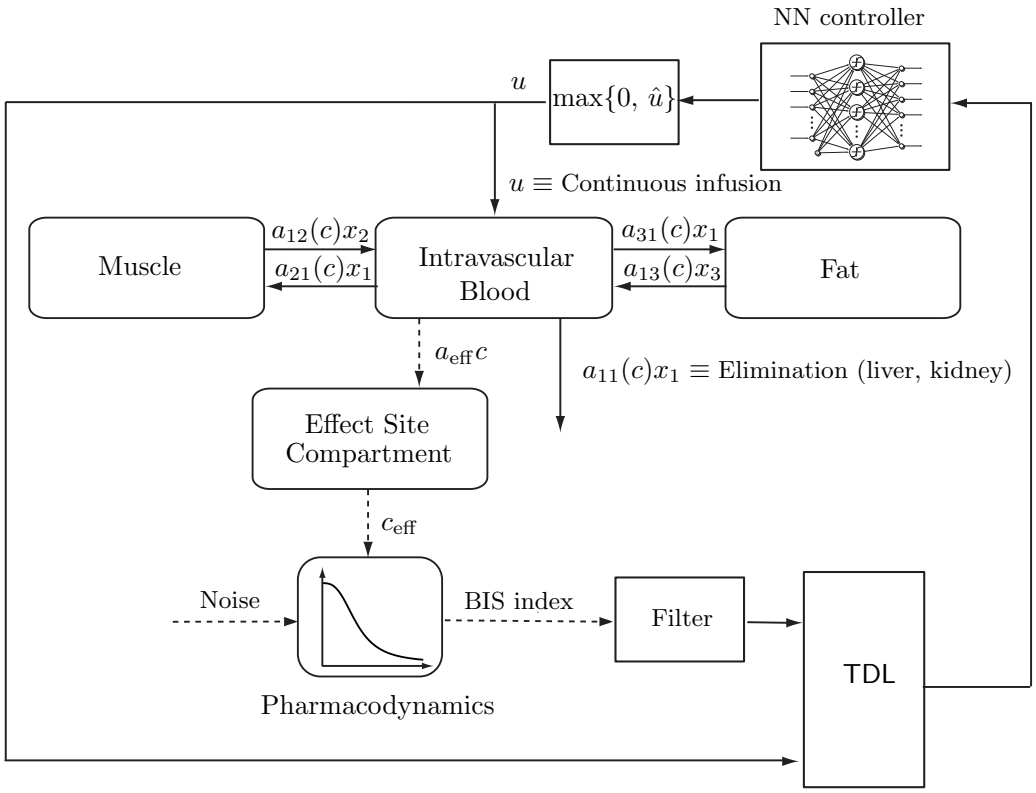

Figure 5.3: Combined pharmacokinetic/pharmacodynamic control model.

EEG signal (no cerebral electrical activity) and an EEG signal of a fully conscious patient; the range between 40 and 60 indicates a moderate hypnotic state [123]. Figure 5.3 shows the combined pharmacokinetic/pharmacodynamic control model for the distribution of propofol.

For set-point regulation define $e(t) \triangleq x(t) - x_{\text{e}}$, where $x_{\text{e}} \in \mathbb{R}^4_+$ is the set point satisfying the equilibrium condition for (5.58)–(5.60) and (5.62) with $x_1(t) \equiv x_{\text{e}1}$, $x_2(t) \equiv x_{\text{e}2}$, $x_3(t) \equiv x_{\text{e}3}$, $x_4(t) = c_{\text{eff}}(t) \equiv \text{EC}_{50}$, and $u(t) \equiv u_{\text{e}}$, so that $f_{\text{e}}(e) = [f_{\text{e}1}(e), f_{\text{e}2}(e), f_{\text{e}3}(e), f_{\text{e}4}(e)]^{\text{T}}$ is given by

$$
\begin{aligned}
f_{\text{e}1}(e) = {} & -[a_{\text{e}}(c) + a_{21}(c) + a_{31}(c)](e_1 + x_{\text{e}1}) + a_{12}(c)(e_2 + x_{\text{e}2}) + a_{13}(c)(e_3 + x_{\text{e}3}) \\
& -[a_{\text{e}}(c_{\text{e}}) + a_{21}(c_{\text{e}}) + a_{31}(c_{\text{e}})]x_{\text{e}1} + a_{12}(c_{\text{e}})x_{\text{e}2} + a_{13}(c_{\text{e}})x_{\text{e}3}, \\
f_{\text{e}2}(e) = {} & a_{21}(c)(e_1 + x_{\text{e}1}) - a_{12}(c)(e_2 + x_{\text{e}2}) - [a_{21}(c_{\text{e}})x_{\text{e}1} - a_{12}(c_{\text{e}})x_{\text{e}2}],
\end{aligned}
$$

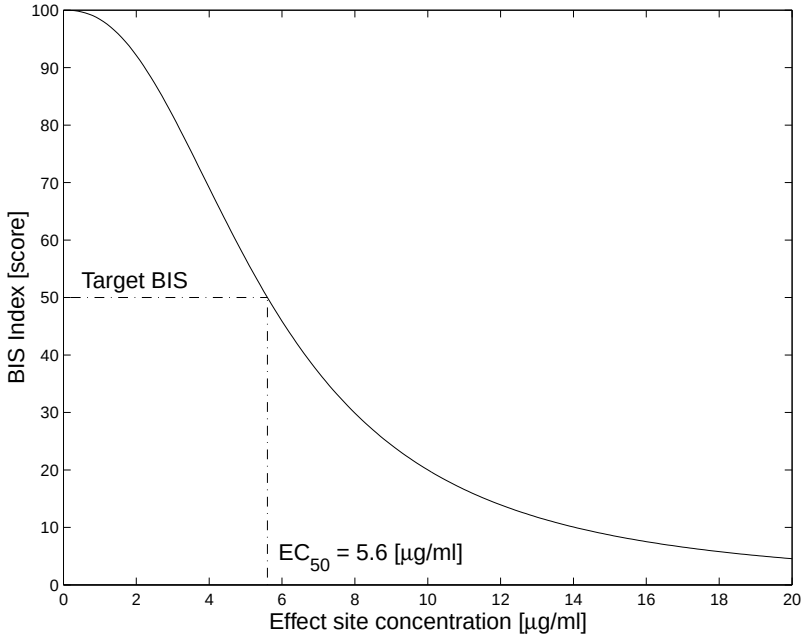

Figure 5.4: BIS Index versus effect site concentration.

$$f_{e3}(e) = a_{31}(c)(e_1 + x_{e1}) - a_{13}(c)(e_3 + x_{e3}) - [a_{31}(c_e)x_{e1} - a_{13}(c_e)x_{e3}],$$

$$f_{e4}(e) = a_{eff}(c - (e_4 + EC_{50})) - a_{eff}(e_e - EC_{50}),$$

where $c_e \triangleq x_{e1}/V_c$. The existence of this equilibrium point follows from the fact that the Jacobian of (5.58)–(5.60) and (5.62) is essentially nonnegative and every solution of (5.58)–(5.60) and (5.62) is bounded [70]. Next, linearizing $f_e(e)$ about 0 and computing the eigenvalues of the resulting Jacobian matrix, it can be shown that x_e is asymptotically stable. Hence, Assumption 5.1 is satisfied for our clinical model.

In the following simulation involving the infusion of the anesthetic drug propofol we set $EC_{50} = 5.6$ μg/ml, $\gamma = 2.39$, and $BIS_0 = 100$, so that the BIS signal is shown in Figure 5.4. The target (desired) BIS value, BIS_{target}, is set at 50. Here, we use the neuroadaptive output feedback controller

$$u(t) = \max\{0, \hat{u}(t)\}, \tag{5.63}$$

where

$$\hat{u}(t) = -\frac{\hat{W}_1^{\mathrm{T}}(t)\sigma_1(\zeta(t))}{\hat{b} + \hat{W}_2^{\mathrm{T}}(t)\sigma_2(\zeta(t))},$$
$$\zeta(t) = [\mathrm{BIS_f}(t-d), \mathrm{BIS_f}(t-2d), u(t-d), u(t-2d)]^{\mathrm{T}},$$

$\hat{b} > 0$, $d > 0$, with update laws

$$\dot{\hat{W}}_1(t) = Q_{\mathrm{BIS_1}}\mathrm{Proj}[\hat{W}_1(t), -\sigma_1(\zeta(t))\xi_{\mathrm{c}}^{\mathrm{T}}(t)\tilde{P}B_0], \quad \hat{W}_1(0) = \hat{W}_{10},\ t \geq 0,$$
$$\dot{\hat{W}}_2(t) = Q_{\mathrm{BIS_2}}\mathrm{Proj}[\hat{W}_2(t), -\sigma_2(\zeta(t))u(t)\xi_{\mathrm{c}}^{\mathrm{T}}(t)\tilde{P}B_0], \quad \hat{W}_2(0) = \hat{W}_{20},$$

where $Q_{\mathrm{BIS_1}}$ and $Q_{\mathrm{BIS_2}}$ are positive constants and $\xi_{\mathrm{c}}(t) \in \mathbb{R}^2$, $t \geq 0$, is the solution to the estimator dynamics

$$\dot{\xi}_{\mathrm{c}}(t) = A\xi_{\mathrm{c}}(t) + L(\mathrm{BIS_f}(t) - y_{\mathrm{c}}(t) - \mathrm{BIS_{target}}), \quad \xi_{\mathrm{c}}(0) = \xi_{\mathrm{c}0}, \quad t \geq 0, \tag{5.64}$$
$$y_{\mathrm{c}}(t) = C\xi_{\mathrm{c}}(t), \tag{5.65}$$

where $A \in \mathbb{R}^{2\times 2}$, $L \in \mathbb{R}^{2\times 1}$, $C = [1, 0]^{\mathrm{T}}$, and $\mathrm{BIS_f}(t)$ is output of the second-order, low-pass asymptotically stable filter

$$\dot{x}_{\mathrm{f}}(t) = A_{\mathrm{f}}x_{\mathrm{f}}(t) + B_{\mathrm{f}}\mathrm{BIS_n}(t),\ x_{\mathrm{f}}(0) = [\mathrm{BIS_f}(0),\, 0]^{\mathrm{T}}, \quad t \geq 0, \tag{5.66}$$
$$\mathrm{BIS_f}(t) = C_{\mathrm{f}}x_{\mathrm{f}}(t), \tag{5.67}$$

where $A_{\mathrm{f}} = \begin{bmatrix} 0 & 1 \\ -\omega_n^2 & -2\zeta\omega_n \end{bmatrix}$, $B_{\mathrm{f}} = [0,\ \omega_n^2]^{\mathrm{T}}$, $C_{\mathrm{f}} = [1, 0]^{\mathrm{T}}$, $\omega_n = 5$ rad/sec, $\zeta = 0.7$, and $\mathrm{BIS_f}(0) = 100$. Here, we model $n(t)$ as a noise signal generated by a SIMULINK band-limited white noise block with a noise power parameter of 0.0001 amplified 100 times. Now, it follows from Theorem 5.1 that there exist positive constants ε and T such that $|\mathrm{BIS}(t) - \mathrm{BIS_{target}}| \leq \varepsilon$, $t \geq T$, where $\mathrm{BIS}(t)$ is given by (5.61) with $n(t) \equiv 0$, for all nonnegative values of the pharmacokinetic transfer and loss coefficients $A_{12}, A_{21}, A_{13}, A_{31}, A_{11}$ as well as all nonnegative coefficients α, $\mathrm{C_{50}}$, and Q_0. A flowchart for the neuroadaptive control algorithm is shown in Figure 5.5.

For our simulation, we assume $V_{\rm c} = (0.228 \text{ l/kg})(M \text{ kg})$, where $M = 70$ kg is the mass of the patient, $A_{21}Q_0 = 0.112$ min^{-1}, $A_{12}Q_0 = 0.055$ min^{-1}, $A_{31}Q_0 = 0.0419$ min^{-1}, $A_{13}Q_0 = 0.0033$ min^{-1}, $A_{\rm e}Q_0 = 0.119$ min^{-1}, $a_{\rm eff} = 3.4657$ min^{-1}, $\alpha = 3$, and $\rm C_{50} = 4$ μg/ml [78, 96]. Note that the parameter values for α and $\rm C_{50}$ probably exaggerate the effect of propofol on cardiac output. They have been selected to accentuate nonlinearity but they are not biologically unrealistic. Furthermore, to illustrate the proposed neuroadaptive controller we switch the pharmacodynamic parameters $\rm EC_{50}$ and γ, respectively, from 5.6 μg/ml and 2.39 to 7.2 μg/ml and 3.39 at $t = 15$ min and back to 5.6 μg/ml and 2.39 at $t = 30$ min. Here, we consider noncardiac surgery since cardiac surgery often utilizes hypothermia which itself changes the BIS signal.

With $A = \left[\begin{array}{cc} 0 & 1 \\ -1 & -1 \end{array} \right]$, $L = [0, 1]^{\rm T}$, $\hat{b} = 1$, $Q_{\rm BIS_1} = 2.0 \times 10^{-4}$ g/min^2, $Q_{\rm BIS_2} = 4.0 \times 10^{-4}$ g/min^2, $d = 0.005$, and initial conditions $x_1(0) = x_2(0) = x_3(0) = 0$ g, $c_{\rm eff}(0) = 0$ g/ml, $\xi_{\rm c}(0) = [0,\, 0]^{\rm T}$, $\hat{W}_1(0) = 1 \times 10^{-3}[-3_{12\times 1}, 1_{12\times 1}]^{\rm T}$, $\hat{W}_2(0) = 0_{24\times 1}$, Figure 5.6 shows the masses of propofol in the three compartments versus time. Figure 5.7 shows the concentrations in the central and effect-site compartments versus time. Note that the effect-site compartment equilibrates with the central compartment in a matter of a few minutes. Figure 5.8 shows the noisy, actual, and filtered controlled BIS signals versus time. Finally, Figure 5.9 shows the control signal (propofol infusion rate) versus time predicated on the actual and filtered BIS signal.

For our simulation we used

$$\sigma_1(\zeta(t)) = \sigma_2(\zeta(t)) = \left[\frac{1}{1 + e^{-ak_1(\rm BIS_f(t-d) - BIS_{target})}}, \cdots, \frac{1}{1 + e^{-ak_6(\rm BIS_f(t-d) - BIS_{target})}}, \right.$$
$$\frac{1}{1 + e^{-ak_1(\rm BIS_f(t-2d) - BIS_{target})}}, \cdots, \frac{1}{1 + e^{-ak_6(\rm BIS_f(t-2d) - BIS_{target})}},$$
$$\frac{1}{1 + e^{-ak_1(u(t-d) - u_0)}}, \cdots, \frac{1}{1 + e^{-ak_6(u(t-d) - u_0)}},$$
$$\left. \frac{1}{1 + e^{-ak_1(u(t-2d) - u_0)}}, \cdots, \frac{1}{1 + e^{-ak_6(u(t-2d) - u_0)}} \right]^{\rm T},$$

where $s_1 = s_2 = 24$, $a = 0.1$, $k_1 = 1$, $k_2 = 2$, $k_3 = 6$, $k_4 = 24$, $k_5 = 120$, $k_6 = 720$, and $u_0 = 15$ mg/min. Even though we did not calculate the analytical bounds given by (5.33) due to the fact that one has to solve an optimization problem with respect to (5.14) and (5.15) to obtain ε_i^* and $w_{i\max}^*$, $i = 1, 2$, the closed-loop BIS signal response shown in Figure 5.8 is clearly acceptable. Furthermore, the basis functions for $\sigma_i(\zeta)$, $i = 1, 2$, are chosen to cover the domain of interest of our pharmacokinetic/pharmacodynamic problem since we know that the BIS index varies from 0 to 100. Hence, the basis functions are distributed over that domain. The number of basis functions, however, is based on trial and error. This goes back to the Stone-Weierstrass theorem which only provides an existence result without any constructive guidelines. Finally, we note that simulations using a larger number of neurons resulted in imperceptible differences in the closed-loop system performance.

The neuroadaptive control algorithm (5.63)–(5.65) does not require knowledge of the pharmacokinetic and pharmacodynamic parameters, in contrast to previous algorithms for closed-loop control of anesthesia [117,131]. However, the neuroadaptive controller (5.63)–(5.65) does not account for time delays due to the proprietary signal-averaging algorithm within the BIS monitor. Given the clinical observation that there is often a substantial delay between observed changes in patient status and a change in the BIS signal, other measures of depth of anesthesia may be needed [147].

5.5. Clinical Evaluation Trials

We have performed fifteen clinical trials with the neuroadaptive controller (5.63)–(5.65) at the Northeast Georgia Medical Center in Gainesville, Georgia [56]. In initial clinical testing, we implemented (5.63)–(5.65) using a Dell Latitude C610 laptop computer with a Pentium (R) III processor running under Windows XP, an Aspect A 2000 BIS monitor (rev 3.23), and a Harvard PHD 2000 programmable research pump.

The BIS monitor sends a data stream, which is updated every 5 sec. This data stream contains the BIS signal as well as other parameters such as date, time, signal quality indicator, raw EEG information, and electromyographic data. The data are sent to the serial port of the laptop computer.

The infusion rate $u(t)$ for the controller is calculated by employing a forward Euler method to update the neural network weights $\hat{W}_1(t)$ and $\hat{W}_2(t)$ every 0.5 sec, using the BIS signal. The infusion rate is communicated to the infusion pump using a 9600 bpm, 8 data bits, 2 stop bits, and zero parity protocol with the aid of a USB-serial port adaptor. An updated infusion rate is sent to the pump every 1 sec. Pharmacokinetic simulations predict that a pump update every 5 sec or less is adequate in the context of the algorithm under evaluation. An update interval of 1 sec was selected in anticipation that future algorithms might benefit from the faster update rate. In order to filter the noisy BIS signal we used a second-order, low-pass filter with natural frequency $\omega_n = 0.01\,\text{rad/sec}$ and damping ratio $\zeta = 0.707$.

The neuroadaptive control algorithm was programmed in Java, an object-oriented programming language chosen for its multi-platform portability tools for rapid prototyping. The program is organized into 5 modules, namely, bisloader, bislogger, controller, pumplogger, and pumploader. Bisloader and bislogger handle communication between the BIS monitor and the computer, while pumploader and pumplogger manage the Harvard pump apparatus. The module bisloader finds the serial port that receives the BIS signal by using the Java class CommPort Identifier, and then invokes bislogger. Bislogger uses the Java class SerialPort EventListener to read the signal, and uses the class StringTokenizer to parse the BIS signal from the input stream. The infusion rate is calculated by the controller module. Finally, pumploader opens the serial port communicating to the pump and establishes the communication protocol, while pumplogger delivers the infusion rate to the pump.

The protocol for clinical evaluation of the system was approved by the Institutional Review Board of Northeast Georgia Medical Center. Patients are enrolled after giving informed consent. Our protocol excludes patients requiring emergency surgery, pediatric patients, hemodynamically unstable patients, and patients for whom we anticipate difficult airway management. Otherwise, all elective surgical patients who can provide informed consent are candidates. Pre-operative management, including administration of anti-anxiolytic drugs, is left to the discretion of the attending anesthesiologist. Propofol is delivered using the BIS-computer-pump system with a target value of 50. In addition to propofol, all patients receive infusions of either sufentanil or fentanyl with loading doses of 0.25 μg/ml or 2 μg/ml and continuous infusions of 0.25 (μg/ml)/hr or 2 (μg/ml)/hr, respectively, to provide analgesia. To ensure patient safety, an independent anesthesia provider observes the progress of the study and can terminate the study if it appears that the patient's safety is being jeopardized by either overdosing or underdosing of propofol.

5.6. Results and Discussion

Patient demographics (for 10 patients) are presented in Table 5.1. The median BIS value after induction was 43. Four of the ten patients required phenylephrine to treat hypotension during induction (average dose 1075 μg with a standard deviation of 809.8 μg). The actual and filtered BIS signals versus time and control signal (propofol infusion rate) versus time for 10 patients are shown in Figures 5.10–5.12. The effect of using the actual (i.e., noisy) versus filtered BIS signal to generate the control signal is illustrated in Figures 5.13–5.16. In particular, Figure 5.14 shows the control signal predicated on the filtered BIS signal shown in Figure 5.13, whereas Figure 5.16 shows control signal predicated on the actual (i.e., noisy) BIS signal shown in Figure 5.15. Several performance measures of the control algorithm such as median BIS, bias (the

Table 5.1: Demographics of Neuroadaptive Control Algorithm

Age	59.0 years (18.0)
Weight	91.8 kg (23.3)
Gender	8 M / 2 F
Procedure	8 CABG †, 1 Thoracoscopy, 1 AVR ‡

* All values are mean with standard deviation in parentheses.
† CABG is Coronary Artery Bypass Grafting.
‡ AVR is Aortic Valve Replacement.

median of measured BIS minus target, normalized to the target), the median absolute value of the performance error (MAPE) (with performance error defined as measured BIS minus the target, normalized to the target) are summarized in Table 5.2. We observed that with induction all patients had some "overshoot" of the target BIS of 50, that is, a BIS value less than 50. In Table 5.3 we present, overshoot, and outside time (the percentage of study time that the individual patients had BIS values outside of the 35-60 range).

As noted in the introduction and [8], several other systems for closed-loop control of intravenous anesthesia have been previously described. The most direct comparison is to the results of Struys *et al.* [131]. The median absolute performance error of their controller was 7.7% in comparison to our 17.7%. The fraction of time that patients in the Struys *et al.* study were outside a BIS range of 35-60 was 11% compared to our 20.5%. Based on these measures, one would surmise that the clinical performance of the controller described by Struys *et al.* is superior. However, there are several factors that make direct comparisons tenuous. First, study designs were quite different. Struys *et al.* supplemented propofol with a continuous infusion of remifentanil while we used a bolus then continuous infusion of sufentanil. The rapid kinetics of remifentanil in comparison to sufentanil implies that opioid levels were more constant over time in the Struys *et al.* study than in ours. A constant opioid concentration could be expected to more effectively blunt arousal responses in the BIS with surgical stimulation. And, as noted by Glass and Rampil in the editorial

accompanying the publication by Struys *et al.*; the remifentanil dose used by Struys *et al.* is sufficient to blunt responses to surgical stimulation and reduce the propofol concentration to that needed to prevent consciousness [43].

Another key difference in study protocols is that Struys *et al.* initiated propofol administration with open-loop control and did not "close" the loop until the BIS reached 50. The controllers evaluated in this study were used for the induction as well as the maintenance of anesthesia. Finally, we note that model-based controllers may be expected to perform better than model-independent controllers as long as the model is correct. The three compartment mammillary pharmacokinetic model and the modified Hill equation pharmacodynamic model are well established and they could be expected to facilitate closed-loop control in the "average" patient who conforms to the models. However, model-based controllers could fail in patients who do not conform to the model and the studies done of closed-loop anesthesia to date do not have sufficient numbers to evaluate failure due to model nonconformance. Furthermore, we know that the three compartment mammilary model is not accurate when the propofol concentration is increased acutely, as occurs during induction and when surgical arousal is not blunted by opioids. Thus, we believe that comparison of controllers will not be definitive until larger numbers of patients are studied, so that one might encounter outlier patients, and with more demanding anesthetic/surgical conditions requiring wider ranges of anesthetic concentrations.

Table 5.2: BIS, Bias and MAPE of Neuroadaptive Control Algorithm

No	median BIS	Bias(%)	MAPE(%)
1	41.2	-17.6	20.1
2	41.2	-17.6	18.8
3	42.2	-15.8	17.4
4	46.5	-7.1	12.4
5	46.0	-8.0	20.4
6	42.7	-14.6	17.2
7	47.2	-5.5	8.1
8	41.1	-17.8	22.3
9	41.9	-16.3	17.0
10	39.5	-21.1	23.1

Table 5.3: Overshoot, Outside Time of Neuroadaptive Control Algorithm

No	Overshoot	Outside Time (%)
1	23.3	27.7
2	22.8	23.0
3	24.7	15.2
4	31.8	18.0
5	30.6	42.2
6	32.6	14.6
7	27.1	12.9
8	19.8	37.8
9	23.7	13.4
10	24.9	36.3

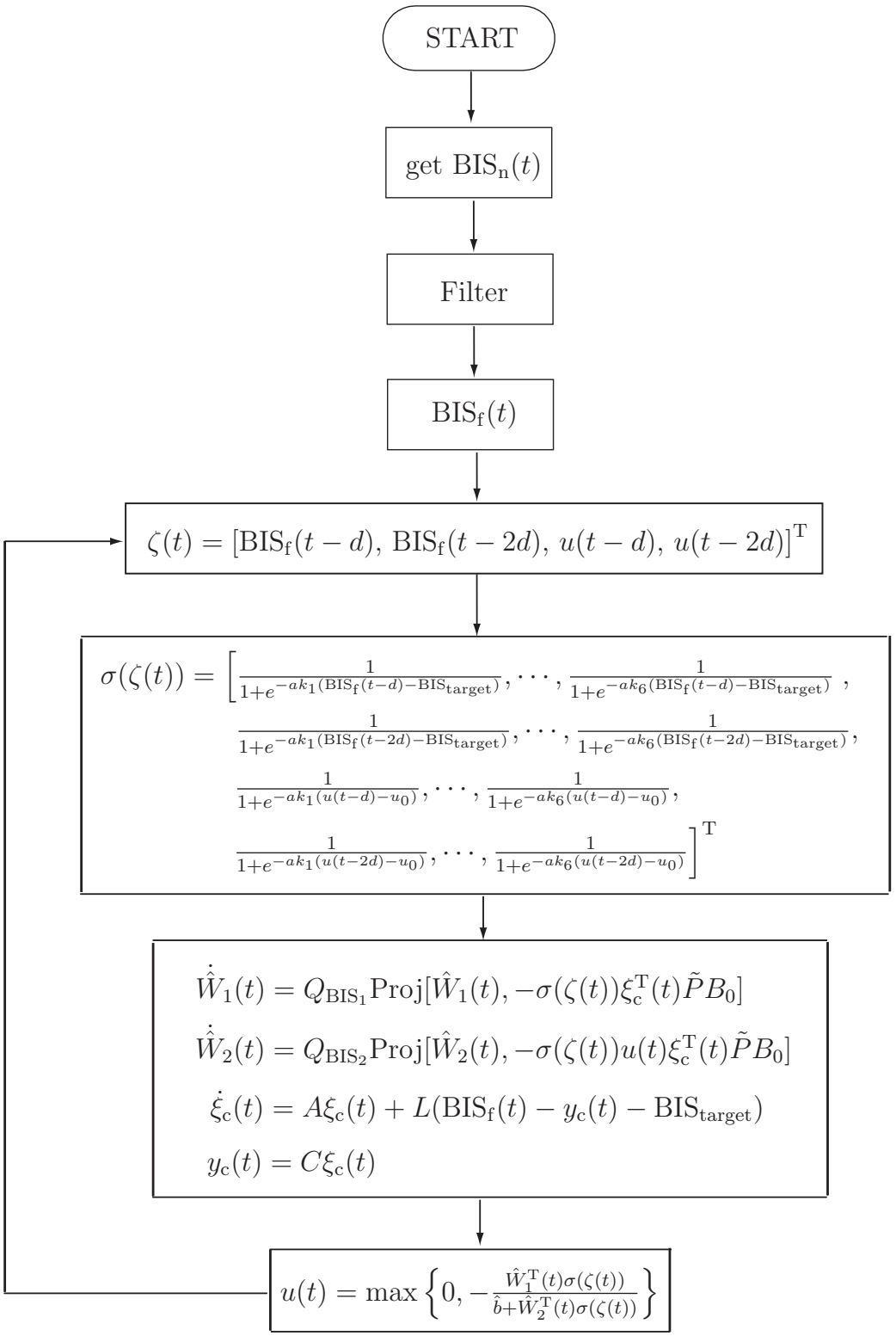

Figure 5.5: Flowchart for the neuroadaptive control algorithm.

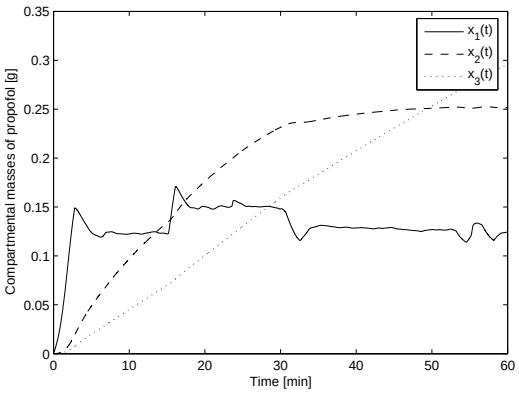

Figure 5.6: Compartmental masses versus time.

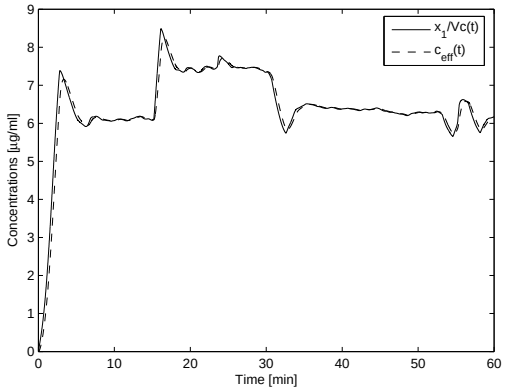

Figure 5.7: Concentrations in central and effect site compartments versus time.

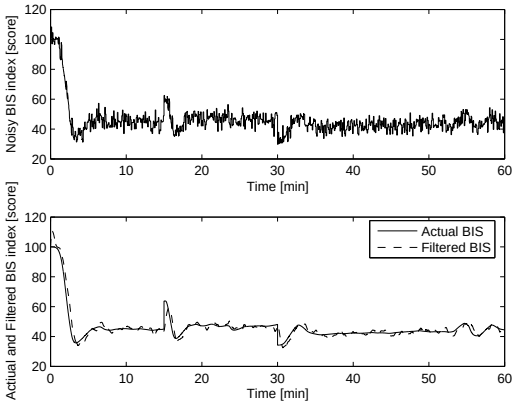

Figure 5.8: BIS signal versus time.

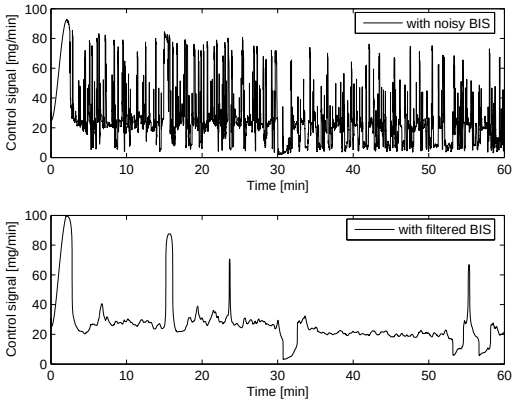

Figure 5.9: Control signal (infusion rate) versus time.

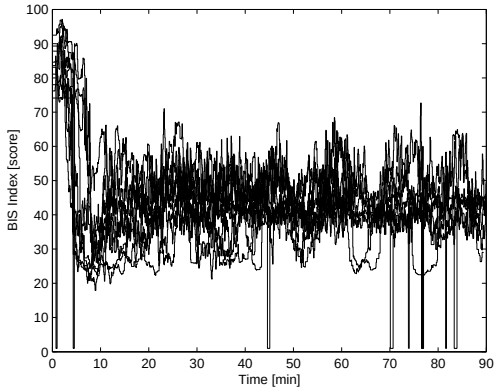

Figure 5.10: Controlled BIS signal versus time for 10 patients.

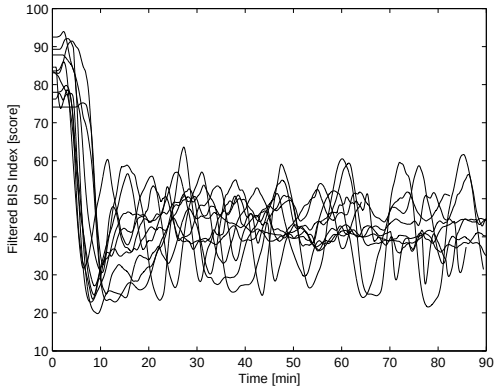

Figure 5.11: Filtered BIS signal versus time for 10 patients.

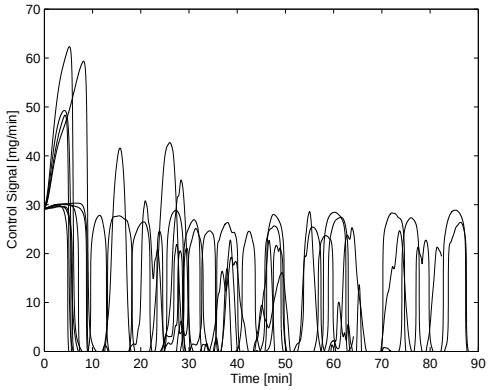

Figure 5.12: Infusion rate versus time for 10 patients.

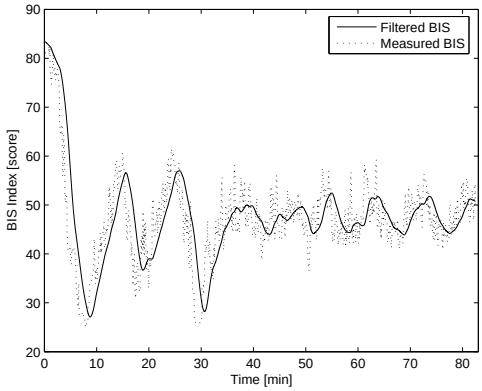

Figure 5.13: Representative measured and filtered BIS signal versus time.

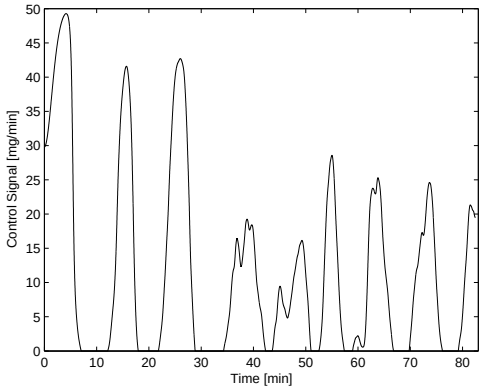

Figure 5.14: Representative infusion rate predicated on filtered BIS signal versus time.

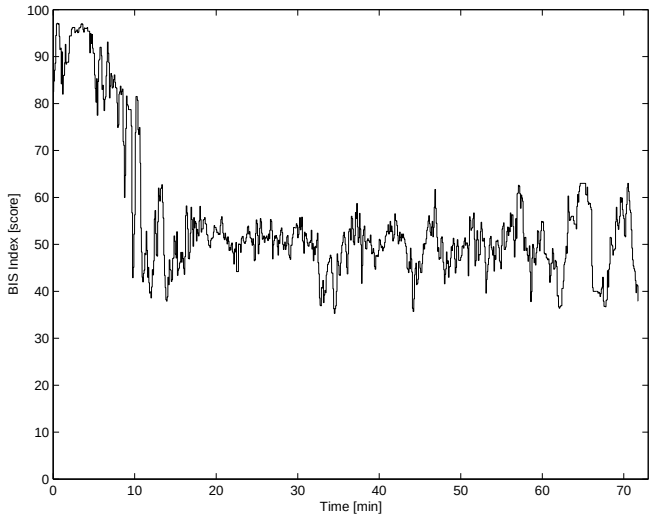

Figure 5.15: Representative measured (noisy) BIS signal versus time.

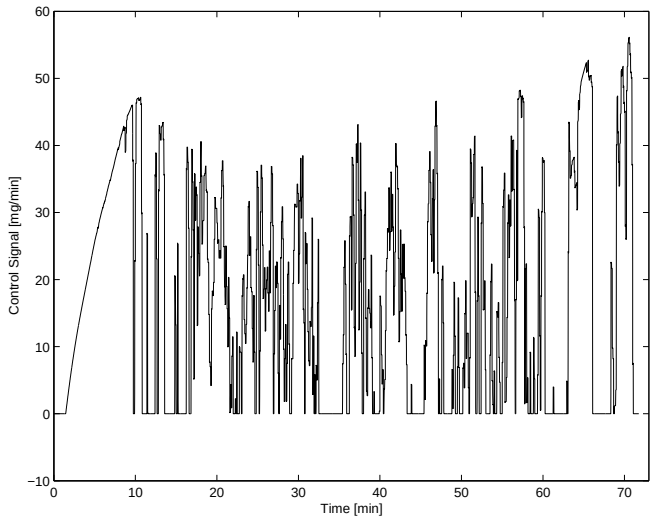

Figure 5.16: Representative infusion rate predicated on measured (noisy) BIS signal versus time.

Chapter 6

Neuroadaptive Output Feedback Control for Nonlinear Nonnegative Dynamical Systems with Actuator Amplitude and Integral Constraints

6.1. Introduction

Actuator nonlinearities arise frequently in practice and can severely degrade closed-loop system performance, and in some cases drive the system to instability, if not accounted for in the control design process. These effects are even more pronounced for adaptive controllers which continue to adapt when the feedback loop has been severed due to the presence of actuator saturation causing unstable controller modes to drift, which in turn leads to severe windup effects and unacceptable transients after saturation. Direct adaptive controllers for adaptive tracking of multivariable nonlinear uncertain dynamical systems with amplitude saturation constraints have been developed in the literature [1, 37, 76, 86, 88, 106, 116, 146].

The presence of control rate saturation may further exacerbate the problem of control amplitude saturation. To address amplitude and rate saturation constraints the authors in [90] construct a reference system (governor or supervisor) to address tracking and regulation in the face of actuator constraints by deriving adaptive update laws that guarantee that the error system dynamics are asymptotically stable and the adaptive controller gains are Lyapunov stable. In the case where the actuator

amplitude and rate are limited, the adaptive control signal to the reference system is modified to effectively robustify the error dynamics to the saturation constraints, and hence, guaranteeing asymptotic stability of the error states.

Even though adaptive and neuroadaptive controllers for drug delivery systems have been developed in the literature [7, 46, 53, 54, 57], adaptive control for drug dosing with actuator saturation effects is rather limited [62]. An implicit assumption inherent in most adaptive control frameworks for clinical pharmacology is that the adaptive control law is implemented without any regard to actuator constraints. Of course, any electromechanical control actuation device (e.g., infusion pump) is subject to amplitude and/or rate constraints leading to saturation nonlinearities enforcing limitations on control amplitudes and control rates. More importantly, in physiological applications, drug infusion rates can vary from patient to patient, and, to avoid overdosing, it is vital that the infusion rate does not exceed patient-specific threshold values. As a consequence, actuator constraints (e.g., infusion pump rate constraints) need to be accounted for in drug delivery systems.

One of the main drawbacks in developing active drug delivery systems is the lack of accurate mathematical models for characterizing the dynamic behavior of drugs on physiological variables. The distribution of drugs in the body depends on transport and metabolic processes, many of which are poorly understood. However, nonnegative and compartmental systems are essential in capturing the behavior of a wide range of dynamical systems involving dynamical models based on conservation laws involving dynamic states whose values are nonnegative [47, 49], and their use in the specific field of pharmacokinetics is essential in developing models for closed-loop control for drug administration [49]. In this chapter, we develop a neuroadaptive control framework for nonnegative dynamical systems with actuator amplitude and control integral constraints. Specifically, building on the work of [37, 46, 116] we develop

an output feedback neural network controller with input constraints that operates over a tapped delay line (TDL) of available input and output measurements. The neuroadaptive laws for the neural network weights are constructed using a linear observer for the nominal normal form system error dynamics.

The proposed approach is applicable to a specific class of nonlinear nonnegative dynamical systems with control amplitude saturation constraints as well as control integral constraints over a given time interval. It is important to note here that our framework does not account for actuator rate constraints. However, since control inputs for drug delivery systems involve drug infusion rates, an actuator amplitude constraint captures a constraint on the drug delivery infusion rate. In addition, since in pharmacological applications involving active drug administration control inputs as well as the system states need to be nonnegative, the proposed neuroadaptive output feedback controller also guarantees that the control signal as well as the physical system states remain nonnegative. Using an electroencephalogram (EEG) measurement as an objective, quantitative measure of consciousness, the proposed framework is used to control the infusion of an anesthetic drug for maintaining a desired constant level of depth of anesthesia during surgery in the face of infusion rate constraints and an integral drug dosing constraint over a specified time interval.

6.2. Neuroadaptive Output Feedback Control with Actuator Constraints

In this section, we consider the problem of characterizing neuroadaptive dynamic output feedback control laws for nonlinear uncertain dynamical systems with actuator amplitude constraints to achieve reference model output tracking. Specifically, consider the controlled nonlinear uncertain dynamical system $\mathcal{G}$ in normal form [67]

given by

$$\dot{x}(t) = A_0 x(t) + B\Lambda \left[h(u(t)) + f(x(t), z(t), \hat{u}(t)) \right], \quad x(0) = x_0, \quad t \geq 0, \tag{6.1}$$

$$\dot{z}(t) = f_z(x(t), z(t)), \quad z(0) = z_0, \tag{6.2}$$

$$y(t) = Cx(t) + W_y^{\mathrm{T}} \sigma_y(\hat{y}(t), \hat{u}(t)), \tag{6.3}$$

where $x(t) \in \mathbb{R}^r$, $t \geq 0$, and $z(t) \in \mathbb{R}^{n-r}$, $t \geq 0$, are the state vectors, $u(t) \in \mathbb{R}^m$, $t \geq 0$, is the control input, $y(t) \in \mathbb{R}^m$, $t \geq 0$, is the system output, $\hat{u}(t) \triangleq [\, u(t - \tau_u),\, u(t - 2\tau_u),\, \ldots,\, u(t - p\tau_u)]$ is a vector of p-delayed values of the control input with $p \geq 1$ and $\tau_u > 0$ given, $\hat{y}(t) \triangleq [\, y(t - \tau_y),\, y(t - 2\tau_y),\, \ldots,\, y(t - q\tau_y)]$ is a vector of q-delayed values of the system output with $q \geq 1$ and $\tau_y > 0$ given, $A_0 \in \mathbb{R}^{r \times r}$ is a known Hurwitz and essentially nonnegative matrix, $B \in \mathbb{R}^{r \times m}$ is a known nonnegative input matrix, $\Lambda \in \mathbb{R}^{m \times m}$ is an *unknown* nonnegative and positive-definite matrix, $h(u(t)) = [h_1(u_1(t), \ldots, h_m(u_m(t))]^{\mathrm{T}}$ is the constrained control input given by

$$h_i(u_i) \triangleq \begin{cases} 0, & \text{if } u_i \leq 0, \\ u_i^*, & \text{if } u_i \geq u_i^*, \\ u_i, & \text{otherwise,} \end{cases} \qquad i = 1, \ldots, m, \tag{6.4}$$

where $u_i^* > 0$, $i = 1, \ldots, m$, are given constants, $f : \mathbb{R}^r \times \mathbb{R}^{n-r} \times \mathbb{R}^{mp} \to \mathbb{R}^m$ is Lipschitz continuous, bounded, and essentially nonnegative with respect to x for all $z \in \mathbb{R}^{n-r}$ and $\hat{u} \in \mathbb{R}^{mp}$ but otherwise *unknown* (that is, $f(\cdot, \cdot)$ is such that $f_i(x, \hat{u}) \geq 0$ if $x_i = 0$, $i = 1, \ldots, n$, for all $z \in \mathbb{R}^{n-r}$ and $\hat{u} \in \mathbb{R}^{mp}$), $f_z : \mathbb{R}^r \times \mathbb{R}^{n-r} \to \mathbb{R}^{n-r}$ is such that (6.2) is input-to-state stable for all $z \in \mathbb{R}^{n-r}$ with $x(t)$ viewed as the input, $C \in \mathbb{R}^{m \times r}$ is a known output matrix, $W_y \in \mathbb{R}^{l \times m}$ is an *unknown* matrix, and $\sigma_y : \mathbb{R}^{mq} \times \mathbb{R}^{mp} \to \mathbb{R}^l$ is a known Lipschitz continuous function that is bounded on $\mathbb{R}^{mq} \times \mathbb{R}^{mp}$.

In order to achieve output tracking, we construct a reference nonnegative dynam-

ical system $\mathcal{G}_{\rm ref}$ given by

$$\dot{x}_{\rm ref}(t) = A_{\rm ref}x_{\rm ref}(t) + B_{\rm ref}r(t), \quad x_{\rm ref}(0) = x_{\rm ref_0}, \quad t \geq 0, \tag{6.5}$$

$$y_{\rm ref}(t) = Cx_{\rm ref}(t), \tag{6.6}$$

where $x_{\rm ref}(t) \in \mathbb{R}^r$, $t \geq 0$, is the reference state vector, $r(t) \in \mathbb{R}^d$, $t \geq 0$, is a bounded piecewise continuous nonnegative reference input, $A_{\rm ref} \in \mathbb{R}^{r\times r}$ is a Hurwitz and essentially nonnegative matrix, and $B_{\rm ref} \in \mathbb{R}^{r\times d}$ is a nonnegative matrix.

As discussed in the Introduction, control (source) inputs of drug delivery systems for physiological and pharmacological processes are usually constrained to be nonnegative as are the system states. Hence, in this chapter we develop neuroadaptive dynamic output feedback control laws for nonnegative systems with nonnegative control inputs. In addition, to account for infusion rate constraints we develop neuroadaptive control laws with actuator constraints. Specifically, for the reference model output tracking problem our goal is to design a nonnegative control input $u(t)$, $t \geq 0$, predicated on the system measurement $y(t)$, $t \geq 0$, such that $\|y(t) - y_{\rm ref}(t)\| < \gamma$ for all $t \geq T$, where $\|\cdot\|$ denotes the Euclidean vector norm on $\mathbb{R}^m$, $\gamma > 0$ is sufficiently small, and $T \in [0, \infty)$, $x(t) \geq\geq 0$, $t \geq 0$, for all $x_0 \in \overline{\mathbb{R}}^n_+$, and the control input $u(\cdot)$ in (6.1) is restricted to the class of *admissible controls* consisting of measurable functions $u(t) = [u_1(t), \ldots, u_m(t)]^{\rm T}$, $t \geq 0$, such that (6.4) holds and

$$\eta_i(t) \triangleq \int_{t-\tau_{\rm s}}^{t} h_i(u_i(s))\mathrm{d}s \leq \eta_i^*, \quad i = 1, \ldots, m, \quad t \geq 0, \tag{6.7}$$

where $\tau_{\rm s} > 0$ and $\eta_i^* > 0$, $i = 1, \ldots, m$, are given constants, and $u_i(t) \equiv 0$ for all $t \in [-\tau_{\rm s}, 0]$ and $i = 1, \ldots, m$. Note that $\eta_i(t)$, $i = 1, \ldots, m$, $t \geq 0$, given by (6.7) satisfies

$$\dot{\eta}_i(t) = h_i(u_i(t)) - h_i(u_i(t - \tau_{\rm s})), \quad \eta_i(0) = 0, \quad t \geq 0. \tag{6.8}$$

Here, we assume that the function $f(x, z, \hat{u})$ can be approximated over a compact set $\mathcal{D}_x \times \mathcal{D}_z \times \mathcal{D}_{\hat{u}}$ by a linear in parameters neural network up to a desired accuracy.

In this case, there exists $\hat{\varepsilon} : \mathbb{R}^r \times \mathbb{R}^{n-r} \times \mathbb{R}^{mp} \to \mathbb{R}^m$ such that $\|\hat{\varepsilon}(x, z, \hat{u})\| < \hat{\varepsilon}^*$ for all $(x, z, \hat{u}) \in \mathcal{D}_x \times \mathcal{D}_z \times \mathcal{D}_{\hat{u}}$, where $\hat{\varepsilon}^* > 0$, and

$$f(x, z, \hat{u}) = W_f^{\mathrm{T}} \hat{\sigma}(x, z, \hat{u}) + \hat{\varepsilon}(x, z, \hat{u}), \quad (x, z, \hat{u}) \in \mathcal{D}_x \times \mathcal{D}_z \times \mathcal{D}_{\hat{u}}, \tag{6.9}$$

where $W_f \in \mathbb{R}^{s \times m}$ is an optimal *unknown* (constant) weight that minimizes the approximation error over $\mathcal{D}_x \times \mathcal{D}_z \times \mathcal{D}_{\hat{u}}$, $\hat{\sigma} : \mathbb{R}^r \times \mathbb{R}^{n-r} \times \mathbb{R}^{mp} \to \mathbb{R}^s$ is a vector of basis functions such that each component of $\hat{\sigma}(\cdot, \cdot, \cdot)$ takes values between 0 and 1, and $\hat{\varepsilon}(\cdot, \cdot, \cdot)$ is the modeling error. Note that s denotes the total number of basis functions or, equivalently, the number of nodes of the neural network.

Since $f(\cdot, \cdot, \cdot)$ is continuous on $\mathbb{R}^r \times \mathbb{R}^{n-r} \times \mathbb{R}^{mp}$ we can choose $\hat{\sigma}(\cdot, \cdot, \cdot)$ from a linear space $\mathcal{X}$ of continuous functions that forms an algebra and separates points in $\mathcal{D}_x \times \mathcal{D}_z \times \mathcal{D}_{\hat{u}}$. In this case, it follows from the Stone-Weierstrass theorem [111, p. 212] that $\mathcal{X}$ is a dense subset of the set of continuous functions on $\mathcal{D}_x \times \mathcal{D}_z \times \mathcal{D}_{\hat{u}}$. Now, as is the case in the standard neuroadaptive control literature [92], we can construct a signal involving the estimates of the optimal weights and basis functions as our adaptive control signal. It is important to note here that we assume that we know the structure and the size of the approximator. This is a standard assumption in the neural network adaptive control literature. In online neural network training, the size and the structure of the optimal approximator are not known and are often chosen by the rule that the larger the size of the neural network and the richer the distribution class of the basis functions over a compact domain, the tighter the resulting approximation error bound $\hat{\varepsilon}(\cdot, \cdot, \cdot)$. This goes back to the Stone-Weierstrass theorem which only provides an existence result without any constructive guidelines.

In order to develop an *output* feedback neuroadaptive controller, we use the approach developed in [87] for reconstructing the system states via the system delayed inputs and outputs. Specifically, we use a *memory unit* as a particular form of

a tapped delay line (TDL) that takes a scalar time series input and provides an $(2mn - r)$-dimensional vector output consisting of the present values of the system outputs and system inputs, and their $2(n-1)m - r$ delayed values given by

$$\begin{aligned}\zeta(t) \triangleq\ & [y_1(t), y_1(t-d), \ldots, y_1(t-(n-1)d), \ldots, y_m(t), y_m(t-d), \ldots, \\ & y_m(t-(n-1)d); u_1(t), u_1(t-d), \ldots, u_1(t-(n-r_1-1)d), \ldots, u_m(t), \\ & u_m(t-d), \ldots, u_m(t-(n-r_m-1)d)]^{\mathrm{T}}, \quad t \geq 0, \end{aligned} \tag{6.10}$$

where r_i denotes the relative degree of $\mathcal{G}$ with respect to the output y_i, $i = 1, \ldots, m$.

The following matching conditions are needed for the main result of this chapter.

Assumption 6.1. There exist $K_{\mathrm{y}} \in \mathbb{R}^{m \times m}$ and $K_{\mathrm{r}} \in \mathbb{R}^{m \times d}$ such that $A_0 + BK_{\mathrm{y}}C = A_{\mathrm{ref}}$ and $BK_{\mathrm{r}} = B_{\mathrm{ref}}$.

Assumption 6.1 involves standard matching conditions for model reference adaptive control appearing in the literature; see, for example, Chapter 5 in [132].

Using the parameterization $\Lambda = \hat{\Lambda} + \Delta\Lambda$, where $\Delta\Lambda \in \mathbb{R}^{m \times m}$ is an unknown symmetric matrix, the dynamics in (6.1) can be rewritten as

$$\dot{x}(t) = A_0 x(t) + B\hat{\Lambda}h(u(t)) + B\left[\Delta\Lambda h(u(t)) + \Lambda f(x(t), z(t), \hat{u}(t))\right], \ x(0) = x_0, \ t \geq 0. \tag{6.11}$$

Define $W \triangleq \left[W_1^{\mathrm{T}}, W_2^{\mathrm{T}}\right]^{\mathrm{T}} \in \mathbb{R}^{(s+m) \times m}$, where $W_1 \triangleq W_f\Lambda$ and $W_2 \triangleq \Delta\Lambda^{\mathrm{T}}$. Using (6.9), (6.11) can be rewritten as

$$\begin{aligned}\dot{x}(t) = \ & A_0 x(t) + B\hat{\Lambda}u(t) + BW^{\mathrm{T}}\sigma(\zeta(t), h(u(t))) + B\hat{\Lambda}\Delta h(t) + B\Lambda\hat{\varepsilon}(x(t), z(t), \hat{u}(t)), \\ & + BW_1^{\mathrm{T}}\left[\hat{\sigma}(x(t), z(t), \hat{u}(t)) - \sigma_\zeta(\zeta(t))\right], \quad x(0) = x_0, \quad t \geq 0, \end{aligned} \tag{6.12}$$

where

$$\sigma(\zeta(t), h(u(t))) \triangleq \left[\sigma_\zeta^{\mathrm{T}}(\zeta(t)), h^{\mathrm{T}}(u(t))\right]^{\mathrm{T}}, \quad t \geq 0, \tag{6.13}$$

$\sigma_\zeta : \mathbb{R}^{2mn-r} \to \mathbb{R}^s$ is a vector of basis functions such that each component of $\sigma_\zeta(\cdot)$ takes values between 0 and 1, and $\Delta h(u(t)) \triangleq h(u(t)) - u(t)$, $t \geq 0$.

Next, consider a sequence of positive numbers $\{\rho_i\}_{i=1}^{\infty}$ such that $\lim_{i\to\infty} \rho_i = 0$ and define the time-dependent set $\Omega_{t,i}$ and saturation impact times $\tau_i^*(t)$ by

$$\Omega_{t,i} \triangleq \{\tau \geq 0 : \eta_i(\tau) = \eta_i^* \text{ and there exists } N > 0 \text{ such that, for all } i \geq N,$$
$$\eta_i(\tau - \rho_i) < \eta_i^*\}, \quad t \geq 0, \quad i = 1, \ldots, m, \tag{6.14}$$

$$\tau_i^*(t) \triangleq \begin{cases} \theta_i + \max\{\tau : \tau \in \Omega_{t,i}\}, & \text{if } \Omega_{t,i} \neq \varnothing, \\ 0, & \text{otherwise,} \end{cases} \quad t \geq 0, \quad i = 1, \ldots, m, \tag{6.15}$$

where $\theta_i > 0$, $i = 1, \ldots, m$, are design parameters.

Now, consider the control input $u(t)$, $t \geq 0$, given by

$$u(t) = \Phi(\eta(t))\psi(t), \quad t \geq 0, \tag{6.16}$$

where $\Phi(\eta(t)) \triangleq \operatorname{diag}[\phi_1(\eta_1(t)), \ldots, \phi_m(\eta_m(t))]$, $t \geq 0$,

$$\phi_i(\eta_i(t)) \triangleq \begin{cases} 1, & \text{if } 0 \leq \eta_i(t) \leq \eta_i^* - \delta_i \text{ and } t \geq \tau_i^*(t), \\ \frac{1}{\delta_i}(\eta_i^* - \eta_i(t)), & \text{if } \eta_i^* - \delta_i \leq \eta_i(t) \leq \eta_i^* \text{ and } t \geq \tau_i^*(t), \\ 0, & \text{otherwise,} \end{cases} \tag{6.17}$$
$$t \geq 0, \quad i = 1, \ldots, m,$$

$0 < \delta_i < \eta_i^*$, $i = 1, \ldots, m$, are design constant parameters (chosen to be sufficiently small), and $\psi(t) \in \mathbb{R}^m$, $t \geq 0$, is given by

$$\psi(t) = \psi_{\mathrm{n}}(t) - \psi_{\mathrm{ad}}(t), \quad t \geq 0, \tag{6.18}$$

where

$$\psi_{\mathrm{n}}(t) = \hat{\Lambda}^{-1}[K_{\mathrm{y}} y(t) + K_{\mathrm{r}} r(t)], \quad t \geq 0, \tag{6.19}$$

$$\psi_{\mathrm{ad}}(t) = \hat{\Lambda}^{-1}\left[\hat{W}^{\mathrm{T}}(t)\sigma(\zeta(t), h(u(t))) + K_{\mathrm{y}}\hat{W}_y^{\mathrm{T}}(t)\sigma_y(\hat{y}(t), \hat{u}(t))\right], \quad t \geq 0, \tag{6.20}$$

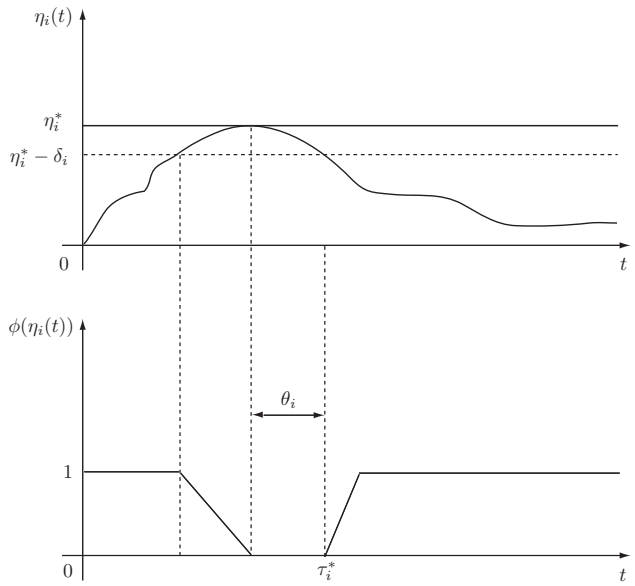

Figure 6.1: Visualization of the effect of $\phi_i(\eta_i(t))$ for a given function $\eta_i(t)$.

and $\hat{W}(t) \in \mathbb{R}^{(s+m)\times m}$, $t \geq 0$, and $\hat{W}_y(t) \in \mathbb{R}^{l\times m}$, $t \geq 0$, are update weights. Note that, for all $t \geq 0$ and $i = 1, \ldots, m$, $0 \leq \phi_i(\eta_i(t)) \leq 1$. Furthermore, if $\eta_i(\hat{t}) = \eta_i^*$ for every $\hat{t} \geq 0$, then $h_i(u_i(\hat{t})) = 0$. Now, it follows from (6.8) that $\dot{\eta}(\hat{t}) = -h_i(u_i(\hat{t} - \tau_{\mathrm{s}})) \leq 0$, $\hat{t} \geq 0$, and hence, $\eta_i(\hat{t})$ is upper bounded by η_i^*. Thus, the integral constraint (6.7) is satisfied. Figure 6.1 shows the interplay between $\eta_i(t)$ and $\phi_i(\eta_i(t))$, $i = 1, \ldots, m$.

Remark 6.1. The choice of $\phi_i(\eta_i)$, $i = 1, \ldots, m$, is not limited to the piecewise linear continuous function given by (6.17). In particular, on the interval $\eta_i^* - \delta_i \leq \eta_i \leq \eta_i^*$, $\phi_i(\eta_i)$ can be chosen as any decreasing continuous function such that $\phi_i(\eta_i^* - \delta_i) = 1$ and $\phi_i(\eta_i^*) = 0$.

Defining the tracking error state $e(t) \triangleq x(t) - x_{\mathrm{ref}}(t)$, $t \geq 0$, and using (6.16), (6.18)–(6.20), and Assumption 6.1, the error dynamics are given by

$$\dot{e}(t) = A_{\mathrm{ref}}e(t) + B\tilde{W}^{\mathrm{T}}(t)\sigma(\zeta(t), h(u(t))) + BK_{\mathrm{y}}\tilde{W}_y^{\mathrm{T}}(t)\sigma_y(\hat{y}(t), \hat{u}(t)) + B\hat{\Lambda}\Delta h(u(t)) + \varepsilon(t), \qquad e(0) = x_0 - x_{\mathrm{ref}_0}, \quad t \geq 0, \tag{6.21}$$

where

$$\varepsilon(t) \triangleq B\hat{\Lambda}(\Phi(t) - I_m)\psi(t) + BW_1^{\mathrm{T}}\left[\hat{\sigma}(x(t), z(t), \hat{u}(t)) - \sigma_\zeta(\zeta(t))\right] + B\Lambda\hat{\varepsilon}(x(t), z(t), \hat{u}(t)), \quad t \geq 0, \tag{6.22}$$

$\tilde{W}(t) \triangleq W - \hat{W}(t)$, $t \geq 0$, and $\tilde{W}_y(t) \triangleq W_y - \hat{W}_y(t)$, $t \geq 0$.

Next, to account for the effects of saturation on the error state $e(t)$, $t \geq 0$, consider the dynamical system given by

$$\dot{e}_{\mathrm{s}}(t) = A_{\mathrm{ref}}e_{\mathrm{s}}(t) + B\hat{\Lambda}\Delta h(u(t)), \quad e_{\mathrm{s}}(0) = e_{\mathrm{s}0}, \quad t \geq 0, \tag{6.23}$$

$$y_{\mathrm{s}}(t) = Ce_{\mathrm{s}}(t), \tag{6.24}$$

where $e_{\mathrm{s}}(t) \in \mathbb{R}^r$, $t \geq 0$, and define the augmented error state $\tilde{e}(t) \triangleq e(t) - e_{\mathrm{s}}(t)$, $t \geq 0$. Now, it follows from (6.21) and (6.23) that

$$\dot{\tilde{e}}(t) = A_{\mathrm{ref}}\tilde{e}(t) + B\left[\tilde{W}^{\mathrm{T}}(t)\sigma(\zeta(t), h(u(t))) + K_{\mathrm{y}}\tilde{W}_y^{\mathrm{T}}(t)\sigma_y(\hat{y}(t), \hat{u}(t))\right] + \varepsilon(t), \quad \tilde{e}(0) = 0, \quad t \geq 0. \tag{6.25}$$

Consider the update laws given by

$$\dot{\hat{W}}(t) = \Gamma_W \mathrm{Proj}[\hat{W}(t), \sigma(\zeta(t), h(u(t)))\xi_{\mathrm{c}}^{\mathrm{T}}(t)PB], \ \hat{W}(0) = \hat{W}_0, \ t \geq 0, \tag{6.26}$$

$$\dot{\hat{W}}_y(t) = \Gamma_y \mathrm{Proj}[\hat{W}_y(t), \sigma_y(\hat{y}(t), \hat{u}(t))\xi_{\mathrm{c}}^{\mathrm{T}}(t)(PBK_y + \tilde{P}L)], \quad \hat{W}_y(0) = \hat{W}_{y0}, \tag{6.27}$$

where $\Gamma_W \in \mathbb{R}^{(s+m)\times(s+m)}$ and $\Gamma_y \in \mathbb{R}^{l\times l}$ are positive definite matrices, $P \in \mathbb{R}^{r\times r}$ is a positive-definite solution of the Lyapunov equation

$$0 = A_{\mathrm{ref}}^{\mathrm{T}}P + PA_{\mathrm{ref}} + R, \tag{6.28}$$

where $R > 0$, and $\tilde{P} \in \mathbb{R}^{n_\xi \times n_\xi}$ is a positive-definite solution of the Lyapunov equation

$$0 = (\hat{A} - L\hat{C})^{\mathrm{T}}\tilde{P} + \tilde{P}(\hat{A} - L\hat{C}) + \tilde{R}, \tag{6.29}$$

where $\tilde{R} > 0$, $\hat{A} \in \mathbb{R}^{n_\xi \times n_\xi}$ is Hurwitz, $L \in \mathbb{R}^{n_\xi \times m}$, $\hat{C} \in \mathbb{R}^{m \times n_\xi}$, and $\xi_{\mathrm{c}}(t) \in \mathbb{R}^{n_\xi}$, $t \geq 0$, is the solution to the estimator dynamics

$$\dot{\xi}_{\mathrm{c}}(t) = \hat{A}\xi_{\mathrm{c}}(t) + L\left[y(t) - y_{\mathrm{ref}}(t) - y_{\mathrm{c}}(t) - y_{\mathrm{s}}(t)\right], \quad \xi_{\mathrm{c}}(0) = \xi_{\mathrm{c}0}, \quad t \geq 0, \tag{6.30}$$

$$y_{\mathrm{c}}(t) = \hat{C}\xi_{\mathrm{c}}(t) + \hat{W}_y^{\mathrm{T}}(t)\sigma_y(\hat{y}(t), \hat{u}(t)). \tag{6.31}$$

Note that since $h(u)$ is bounded for all $u \in \mathbb{R}^m$ and $f(x, z, \hat{u})$ is bounded for all $(x, z, \hat{u}) \in \mathbb{R}^r \times \mathbb{R}^{n-r} \times \mathbb{R}^{mp}$, it follows that $x(t)$, $t \geq 0$, is bounded for all $t \geq 0$, and hence, $\psi_{\mathrm{n}}(t)$ is bounded for all $t \geq 0$. Now, since the projection operator used in the update laws (6.26) and (6.27) guarantees the boundness of the update weights $\hat{W}(t)$, $t \geq 0$, and $\hat{W}_y(t)$, $t \geq 0$, it follows that there exist $u^* > 0$ and $\delta^* > 0$ such that $\|u(t)\| \leq u^*$ and $\|\Delta h(u(t))\| \leq \delta^*$ for all $t \geq 0$. Furthermore, note that there exists $\varepsilon^* > 0$ such that $\|\varepsilon(t)\| \leq \varepsilon^*$ for all $t \geq 0$ such that $(x(t), z(t), \hat{u}(t)) \in \mathcal{D}_x \times \mathcal{D}_z \times \mathcal{D}_{\hat{u}}$. Finally, there exist $\alpha_1 > 0$ and $\alpha_2 > 0$ such that $\|\tilde{W}^{\mathrm{T}}(t)\sigma(\zeta(t), h(u(t)))\| \leq \alpha_1$ and $\|\tilde{W}_y^{\mathrm{T}}(t)\sigma_y(\hat{y}(t), \hat{u}(t))\| \leq \alpha_2$ for all $t \geq 0$.

For the statement of the main result of this chapter, let $\|\cdot\|' : \mathbb{R}^{r \times r} \to \mathbb{R}$ be the matrix norm equi-induced by the vector norm $\|\cdot\|'' : \mathbb{R}^r \to \mathbb{R}$, let $\|\cdot\|''' : \mathbb{R}^{r \times m} \to \mathbb{R}$ be the matrix norm induced by the vector norms $\|\cdot\|'' : \mathbb{R}^r \to \mathbb{R}$ and $\|\cdot\|'''' : \mathbb{R}^m \to \mathbb{R}$, and let $\|\cdot\|^* : \mathbb{R}^{n_\xi \times n_\xi} \to \mathbb{R}$ be the matrix norm equi-induced by the vector norm $\|\cdot\|^{**} : \mathbb{R}^{n_\xi} \to \mathbb{R}$.

Theorem 6.1. Consider the nonlinear uncertain dynamical system $\mathcal{G}$ given by (6.1)–(6.3) with $u(t)$, $t \geq 0$, given by (6.16)–(6.20) and reference model $\mathcal{G}_{\mathrm{ref}}$ given by (6.5) and (6.6) with tracking error dynamics given by (6.21). Assume Assumption 6.1 holds, $\lambda_{\min}(R) > 1$, and $\lambda_{\min}(\tilde{R}) > \|\tilde{P}L\hat{C}\|^{*2}$. Then there exists a compact positively invariant set $\mathcal{D}_\alpha \subset \mathbb{R}^r \times \mathbb{R}^r \times \mathbb{R}^{n_\xi} \times \mathbb{R}^{(s+m)\times m} \times \mathbb{R}^{l \times m}$ such that $(0, 0, 0, W, W_y) \in \mathcal{D}_\alpha$, where $W \in \mathbb{R}^{(s+m)\times m}$ and $W_y \in \mathbb{R}^{l \times m}$, and the solution $(e(t), e_{\mathrm{s}}(t), \xi_{\mathrm{c}}(t), \hat{W}(t), \hat{W}_y(t))$, $t \geq 0$, of the closed-loop system given by (6.1)–(6.3),

(6.16), (6.23), (6.24), (6.26), (6.27), (6.30) and (6.31) is ultimately bounded for all $(e(0), e_{\rm s}(0), \xi_{\rm c}(0), \hat{W}(0), \hat{W}_y(0)) \in \mathcal{D}_\alpha$ with ultimate bound $\|y(t) - y_{\rm ref}(t)\| < \gamma$, $t \geq T$, where

$$\gamma > \Bigg(\Big[(\lambda_{\min}(R) - 1)^{-\frac{1}{2}} \sqrt{\nu} + \alpha_e \Big]^2 + \Big[(\lambda_{\min}(\tilde{R}) - \|\tilde{P} L \hat{C}\|^{*2})^{-\frac{1}{2}} \sqrt{\nu} + \alpha_\xi \Big]^2 + \lambda_{\max}(\Gamma_W^{-1}) \hat{w}^2{}_{\max} + \lambda_{\max}(\Gamma_y^{-1}) \hat{w}_{y\max}^2 \Bigg)^{\frac{1}{2}}, \tag{6.32}$$

$$\nu \triangleq (\lambda_{\min}(R) - 1) \alpha_e^2 + (\lambda_{\min}(\tilde{R}) - \|\tilde{P} L \hat{C}\|^{*2}) \alpha_\xi^2, \tag{6.33}$$

$$\alpha_e \triangleq \frac{1}{\lambda_{\min}(R) - 1} \Big(\|P\|' \varepsilon^* + \|PB\|''' \alpha_1 + \|PBK_y\|''' \alpha_2 \Big), \tag{6.34}$$

$$\alpha_\xi \triangleq \frac{1}{\lambda_{\min}(\tilde{R}) - \|\tilde{P} L \hat{C}\|^{*2}} \Big(\|PB\|''' \alpha_1 + \|PBK_y\|''' \alpha_2 \Big), \tag{6.35}$$

and $\hat{w}_{\max}$ and $\hat{w}_{y\max}$ are norm bounds imposed on $\hat{W}$ and $\hat{W}_y$, respectively. Furthermore, $u(t)$ satisfies (6.7) for all $t \geq 0$, $h(u(t)) \geq\geq 0$, $t \geq 0$, and $x(t) \geq\geq 0$, $t \geq 0$, for all $x_0 \in \overline{\mathbb{R}}_+^r$.

Proof. Ultimate boundness of the closed-loop system follows by considering the Lyapunov-like function candidate

$$V(\tilde{e}, \xi_{\rm c}, \tilde{W}, \tilde{W}_y) = \tilde{e}^{\rm T} P \tilde{e} + \xi_{\rm c}^{\rm T} \tilde{P} \xi_{\rm c} + \operatorname{tr} \tilde{W}^{\rm T} \Gamma_W^{-1} \tilde{W} + \operatorname{tr} \tilde{W}_y^{\rm T} \Gamma_y^{-1} \tilde{W}_y, \tag{6.36}$$

where $P > 0$ and $\tilde{P} > 0$ satisfy, respectively, (6.28) and (6.29). Note that (6.36) satisfies $\alpha(\|z\|) \leq V(z) \leq \beta(\|z\|)$ with $z = [\tilde{e}^{\rm T}, \xi_{\rm c}^{\rm T}, (\operatorname{vec} \tilde{W})^{\rm T}, (\operatorname{vec} \tilde{W}_y)^{\rm T}]^{\rm T}$ and $\alpha(\|z\|) = \beta(\|z\|) = \|z\|^2$, where $\|z\|^2 \triangleq \tilde{e}^{\rm T} P \tilde{e} + \xi_{\rm c}^{\rm T} \tilde{P} \xi_{\rm c} + \operatorname{tr} \tilde{W}^{\rm T} \Gamma_W^{-1} \tilde{W} + \operatorname{tr} \tilde{W}_y^{\rm T} \Gamma_y^{-1} \tilde{W}_y$ and $\operatorname{vec}(\cdot)$ denotes the column stacking operator. Furthermore, note that $\alpha(\cdot)$ is a class $\mathcal{K}_\infty$ function. Now, using (6.26)–(6.27), and after considerable, albeit standard, algebraic manipulations, the time derivative of $V(\tilde{e}, \xi_{\rm c}, \tilde{W}, \tilde{W}_y)$ along the closed-loop system trajectories satisfies

$$\dot{V}(\tilde{e}(t), \xi_{\rm c}(t), \tilde{W}(t), \tilde{W}_y(t)) \leq - \big(\lambda_{\min}(RP^{-1}) - 1 \big) \big(\|\tilde{e}(t)\| - \alpha_e \big)^2 + \nu - \Big(\lambda_{\min}(\tilde{R}) - \|\tilde{P} L \hat{C}\|^{*2} \Big) \big(\|\xi_{\rm c}(t)\| - \alpha_\xi \big)^2, \ t \geq 0. \tag{6.37}$$

Now, for

$$\|\tilde{e}\| \geq \alpha_{\tilde{e}} \triangleq \sqrt{\frac{\nu}{\lambda_{\min}(RP^{-1}) - 1}} + \alpha_e, \tag{6.38}$$

or

$$\|\xi_{\mathrm{c}}\| \geq \alpha_{\xi_{\mathrm{c}}} \triangleq \sqrt{\frac{\nu}{\lambda_{\min}(\tilde{R}) - \|\tilde{P}L\hat{C}\|^{*2}}} + \alpha_\xi, \tag{6.39}$$

it follows that $\dot{V}(\tilde{e}(t), \xi_{\mathrm{c}}(t), \tilde{W}(t), \tilde{W}_y(t) \leq 0$ for all $t \geq 0$, that is, $\dot{V}(\tilde{e}(t), \xi_{\mathrm{c}}(t), \tilde{W}(t), \tilde{W}_y(t) \leq 0$ for all $(\tilde{e}(t), \xi_{\mathrm{c}}(t), \tilde{W}(t), \tilde{W}_y(t) \in \tilde{\mathcal{D}}_{\mathrm{e}} \backslash \tilde{\mathcal{D}}_{\mathrm{r}}$ and $t \geq 0$, where

$$\tilde{\mathcal{D}}_{\mathrm{e}} \triangleq \Big\{(\tilde{e}, \xi_{\mathrm{c}}, \tilde{W}, \tilde{W}_y) \in \mathbb{R}^r \times \mathbb{R}^{n_\xi} \times \mathbb{R}^{(s+m)\times m} \times \mathbb{R}^{l\times m} : (x, z, \hat{u}) \in \mathcal{D}_x \times \mathcal{D}_z \times \mathcal{D}_{\hat{u}}\Big\}, \tag{6.40}$$

$$\tilde{\mathcal{D}}_{\mathrm{r}} \triangleq \Big\{(\tilde{e}, \xi_{\mathrm{c}}, \tilde{W}, \tilde{W}_y) \in \mathbb{R}^r \times \mathbb{R}^{n_\xi} \times \mathbb{R}^{(s+m)\times m} \times \mathbb{R}^{l\times m} : \|\tilde{e}\| \leq \alpha_{\tilde{e}},\ \|\xi_{\mathrm{c}}\| \leq \alpha_{\xi_{\mathrm{c}}},\Big\}. \tag{6.41}$$

Next, define

$$\tilde{\mathcal{D}}_\alpha \triangleq \Big\{(\tilde{e}, \xi_{\mathrm{c}}, \tilde{W}, \tilde{W}_y) \in \mathbb{R}^r \times \mathbb{R}^{n_\xi} \times \mathbb{R}^{(s+m)\times m} \times \mathbb{R}^{l\times m} : V(\tilde{e}, \xi_{\mathrm{c}}, \tilde{W}, \tilde{W}_y) \leq \alpha\Big\}, \tag{6.42}$$

where α is the maximum value such that $\tilde{\mathcal{D}}_\alpha \subseteq \tilde{\mathcal{D}}_{\mathrm{e}}$, and define

$$\tilde{\mathcal{D}}_\eta \triangleq \Big\{(\tilde{e}, \xi_{\mathrm{c}}, \tilde{W}, \tilde{W}_y) \in \mathbb{R}^r \times \mathbb{R}^{n_\xi} \times \mathbb{R}^{(s+m)\times m} \times \mathbb{R}^{l\times m} : V(\tilde{e}, \xi_{\mathrm{c}}, \tilde{W}, \tilde{W}_y) \leq \eta\Big\}, \tag{6.43}$$

where

$$\eta > \beta(\mu) = \mu = \alpha_{\tilde{e}}^2 + \alpha_{\xi_{\mathrm{c}}}^2 + \lambda_{\max}(\Gamma_W^{-1})\hat{w}^2{}_{\max} + \lambda_{\max}(\Gamma_y^{-1})\hat{w}_{y\max}^2. \tag{6.44}$$

To show ultimate boundedness of the closed-loop system (6.1)–(6.3), (6.16), (6.23)–(6.27), (6.30) and (6.31) assume that $\tilde{\mathcal{D}}_\eta \subset \tilde{\mathcal{D}}_\alpha$. Now, since $\dot{V}(\tilde{e}, \xi_{\mathrm{c}}, \tilde{W}, \tilde{W}_y) \leq 0$ for all

$(\tilde{e}, \xi_{\rm c}, \tilde{W}, \tilde{W}_y) \in \tilde{\mathcal{D}}_{\rm e} \backslash \tilde{\mathcal{D}}_{\rm r}$ and $\tilde{\mathcal{D}}_{\rm r} \subset \tilde{\mathcal{D}}_\alpha$, it follows that $\tilde{\mathcal{D}}_\alpha$ is positively invariant. Hence, if $(\tilde{e}(0), \xi_{\rm c}(0), \tilde{W}(0), \tilde{W}_y(0)) \in \tilde{\mathcal{D}}_\alpha$, then it follows from Theorem 4.14 of [48] that the solution $(\tilde{e}(t), \xi_{\rm c}(t), \tilde{W}(t), \tilde{W}_y(t))$, $t \geq 0$, to (6.25), (6.26), (6.27), (6.30) and (6.31) is ultimately bounded with respect to $(\tilde{e}(t), \xi_{\rm c}(t), \tilde{W}(t), \tilde{W}_y(t))$ uniformly in $z(0)$ with ultimate bound given by $\gamma = \alpha^{-1}(\eta) = \sqrt{\eta}$, which yields (6.32). In addition, since (6.2) is input-to-state stable with $x(t)$ viewed as the input, it follows from Proposition 4.4 of [48] that the solution $z(t)$, $t \geq 0$, to (6.2) is also ultimately bounded.

The nonnegativity of $h(u(t))$, $t \geq 0$, is immediate from (6.4). The fact that $u(t)$, $t \geq 0$, satisfies (6.7) follows from (6.16), (6.17), and the fact that $h(u) \geq\geq 0$ for all $u \in \mathbb{R}^m$. Since A_0 is essentially nonnegative, $B\Lambda \geq\geq 0$, $h(u(t)) \geq\geq 0$, $t \geq 0$, and $f(x, z, \hat{u})$ is essentially nonnegative with respect to x for all $z \in \mathbb{R}^{n-r}$ and $\hat{u} \in \mathbb{R}^{mp}$, it follows from (6.1) and Proposition 5.1 that $x(t) \geq\geq 0$, $t \geq 0$, for all $x_0 \in \overline{\mathbb{R}}^r_+$. This completes the proof. □

A block diagram showing the neuroadaptive control architecture given in Theorem 6.1 is shown in Figure 6.2.

Remark 6.2. To apply Theorem 6.1 to the set-point regulation problem, let $x_{\rm e} \in \overline{\mathbb{R}}^r_+$ and $r(t) \equiv r^*$ be such that $0 = A_{\rm ref} x_{\rm e} + B_{\rm ref} r^*$ and $y_{\rm ref}(t) \equiv y_{\rm d} = C x_{\rm e}$, where $y_{\rm d} \in \overline{\mathbb{R}}^m_+$ is a given desired set-point. In this case, the control signal $u(t)$ is given by (6.16) and (6.18) with $\psi_{\rm n}(t) \equiv 0$.

Example 6.1. To illustrate the performance of the controller given by (6.16), we consider the dynamical system given by (6.1), with $A_0 = \left[\begin{array}{cc} -1 & 2 \\ 0.5 & -3 \end{array} \right]$, $B = I_2$, $\Lambda = I_2$, $x_0 = [0.1, 0.05]^{\rm T}$, $f(x, z, \hat{u}) = W^{\rm T}\sigma(x)$, where $W = {\rm diag}[0.2, 0.3]$, $\sigma(x) = [1 - \sin(\omega_1(x_1 + x_2)), 1 - \cos(\omega_2(x_1 + x_2))]^{\rm T}$, where $\omega_1 = 3$ rad/sec and $\omega_2 = 5$ rad/sec, and with output given by (6.3), where $C = I_2$ and $W_y \equiv 0$. The reference model

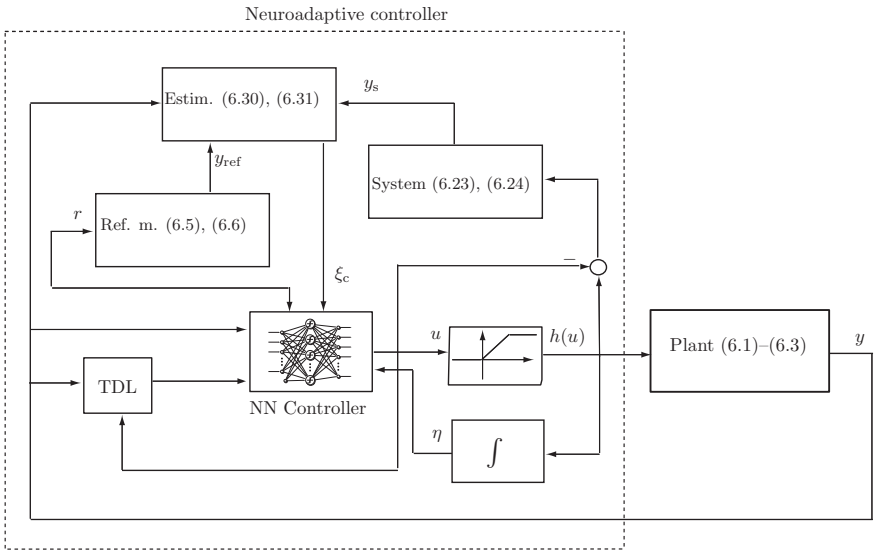

Figure 6.2: Block diagram of the closed-loop system.

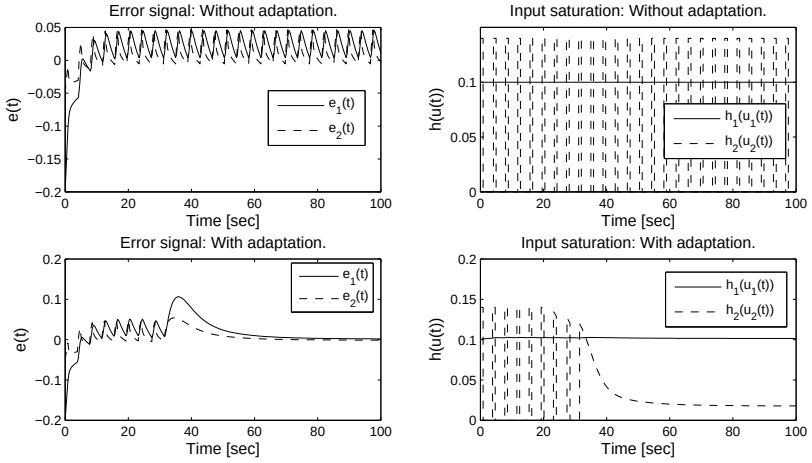

Figure 6.3: Error signals and saturated input signals versus time.

is given by (6.5) and (6.6), where $A_{\rm ref} = A_0$, $B_{\rm ref} = B$, $r(t) = [0.1, 0.15]^{\rm T}$, and $x_{\rm ref0} = [0.3, 0.1]^{\rm T}$. For our simulation we let $u_1^* = 0.12$, $u_2^* = 0.14$, $\eta_1^* = 0.13$, $\eta_2^* = 0.12$, $\Gamma_W = I_2$, and $\hat{W}_0 = 0_{2\times 2}$.

Figures 6.3 and 6.4 show the system error signals, saturated input signals, and system states versus time with and without adaptation. Figures 6.5 and 6.6 show the control input signals and integrated input signals versus time. As can be seen from

the figures, in the absence of adaptation the system errors, system states, and control signals are oscillatory with large amplitudes, whereas the closed-loop system errors, states, and control signals with the adaptive controller given by Theorem 6.1 show a satisfactory response.

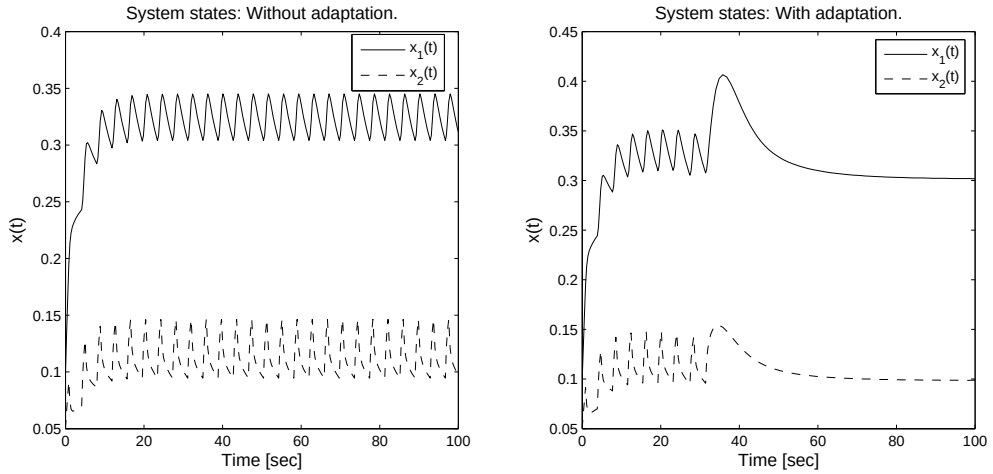

Figure 6.4: System states versus time.

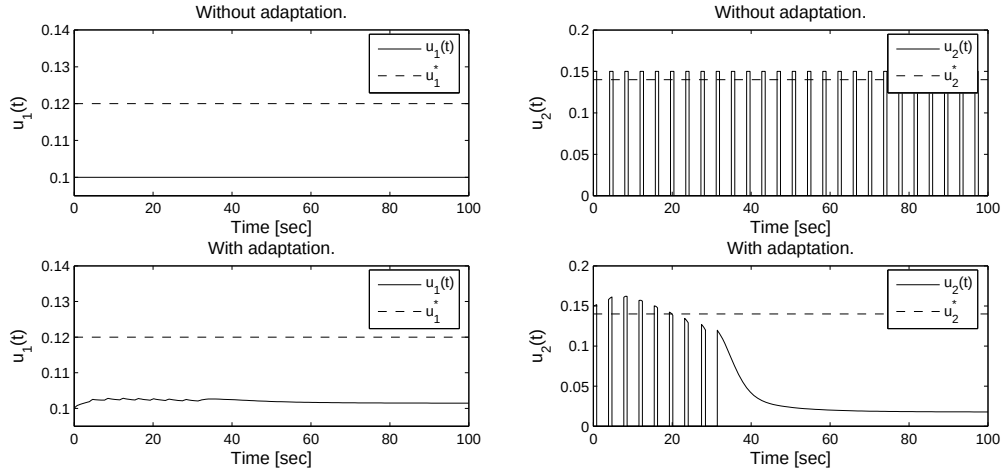

Figure 6.5: Control input versus time.

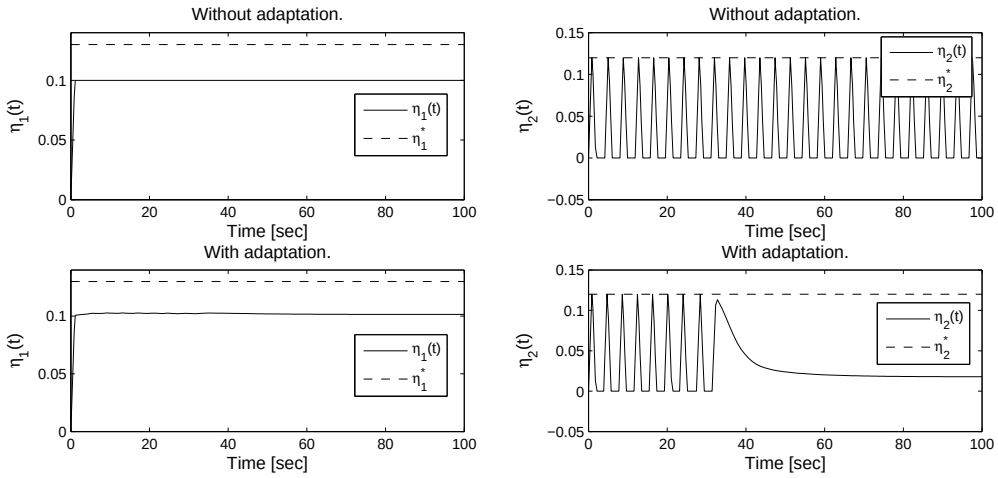

Figure 6.6: η versus time.

6.3. Neuroadaptive Output Feedback Control for General Anesthesia with Drug Infusion Constraints

To illustrate the application of the neuroadaptive control framework presented in Section 6.2 for general anesthesia, we consider the intravenous anesthetic propofol model developed in Section 5.4. The pharmacokinetics of propofol are described by the three compartment model shown in Figure 6.7, where x_1 denotes the mass of drug in the central compartment. The remainder of the drug in the body is assumed to reside in two peripheral compartments, one identified with muscle and one with fat; the masses in these compartments are denoted by x_2 and x_3, respectively.

A mass balance of the three-state compartmental model yields

$$\dot{x}_1(t) = -[a_{11}(c(t)) + a_{21}(c(t)) + a_{31}(c(t))]x_1(t) + a_{12}(c(t))x_2(t) + a_{13}(c(t))x_3(t) + h(u(t)), \quad x_1(0) = x_{10}, \quad t \geq 0, \tag{6.45}$$

$$\dot{x}_2(t) = a_{21}(c(t))x_1(t) - a_{12}(c(t))x_2(t), \quad x_2(0) = x_{20}, \tag{6.46}$$

$$\dot{x}_3(t) = a_{31}(c(t))x_1(t) - a_{13}(c(t))x_3(t), \quad x_3(0) = x_{30}, \tag{6.47}$$

where $c(t) = x_1(t)/V_{\mathrm{c}}$, V_{c} is the volume of the central compartment (about 15 l for

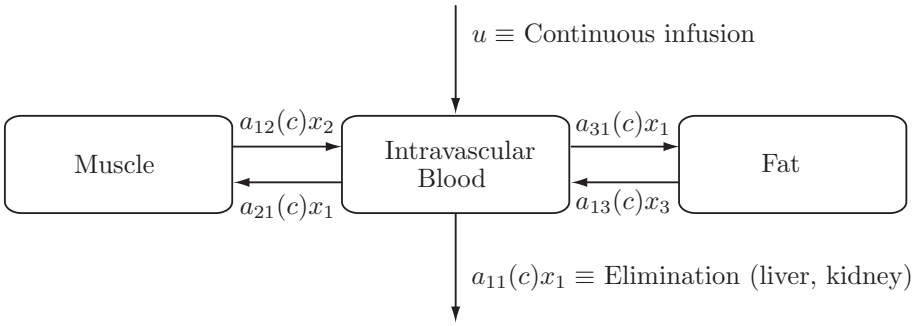

Figure 6.7: Pharmacokinetic model for drug distribution during anesthesia.

a 70 kg patient), $a_{ij}(c)$, $i \neq j$, is the rate of transfer of drug from the jth compartment to the ith compartment, $a_{11}(c)$ is the rate of drug metabolism and elimination (metabolism typically occurs in the liver), and $h(u(t))$, $t \geq 0$, is the constrained infusion rate of the anesthetic drug propofol into the central compartment. The transfer coefficients are assumed to be functions of the drug concentration c since it is well known that the pharmacokinetics of propofol are influenced by cardiac output [134] and, in turn, cardiac output is influenced by propofol plasma concentrations, both due to *venodilation* (pooling of blood in dilated veins) [101] and myocardial depression [68]. Finally, note that the compartmental model (6.45)–(6.47) is already in the normal form basis (6.1) and (6.2) with $n = r$.

To consider drug effect rather than drug concentration, we use a BIS measurement predicated on an effect-site compartment as in Section 5.4. In the following numerical simulation we consider a set-point regulation problem with a desired level of hypnosis corresponding to $\mathrm{BIS}_{\mathrm{Target}} = 50$. In the following simulation involving the infusion of the anesthetic drug propofol we set $\mathrm{EC}_{50} = 5.6$ μg/ml, $\gamma = 2.39$, and $\mathrm{BIS}_0 = 100$, so that the BIS signal is shown in Figure 6.8. Here, we use the neuroadaptive output feedback controller

$$u(t) = \phi(\eta(t))\psi(t), \tag{6.48}$$

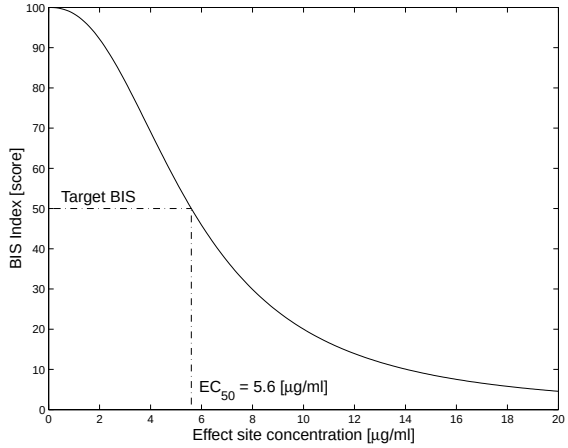

Figure 6.8: BIS Index versus effect site concentration.

where

$$\phi(\eta(t)) = \begin{cases} 1, & \text{if } 0 \leq \eta(t) \leq \eta^* - \delta \text{ and } t \geq \tau^*(t), \\ \frac{1}{\delta}(\eta^* - \eta(t)), & \text{if } \eta^* - \delta \leq \eta(t) \leq \eta^* \text{ and } t \geq \tau^*(t), \\ 0, & \text{otherwise,} \end{cases} \qquad t \geq 0, \tag{6.49}$$

$$\eta(t) = \int_{t-\tau_{\rm s}}^{t} h(u(s))\mathrm{d}s \leq \eta^*, \quad t \geq 0, \tag{6.50}$$

$$h(u(t)) = \begin{cases} 0, & \text{if } u(t) \leq 0, \\ u^*, & \text{if } u(t) \geq u^*, \\ u(t), & \text{otherwise,} \end{cases} \qquad t \geq 0, \tag{6.51}$$

$\delta = 0.005$, $\eta^* = 0.15\,\mathrm{g}$, $\tau_{\rm s} = 10\,\mathrm{sec}$, $\theta = 5\,\mathrm{sec}$, and $u^* = 0.32\,\mathrm{g/min}$. Note that (6.51) guarantees an infusion rate constraint of $0.32\,\mathrm{g/min}$, whereas (6.50) ensures a drug dosing constraint of $0.15\,\mathrm{g}$ over a period of $10\,\mathrm{seconds}$.

Next, let

$$\psi(t) = \psi_{\rm n}(t) - \psi_{\rm ad}(t), \tag{6.52}$$

where $\psi_{\rm n}(t) \equiv 0$ and $\psi_{\rm ad}(t) = \hat{W}^{\rm T}(t)\sigma(\zeta(t))$, $t \geq 0$, where

$$\zeta(t) = [\mathrm{BIS_f}(t-d), \mathrm{BIS_f}(t-2d), h(u(t-d)), h(u(t-2d))]^{\rm T}, \tag{6.53}$$

$d > 0$, and

$$\dot{\hat{W}}(t) = Q_{\rm BIS}\mathrm{Proj}[\hat{W}_1(t), \sigma(\zeta(t))\xi_{\rm c}^{\rm T}(t)PB], \quad \hat{W}(0) = \hat{W}_0, \quad t \geq 0, \tag{6.54}$$

where $Q_{\rm BIS}$ is a positive constant and $\xi_{\rm c}(t) \in \mathbb{R}^2$, $t \geq 0$, is the solution to the estimator dynamics

$$\dot{\xi}_{\rm c}(t) = \hat{A}\xi_{\rm c}(t) + L(\mathrm{BIS}(t) - \mathrm{BIS}_{\rm Target} - y_{\rm c}(t) - y_{\rm s}(t)), \ \xi_{\rm c}(0) = \xi_{\rm c0}, \ t \geq 0, \tag{6.55}$$

$$y_{\rm c}(t) = \hat{C}\xi_{\rm c}(t), \tag{6.56}$$

where $\hat{A} \in \mathbb{R}^{2\times 2}$, $L \in \mathbb{R}^{2\times 1}$, $\hat{C} \in \mathbb{R}^{1\times 2}$, and $y_{\rm s}(t)$, $t \geq 0$, is the output of the dynamical system

$$\dot{e}_{\rm s}(t) = A_0 e_{\rm s}(t) + B\Delta h(u(t)), \quad e_{\rm s}(0) = e_{\rm s0}, \quad t \geq 0, \tag{6.57}$$

$$y_{\rm s}(t) = Ce_{\rm s}(t). \tag{6.58}$$

Here, we assume that $W_y = 0$ so that $\hat{W}(t) \equiv 0$. Now, it follows from Theorem 6.1 that there exist positive constants γ and T such that $|\mathrm{BIS}(t) - \mathrm{BIS}_{\rm target}| \leq \gamma$, $t \geq T$, where $\mathrm{BIS}(t)$ is given by (5.61), for all nonnegative values of the pharmacokinetic transfer and loss coefficients $A_{12}, A_{21}, A_{13}, A_{31}, A_{11}$ as well as all nonnegative coefficients α, C_{50}, and Q_0.

For our simulation we assume $V_{\rm c} = (0.228 \text{ l/kg})(M \text{ kg})$, where $M = 70$ kg is the mass of the patient, $A_{21}Q_0 = 0.112 \text{ min}^{-1}$, $A_{12}Q_0 = 0.055 \text{ min}^{-1}$, $A_{31}Q_0 = 0.0419 \text{ min}^{-1}$, $A_{13}Q_0 = 0.0033 \text{ min}^{-1}$, $A_{\rm e}Q_0 = 0.119 \text{ min}^{-1}$, $a_{\rm eff} = 3.4657 \text{ min}^{-1}$, $\alpha = 3$, and $\mathrm{C}_{50} = 4$ μg/ml [78, 96]. Note that the parameter values for α and C_{50} probably exaggerate the effect of propofol on cardiac output. They have been selected to accentuate nonlinearity but they are not biologically unrealistic. Furthermore, to illustrate the efficacy of the proposed neuroadaptive controller we switch the pharmacodynamic parameters EC_{50} and γ, respectively, from 5.6 μg/ml and 2.39 to 7.2 μg/ml and 3.39 at $t = 15$ min and back to 5.6 μg/ml and 2.39 at $t = 30$ min. Here, we

consider noncardiac surgery since cardiac surgery often utilizes hypothermia which itself changes the BIS signal.

With

$$A_0 = \begin{bmatrix} -0.2729 & 0.0550 & 0.0033 \\ 0.1120 & -0.0550 & 0 \\ 0.0419 & 0 & -0.0033 \end{bmatrix}, \quad B = \begin{bmatrix} 1 \\ 0 \\ 0 \end{bmatrix}, \quad C = [1,\, 0,\, 0]^{\mathrm{T}},$$

$\hat{A} = \begin{bmatrix} 0 & 1 \\ -1 & -1 \end{bmatrix}$, $L = [0,1]^{\mathrm{T}}$, $\hat{C} = [1,0]$, $Q_{\mathrm{BIS}} = 2.0 \times 10^{-4}$ g/min^2, $d = 0.005$, and initial conditions $x_1(0) = x_2(0) = x_3(0) = 0$ g, $c_{\mathrm{eff}}(0) = 0$ g/ml, $\xi_{\mathrm{c}}(0) = [0,\, 0]^{\mathrm{T}}$, $e_{\mathrm{s}0} = [0,\, 0,\, 0]^{\mathrm{T}}$, and $\hat{W}(0) = 1 \times 10^{-3}[-3_{12\times 1}, 1_{12\times 1}]^{\mathrm{T}}$, Figure 6.9 shows the masses of propofol in the three compartments versus time, and the concentrations in the central and effect-site compartments versus time. Note that the effect-site compartment equilibrates with the central compartment in a matter of several minutes. Figure 6.10 shows the BIS signal versus time and the amount of propofol delivered over a 10-second window versus time, and the constrained $h(u(t))$ and unconstrained $u(t)$ propofol infusion rate versus time. Note that during the controller operation $\eta(t)$ is far below the clinical critical value η^*.

For our simulation we used

$$\begin{aligned} \sigma(\zeta(t)) = \Bigg[& \frac{1}{1+e^{-ak_1(\mathrm{BIS_f}(t-d)-\mathrm{BIS_{target}})}}, \cdots, \frac{1}{1+e^{-ak_6(\mathrm{BIS_f}(t-d)-\mathrm{BIS_{target}})}}, \\ & \frac{1}{1+e^{-ak_1(\mathrm{BIS_f}(t-2d)-\mathrm{BIS_{target}})}}, \cdots, \frac{1}{1+e^{-ak_6(\mathrm{BIS_f}(t-2d)-\mathrm{BIS_{target}})}}, \\ & \frac{1}{1+e^{-ak_1(u(t-d)-u_0)}}, \cdots, \frac{1}{1+e^{-ak_6(u(t-d)-u_0)}}, \\ & \frac{1}{1+e^{-ak_1(u(t-2d)-u_0)}}, \cdots, \frac{1}{1+e^{-ak_6(u(t-2d)-u_0)}} \Bigg]^{\mathrm{T}}, \end{aligned} \tag{6.59}$$

where $s = 24$, $a = 0.1$, $k_1 = 1$, $k_2 = 2$, $k_3 = 6$, $k_4 = 24$, $k_5 = 120$, $k_6 = 720$, and $u_0 = 15\,\mathrm{mg/min}$. Even though we did not calculate the analytical bounds given by (6.32) due to the fact that one has to solve an optimization problem with respect to (6.34) and (6.35) to obtain α_e and α_ξ, the closed-loop BIS signal response shown in

Figure 6.10 is clearly acceptable. Furthermore, the basis function for $\sigma(\zeta)$ is chosen to cover the domain of interest of our pharmacokinetic/pharmacodynamic problem since we know that the BIS index varies from 0 to 100. Hence, the basis functions are distributed over that domain. The number of basis functions, however, is based on trial and error. As noted in Section 6.2, this goes back to the Stone-Weierstrass theorem which only provides an existence result without any constructive guidelines. Finally, we note that simulations using a larger number of neurons resulted in imperceptible differences in the closed-loop system performance.

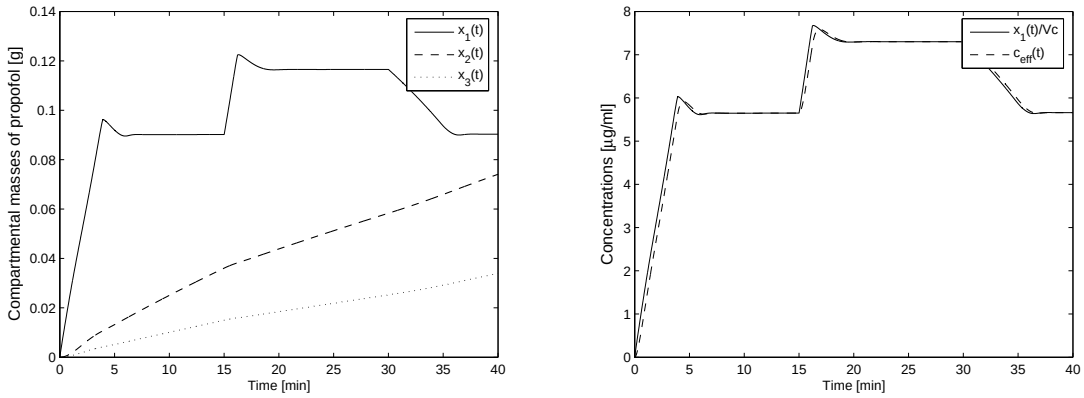

Figure 6.9: Compartmental masses, and concentrations in the central and effect site compartments versus time.

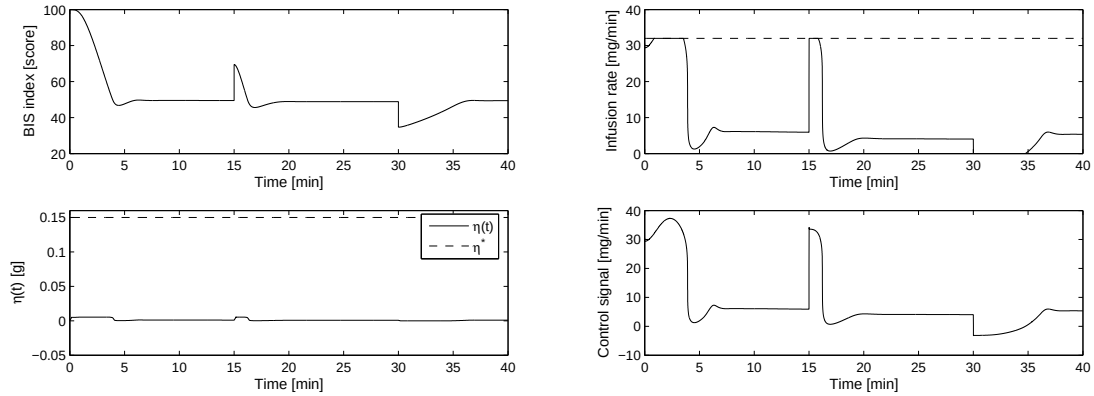

Figure 6.10: BIS signal, η, infusion rate $h(u(t))$, and control signal $u(t)$ versus time.

Chapter 7

Pressure- and Work-Limited Neuroadaptive Control for Mechanical Ventilation of Critical Care Patients

7.1. Introduction

The lungs are particularly vulnerable to acute, critical illness. Respiratory failure can result not only from primary lung pathology, such as pneumonia, but also as a secondary consequence of heart failure or inflammatory illness, such as sepsis or trauma. When this occurs it is essential to support patients while the fundamental disease process is addressed. For example, a patient with pneumonia may require mechanical ventilation while the pneumonia is being treated with antibiotics that will eventually effectively "cure" the disease. Since the lungs are vulnerable to critical illness, and respiratory failure is common, support of patients with mechanical ventilation is very common in the intensive care unit.

The goal of mechanical ventilation is to ensure adequate ventilation, which involves a magnitude of gas exchange that leads to the desired blood level of carbon dioxide, and adequate oxygenation, which involves a blood concentration of oxygen that will ensure organ function. Achieving these goals is complicated by the fact that mechanical ventilation can actually cause acute lung injury, either by inflating the lungs to excessive volumes or by using excessive pressures to inflate the lungs. The

challenge to mechanical ventilation is to produce the desired blood levels of carbon dioxide and oxygen without causing further acute lung injury.

The earliest primary modes of ventilation can be classified, approximately, as volume-controlled or pressure-controlled [133]. In volume-controlled ventilation, the lungs are inflated (by the mechanical ventilator) to a specified volume and then allowed to passively deflate to the baseline volume. The mechanical ventilator controls the volume of each breath and the number of breaths per minute. In pressure-controlled ventilation, the lungs are inflated to a given peak pressure. The ventilator controls this peak pressure as well as the number of breaths per minute.

The primary determinant of the level of carbon dioxide in the blood is minute ventilation, which is defined as the tidal volume (the volume of each breath) multiplied by the number of breaths per minute [97, 141]. With volume-controlled ventilation both tidal volume and the number of breaths are determined by the machine (the ventilator) and typically the tidal volumes and breaths per minute are selected by the clinician caring for the patient. In pressure-controlled ventilation, the tidal volume is not directly controlled. The ventilator determines the pressure that inflates the lungs and the tidal volume is proportional to this driving pressure and the compliance, or "stiffness," of the lungs. Consequently, the minute ventilation is not directly controlled by the ventilator and any change in lung compliance (such as improvement or deterioration in the underlying lung pathology) can result in changes in tidal volume, minute ventilation, and ultimately the blood concentration of carbon dioxide.

The concentration of oxygen in the blood is determined by the underlying lung pathology, the concentration of oxygen in the gas delivered by the mechanical ventilator, and also by the pressure that is used to inflate the lungs. In very general terms, oxygenation can be improved by higher mean pressures in the lungs, although higher peak pressures during the inflation-deflation cycle are associated with lung

injury [10, 81].

With the increasing availability of micro-chip technology, it has been possible to design mechanical ventilators that have control algorithms that are more sophisticated than simple volume or pressure control. Examples are proportional-assist ventilation [144, 145], adaptive support ventilation [85], and neurally adjusted ventilation [125]. The common theme in modern ventilation control algorithms is the use of pressure-limited ventilation while also guaranteeing adequate minute ventilation. One of the challenges in the design of efficient control algorithms is that the fundamental physiological variables defining lung function, the resistance to gas flow and the compliance of the lung units, are not constant but rather vary with lung volume. This is particularly true for compliance, strictly defined as $\frac{\mathrm{d}V}{\mathrm{d}P}$, where V is the lung unit volume and P is the pressure driving inflation. More simply, lung volume is a nonlinear function of driving pressure.

In this chapter, we apply the adaptive control architecture of Chapter 6 to control lung volume and minute ventilation with input pressure constraints that also accounts for spontaneous breathing by the patient. Specifically, we develop a pressure- and work-limited neuroadaptive controller for mechanical ventilation based on a nonlinear multi-compartmental lung model. The control framework does not rely on any averaged data and is designed to automatically adjust the input pressure to the patient's physiological characteristics capturing lung resistance and compliance modeling uncertainty. Moreover, the controller accounts for input pressure constraints as well as work of breathing constraints. Finally, the effect of spontaneous breathing is incorporated within the lung model and the control framework.

7.2. Neuroadaptive Output Feedback Control with Actuator Constraints

In this section, we consider the problem of characterizing neuroadaptive dynamic output feedback control laws for nonlinear uncertain dynamical systems with actuator amplitude constraints to achieve reference model output tracking. While our framework here is very similar to the framework developed in Chapter 6 and is applicable to general nonnegative and compartmental dynamical systems [49] with actuator amplitude constraints, the main focus of this chapter is the application of this framework to pressure-limited control of mechanical ventilation.

Consider the controlled nonlinear uncertain dynamical system $\mathcal{G}$ given by

$$\dot{x}(t) = A_0x(t) + B\Lambda f(x(t), h(u(t)), \theta(t)) + B\Lambda h(u(t)),\ x(0) = x_0,\ t \geq 0, \quad (7.1)$$

$$y(t) = Cx(t), \quad (7.2)$$

where $x(t) \in \mathbb{R}^n$, $t \geq 0$, is the state vector, $u(t) \in \mathbb{R}^m$, $t \geq 0$, is the control input, $y(t) \in \mathbb{R}^m$, $t \geq 0$, is the system output, $A_0 \in \mathbb{R}^{n\times n}$ is a known Hurwitz and essentially nonnegative matrix, $B \in \mathbb{R}^{r\times m}$ is a known nonnegative input matrix, $\Lambda \in \mathbb{R}^{m\times m}$ is an *unknown* nonnegative and positive-definite matrix, $h(u(t)) = [h_1(u_1(t), \ldots, h_m(u_m(t))]^{\mathrm{T}}$ is the constrained control input given by (6.4) where $\theta : \mathbb{R} \to \mathcal{D}_\theta$ is a known bounded continuous function, where $\mathcal{D}_\theta \subset \mathbb{R}$ is a compact set, $f : \mathbb{R}^n \times \mathbb{R}^m \times \mathcal{D}_\theta \to \mathbb{R}^m$ is Lipschitz continuous and essentially nonnegative for all $u \in \mathbb{R}^m$ and $\theta \in \mathcal{D}_\theta$ but otherwise *unknown* (that is, $f(\cdot, \cdot, \cdot)$ is such that $f_i(x, h(u), \theta) \geq 0$ if $x_i = 0$, $i = 1, \ldots, n$, for all $u \in \mathbb{R}^m$ and $\theta \in \mathcal{D}_\theta$), and $C \in \mathbb{R}^{m\times n}$ is a known output matrix. For the mechanical ventilation problem, the control input $u(t)$, $t \geq 0$, represents the pressure input to the ventilator and the control input constraint (6.4) captures pressure amplitude limitations. Furthermore, as we see in Section 7.4, the function $\theta(t)$, $t \geq 0$, is introduced to account for a contin-

uous transition of the respiratory parameters (e.g., lung resistance and compliance) from inspiration to expiration.

In this Chapter, in order to achieve output tracking, we use a reference nonnegative dynamical system $\mathcal{G}_{\rm ref}$ of the form given by (6.5) and (6.6). Control (source) inputs for mechanical ventilation involving pressure control are usually constrained to be nonnegative as are the system states, which typically correspond to compartmental volumes. Hence, in this chapter we develop neuroadaptive dynamic output feedback control laws for nonnegative systems with nonnegative control inputs. Specifically, for the reference model output tracking problem our goal is to design a nonnegative control input $u(t)$, $t \geq 0$, predicated on the system measurement $y(t)$, $t \geq 0$, such that $\|y(t) - y_{\rm ref}(t)\| < \gamma$ for all $t \geq T$, where $\|\cdot\|$ denotes the Euclidean vector norm on $\mathbb{R}^m$, $\gamma > 0$ is sufficiently small, and $T \in [0, \infty)$, $x(t) \geq\geq 0$, $t \geq 0$, for all $x_0 \in \overline{\mathbb{R}}^n_+$, and the control input $u(\cdot)$ in (7.1) is restricted to the class of *admissible controls* consisting of measurable functions $u(t) = [u_1(t), \ldots, u_m(t)]^{\rm T}$, $t \geq 0$, such that (6.4) and (6.7) hold. For the mechanical ventilation problem, the pressure control integral constraint (6.7) enforces an upper bound on the amount of work performed by the ventilator.

Here, we assume that the function $f(x, h(u), \theta)$ can be approximated over a compact set $\mathcal{D}_x \times \mathcal{D}_u \times \mathcal{D}_\theta$ by a linear in parameters neural network up to a desired accuracy. In this case, there exists $\hat{\varepsilon} : \mathbb{R}^n \times \mathbb{R}^m \times \mathcal{D}_\theta \to \mathbb{R}^m$ such that $\|\hat{\varepsilon}(x, h(u), \theta)\| < \hat{\varepsilon}^*$ for all $(x, h(u), \theta) \in \mathcal{D}_x \times \mathcal{D}_u \times \mathcal{D}_\theta$, where $\hat{\varepsilon}^* > 0$, and

$$f(x, h(u), \theta) = W_f^{\rm T} \hat{\sigma}(x, u, \theta) + \hat{\varepsilon}(x, u, \theta), \quad (x, u, \theta) \in \mathcal{D}_x \times \mathcal{D}_u \times \mathcal{D}_\theta, \tag{7.3}$$

where $W_f \in \mathbb{R}^{s \times m}$ is an optimal *unknown* (constant) weight that minimizes the approximation error over $\mathcal{D}_x \times \mathcal{D}_u \times \mathcal{D}_\theta$, $\hat{\sigma} : \mathbb{R}^n \times \mathbb{R}^m \times \mathcal{D}_\theta \to \mathbb{R}^s$ is a vector of basis functions such that each component of $\hat{\sigma}(\cdot, \cdot, \cdot)$ takes values between 0 and 1, and

$\hat{\varepsilon}(\cdot,\cdot,\cdot)$ is the modeling error. Note that s denotes the total number of basis functions or, equivalently, the number of nodes of the neural network.

In order to develop an *output* feedback neuroadaptive controller, we use the approach developed in [87] for reconstructing the system states via the system delayed inputs and outputs. Specifically, we use a *memory unit* as a particular form of a tapped delay line (TDL) that takes a scalar time series input and provides an $(2mn - r)$-dimensional vector output consisting of the present values of the system outputs and system inputs, and their $2(n-1)m - r$ delayed values given by

$$\begin{aligned}\kappa(t) \triangleq\ & [y_1(t), y_1(t-d), \ldots, y_1(t-(n-1)d), \ldots, y_m(t), y_m(t-d), \ldots,\\ & y_m(t-(n-1)d); u_1(t), u_1(t-d), \ldots, u_1(t-(n-r_1-1)d), \ldots, u_m(t),\\ & u_m(t-d), \ldots, u_m(t-(n-r_m-1)d)]^{\mathrm{T}}, \quad t \geq 0, \end{aligned} \tag{7.4}$$

where r_i denotes the relative degree of $\mathcal{G}$ with respect to the output y_i, $i = 1, \ldots, m$, and $r \triangleq r_1 + \cdots + r_m$ denotes the (vector) relative degree of $\mathcal{G}$.

The following matching conditions are needed for the main result of this chapter.

Assumption 7.1. There exist $K_{\mathrm{y}} \in \mathbb{R}^{m\times m}$ and $K_{\mathrm{r}} \in \mathbb{R}^{m\times d}$ such that $A_0 + BK_{\mathrm{y}}C = A_{\mathrm{ref}}$ and $BK_{\mathrm{r}} = B_{\mathrm{ref}}$.

Assumption 7.1 involves standard matching conditions for model reference adaptive control appearing in the literature; see, for example, Chapter 5 in [132].

Using the parameterization $\Lambda = \hat{\Lambda} + \Delta\Lambda$, where $\Delta\Lambda \in \mathbb{R}^{m\times m}$ is an unknown symmetric matrix, the dynamics in (7.1) can be rewritten as

$$\begin{aligned}\dot{x}(t) = A_0 x(t) + B\hat{\Lambda}h(u(t)) + B\left[\Delta\Lambda h(u(t)) + \Lambda f(x(t), h(u(t)), \theta(t))\right],\\ x(0) = x_0,\ t \geq 0. \end{aligned} \tag{7.5}$$

Define $W \triangleq \left[W_1^{\mathrm{T}}, W_2^{\mathrm{T}}\right]^{\mathrm{T}} \in \mathbb{R}^{(s+m)\times m}$, where $W_1 \triangleq W_f\Lambda$ and $W_2 \triangleq \Delta\Lambda^{\mathrm{T}}$, and $\zeta(t) \triangleq \left[\kappa^{\mathrm{T}}(t),\, \theta(t)\right]^{\mathrm{T}}$, $t \geq 0$. Using (7.3), (7.5) can be rewritten as

$$\begin{aligned}\dot{x}(t) = {} & A_0x(t) + B\hat{\Lambda}u(t) + BW^{\mathrm{T}}\sigma(\zeta(t), h(u(t))) + B\Lambda\hat{\varepsilon}(x(t), u(t), \theta(t)), \\ & + B\hat{\Lambda}\Delta h(t) + BW_1^{\mathrm{T}}\left[\hat{\sigma}(x(t), u(t), \theta(t)) - \sigma_\zeta(\zeta(t))\right], \quad x(0) = x_0, \quad t \geq 0,\end{aligned} \tag{7.6}$$

where

$$\sigma(\zeta(t), h(u(t))) \triangleq \left[\sigma_\zeta^{\mathrm{T}}(\zeta(t)), h^{\mathrm{T}}(u(t))\right]^{\mathrm{T}}, \tag{7.7}$$

$\sigma_\zeta : \mathbb{R}^{2mn-r+1} \to \mathbb{R}^s$ is a vector of basis functions such that each component of $\sigma_\zeta(\cdot)$ takes values between 0 and 1, and $\Delta h(u(t)) \triangleq h(u(t)) - u(t)$, $t \geq 0$.

Next, we develop a control architecture similar to the one developed in Chapter 6. Specifically, consider the control input $u(t)$, $t \geq 0$, given by

$$u(t) = \Phi(\eta(t))\psi(t), \quad t \geq 0, \tag{7.8}$$

where $\Phi(\eta(t)) \triangleq \operatorname{diag}\left[\phi_1(\eta_1(t)), \ldots, \phi_m(\eta_m(t))\right]$, $t \geq 0$, and ϕ_i are defined as in (6.17), and and $\psi(t) \in \mathbb{R}^m$, $t \geq 0$, is given by

$$\psi(t) = \psi_{\mathrm{n}}(t) - \psi_{\mathrm{ad}}(t), \quad t \geq 0, \tag{7.9}$$

where

$$\psi_{\mathrm{n}}(t) = \hat{\Lambda}^{-1}[K_{\mathrm{y}}y(t) + K_{\mathrm{r}}r(t)], \quad t \geq 0, \tag{7.10}$$

$$\psi_{\mathrm{ad}}(t) = \hat{\Lambda}^{-1}\hat{W}^{\mathrm{T}}(t)\sigma(\zeta(t), h(u(t))), \quad t \geq 0, \tag{7.11}$$

and $\hat{W}(t) \in \mathbb{R}^{(s+m)\times m}$, $t \geq 0$, is an update weight.

After going through analogous steps as in Chapter 6 we arrive at the main result of this section. Consider the update law given by

$$\dot{\hat{W}}(t) = \Gamma_W \mathrm{Proj}[\hat{W}(t), \sigma(\zeta(t), h(u(t)))\xi_{\mathrm{c}}^{\mathrm{T}}(t)PB], \ \hat{W}(0) = \hat{W}_0, \ t \geq 0, \tag{7.12}$$

where $\Gamma_W \in \mathbb{R}^{(s+m)\times(s+m)}$ is a positive definite matrix, $P \in \mathbb{R}^{n\times n}$ is a positive-definite solution of the Lyapunov equation

$$0 = A_{\mathrm{ref}}^{\mathrm{T}} P + P A_{\mathrm{ref}} + R, \tag{7.13}$$

where $R > 0$, and $\tilde{P} \in \mathbb{R}^{n_\xi \times n_\xi}$ is a positive-definite solution of the Lyapunov equation

$$0 = (\hat{A} - L\hat{C})^{\mathrm{T}} \tilde{P} + \tilde{P}(\hat{A} - L\hat{C}) + \tilde{R}, \tag{7.14}$$

where $\tilde{R} > 0$, $\hat{A} \in \mathbb{R}^{n_\xi \times n_\xi}$ is Hurwitz, $L \in \mathbb{R}^{n_\xi \times m}$, $\hat{C} \in \mathbb{R}^{m \times n_\xi}$, and $\xi_{\mathrm{c}}(t) \in \mathbb{R}^{n_\xi}$, $t \geq 0$, is the solution to the estimator dynamics

$$\dot{\xi}_{\mathrm{c}}(t) = \hat{A}\xi_{\mathrm{c}}(t) + L\left[y(t) - y_{\mathrm{ref}}(t) - y_{\mathrm{c}}(t) - y_{\mathrm{s}}(t)\right], \quad \xi_{\mathrm{c}}(0) = \xi_{\mathrm{c}0}, \quad t \geq 0, \tag{7.15}$$

$$y_{\mathrm{c}}(t) = \hat{C}\xi_{\mathrm{c}}(t). \tag{7.16}$$

Now, since the projection operator used in the update law (7.12) guarantees the boundness of the update weight $\hat{W}(t)$, $t \geq 0$, it follows that there exist $u^* > 0$ and $\delta^* > 0$ such that $\|u(t)\| \leq u^*$ and $\|\Delta h(u(t))\| \leq \delta^*$ for all $t \geq 0$. Furthermore, note that there exists $\varepsilon^* > 0$ such that $\|\varepsilon(t)\| \leq \varepsilon^*$ for all $t \geq 0$ such that $(x(t), u(t), \theta(t)) \in \mathcal{D}_x \times \mathcal{D}_u \times \mathcal{D}_\theta$. Finally, there exists $\alpha_1 > 0$ such that $\|\tilde{W}^{\mathrm{T}}(t)\sigma(\zeta(t), h(u(t)))\| \leq \alpha_1$ for all $t \geq 0$.

For the statement of the main result of this section, let $\|\cdot\|' : \mathbb{R}^{n\times n} \to \mathbb{R}$ be the matrix norm equi-induced by the vector norm $\|\cdot\|'' : \mathbb{R}^n \to \mathbb{R}$, let $\|\cdot\|''' : \mathbb{R}^{n\times m} \to \mathbb{R}$ be the matrix norm induced by the vector norms $\|\cdot\|'' : \mathbb{R}^n \to \mathbb{R}$ and $\|\cdot\|'''' : \mathbb{R}^m \to \mathbb{R}$, and let $\|\cdot\|^* : \mathbb{R}^{n_\xi \times n_\xi} \to \mathbb{R}$ be the matrix norm equi-induced by the vector norm $\|\cdot\|^{**} : \mathbb{R}^{n_\xi} \to \mathbb{R}$. Furthermore, recall the definition of ultimate boundness of a state trajectory given in [48, p. 241].

Theorem 7.1. Consider the nonlinear uncertain dynamical system $\mathcal{G}$ given by (7.1) and (7.2) with $u(t)$, $t \geq 0$, given by (7.8)–(7.11) and reference model $\mathcal{G}_{\mathrm{ref}}$ given

by (6.5) and (6.6). Assume Assumption 7.1 holds, $\lambda_{\min}(R) > 1$, and $\lambda_{\min}(\tilde{R}) > \|\tilde{P}L\hat{C}\|^{*2}$. Then there exists a compact positively invariant set $\mathcal{D}_\alpha \subset \mathbb{R}^n \times \mathbb{R}^n \times \mathbb{R}^{n_\xi} \times \mathbb{R}^{(s+m)\times m}$ such that $(0, 0, 0, W) \in \mathcal{D}_\alpha$, where $W \in \mathbb{R}^{(s+m)\times m}$, and the solution $(e(t), e_{\mathrm{s}}(t), \xi_{\mathrm{c}}(t), \hat{W}(t))$, $t \geq 0$, of the closed-loop system given by (7.1), (7.2), (7.8), (7.12), (7.15), and (7.16) is ultimately bounded for all $(e(0), e_{\mathrm{s}}(0), \xi_{\mathrm{c}}(0), \hat{W}(0)) \in \mathcal{D}_\alpha$ with ultimate bound $\|y(t) - y_{\mathrm{ref}}(t)\| < \gamma$, $t \geq T$, where

$$\gamma > \Bigg(\Big[(\lambda_{\min}(R) - 1)^{-\frac{1}{2}}\sqrt{\nu} + \alpha_e\Big]^2 + \Big[(\lambda_{\min}(\tilde{R}) - \|\tilde{P}L\hat{C}\|^{*2})^{-\frac{1}{2}}\sqrt{\nu} + \alpha_\xi\Big]^2 + \lambda_{\max}(\Gamma_W^{-1})\hat{w}^2{}_{\max}\Bigg)^{\frac{1}{2}}, \tag{7.17}$$

$$\nu \triangleq (\lambda_{\min}(R) - 1)\alpha_e^2 + (\lambda_{\min}(\tilde{R}) - \|\tilde{P}L\hat{C}\|^{*2})\alpha_\xi^2, \tag{7.18}$$

$$\alpha_e \triangleq \frac{1}{\lambda_{\min}(R) - 1}\Big(\|P\|'\varepsilon^* + \|PB\|'''\alpha_1\Big), \tag{7.19}$$

$$\alpha_\xi \triangleq \frac{1}{\lambda_{\min}(\tilde{R}) - \|\tilde{P}L\hat{C}\|^{*2}}\|PB\|'''\alpha_1, \tag{7.20}$$

and $\hat{w}_{\max}$ is a norm bound imposed on $\hat{W}$. Furthermore, $u(t)$ satisfies (6.7) for all $t \geq 0$, $h(u(t)) \geq\geq 0$, $t \geq 0$, and $x(t) \geq\geq 0$, $t \geq 0$, for all $x_0 \in \overline{\mathbb{R}}_+^n$.

Proof. This is a restatement of Theorem 6.1 with the additional parameter $\theta(t)$, $t \geq 0$, introduced in the nonlinear uncertain dynamics (7.1).

7.3. Nonlinear Multi-Compartment Model for a Pressure-Limited Respirator

In this section, we extend the linear multi-compartment lung model of [22] to develop a nonlinear model for the dynamic behavior of a multi-compartment respiratory system in response to an arbitrary applied inspiratory pressure. Here, we assume that the bronchial tree has a dichotomy architecture [140]; that is, in every generation each airway unit branches in two airway units of the subsequent generation. In addition, we assume that lung compliance is a nonlinear function of lung volume. First, for

simplicity of exposition, we consider a single-compartment lung model as shown in Figure 7.1. In this model, the lungs are represented as a single lung unit with nonlin-

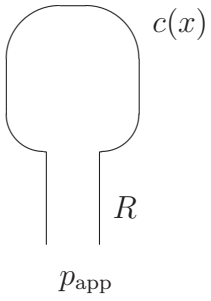

Figure 7.1: Single-compartment lung model.

ear compliance $c(x)$ connected to a pressure source by an airway unit with resistance (to air flow) of R. At time $t = 0$, an arbitrary pressure $p_{\text{in}}(t)$ is applied to the opening of the parent airway, where $p_{\text{in}}(t)$ is determined by the mechanical ventilator. This pressure is applied to the airway opening over the time interval $0 \leq t \leq T_{\text{in}}$, which is the inspiratory part of the breathing cycle. At time $t = T_{\text{in}}$, the applied airway pressure is released and expiration takes place passively, that is, the external pressure is only the atmospheric pressure $p_{\text{ex}}(t)$ during the time interval $T_{\text{in}} \leq t \leq T_{\text{in}} + T_{\text{ex}}$, where T_{ex} is the duration of expiration.

The state equation for inspiration (inflation of lung) is given by

$$R_{\text{in}}\dot{x}(t) + \frac{1}{c_{\text{in}}(x)}x(t) = p_{\text{in}}(t), \qquad x(0) = x_0^{\text{in}}, \qquad 0 \leq t \leq T_{\text{in}}, \tag{7.21}$$

where $x(t) \in \mathbb{R}$, $t \geq 0$, is the lung volume, $R_{\text{in}} \in \mathbb{R}$ is the resistance to air flow during the inspiration period, $c_{\text{in}} : \mathbb{R} \to \mathbb{R}_+$ is a nonlinear function defining the lung compliance at inspiration, $x_0^{\text{in}} \in \mathbb{R}_+$ is the lung volume at the start of the inspiration and serves as the system initial condition. Equation (7.21) is simply a pressure balance equation where the total pressure $p_{\text{in}}(t), t \geq 0$, applied to the compartment is proportional to the volume of the compartment via the compliance and the rate of

change of the compartmental volume via the resistance. We assume that expiration is passive (due to elastic stretch of lung unit). During the expiration process, the state equation is given by

$$R_{\rm ex}\dot{x}(t) + \frac{1}{c_{\rm ex}(x)}x(t) = p_{\rm ex}(t), \qquad x(T_{\rm in}) = x_0^{\rm ex}, \qquad T_{\rm in} \le t \le T_{\rm in} + T_{\rm ex}, \quad (7.22)$$

where $x(t) \in \mathbb{R}$, $t \ge 0$, is the lung volume, $R_{\rm ex} \in \mathbb{R}$ is the resistance to air flow during the expiration period, $c_{\rm ex} : \mathbb{R} \to \mathbb{R}_+$ is a nonlinear function defining the lung compliance at expiration, and $x_0^{\rm ex} \in \mathbb{R}_+$ is the lung volume at the start of expiration.

Next, we develop the state equations for inspiration and expiration for a 2^n-compartment model, where $n \ge 0$. In this model, the lungs are represented as 2^n lung units which are connected to the pressure source by n generations of airway units, where each airway is divided into two airways of the subsequent generation leading to 2^n compartments (see Figure 7.2 for a four-compartment model).

Let $x_i,\ i = 1, 2, \ldots, 2^n$, denote the lung volume in the i-th compartment, $c_i^{\rm in}(x_i),\ i = 1, 2, \ldots, 2^n$, denote the compliance of each compartment as a nonlinear function of the volume of i-th compartment, and let $R_{j,i}^{\rm in}$ (resp., $R_{j,i}^{\rm ex}$), $i = 1, 2, \ldots, 2^j,\ j = 0, \ldots, n$, denote the resistance (to air flow) of the i-th airway in the j-th generation during the inspiration (resp., expiration) period with $R_{01}^{\rm in}$ (resp., $R_{01}^{\rm ex}$) denoting the inspiration (resp., expiration) of the *parent* (i.e., 0-th generation) airway. As in the single-compartment model we assume that a pressure of $p_{\rm in}(t), t \ge 0$, is applied during inspiration. Now, the state equations for inspiration are given by

$$R_{n,i}^{\rm in}\dot{x}_i(t) + \frac{1}{c_i^{\rm in}(x_i(t))}x_i(t) + \sum_{j=0}^{n-1} R_{j,k_j}^{\rm in} \sum_{l=(k_j-1)2^{n-j}+1}^{k_j 2^{n-j}} \dot{x}_l(t) = p_{\rm in}(t),$$
$$x_i(0) = x_{i0}^{\rm in}, \quad 0 \le t \le T_{\rm in}, \quad i = 1, 2, \ldots, 2^n, \quad (7.23)$$

where $c_i^{\rm in}(x_i),\ i = 1, 2, \ldots, 2^n$, are nonlinear functions of x_i, $i = 1, 2, \ldots, 2^n$, given by

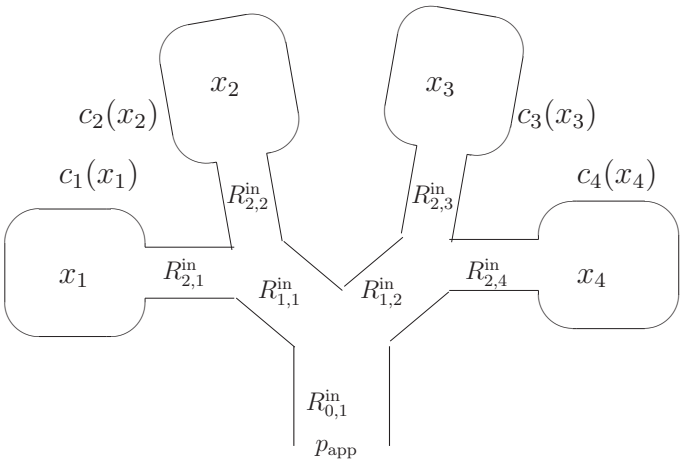

Figure 7.2: Four-compartment lung model.

([28])

$$c_i^{\text{in}}(x_i) \triangleq \begin{cases} a_{i_1}^{\text{in}} + b_{i_1}^{\text{in}} x_i, & \text{if } 0 \le x_i \le x_{i_1}^{\text{in}}, \\ a_{i_2}^{\text{in}}, & \text{if } x_{i_1}^{\text{in}} \le x_i \le x_{i_2}^{\text{in}}, \\ a_{i_3}^{\text{in}} + b_{i_3}^{\text{in}} x_i, & \text{if } x_{i_2}^{\text{in}} \le x_i \le V_{\text{T}}, \end{cases} \qquad i = 1, \ldots, 2^n, \tag{7.24}$$

where $a_{i_j}^{\text{in}}$, $j = 1, 2, 3$, and $b_{i_j}^{\text{in}}$, $j = 1, 3$, are unknown parameters with $b_{i_1}^{\text{in}} > 0$ and $b_{i_3}^{\text{in}} < 0$, $x_{i_j}^{\text{in}}$, $j = 1, 2$, are unknown volume ranges wherein the compliance is constant, V_{T} denotes tidal volume, and

$$k_j = \lfloor \frac{k_{j+1} - 1}{2} \rfloor + 1, \quad j = 0, \ldots, n-1, \quad k_n = i, \tag{7.25}$$

where $\lfloor q \rfloor$ denotes the *floor function* which gives the largest integer less than or equal to the positive number q. Figure 7.3 shows a typical piecewise linear compliance function for inspiration. A similar compliance representation holds for expiration.

To further elucidate the inspiration state equation for a 2^n-compartment model, consider the four-compartment model shown in Figure 7.2 corresponding to a two generation lung model. Let x_i, $i = 1, 2, 3, 4$, denote the compartmental volumes. Now, the pressure $\frac{1}{c_i^{\text{in}}(x_i(t))} x_i(t)$ due to the compliance in i-th compartment will be equal to the difference between the external pressure applied and the resistance to

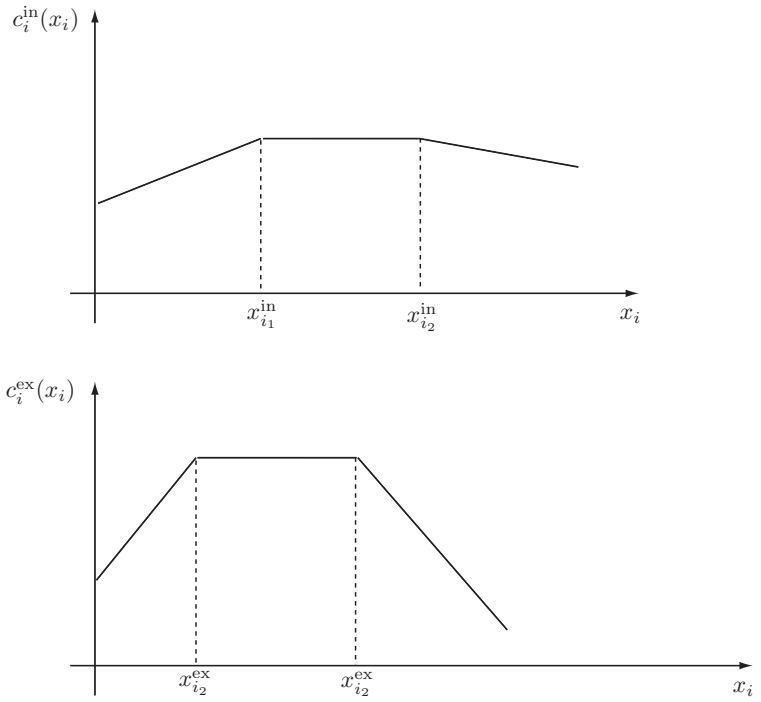

Figure 7.3: Typical inspiration and expiration compliance functions as function of compartmental volumes.

air flow at every airway in the path leading from the pressure source to the i-th compartment. In particular, for $i = 3$ (see Figure 7.2),

$$\frac{1}{c_3^{\text{in}}(x_3(t))}x_3(t) = p_{\text{in}}(t) - R_{0,1}^{\text{in}}[\dot{x}_1(t)+\dot{x}_2(t)+\dot{x}_3(t)+\dot{x}_4(t)] - R_{1,2}^{\text{in}}[\dot{x}_3(t)+\dot{x}_4(t)] - R_{2,3}^{\text{in}}\dot{x}_3(t),$$

or, equivalently,

$$R_{2,3}^{\text{in}}\dot{x}_3(t)+R_{1,2}^{\text{in}}[\dot{x}_3(t)+\dot{x}_4(t)]+R_{0,1}^{\text{in}}[\dot{x}_1(t)+\dot{x}_2(t)+\dot{x}_3(t)+\dot{x}_4(t)]+\frac{1}{c_3^{\text{in}}(x_3(t))}x_3(t) = p_{\text{in}}(t).$$

Next, we consider the state equation for the expiration process. As in the single-compartment model we assume that the expiration process is passive and the external pressure applied is $p_{\text{ex}}(t), t \geq 0$. Following an identical procedure as in the inspiration case, we obtain the state equation for expiration as

$$R_{n,i}^{\text{ex}}\dot{x}_i(t) + \sum_{j=0}^{n-1} R_{j,k_j}^{\text{ex}} \sum_{l=(k_j-1)2^{n-j}+1}^{k_j 2^{n-j}} \dot{x}_l(t) + \frac{1}{c_i^{\text{ex}}(x_i(t))}x_i(t) = p_{\text{ex}}(t),$$
$$x_i(T_{\text{in}}) = x_{i_0}^{\text{ex}}, \quad T_{\text{in}} \leq t \leq T_{\text{ex}} + T_{\text{in}}, \quad i = 1, 2, \ldots, 2^n, \tag{7.26}$$

where

$$c_i^{\rm ex}(x_i) \triangleq \begin{cases} a_{i_1}^{\rm ex} + b_{i_1}^{\rm ex} x_i, & \text{if } 0 \le x_i \le x_{i_1}^{\rm ex}, \\ a_{i_2}^{\rm ex}, & \text{if } x_{i_1}^{\rm ex} \le x_i \le x_{i_2}^{\rm ex}, \\ a_{i_3}^{\rm ex} + b_{i_3}^{\rm ex} x_i, & \text{if } x_{i_2}^{\rm ex} \le x_i \le V_{\rm T}, \end{cases} \qquad i = 1, \ldots, 2^n, \tag{7.27}$$

$a_{i_j}^{\rm ex}$, $j = 1, 2, 3$, and $b_{i_j}^{\rm ex}$, $j = 1, 3$, are unknown parameters with $b_{i_1}^{\rm ex} > 0$ and $b_{i_3}^{\rm ex} < 0$, $x_{i_j}^{\rm ex}$, $j = 1, 2$, are unknown volume ranges wherein the compliance is constant, and k_j is given by (7.25).

7.4. Neuroadaptive Control for Pressure- and Work-Limited Mechanical Ventilation

In this section, we illustrate the efficacy of the neuroadaptive control framework of Section 7.2 on the nonlinear multi-compartmental lung model developed in Section 7.3. First, however, we rewrite the state equations (7.23) and (7.26) for inspiration and expiration, respectively, in the form of (7.1). Specifically, define the state vector $x \triangleq [x_1, x_2, \ldots, x_{2^n}]^{\rm T}$, where x_i denotes the lung volume of the i-th compartment. Now, the state equation (7.23) for inspiration can be rewritten as

$$R_{\rm in}\dot{x}(t) + C_{\rm in}(x(t))x(t) = p_{\rm in}(t)\mathbf{e}, \quad x(0) = x_0^{\rm in}, \quad 0 \le t \le T_{\rm in}, \tag{7.28}$$

where $\mathbf{e} \triangleq [1, \ldots, 1]^{\rm T}$ denotes the ones vector of order 2^n, $C_{\rm in}(x)$ is a diagonal matrix function given by

$$C_{\rm in}(x) \triangleq \operatorname{diag}\left[\frac{1}{c_1^{\rm in}(x_1)}, \cdots, \frac{1}{c_{2^n}^{\rm in}(x_{2^n})}\right], \tag{7.29}$$

and

$$R_{\rm in} \triangleq \sum_{j=0}^{n} \sum_{k=1}^{2^j} R_{j,k}^{\rm in}\ Z_{j,k}\ Z_{j,k}^{\rm T}, \tag{7.30}$$

where $Z_{j,k} \in \mathbb{R}^{2^n}$ is such that the l-th element of $Z_{j,k}$ is 1 for all $l = (k-1)2^{n-j} + 1,\ (k-1)2^{n-j} + 2, \ldots, k2^{n-j}, k = 1, \ldots, 2^j, j = 0, 1, \ldots, n$, and zero elsewhere.

Similarly, the state equation (7.26) for expiration can be rewritten as

$$R_{\rm ex}\dot{x}(t) + C_{\rm ex}(x(t))x(t) = p_{\rm ex}(t)\mathbf{e}, \quad x(T_{\rm in}) = x_0^{\rm ex}, \quad T_{\rm in} \le t \le T_{\rm ex} + T_{\rm in}, \quad (7.31)$$

where

$$C_{\rm ex}(x) \triangleq \text{diag}\left[\frac{1}{c_1^{\rm ex}(x_1)}, \cdots, \frac{1}{c_{2^n}^{\rm ex}(x_{2^n})}\right], \quad (7.32)$$

and

$$R_{\rm ex} \triangleq \sum_{j=0}^{n}\sum_{k=1}^{2^j} R_{j,k}^{\rm ex}\ Z_{j,k}\ Z_{j,k}^{\rm T}. \quad (7.33)$$

Now, since, by Proposition 4.1 of [22], $R_{\rm in}$ and $R_{\rm ex}$ are invertible, it follows that (7.28) and (7.31) can be equivalently written as

$$\dot{x}(t) = A_{\rm in}(x(t))x(t) + B_{\rm in}p_{\rm in}(t), \quad x(0) = x_0^{\rm in}, \quad 0 \le t \le T_{\rm in}, \quad (7.34)$$

$$\dot{x}(t) = A_{\rm ex}(x(t))x(t) + B_{\rm ex}p_{\rm ex}(t), \quad x(T_{\rm in}) = x_0^{\rm ex}, \quad T_{\rm in} \le t \le T_{\rm ex} + T_{\rm in}, \quad (7.35)$$

where $A_{\rm in}(x) \triangleq -R_{\rm in}^{-1}C_{\rm in}(x)$, $B_{\rm in} \triangleq R_{\rm in}^{-1}\mathbf{e}$, $A_{\rm ex}(x) \triangleq -R_{\rm ex}^{-1}C_{\rm ex}(x)$, and $B_{\rm ex} \triangleq R_{\rm ex}^{-1}\mathbf{e}$.

To account for a continuous transition of the lung resistance and compliance parameters between the inspiration and expiration phase, consider the bounded continuous periodic function $\theta(t) \in \mathbb{R}$, $t \ge 0$, given by

$$\theta(t) \triangleq \begin{cases} 1, & \text{if } 0 \le t \le T_{\rm in} - \varepsilon_{\rm in}, \\ \frac{1}{\varepsilon_{\rm in}}(T_{\rm in} - t), & \text{if } T_{\rm in} - \varepsilon_{\rm in} \le t \le T_{\rm in}, \\ 0, & \text{if } T_{\rm in} \le t \le T_{\rm in} + T_{\rm ex} - \varepsilon_{\rm ex}, \\ \frac{1}{\varepsilon_{\rm ex}}(t + \varepsilon_{\rm ex} - T_{\rm in} - T_{\rm ex}), & \text{if } T_{\rm in} + T_{\rm ex} - \varepsilon_{\rm ex} \le t \le T_{\rm in} + T_{\rm ex}, \end{cases} \quad (7.36)$$

where $\varepsilon_{\rm in} > 0$ and $\varepsilon_{\rm ex} > 0$ are sufficiently small constants representing the transition times form inspiration to expiration and vice versa, respectively, and $\theta(t) = \theta(t + T_{\rm in} + T_{\rm ex})$ for all $t \ge 0$. Now, (7.34) and (7.35) can be written as

$$\dot{x}(t) = \left[\theta(t)A_{\rm in}(x(t)) + (1 - \theta(t))A_{\rm ex}(x(t))\right]x(t) + \left[\theta(t)B_{\rm in} + (1 - \theta(t))B_{\rm ex}\right]h(u(t))$$
$$+P_{\rm musc}(\mathbf{e}^{\rm T}x(t)) + P_{\rm ex}, \quad x(0) = x_{\rm in}(0), \quad t \ge 0, \quad (7.37)$$

where $u(t) \triangleq p_{\rm k}(t)$, ${\rm k} \in \{{\rm in}, {\rm ex}\}$, $t \geq 0$, $h(u(t))$, $t \geq 0$, is a saturation constraint on the applied airway pressure given by

$$h(u) \triangleq \begin{cases} 0, & \text{if } u \leq 0, \\ P_{\max}, & \text{if } u \geq P_{\max}, \\ u, & \text{otherwise}, \end{cases} \tag{7.38}$$

$P_{\rm ex} \in \mathbb{R}^{2^n}$ denotes the end-expiratory pressure due to air remaining in the lung after the completion of each breath [28], $P_{\max}$ denotes the peak pressure of the ventilator, and $P_{\rm musc}(\mathbf{e}^{\rm T}x(t))$, $t \geq 0$, introduced in (7.37) represents a nonnegative pressure term due to the lung muscle activity of a patient and accounts for the effect of spontaneous breathing of a patient in the lung model.

Here, we assume that $P_{\rm musc}(\mathbf{e}^{\rm T}x)$ is a nonlinear function given by

$$P_{\rm musc}(\mathbf{e}^{\rm T}x) = W_{\rm m}^{\rm T}\sigma_{\rm m}(\mathbf{e}^{\rm T}x), \tag{7.39}$$

where $W_{\rm m} \in \mathbb{R}^{l_m \times 2^n} \geq\geq 0$ is an unknown matrix and $\sigma_{\rm m}(\mathbf{e}^{\rm T}x) \in \mathbb{R}^{l_m} \geq\geq 0$ is a known function. Note that since, by Proposition 4.1 of [22] ,$-R_{\rm in}^{-1}$ and $-R_{\rm ex}^{-1}$ are essentially nonnegative, $C_{\rm in}(x)$ and $C_{\rm ex}(x)$ are diagonal, and $\theta(t) \geq 0$, $t \geq 0$, it follows that $A_{\rm in}(x)$ and $A_{\rm ex}(x)$ in (7.37) are essentially nonnegative. Hence, since $h(u(t)) \geq\geq 0$, $t \geq 0$, $P_{\rm musc}(\mathbf{e}^{\rm T}x(t)) \geq\geq 0$, $t \geq 0$, and $P_{\rm ex} \geq\geq 0$, it follows from Proposition 5.1 that $x(t) \geq\geq 0$, $t \geq 0$, for all $x_{\rm in}(0) \in \overline{\mathbb{R}}_+^{2^n}$.

Next, we rewrite (7.37) in the form of (7.1) and (7.2) as

$$\dot{x}(t) = A_0x(t) + B_0h(u(t)) + f(x(t), h(u(t)), \theta(t)),\ x(0) = x_{\rm in}(0),\ t \geq 0, \tag{7.40}$$

$$y(t) = Cx(t), \tag{7.41}$$

where $A_0 = -R_{\rm av}^{-1}C_{\rm av}$, $B_0 = R_{\rm av}^{-1}\mathbf{e}$, and $C = \mathbf{e}^{\rm T}$, and $R_{\rm av}$ and $C_{\rm av}$ are nominal parameter matrices given by

$$R_{\rm av} \triangleq \sum_{j=0}^{n}\sum_{k=1}^{2^j} R_{j,k}^{\rm av}\ Z_{j,k}\ Z_{j,k}^{\rm T}, \quad C_{\rm av} \triangleq {\rm diag}\left[\frac{1}{c_1^{\rm av}}, \cdots, \frac{1}{c_{2^n}^{\rm av}}\right], \tag{7.42}$$

where $R_{j,i}^{\mathrm{av}}$, $i = 1, 2, \ldots, 2^j$, $j = 0, \ldots, n$, denote the nominal resistance (to air flow) of the i-th airway in the j-th generation, and c_i^{av}, $i = 1, 2, \ldots, 2^n$, denote the nominal compliance of each compartment. Now, the nonlinear unknown function $f(x, h(u), \theta)$ capturing resistance and compliance uncertainty in (7.40) during the inspiration and expiration phases is given by

$$f(x, h(u), \theta) = [\theta(A_{\mathrm{in}}(x) - A_0) + (1 - \theta)(A_{\mathrm{ex}}(x) - A_0)]\, x + P_{\mathrm{musc}}(\mathbf{e}^{\mathrm{T}} x) + [\theta(B_{\mathrm{in}} - B_0) + (1 - \theta)(B_{\mathrm{ex}} - B_0)]\, h(u) + P_{\mathrm{ex}}. \quad (7.43)$$

Finally, to account for work limitation constraints by the mechanical ventilator over an inspiration-expiration cycle, we assume that the constraint (6.7) holds and is given by $\eta(t) \triangleq \int_{t-\tau_l}^{t} h(u(s))\mathrm{d}s \leq \eta^*$, $t \geq 0$, $\tau_l > 0$, where $\eta^* > 0$.

Our goal here is to design a neuroadaptive controller satisfying the aforementioned input constraints while guaranteeing output tracking of a clinically plausible reference model. For the system given by (7.40) and (7.41), which is a special case of (7.1) and (7.2), we consider an output tracking problem with a reference model of the form given by (6.5) and (6.6), and design a neuroadaptive controller using Theorem 7.1.

For our simulation we consider a two-compartment lung model and use the values for lung resistance and compliance found in [28]. In particular, we set $c_1^{\mathrm{av}} = 0.022\,\ell/\mathrm{cm\ H_2O}$, $c_2^{\mathrm{av}} = 0.03\,\ell/\mathrm{cm\ H_2O}$, $a_{i_1}^{\mathrm{in}} = 0.018\,\ell/\mathrm{cm\ H_2O}$, $b_{i_1}^{\mathrm{in}} = 0.0233$, $a_{i_2}^{\mathrm{in}} = 0.025\,\ell/\mathrm{cm\ H_2O}$, $a_{i_3}^{\mathrm{in}} = 0.024\,\ell/\mathrm{cm\ H_2O}$, $b_{i_3}^{\mathrm{in}} = -0.0067$, $x_{i_1}^{\mathrm{in}} = 0.3\,\ell$, $x_{i_2}^{\mathrm{in}} = 0.48\,\ell$, $x_{i_3}^{\mathrm{in}} = 0.63\,\ell$, $i = 1, 2$, $a_{i_1}^{\mathrm{ex}} = 0.02\,\ell/\mathrm{cm\ H_2O}$, $b_{i_1}^{\mathrm{ex}} = 0.078$, $a_{i_2}^{\mathrm{ex}} = 0.038\,\ell/\mathrm{cm\ H_2O}$, $a_{i_3}^{\mathrm{ex}} = 0.1025\,\ell/\mathrm{cm\ H_2O}$, $b_{i_3}^{\mathrm{ex}} = -0.15$, $x_{i_1}^{\mathrm{ex}} = 0.23\,\ell$, $x_{i_2}^{\mathrm{ex}} = 0.43\,\ell$, $x_{i_3}^{\mathrm{ex}} = 0.63\,\ell$, $i = 1, 2$, $R_{0,1}^{\mathrm{av}} = 6.29\ \mathrm{cm\ H_2O}/\ell/\mathrm{sec}$, $R_{1,1}^{\mathrm{av}} = 30.67\ \mathrm{cm\ H_2O}/\ell/\mathrm{sec}$, $R_{1,2}^{\mathrm{av}} = 13\ \mathrm{cm\ H_2O}/\ell/\mathrm{sec}$, $R_{0,1}^{\mathrm{in}} = 6\ \mathrm{cm\ H_2O}/\ell/\mathrm{sec}$, $R_{1,1}^{\mathrm{in}} = 25\ \mathrm{cm\ H_2O}/\ell/\mathrm{sec}$, $R_{1,2}^{\mathrm{in}} = 10\ \mathrm{cm\ H_2O}/\ell/\mathrm{sec}$, $R_{0,1}^{\mathrm{ex}} = 6\ \mathrm{cm\ H_2O}/\ell/\mathrm{sec}$, $R_{1,1}^{\mathrm{ex}} = 40\ \mathrm{cm\ H_2O}/\ell/\mathrm{sec}$, $R_{1,2}^{\mathrm{ex}} = 20\ \mathrm{cm\ H_2O}/\ell/\mathrm{sec}$, $T_{\mathrm{in}} = 5$ sec, $T_{\mathrm{ex}} = 10$ sec, $\varepsilon_{\mathrm{in}} = \varepsilon_{\mathrm{ex}} = 0.001$ sec, $P_{\mathrm{ex}}(t) = \theta(t)P_{\mathrm{ex}}^1 +$

$(1-\theta(t))P_{\rm ex}^2$, $P_{\rm ex}^1 = [-0.1105, -0.3113]^{\rm T}$ cm H_2O, $P_{\rm ex}^2 = [-0.0894, -0.1964]^{\rm T}$ cm H_2O, $W_{\rm m} = [0.01, 0.03; 0.02, 0.01]^{\rm T}$, and $\sigma_{\rm m}(y) = [1/(1+e^{-0.2y}), 1/(1+e^{-0.3y})]^{\rm T}$.

With $A_{\rm ref} = A_0$, $B_{\rm ref} = 0.6B$, $r(t) = 17\theta(t)+5$ cm H_2O, $K_{\rm r} = 0.6$, $\sigma(\zeta(t), h(u(t))) = \left[1/(1+e^{-ay(t)}), 1/(1+e^{-ay(t-d)}), 1/(1+e^{-aP(t)}), \theta(t), \sigma_{\rm m}^{\rm T}(y)\right]^{\rm T}$, $t \geq 0$, $a = 0.02$, $x_0 = x_{\rm ref0} = [0, 0]^{\rm T}$, $\hat{W}_0 = 0_{6\times 2}$, $\Gamma_W = 100I_6$, peak pressure limit $P_{\max} = 19$ cm H_2O, and $\eta^* = 43$ sec·cm H_2O, Figures 7.4, 7.5, and 7.6 show the delivered air volume $V(t) = \mathbf{e}^{\rm T}x(t)$ versus time, the constrained pressure $P(t) = h(u(t))$ versus time, and the integrated constrained pressure over the time interval $\tau_l = 5$ sec with and without adaptation for the pressure-limited input $h(u(t))$, $t \geq 0$. Figures 7.7 and 7.8 show the delivered air volume versus time and the unconstrained pressure input $u(t)$, $t \geq 0$, versus time with and without adaptation. Here, "with adaptation" refers to the control signal (7.8) with the adaptive signal $\psi_{\rm ad}(t)$, $t \geq 0$, given by (7.11), and "without adaptation" refers to the control signal (7.8) with $\psi_{\rm ad}(t) \equiv 0$.

As can be seen from Figure 7.4, the delivered air volume significantly exceeds the desired values in the absence of adaptation, whereas satisfactory tracking of the desired air volume is achieved with adaptation. As discussed in the Introduction, failure to adequately regulate the mode and parameters of ventilatory support can result in failure to oxygenate, failure to achieve adequate lung expansion, or overexpansion of the lung resulting in lung tissue rupture. These problems oftentimes occur when open-loop volume-control or pressure-control is employed, or when averaged respiratory data is used to choose the parameters for a closed-loop ventilation control algorithm. In contrast, the proposed neuroadaptive control algorithm avoids reliance on average respiratory data and achieves system performance without excessive reliance on system model parameters.

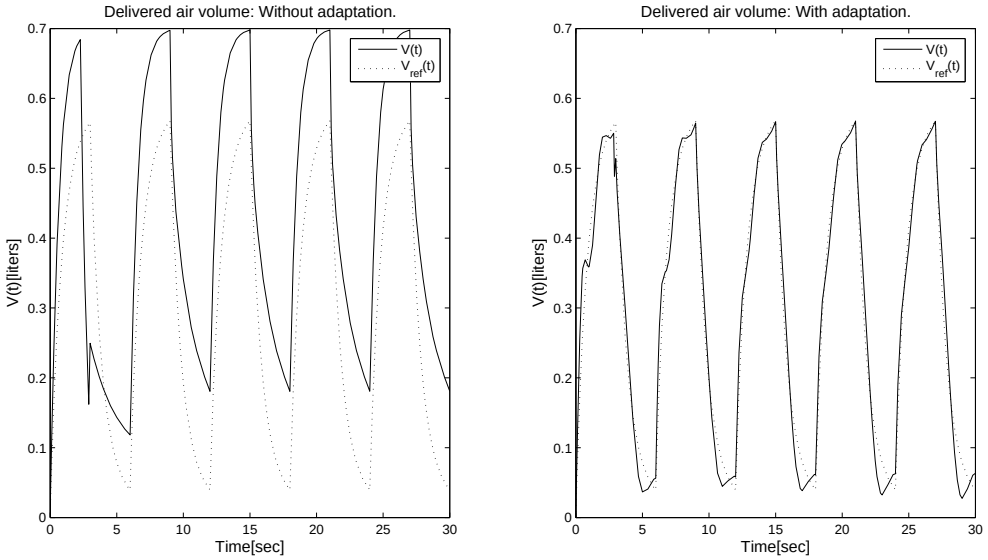

Figure 7.4: Delivered air volume $V(t) = \mathbf{e}^{\mathrm{T}} x(t)$ versus time with pressure-limited input $h(u(t))$.

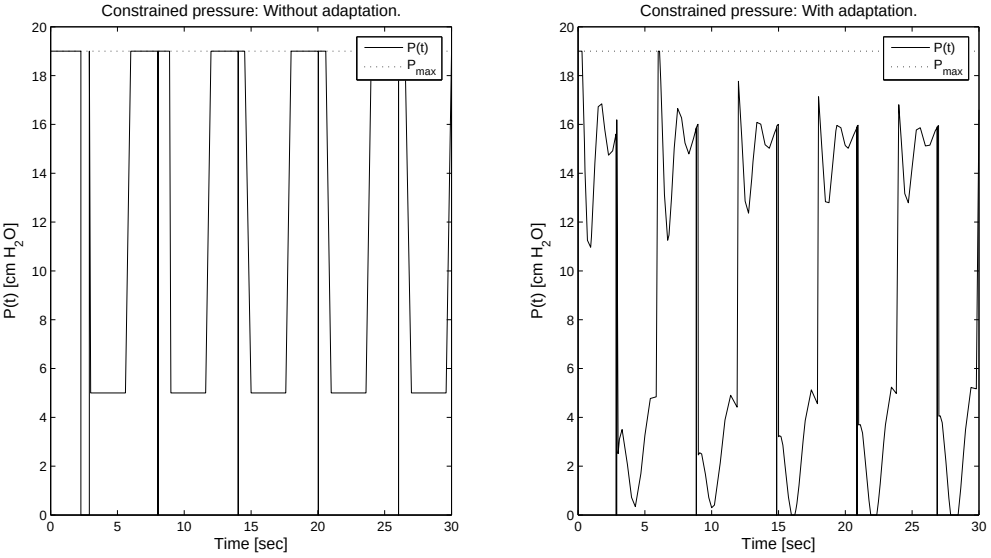

Figure 7.5: Constrained pressure $P(t) = h(u(t))$ versus time.

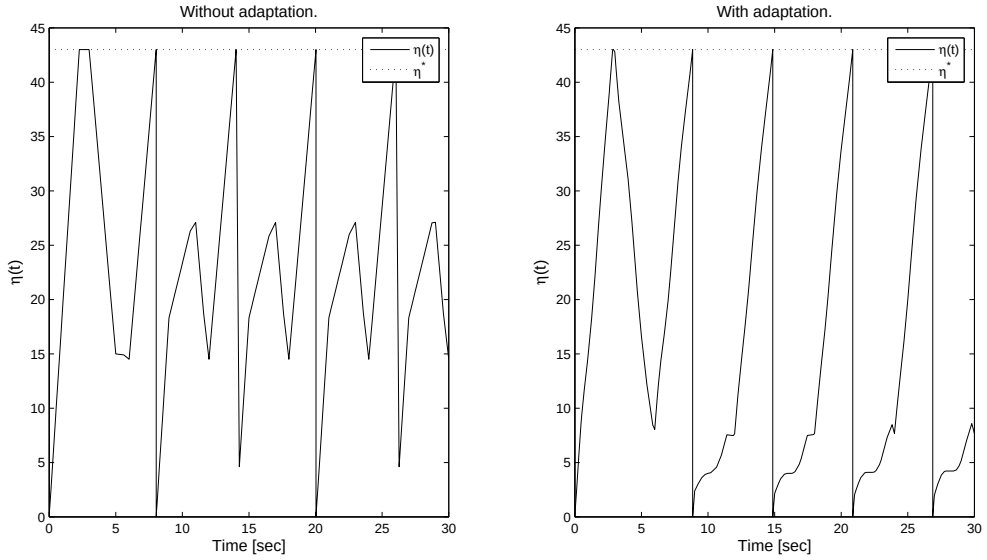

Figure 7.6: $\eta(t)$ versus time.

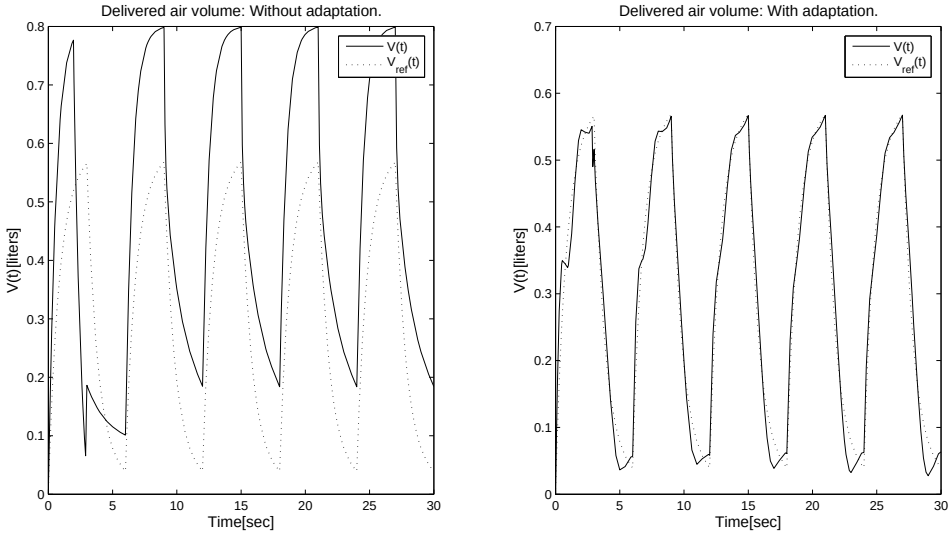

Figure 7.7: Delivered air volume $V(t) = \mathbf{e}^{\mathrm{T}} x(t)$ versus time with unconstrained pressure input $u(t)$.

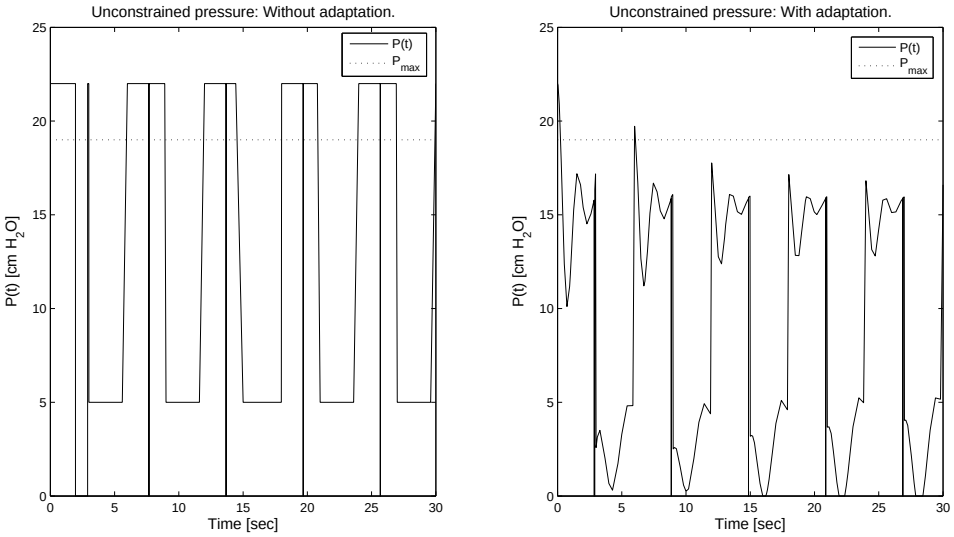

Figure 7.8: Unconstrained pressure $P(t) = u(t)$ versus time.

Chapter 8

Neural Network Hybrid Adaptive Control for Nonlinear Uncertain Impulsive Dynamical Systems

8.1. Introduction

Modern complex engineering systems involve multiple modes of operation placing stringent demands on controller design and implementation of increasing complexity. Such systems typically possess a multiechelon hierarchical *hybrid* control architecture characterized by continuous-time dynamics at the lower levels of the hierarchy and discrete-time dynamics at the higher levels of the hierarchy (see [4, 51, 98] and the numerous references therein). The lower-level units directly interact with the dynamical system to be controlled while the higher-level units receive information from the lower-level units as inputs and provide (possibly discrete) output commands which serve to coordinate and reconcile the (sometimes competing) actions of the lower-level units. The hierarchical controller organization reduces processor cost and controller complexity by breaking up the processing task into relatively small pieces and decomposing the fast and slow control functions. Typically, the higher-level units perform logical checks that determine system mode operation, while the lower-level units execute continuous-variable commands for a given system mode of operation. The mathematical description of many of these systems can be characterized by impulsive differential equations [9, 50, 51, 84, 112].

The purpose of feedback control is to achieve desirable system performance in the face of system uncertainty. To this end, adaptive control along with robust control theory have been developed to address the problem of system uncertainty in control-system design. In contrast to fixed-gain robust controllers, which maintain specified constants within the feedback control law to *sustain* robust performance, adaptive controllers directly or indirectly adjust feedback gains to maintain closed-loop stability and *improve* performance in the face of system uncertainties. Specifically, indirect adaptive controllers utilize parameter update laws to identify unknown system parameters and adjust feedback gains to account for system variation, while direct adaptive controllers directly adjust the controller gains in response to plant variations. The inherent nonlinearities and system uncertainties in hierarchical hybrid control systems and the increasingly stringent performance requirements required for controlling such modern complex embedded systems necessitates the development of hybrid adaptive nonlinear control methodologies.

In a recent paper [55], a hybrid adaptive control framework for adaptive stabilization of multivariable nonlinear uncertain impulsive dynamical systems was developed. In particular, a Lyapunov-based hybrid adaptive control framework was developed that guarantees partial asymptotic stability of the closed-loop system; that is, asymptotic stability with respect to part of the closed-loop system states associated with the hybrid plant dynamics. Furthermore, the remainder of the state associated with the adaptive controller gains was shown to be Lyapunov stable. As is the case in the continuous and discrete-time adaptive control literature [5, 45, 66, 83, 103], the system errors in [55] are captured by a constant linearly parameterized uncertainty model of a known structure but unknown variation. This uncertainty characterization allows the system nonlinearities to be parameterized by a *finite* linear combination of basis functions within a class of function approximators such as rational functions,

spline functions, radial basis functions, sigmoidal functions, and wavelets. However, this linear parametrization of basis functions cannot, in general, exactly capture the unknown system nonlinearity.

Neural network-based adaptive control algorithms have been extensively developed in the literature, wherein Lyapunov-like functions are used to ensure that the neural network controllers can guarantee *ultimate boundedness* of the closed-loop system states rather than closed-loop asymptotic stability. Ultimate boundness ensures that the plant states converge to a *neighborhood* of the origin (see, for example, [40,92,129] for continuous-time systems and [26,38,73] for discrete-time systems). The reason why stability in the sense of Lyapunov is not guaranteed stems from the fact that the uncertainties in the system dynamics cannot be perfectly captured by neural networks using the universal function approximation property and the residual approximation error is characterized via *a norm bound* over a given compact set. Ultimate boundedness guarantees, however, are often conservative since standard Lyapunov-like theorems that are typically used to show ultimate boundedness of the closed-loop hybrid system states provide only *sufficient conditions*, while neural network controllers may possibly achieve plant state convergence to an equilibrium point.

In this chapter, we develop a neural hybrid adaptive control framework for a class of nonlinear uncertain impulsive dynamical systems which ensures state convergence to a Lyapunov stable equilibrium as well as boundedness of the neural network weighting gains. Specifically, the proposed framework is Lyapunov-based and guarantees partial asymptotic stability of the closed-loop hybrid system; that is, Lyapunov stability of the overall closed-loop states and convergence of the plant state. The neuroadaptive controllers are constructed *without* requiring explicit knowledge of the hybrid system dynamics other than the fact that the plant dynamics are continuously

differentiable and that the approximation error of the unknown system nonlinearities lies in a small gain-type *norm bounded* conic sector over a compact set. Hence, the overall neuroadaptive control framework captures the residual approximation error inherent in linear parameterizations of system uncertainty via basis functions. Furthermore, the proposed neuroadaptive control architecture is modular in the sense that if a nominal linear design model is available, then the neuroadaptive controller can be augmented to the nominal design to account for system nonlinearities and system uncertainty.

Finally, we emphasize that we do not impose any linear growth condition on the system resetting (discrete) dynamics. In the literature on classical (non-neural) adaptive control theory for discrete-time systems, it is typically assumed that the nonlinear system dynamics have the linear growth rate which is necessary in proving Lyapunov stability rather than practical stability (ultimate boundedness). Our novel characterization of the system uncertainties (i.e., the small gain-type bound on the norm of the modeling error) allows us to prove asymptotic stability without requiring a linear growth condition on the system dynamics.

8.2. Mathematical Preliminaries

In this section, we introduce notation, definitions, and some key results concerning impulsive dynamical systems [9, 21, 50, 51, 84, 112]. Let $\mathbb{R}$ denote the set of real numbers, $\mathbb{R}^n$ denote the set of $n \times 1$ real column vectors, $(\cdot)^{\mathrm{T}}$ denote transpose, $(\cdot)^{\dagger}$ denote the Moore-Penrose generalized inverse, $\overline{\mathbb{Z}}_+$ denote the set of nonnegative integers, $\mathbb{N}^n$ (resp., $\mathbb{P}^n$) denote the set of $n \times n$ nonnegative (resp., positive) definite matrices, and I_n denote the $n \times n$ identity matrix. Furthermore, we write $\mathrm{tr}(\cdot)$ for the trace operator, $\ln(\cdot)$ for the natural log operator, $\lambda_{\min}(M)$ (resp., $\lambda_{\max}(M)$) for the minimum (resp., maximum) eigenvalue of the Hermitian matrix M, $\sigma_{\max}(M)$ for

the maximum singular value of the matrix M, $V'(x)$ for the Fréchet derivative of V at x, and $\mathrm{dist}(p, \mathcal{M})$ for the smallest distance from a point p to any point in the set $\mathcal{M}$, that is, $\mathrm{dist}(p, \mathcal{M}) \triangleq \inf_{x \in \mathcal{M}} \|p - x\|$.

In this section, we consider controlled *state-dependent* [51] impulsive dynamical systems $\mathcal{G}$ of the form

$$\dot{x}(t) = f_{\mathrm{c}}(x(t)) + G_{\mathrm{c}}(x(t))u_{\mathrm{c}}(t), \quad x(0) = x_0, \quad x(t) \notin \mathcal{Z}_x, \tag{8.1}$$

$$\Delta x(t) = f_{\mathrm{d}}(x(t)) + G_{\mathrm{d}}(x(t))u_{\mathrm{d}}(t), \quad x(t) \in \mathcal{Z}_x, \tag{8.2}$$

where $t \geq 0$, $x(t) \in \mathcal{D} \subseteq \mathbb{R}^n$, $\mathcal{D}$ is an open set with $0 \in \mathcal{D}$, $\Delta x(t) \triangleq x(t^+) - x(t)$, $u_{\mathrm{c}}(t) \in \mathcal{U}_{\mathrm{c}} \subseteq \mathbb{R}^{m_{\mathrm{c}}}$, $u_{\mathrm{d}}(t_k) \in \mathcal{U}_{\mathrm{d}} \subseteq \mathbb{R}^{m_{\mathrm{d}}}$, t_k denotes the kth instant of time at which $x(t)$ intersects $\mathcal{Z}_x$ for a particular trajectory $x(t)$, $f_{\mathrm{c}} : \mathcal{D} \to \mathbb{R}^n$ is Lipschitz continuous and satisfies $f_{\mathrm{c}}(0) = 0$, $G_{\mathrm{c}} : \mathcal{D} \to \mathbb{R}^{n \times m_{\mathrm{c}}}$, $f_{\mathrm{d}} : \mathcal{Z}_x \to \mathbb{R}^n$ is continuous, $G_{\mathrm{d}} : \mathcal{Z}_x \to \mathbb{R}^{n \times m_{\mathrm{d}}}$ is such that $\operatorname{rank} G_{\mathrm{d}}(x) = m_{\mathrm{d}}$, $x \in \mathcal{Z}_x$, and $\mathcal{Z}_x \subset \mathcal{D}$ is the *resetting set*. Here, we assume that $u_{\mathrm{c}}(\cdot)$ and $u_{\mathrm{d}}(\cdot)$ are restricted to the class of *admissible* inputs consisting of measurable functions such that $(u_{\mathrm{c}}(t), u_{\mathrm{d}}(t_k)) \in \mathcal{U}_{\mathrm{c}} \times \mathcal{U}_{\mathrm{d}}$ for all $t \geq 0$ and $k \in \mathbb{Z}_{[0,t)} \triangleq \{k : 0 \leq t_k < t\}$, where the constrained set $\mathcal{U}_{\mathrm{c}} \times \mathcal{U}_{\mathrm{d}}$ is given with $(0, 0) \in \mathcal{U}_{\mathrm{c}} \times \mathcal{U}_{\mathrm{d}}$. We refer to the differential equation (8.1) as the *continuous-time dynamics*, and we refer to the difference equation (8.2) as the *resetting law*.

The equations of motion for the closed-loop impulsive dynamical system (8.1) and (8.2) with hybrid adaptive *feedback* controllers $u_{\mathrm{c}}(\cdot)$ and $u_{\mathrm{d}}(\cdot)$ has the form

$$\dot{\tilde{x}}(t) = \tilde{f}_{\mathrm{c}}(\tilde{x}(t)), \quad \tilde{x}(0) = \tilde{x}_0, \quad \tilde{x}(t) \notin \mathcal{Z}_{\tilde{x}}, \tag{8.3}$$

$$\Delta \tilde{x}(t) = \tilde{f}_{\mathrm{d}}(\tilde{x}(t)), \quad \tilde{x}(t) \in \mathcal{Z}_{\tilde{x}}, \tag{8.4}$$

where $t \geq 0$, $\tilde{x}(t) \in \tilde{\mathcal{D}} \subseteq \mathbb{R}^{\tilde{n}}$, $\tilde{x}(t)$ denotes the closed-loop state involving the system state and the adaptive gains, $\tilde{f}_{\mathrm{c}} : \tilde{\mathcal{D}} \to \mathbb{R}^{\tilde{n}}$ and $\tilde{f}_{\mathrm{d}} : \tilde{\mathcal{D}} \to \mathbb{R}^{\tilde{n}}$ denote the closed-loop continuous-time and resetting dynamics, respectively, with $\tilde{f}_{\mathrm{c}}(\tilde{x}_{\mathrm{e}}) = 0$, where

$\tilde{x}_{\mathrm{e}} \in \tilde{\mathcal{D}} \backslash \mathcal{Z}_{\tilde{x}}$ denotes the closed-loop equilibrium point, and $\tilde{n}$ denotes the dimension of the closed-loop system state. A function $\tilde{x} : \mathcal{I}_{\tilde{x}_0} \to \tilde{\mathcal{D}}$ is a *solution* to the impulsive system (8.3) and (8.4) on the interval $\mathcal{I}_{\tilde{x}_0} \subseteq \mathbb{R}$ with initial condition $\tilde{x}(0) = \tilde{x}_0$, where $\mathcal{I}_{\tilde{x}_0}$ denotes the maximal interval of existence of a solution to (8.3) and (8.4), if $\tilde{x}(\cdot)$ is left-continuous and $\tilde{x}(t)$ satisfies (8.3) and (8.4) for all $t \in \mathcal{I}_{\tilde{x}_0}$. For further discussion on solutions to impulsive differential equations, see [9, 51, 84, 112]. For convenience, we use the notation $s(t, \tilde{x}_0)$ to denote the solution $\tilde{x}(t)$ of (8.3) and (8.4) at time $t \geq 0$ with initial condition $\tilde{x}(0) = \tilde{x}_0$.

In this section, we assume that Assumptions A1 and A2 established in [50, 51] hold; that is, the resetting set is such that resetting removes $\tilde{x}(t_k)$ from the resetting set and no trajectory can intersect the interior of $\mathcal{Z}_{\tilde{x}}$. Hence, as shown in [50, 51], the resetting times are well defined and distinct. Since the resetting times are well defined and distinct and since the solution to (8.3) exists and is unique it follows that the solution of the impulsive dynamical system (8.3) and (8.4) also exists and is unique over a forward time interval. However, it is important to note that the analysis of impulsive dynamical systems can be quite involved. In particular, such systems can exhibit Zenoness and beating as well as confluence, wherein solutions exhibit infinitely many resettings in a finite time, encounter the same resetting surface a finite or infinite number of times in zero time, and coincide after a certain point in time. In this section we allow for the possibility of confluence and Zeno solutions; however, A2 precludes the possibility of beating. Furthermore, since not every bounded solution of an impulsive dynamical system over a forward time interval can be extended to infinity due to Zeno solutions, we assume that existence and uniqueness of solutions are satisfied in forward time. For details see [51].

Next, we provide a key result from [21, 50, 51] involving an invariant set stability theorem for hybrid dynamical systems. For the statement of this result the following

key assumption is needed.

Assumption 8.1 [21, 50, 51]. Let $s(t, \tilde{x}_0)$, $t \geq 0$, denote the solution of (8.3) and (8.4) with initial condition $\tilde{x}_0 \in \tilde{\mathcal{D}}$. Then for every $\tilde{x}_0 \in \tilde{\mathcal{D}}$, there exists a dense subset $\mathcal{T}_{\tilde{x}_0} \subseteq [0, \infty)$ such that $[0, \infty) \backslash \mathcal{T}_{\tilde{x}_0}$ is (finitely or infinitely) countable and for every $\epsilon > 0$ and $t \in \mathcal{T}_{\tilde{x}_0}$, there exists $\delta(\epsilon, \tilde{x}_0, t) > 0$ such that if $\|\tilde{x}_0 - y\| < \delta(\epsilon, \tilde{x}_0, t)$, $y \in \tilde{\mathcal{D}}$, then $\|s(t, \tilde{x}_0) - s(t, y)\| < \epsilon$.

Assumption 8.1 is a generalization of the standard continuous dependence property for dynamical systems with continuous flows to dynamical systems with left-continuous flows. Specifically, by letting $\mathcal{T}_{\tilde{x}_0} = \overline{\mathcal{T}}_{\tilde{x}_0} = [0, \infty)$, where $\overline{\mathcal{T}}_{\tilde{x}_0}$ denotes the closure of the set $\mathcal{T}_{\tilde{x}_0}$, Assumption 8.1 specializes to the classical continuous dependence of solutions of a given dynamical system with respect to the system's initial conditions $\tilde{x}_0 \in \tilde{\mathcal{D}}$ [135]. Since solutions of impulsive dynamical systems are *not* continuous in time and solutions are *not* continuous functions of the system initial conditions, Assumption 8.1 is needed to apply the hybrid invariance principle developed in [21, 50] to hybrid adaptive systems. Henceforth, we assume that the hybrid adaptive feedback controllers $u_{\mathrm{c}}(\cdot)$ and $u_{\mathrm{d}}(\cdot)$ are such that closed-loop hybrid system (8.3) and (8.4) satisfies Assumption 8.1. Necessary and sufficient conditions that guarantee that the nonlinear impulsive dynamical system $\tilde{\mathcal{G}}$ given by (8.1) and (8.2) satisfies Assumption 8.1 are given in [21, 51]. A sufficient condition that guarantees that the trajectories of the closed-loop nonlinear impulsive dynamical system (8.3) and (8.4) satisfy Assumption 8.1 are Lipschitz continuity of $\tilde{f}_{\mathrm{c}}(\cdot)$ and the existence of a continuously differentiable function $\mathcal{X} : \tilde{\mathcal{D}} \to \mathbb{R}$ such that the resetting set is given by $\mathcal{Z}_{\tilde{x}} = \{\tilde{x} \in \tilde{\mathcal{D}} : \mathcal{X}(\tilde{x}) = 0\}$, where $\mathcal{X}'(\tilde{x}) \neq 0$, $\tilde{x} \in \mathcal{Z}_{\tilde{x}}$, and $\mathcal{X}'(\tilde{x})\tilde{f}_{\mathrm{c}}(\tilde{x}) \neq 0$, $\tilde{x} \in \mathcal{Z}_{\tilde{x}}$. The last condition above ensures that the solution of the closed-loop hybrid system is not tangent to the resetting set $\mathcal{Z}_{\tilde{x}}$ for all initial conditions $\tilde{x}_0 \in \tilde{\mathcal{D}}$. For further discussion on Assumption 8.1, see [21, 50, 51].

The following theorem proven in [21, 50] is needed to develop the main results of this section.

Theorem 8.1 [21, 50]. Consider the nonlinear impulsive dynamical system $\tilde{\mathcal{G}}$ given by (8.3) and (8.4), assume $\tilde{\mathcal{D}}_{\rm c} \subset \tilde{\mathcal{D}}$ is a compact positively invariant set with respect to (8.3) and (8.4), and assume that there exists a continuously differentiable function $V : \tilde{\mathcal{D}}_{\rm c} \to \mathbb{R}$ such that

$$V'(\tilde{x})\tilde{f}_{\rm c}(\tilde{x}) \leq 0, \quad \tilde{x} \in \tilde{\mathcal{D}}_{\rm c}, \quad \tilde{x} \notin \mathcal{Z}_{\tilde{x}}, \tag{8.5}$$

$$V(\tilde{x} + \tilde{f}_{\rm d}(\tilde{x})) \leq V(\tilde{x}), \quad \tilde{x} \in \tilde{\mathcal{D}}_{\rm c}, \quad \tilde{x} \in \mathcal{Z}_{\tilde{x}}. \tag{8.6}$$

Let $\mathcal{R} \triangleq \{\tilde{x} \in \tilde{\mathcal{D}}_{\rm c} : \tilde{x} \notin \mathcal{Z}_{\tilde{x}}, V'(\tilde{x})\tilde{f}_{\rm c}(\tilde{x}) = 0\} \cup \{\tilde{x} \in \tilde{\mathcal{D}}_{\rm c} : \tilde{x} \in \mathcal{Z}_{\tilde{x}}, V(\tilde{x} + \tilde{f}_{\rm d}(\tilde{x})) = V(\tilde{x})\}$ and let $\mathcal{M}$ denote the largest invariant set contained in $\mathcal{R}$. If $\tilde{x}_0 \in \tilde{\mathcal{D}}_{\rm c}$, then $\tilde{x}(t) \to \mathcal{M}$ as $t \to \infty$. Finally, if $\tilde{\mathcal{D}} = \mathbb{R}^{\tilde{n}}$ and $V(\tilde{x}) \to \infty$ as $\|\tilde{x}\| \to \infty$, then $\tilde{x}(t) \to \mathcal{M}$ as $t \to \infty$ for all $\tilde{x}_0 \in \mathbb{R}^{\tilde{n}}$.

8.3. Hybrid Adaptive Stabilization for Nonlinear Hybrid Dynamical Systems using Neural Networks

In this section, we consider the problem of neural hybrid adaptive stabilization for nonlinear uncertain hybrid systems. Specifically, we consider the controlled state-dependent impulsive dynamical system (8.1) and (8.2) with $\mathcal{D} = \mathbb{R}^n$, $\mathcal{U}_{\rm c} = \mathbb{R}^{m_{\rm c}}$, and $\mathcal{U}_{\rm d} = \mathbb{R}^{m_{\rm d}}$, where $f_{\rm c} : \mathbb{R}^n \to \mathbb{R}^n$ and $f_{\rm d} : \mathbb{R}^n \to \mathbb{R}^n$ are continuously differentiable and satisfy $f_{\rm c}(0) = 0$ and $f_{\rm d}(0) = 0$, and $G_{\rm c} : \mathbb{R}^n \to \mathbb{R}^{n \times m_{\rm c}}$ and $G_{\rm d} : \mathbb{R}^n \to \mathbb{R}^{n \times m_{\rm d}}$.

In this section, we assume that $f_{\rm c}(\cdot)$ and $f_{\rm d}(\cdot)$ are unknown functions, and $f_{\rm c}(\cdot)$, $G_{\rm c}(\cdot)$, $f_{\rm d}(\cdot)$, and $G_{\rm d}(\cdot)$ are given by

$$f_{\rm c}(x) = A_{\rm c}x + \Delta f_{\rm c}(x), \quad G_{\rm c}(x) = B_{\rm c}G_{\rm cn}(x), \tag{8.7}$$

$$f_{\rm d}(x) = (A_{\rm d} - I_n)x + \Delta f_{\rm d}(x), \quad G_{\rm d}(x) = B_{\rm d}G_{\rm dn}(x), \tag{8.8}$$

where $A_{\rm c} \in \mathbb{R}^{n\times n}$, $A_{\rm d} \in \mathbb{R}^{n\times n}$, $B_{\rm c} \in \mathbb{R}^{n\times m_{\rm c}}$, and $B_{\rm d} \in \mathbb{R}^{n\times m_{\rm d}}$ are known matrices, $G_{\rm cn} : \mathbb{R}^n \to \mathbb{R}^{m_{\rm c}\times m_{\rm c}}$ and $G_{\rm dn} : \mathbb{R}^n \to \mathbb{R}^{m_{\rm d}\times m_{\rm d}}$ are known matrix functions such that $\det G_{\rm cn}(x) \neq 0$, $x \in \mathbb{R}^n$, and $\det G_{\rm dn}(x) \neq 0$, $x \in \mathbb{R}^n$, and $\Delta f_{\rm c} : \mathbb{R}^n \to \mathbb{R}^n$ and $\Delta f_{\rm d} : \mathbb{R}^n \to \mathbb{R}^n$ are unknown functions belonging to the uncertainty sets $\mathcal{F}_{\rm c}$ and $\mathcal{F}_{\rm d}$, respectively, given by

$$\mathcal{F}_{\rm c} = \{\Delta f_{\rm c} : \mathbb{R}^n \to \mathbb{R}^n : \Delta f_{\rm c}(0) = 0,\, \Delta f_{\rm c}(x) = B_{\rm c}\delta_{\rm c}(x),\, x \in \mathbb{R}^n\}, \tag{8.9}$$

$$\mathcal{F}_{\rm d} = \{\Delta f_{\rm d} : \mathbb{R}^n \to \mathbb{R}^n : \Delta f_{\rm d}(0) = 0,\, \Delta f_{\rm d}(x) = B_{\rm d}\delta_{\rm d}(x),\, x \in \mathbb{R}^n\}, \tag{8.10}$$

where $\delta_{\rm c} : \mathbb{R}^n \to \mathbb{R}^{m_{\rm c}}$ and $\delta_{\rm d} : \mathbb{R}^n \to \mathbb{R}^{m_{\rm d}}$ are uncertain continuously differentiable functions such that $\delta_{\rm c}(0) = 0$ and $\delta_{\rm d}(0) = 0$. It is important to note that since $\delta_{\rm c}(x)$ and $\delta_{\rm d}(x)$ are continuously differentiable and $\delta_{\rm c}(0) = 0$ and $\delta_{\rm d}(0) = 0$, it follows that there exist continuous matrix functions $\Delta_{\rm c} : \mathbb{R}^n \to \mathbb{R}^{m_{\rm c}\times n}$ and $\Delta_{\rm d} : \mathbb{R}^n \to \mathbb{R}^{m_{\rm d}\times n}$ such that $\delta_{\rm c}(x) = \Delta_{\rm c}(x)x$, $x \in \mathbb{R}^n$, and $\delta_{\rm d}(x) = \Delta_{\rm d}(x)x$, $x \in \mathbb{R}^n$. Furthermore, we assume that the continuous matrix functions $\Delta_{\rm c}(\cdot)$ and $\Delta_{\rm d}(\cdot)$ can be approximated over a compact set $\mathcal{D}_{\rm c} \subset \mathbb{R}^n$ by a linear in the parameters neural network up to a desired accuracy so that

$$\mathrm{col}_i(\Delta_{\rm c}(x)) = W_{{\rm c}i}^{\rm T}\sigma_{\rm c}(x) + \varepsilon_{{\rm c}i}(x), \quad x \in \mathcal{D}_{\rm c}, \quad i = 1, \cdots, n, \tag{8.11}$$

$$\mathrm{col}_i(\Delta_{\rm d}(x)) = W_{{\rm d}i}^{\rm T}\sigma_{\rm d}(x) + \varepsilon_{{\rm d}i}(x), \quad x \in \mathcal{D}_{\rm c}, \quad i = 1, \cdots, n, \tag{8.12}$$

where $\mathrm{col}_i(\Delta(\cdot))$ denotes the ith column of the matrix $\Delta(\cdot)$, $W_{{\rm c}i}^{\rm T} \in \mathbb{R}^{m_{\rm c}\times s_{\rm c}}$ and $W_{{\rm d}i}^{\rm T} \in \mathbb{R}^{m_{\rm d}\times s_{\rm d}}$, $i = 1, \cdots, n$, are optimal *unknown* (constant) weights that minimize the approximation error over $\mathcal{D}_{\rm c}$, $\varepsilon_{{\rm c}i} : \mathbb{R}^n \to \mathbb{R}^{m_{\rm c}}$ and $\varepsilon_{{\rm d}i} : \mathbb{R}^n \to \mathbb{R}^{m_{\rm d}}$, $i = 1, \cdots, n$, are modeling errors such that $\sigma_{\max}(\Upsilon_{\rm c}(x)) \leq \gamma_{\rm c}^{-1}$ and $\sigma_{\max}(\Upsilon_{\rm d}(x)) \leq \gamma_{\rm d}^{-1}$, $x \in \mathbb{R}^n$, where $\Upsilon_{\rm c}(x) \triangleq [\varepsilon_{{\rm c}1}(x), \cdots, \varepsilon_{{\rm c}n}(x)]$, $\Upsilon_{\rm d}(x) \triangleq [\varepsilon_{{\rm d}1}(x), \cdots, \varepsilon_{{\rm d}n}(x)]$, and $\gamma_{\rm c}, \gamma_{\rm d} > 0$, and $\sigma_{\rm c} : \mathbb{R}^n \to \mathbb{R}^{s_{\rm c}}$ and $\sigma_{\rm d} : \mathbb{R}^n \to \mathbb{R}^{s_{\rm d}}$ are given basis functions such that each component of $\sigma_{\rm c}(\cdot)$ and $\sigma_{\rm d}(\cdot)$ takes values between 0 and 1.

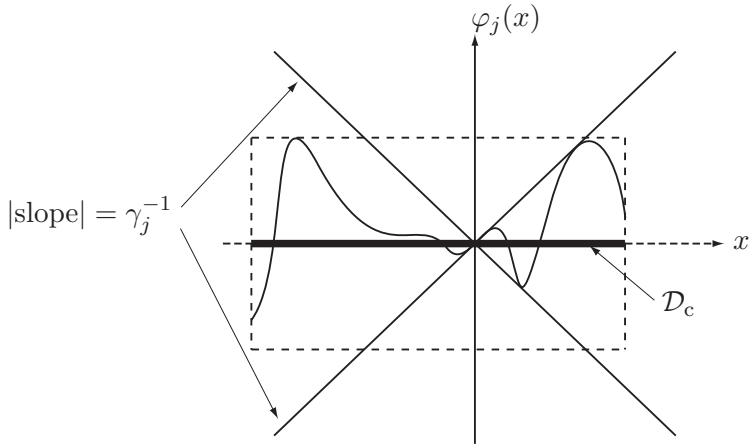

Figure 8.1: Visualization of function $\varphi_j(\cdot)$, $j = \text{c}, \text{d}$

Next, defining

$$\varphi_{\text{c}}(x) \triangleq \delta_{\text{c}}(x) - W_{\text{c}}^{\text{T}}[x \otimes \sigma_{\text{c}}(x)], \tag{8.13}$$

$$\varphi_{\text{d}}(x) \triangleq \delta_{\text{d}}(x) - W_{\text{d}}^{\text{T}}[x \otimes \sigma_{\text{d}}(x)], \tag{8.14}$$

where $W_{\text{c}}^{\text{T}} \triangleq [W_{\text{c}1}^{\text{T}}, \cdots, W_{\text{c}n}^{\text{T}}] \in \mathbb{R}^{m_{\text{c}} \times n s_{\text{c}}}$, $W_{\text{d}}^{\text{T}} \triangleq [W_{\text{d}1}^{\text{T}}, \cdots, W_{\text{d}n}^{\text{T}}] \in \mathbb{R}^{m_{\text{d}} \times n s_{\text{d}}}$, and $\otimes$ denotes Kronecker product, it follows from (8.11) and (8.12), and Cauchy-Schwarz inequality that

$$\begin{aligned}
\varphi_j^{\text{T}}(x)\varphi_j(x) &= \|\Delta_j(x)x - W_j^{\text{T}}(x \otimes \sigma_j(x))\|^2 \\
&= \|\Delta_j(x)x - \Sigma_j(x)x\|^2 \\
&= \|\Upsilon_j(x)x\|^2 \\
&\leq \gamma_j^{-2} x^{\text{T}} x, \quad x \in \mathcal{D}_{\text{c}}, \quad j = \text{c}, \text{d},
\end{aligned} \tag{8.15}$$

where $\|\cdot\|$ denotes the Euclidean norm on $\mathbb{R}^{s_{\text{c}}}$ or $\mathbb{R}^{s_{\text{d}}}$ and $\Sigma_j(x) \triangleq [W_{j1}^{\text{T}}\sigma_j(x), \cdots, W_{jn}^{\text{T}}\sigma_j(x)]$, $j = \text{c}, \text{d}$. This corresponds to a nonlinear small gain-type norm bounded uncertainty characterization for $\varphi_j(\cdot)$, $j = \text{c}, \text{d}$ (see Figure 8.1).

Theorem 8.2. Consider the nonlinear uncertain hybrid dynamical system $\mathcal{G}$ given by (8.1) and (8.2) where $f_{\text{c}}(\cdot)$, $G_{\text{c}}(\cdot)$, $f_{\text{d}}(\cdot)$, and $G_{\text{d}}(\cdot)$ are given by (8.7) and (8.8),

and $\Delta f_{\rm c} : \mathbb{R}^n \to \mathbb{R}^n$ and $\Delta f_{\rm d} : \mathbb{R}^n \to \mathbb{R}^n$ belong to the uncertainty sets $\mathcal{F}_{\rm c}$ and $\mathcal{F}_{\rm d}$, respectively. For given $\gamma_{\rm c}, \gamma_{\rm d} > 0$, assume there exists a positive-definite matrix $P \in \mathbb{R}^{n\times n}$ such that

$$0 = A_{\rm cs}^{\rm T}P + PA_{\rm cs} + \gamma_{\rm c}^{-2}PB_{\rm c}B_{\rm c}^{\rm T}P + I_n + R_{\rm c}, \tag{8.16}$$

$$P = A_{\rm d}^{\rm T}PA_{\rm d} - A_{\rm d}^{\rm T}PB_{\rm d}(B_{\rm d}^{\rm T}PB_{\rm d})^{-1}B_{\rm d}^{\rm T}PA_{\rm d} + (\alpha+\beta)I_n + R_{\rm d}, \tag{8.17}$$

where $A_{\rm cs} \triangleq A_{\rm c} + B_{\rm c}K_{\rm c}$, $K_{\rm c} \in \mathbb{R}^{m_{\rm c}\times n}$, $R_{\rm c} \in \mathbb{R}^{n\times n}$ and $R_{\rm d} \in \mathbb{R}^{n\times n}$ are positive definite, $\alpha > 0$, and β satisfies

$$\beta \geq \gamma_{\rm d}^{-2}\Big(\lambda_{\max}(B_{\rm d}^{\rm T}PB_{\rm d}) + a\frac{1 + x^{\rm T}Px}{c + [x\otimes\sigma_{\rm d}(x)]^{\rm T}[x\otimes\sigma_{\rm d}(x)]}\Big), \quad x \in \mathcal{Z}_x, \tag{8.18}$$

where

$$a = \max\{c, n/\lambda_{\min}(P)\}\lambda_{\max}\Big(B_{\rm d}^{\rm T}PB_{\rm d}\Big(I_m + \tfrac{1}{\alpha\gamma_{\rm d}^2}B_{\rm d}^{\rm T}PB_{\rm d}\Big)\Big) \tag{8.19}$$

and $c > 0$. Finally, let $A_{\rm ds} \triangleq A_{\rm d} + B_{\rm d}K_{\rm d}$, where $K_{\rm d} \triangleq -(B_{\rm d}^{\rm T}PB_{\rm d})^{-1}B_{\rm d}^{\rm T}PA_{\rm d}$, and let $Q_{\rm c} \in \mathbb{R}^{m_{\rm c}}$ and $Y \in \mathbb{R}^{s_{\rm c}}$ be positive definite. Then the neural hybrid adaptive feedback control law

$$u_{\rm c}(t) = G_{\rm cn}^{-1}(x(t))\Big[K_{\rm c}x(t) - \hat{W}_{\rm c}^{\rm T}(t)[x(t)\otimes\sigma_{\rm c}(x(t))]\Big], \quad x(t) \notin \mathcal{Z}_x, \tag{8.20}$$

$$u_{\rm d}(t) = G_{\rm dn}^{-1}(x(t))\Big[K_{\rm d}x(t) - \hat{W}_{\rm d}^{\rm T}(t)[x(t)\otimes\sigma_{\rm d}(x(t))]\Big], \quad x(t) \in \mathcal{Z}_x, \tag{8.21}$$

where $\hat{W}_{\rm c}^{\rm T}(t) \in \mathbb{R}^{m_{\rm c}\times ns_{\rm c}}$, $t \geq 0$, $\hat{W}_{\rm d}^{\rm T}(t) \in \mathbb{R}^{m_{\rm d}\times ns_{\rm d}}$, $t \geq 0$, and $\sigma_{\rm c} : \mathbb{R}^n \to \mathbb{R}^{s_{\rm c}}$ and $\sigma_{\rm d} : \mathbb{R}^n \to \mathbb{R}^{s_{\rm d}}$ are given basis functions, with update laws

$$\dot{\hat{W}}_{\rm c}^{\rm T}(t) = \tfrac{1}{1+x(t)^{\rm T}Px(t)}Q_{\rm c}B_{\rm c}^{\rm T}Px(t)[x(t)\otimes\sigma_{\rm c}(x(t))]^{\rm T}Y, \quad \hat{W}_{\rm c}^{\rm T}(0) = \hat{W}_{\rm c0}^{\rm T}, \quad x(t) \notin \mathcal{Z}_x, \tag{8.22}$$

$$\Delta\hat{W}_{\rm c}^{\rm T}(t) = 0, \quad x(t) \in \mathcal{Z}_x, \tag{8.23}$$

$$\dot{\hat{W}}_{\rm d}^{\rm T}(t) = 0, \quad \hat{W}_{\rm d}^{\rm T}(0) = \hat{W}_{\rm d0}^{\rm T}, \quad x(t) \notin \mathcal{Z}_x, \tag{8.24}$$

$$\Delta\hat{W}_{\rm d}^{\rm T}(t) = \tfrac{1}{c+[x(t)\otimes\sigma_{\rm d}(x(t))]^{\rm T}[x(t)\otimes\sigma_{\rm d}(x(t))]}B_{\rm d}^{\dagger}[x(t^+) - A_{\rm ds}x(t)][x(t)\otimes\sigma_{\rm d}(x(t))]^{\rm T}, \quad x(t) \in \mathcal{Z}_x, \tag{8.25}$$

where $\Delta\hat{W}_{\rm c}^{\rm T}(t) \triangleq \hat{W}_{\rm c}^{\rm T}(t^+) - \hat{W}_{\rm c}^{\rm T}(t)$ and $\Delta\hat{W}_{\rm d}^{\rm T}(t) \triangleq \hat{W}_{\rm d}^{\rm T}(t^+) - \hat{W}_{\rm d}^{\rm T}(t)$, guarantees that there exists a positively invariant set $\mathcal{D}_\alpha \subset \mathbb{R}^n \times \mathbb{R}^{m_{\rm c}\times ns_{\rm c}} \times \mathbb{R}^{m_{\rm d}\times ns_{\rm d}}$ such that $(0, W_{\rm c}^{\rm T}, W_{\rm d}^{\rm T}) \in \mathcal{D}_\alpha$, where $W_{\rm c}^{\rm T} \in \mathbb{R}^{m_{\rm c}\times ns_{\rm c}}$ and $W_{\rm d}^{\rm T} \in \mathbb{R}^{m_{\rm d}\times ns_{\rm d}}$, and the solution $(x(t), \hat{W}_{\rm c}^{\rm T}(t), \hat{W}_{\rm d}^{\rm T}(t)) \equiv (0, W_{\rm c}^{\rm T}, W_{\rm d}^{\rm T})$ of the closed-loop system given by (8.1), (8.2), and (8.20)–(8.25) is Lyapunov stable and $x(t) \to 0$ as $t \to \infty$ for all $\Delta f_{\rm c}(\cdot) \in \mathcal{F}_{\rm c}$, $\Delta f_{\rm d}(\cdot) \in \mathcal{F}_{\rm d}$, and $(x_0, \hat{W}_{\rm c0}^{\rm T}, \hat{W}_{\rm d0}^{\rm T}) \in \mathcal{D}_\alpha$.

Proof. First, note that

$$\begin{aligned} A_{\rm ds}^{\rm T}PB_{\rm d}B_{\rm d}^{\rm T}PA_{\rm ds} &= (A_{\rm d} + B_{\rm d}K_{\rm d})^{\rm T}PB_{\rm d}B_{\rm d}^{\rm T}P(A_{\rm d} + B_{\rm d}K_{\rm d}) \\ &= (A_{\rm d} - B_{\rm d}(B_{\rm d}^{\rm T}PB_{\rm d})^{-1}B_{\rm d}^{\rm T}PA_{\rm d})^{\rm T}PB_{\rm d}B_{\rm d}^{\rm T}P(A_{\rm d} - B_{\rm d}(B_{\rm d}^{\rm T}PB_{\rm d})^{-1}B_{\rm d}^{\rm T} \\ &\quad \cdot PA_{\rm d}) \\ &= 0, \end{aligned} \tag{8.26}$$

and hence, since $A_{\rm ds}^{\rm T}PB_{\rm d}B_{\rm d}^{\rm T}PA_{\rm ds}$ is nonnegative definite, $A_{\rm ds}^{\rm T}PB_{\rm d} = 0$. Furthermore, note that

$$P = A_{\rm ds}^{\rm T}PA_{\rm ds} + (\alpha + \beta)I_n + R_{\rm d}. \tag{8.27}$$

Now, with $u_{\rm c}(t)$, $t \geq 0$, and $u_{\rm d}(t_k)$, $k \in \mathbb{Z}$, given by (8.20) and (8.21), respectively, it follows from (8.7) and (8.8) that the closed-loop hybrid system (8.1) and (8.2) is given by

$$\dot{x}(t) = f_{\rm c}(x(t)) + B_{\rm c}\Big[K_{\rm c}x(t) - \hat{W}_{\rm c}^{\rm T}(t)[x(t) \otimes \sigma_{\rm c}(x(t))]\Big], \quad x(0) = x_0, \quad x(t) \notin \mathcal{Z}_x, \tag{8.28}$$

$$\Delta x(t) = f_{\rm d}(x(t)) + B_{\rm d}\Big[K_{\rm d}x(t) - \hat{W}_{\rm d}^{\rm T}(t)[x(t) \otimes \sigma_{\rm d}(x(t))]\Big], \quad x(t) \in \mathcal{Z}_x, \tag{8.29}$$

or, equivalently, using (8.11) and (8.12),

$$\dot{x}(t) = A_{\rm cs}x(t) + B_{\rm c}\Big[\varphi_{\rm c}(x(t)) - \tilde{W}_{\rm c}^{\rm T}(t)[x(t) \otimes \sigma_{\rm c}(x(t))]\Big], \quad x(0) = x_0, \quad x(t) \notin \mathcal{Z}_x, \tag{8.30}$$

$$\Delta x(t) = (A_{\rm ds} - I_n)x(t) + B_{\rm d}\Big[\varphi_{\rm d}(x(t)) - \tilde{W}_{\rm d}^{\rm T}(t)[x(t) \otimes \sigma_{\rm d}(x(t))]\Big], \ x(t) \in \mathcal{Z}_x, \tag{8.31}$$

where $\tilde{W}_{\mathrm{c}}^{\mathrm{T}}(t) \triangleq \hat{W}_{\mathrm{c}}^{\mathrm{T}}(t) - W_{\mathrm{c}}^{\mathrm{T}}$ and $\tilde{W}_{\mathrm{d}}^{\mathrm{T}}(t) \triangleq \hat{W}_{\mathrm{d}}^{\mathrm{T}}(t) - W_{\mathrm{d}}^{\mathrm{T}}$. Furthermore, define $\tilde{\sigma}_{\mathrm{d}}(x) \triangleq x \otimes \sigma_{\mathrm{d}}(x)$ and note that adding and subtracting $W_{\mathrm{d}}^{\mathrm{T}}$ to and from (8.25) and using (8.31) it follows that

$$\begin{aligned}\tilde{W}_{\mathrm{d}}^{\mathrm{T}}(t^+) &= \tilde{W}_{\mathrm{d}}^{\mathrm{T}}(t) + \tfrac{1}{c+\tilde{\sigma}_{\mathrm{d}}^{\mathrm{T}}(x(t))\tilde{\sigma}_{\mathrm{d}}(x(t))} B_{\mathrm{d}}^{\dagger}\Big[B_{\mathrm{d}}[\varphi_{\mathrm{d}}(x(t)) - \tilde{W}_{\mathrm{d}}^{\mathrm{T}}(t)\tilde{\sigma}_{\mathrm{d}}(x(t))]\Big] \\ &\quad \cdot [x(t) \otimes \sigma_{\mathrm{d}}(x(t))]^{\mathrm{T}} \\ &= \tilde{W}_{\mathrm{d}}^{\mathrm{T}}(t) + \tfrac{1}{c+\tilde{\sigma}_{\mathrm{d}}^{\mathrm{T}}(x(t))\tilde{\sigma}_{\mathrm{d}}(x(t))}[\varphi_{\mathrm{d}}(x(t)) - \tilde{W}_{\mathrm{d}}^{\mathrm{T}}(t)\tilde{\sigma}_{\mathrm{d}}(x(t))]\tilde{\sigma}_{\mathrm{d}}^{\mathrm{T}}(x(t)), \quad x(t) \in \mathcal{Z}_x. \end{aligned} \tag{8.32}$$

To show Lyapunov stability of the closed-loop hybrid system (8.22)–(8.24) and (8.30)–(8.32), consider the Lyapunov function candidate

$$V(x, \hat{W}_{\mathrm{c}}^{\mathrm{T}}, \hat{W}_{\mathrm{d}}^{\mathrm{T}}) = \ln(1 + x^{\mathrm{T}}Px) + \operatorname{tr} Q_{\mathrm{c}}^{-1}\tilde{W}_{\mathrm{c}}^{\mathrm{T}}Y^{-1}\tilde{W}_{\mathrm{c}} + a\operatorname{tr}\tilde{W}_{\mathrm{d}}\tilde{W}_{\mathrm{d}}^{\mathrm{T}}. \tag{8.33}$$

Note that $V(0, W_{\mathrm{c}}^{\mathrm{T}}, W_{\mathrm{d}}^{\mathrm{T}}) = 0$ and, since P, Q_{c}, and Y are positive definite and $a > 0$, $V(x, \hat{W}_{\mathrm{c}}^{\mathrm{T}}, \hat{W}_{\mathrm{d}}^{\mathrm{T}}) > 0$ for all $(x, \hat{W}_{\mathrm{c}}^{\mathrm{T}}, \hat{W}_{\mathrm{d}}^{\mathrm{T}}) \neq (0, W_{\mathrm{c}}^{\mathrm{T}}, W_{\mathrm{d}}^{\mathrm{T}})$. In addition, $V(x, \hat{W}_{\mathrm{c}}^{\mathrm{T}}, \hat{W}_{\mathrm{d}}^{\mathrm{T}})$ is radially unbounded. Now, letting $x(t)$ denote the solution to (8.30) and using (8.22) and (8.24), it follows that the Lyapunov derivative along the closed-loop system trajectories over the time interval $t \in (t_k, t_{k+1}]$, $k \in \overline{\mathbb{Z}}_+$, is given by

$$\begin{aligned}&\dot{V}(x(t), \hat{W}_{\mathrm{c}}^{\mathrm{T}}(t), \hat{W}_{\mathrm{d}}^{\mathrm{T}}(t)) \\ &\quad = \tfrac{2x^{\mathrm{T}}(t)P}{1+x^{\mathrm{T}}(t)Px(t)}\Big[A_{\mathrm{cs}}x(t) + B_{\mathrm{c}}\Big[\varphi_{\mathrm{c}}(x(t)) - \tilde{W}_{\mathrm{c}}^{\mathrm{T}}(t)[x(t) \otimes \sigma_{\mathrm{c}}(x(t))]\Big]\Big] \\ &\qquad + 2\operatorname{tr} Q_{\mathrm{c}}^{-1}\tilde{W}_{\mathrm{c}}^{\mathrm{T}}(t)Y^{-1}\dot{\hat{W}}_{\mathrm{c}}(t) \\ &\quad \leq -x^{\mathrm{T}}(t)(R_{\mathrm{c}} + \gamma^{-2}PB_{\mathrm{c}}B_{\mathrm{c}}^{\mathrm{T}}P + I_n)x(t) \\ &\qquad + 2x^{\mathrm{T}}(t)PB_{\mathrm{c}}\Big[\varphi_{\mathrm{c}}(x(t)) - \tilde{W}_{\mathrm{c}}^{\mathrm{T}}(t)[x(t) \otimes \sigma_{\mathrm{c}}(x(t))]\Big] \\ &\qquad + 2\operatorname{tr}\tilde{W}^{\mathrm{T}}(t)\left(B_{\mathrm{c}}^{\mathrm{T}}Px(t)[x(t) \otimes \sigma_{\mathrm{c}}(x(t))]^{\mathrm{T}}\right)^{\mathrm{T}} \\ &\quad = -x^{\mathrm{T}}(t)R_{\mathrm{c}}x(t) - x^{\mathrm{T}}(t)(\gamma^{-2}PB_{\mathrm{c}}B_{\mathrm{c}}^{\mathrm{T}}P + I_n)x(t) \\ &\qquad + 2x^{\mathrm{T}}(t)PB_{\mathrm{c}}\varphi_{\mathrm{c}}(x(t))\end{aligned}$$

$$
\begin{aligned}
&\leq -x^{\mathrm{T}}(t)R_{\mathrm{c}}x(t)\\
&\quad -[\gamma^{-1}B_{\mathrm{c}}^{\mathrm{T}}Px(t)-\gamma\varphi_{\mathrm{c}}(x(t))]^{\mathrm{T}}[\gamma^{-1}B_{\mathrm{c}}^{\mathrm{T}}Px(t)-\gamma\varphi_{\mathrm{c}}(x(t))]\\
&\leq -x^{\mathrm{T}}(t)R_{\mathrm{c}}x(t)\\
&\leq 0, \quad t_k < t \leq t_{k+1}. \qquad (8.34)
\end{aligned}
$$

Next, using (8.23), (8.27), and (8.32), the Lyapunov difference along the closed-loop system trajectories at the resetting times t_k, $k \in \overline{\mathbb{Z}}_+$, is given by

$$
\begin{aligned}
&\Delta V(x(t_k),\hat{W}_{\mathrm{c}}^{\mathrm{T}}(t_k),\hat{W}_{\mathrm{d}}^{\mathrm{T}}(t_k))\\
&\triangleq V(x(t_k^+),\hat{W}_{\mathrm{c}}^{\mathrm{T}}(t_k^+),\hat{W}_{\mathrm{d}}^{\mathrm{T}}(t_k^+))-V(x(t_k),\hat{W}_{\mathrm{c}}^{\mathrm{T}}(t_k),\hat{W}_{\mathrm{d}}^{\mathrm{T}}(t_k))\\
&= \ln\Big(1+\Big[A_{\mathrm{ds}}x(t_k)+B_{\mathrm{d}}[\varphi_{\mathrm{d}}(x(t_k))-\tilde{W}_{\mathrm{d}}^{\mathrm{T}}(t_k)[x(t_k)\otimes\sigma_{\mathrm{d}}(x(t_k))]]\Big]\\
&\quad \cdot P\Big[A_{\mathrm{ds}}x(t_k)+B_{\mathrm{d}}[\varphi_{\mathrm{d}}(x(t_k))-\tilde{W}_{\mathrm{d}}^{\mathrm{T}}(t_k)[x(t_k)\otimes\sigma_{\mathrm{d}}(x(t_k))]]\Big]\Big)\\
&\quad +a\mathrm{tr}\Big(\tilde{W}_{\mathrm{d}}^{\mathrm{T}}(t_k)+\tfrac{1}{c+\tilde{\sigma}_{\mathrm{d}}^{\mathrm{T}}(x(t_k))\tilde{\sigma}_{\mathrm{d}}(x(t_k))}\Big[\varphi_{\mathrm{d}}(x(t_k))-\tilde{W}_{\mathrm{d}}^{\mathrm{T}}(t_k)\tilde{\sigma}_{\mathrm{d}}(x(t_k))\Big]\tilde{\sigma}_{\mathrm{d}}^{\mathrm{T}}(x(t_k))\Big)^{\mathrm{T}}\\
&\quad \cdot\Big(\tilde{W}_{\mathrm{d}}^{\mathrm{T}}(t_k)+\tfrac{1}{c+\tilde{\sigma}_{\mathrm{d}}^{\mathrm{T}}(x(t_k))\tilde{\sigma}_{\mathrm{d}}(x(t_k))}\Big[\varphi_{\mathrm{d}}(x(t_k))-\tilde{W}_{\mathrm{d}}^{\mathrm{T}}(t_k)\tilde{\sigma}_{\mathrm{d}}(x(t_k))\Big]\tilde{\sigma}_{\mathrm{d}}^{\mathrm{T}}(x(t_k))\Big)\\
&\quad -\ln(1+x^{\mathrm{T}}(t_k)Px(t_k))-a\mathrm{tr}\tilde{W}_{\mathrm{d}}(t_k)\tilde{W}_{\mathrm{d}}^{\mathrm{T}}(t_k)\\
&= \ln\Big(1+\Big[x^{\mathrm{T}}(t_k)A_{\mathrm{ds}}^{\mathrm{T}}PA_{\mathrm{ds}}x(t_k)+2x^{\mathrm{T}}(t_k)A_{\mathrm{ds}}^{\mathrm{T}}PB_{\mathrm{d}}\varphi_{\mathrm{d}}(x(t_k))\\
&\quad -2x^{\mathrm{T}}(t_k)A_{\mathrm{ds}}^{\mathrm{T}}PB_{\mathrm{d}}\tilde{W}_{\mathrm{d}}^{\mathrm{T}}(t_k)\tilde{\sigma}_{\mathrm{d}}(x(t_k))+\varphi_{\mathrm{d}}^{\mathrm{T}}(x(t_k))B_{\mathrm{d}}PB_{\mathrm{d}}\varphi_{\mathrm{d}}(x(t_k))\\
&\quad -2\varphi_{\mathrm{d}}^{\mathrm{T}}(x(t_k))B_{\mathrm{d}}PB_{\mathrm{d}}\tilde{W}_{\mathrm{d}}^{\mathrm{T}}(t_k)\tilde{\sigma}_{\mathrm{d}}(x(t_k))+\tilde{\sigma}_{\mathrm{d}}^{\mathrm{T}}(x(t_k))\tilde{W}_{\mathrm{d}}(t_k)B_{\mathrm{d}}PB_{\mathrm{d}}\tilde{W}_{\mathrm{d}}^{\mathrm{T}}(t_k)\tilde{\sigma}_{\mathrm{d}}(x(t_k))\\
&\quad -x^{\mathrm{T}}(t_k)Px(t_k)\Big]\left[1+x^{\mathrm{T}}(t_k)Px(t_k)\right]^{-1}\Big)+a\mathrm{tr}\tilde{W}_{\mathrm{d}}(t_k)\tilde{W}_{\mathrm{d}}^{\mathrm{T}}(t_k)\\
&\quad +\tfrac{2a}{c+\tilde{\sigma}_{\mathrm{d}}^{\mathrm{T}}(x(t_k))\tilde{\sigma}_{\mathrm{d}}(x(t_k))}\mathrm{tr}\,W_{\mathrm{d}}(t_k)\Big[\varphi_{\mathrm{d}}(x(t_k))-\tilde{W}_{\mathrm{d}}^{\mathrm{T}}(t_k)\tilde{\sigma}_{\mathrm{d}}(x(t_k))\Big]\tilde{\sigma}_{\mathrm{d}}^{\mathrm{T}}(x(t_k))\\
&\quad +\tfrac{a}{(c+\tilde{\sigma}_{\mathrm{d}}^{\mathrm{T}}(x(t_k))\tilde{\sigma}_{\mathrm{d}}(x(t_k)))^2}\mathrm{tr}\,\tilde{\sigma}_{\mathrm{d}}(x(t_k))\Big[\varphi_{\mathrm{d}}^{\mathrm{T}}(x(t_k))-\tilde{\sigma}_{\mathrm{d}}^{\mathrm{T}}(x(t_k))\tilde{W}_{\mathrm{d}}(t_k)\Big]\Big[\varphi_{\mathrm{d}}(x(t_k))\\
&\quad -\tilde{W}_{\mathrm{d}}^{\mathrm{T}}(t_k)\tilde{\sigma}_{\mathrm{d}}(x(t_k))\Big]\tilde{\sigma}_{\mathrm{d}}^{\mathrm{T}}(x(t_k))-a\mathrm{tr}\,\tilde{W}_{\mathrm{d}}(t_k)\tilde{W}_{\mathrm{d}}^{\mathrm{T}}(t_k)\\
&\leq \Big[-x^{\mathrm{T}}(t_k)((\alpha+\beta)I_n+R_{\mathrm{d}})x(t_k)+\varphi_{\mathrm{d}}^{\mathrm{T}}(x(t_k))B_{\mathrm{d}}^{\mathrm{T}}PB_{\mathrm{d}}\varphi_{\mathrm{d}}(x(t_k))\\
&\quad -2\varphi_{\mathrm{d}}^{\mathrm{T}}(x(t_k))B_{\mathrm{d}}^{\mathrm{T}}PB_{\mathrm{d}}\tilde{W}_{\mathrm{d}}^{\mathrm{T}}(t_k)\tilde{\sigma}_{\mathrm{d}}(x(t_k))\\
&\quad +\tilde{\sigma}_{\mathrm{d}}^{\mathrm{T}}(x(t_k))\tilde{W}_{\mathrm{d}}(t_k)B_{\mathrm{d}}^{\mathrm{T}}PB_{\mathrm{d}}\tilde{W}_{\mathrm{d}}^{\mathrm{T}}(t_k)\tilde{\sigma}_{\mathrm{d}}(x(t_k))\Big]\left[1+x^{\mathrm{T}}(t_k)Px(t_k)\right]^{-1}
\end{aligned}
$$

$$
\begin{aligned}
&+\tfrac{2a}{c+\tilde{\sigma}_{\mathrm{d}}^{\mathrm{T}}(x(t_k))\tilde{\sigma}_{\mathrm{d}}(x(t_k))}\mathrm{tr}\,\tilde{W}_{\mathrm{d}}(t_k)\Big[\varphi_{\mathrm{d}}(x(t_k))-\tilde{W}_{\mathrm{d}}^{\mathrm{T}}(t_k)\tilde{\sigma}_{\mathrm{d}}(x(t_k))\Big]\tilde{\sigma}_{\mathrm{d}}^{\mathrm{T}}(x(t_k))\\
&+\tfrac{a}{c+\tilde{\sigma}_{\mathrm{d}}^{\mathrm{T}}(x(t_k))\tilde{\sigma}_{\mathrm{d}}(x(t_k))}\mathrm{tr}\,\Big[\varphi_{\mathrm{d}}^{\mathrm{T}}(x(t_k))-\tilde{\sigma}_{\mathrm{d}}^{\mathrm{T}}(x(t_k))\tilde{W}_{\mathrm{d}}(t_k)\Big]\Big[\varphi_{\mathrm{d}}(x(t_k))\\
&-\tilde{W}_{\mathrm{d}}^{\mathrm{T}}(t_k)\tilde{\sigma}_{\mathrm{d}}(x(t_k))\Big]\\
\leq\ &\Big[-x^{\mathrm{T}}(t_k)((\alpha+\beta)I_n+R_{\mathrm{d}})x(t_k)+\varphi_{\mathrm{d}}^{\mathrm{T}}(x(t_k))B_{\mathrm{d}}^{\mathrm{T}}PB_{\mathrm{d}}\varphi_{\mathrm{d}}(x(t_k))\\
&-2\varphi_{\mathrm{d}}^{\mathrm{T}}(x(t_k))B_{\mathrm{d}}^{\mathrm{T}}PB_{\mathrm{d}}\tilde{W}_{\mathrm{d}}^{\mathrm{T}}(t_k)\tilde{\sigma}_{\mathrm{d}}(x(t_k))\\
&+\tilde{\sigma}_{\mathrm{d}}^{\mathrm{T}}(x(t_k))\tilde{W}_{\mathrm{d}}(t_k)B_{\mathrm{d}}^{\mathrm{T}}PB_{\mathrm{d}}\tilde{W}_{\mathrm{d}}^{\mathrm{T}}(t_k)\tilde{\sigma}_{\mathrm{d}}(x(t_k))\Big]\left[1+x^{\mathrm{T}}(t_k)Px(t_k)\right]^{-1}\\
&+\tfrac{2a}{c+\tilde{\sigma}_{\mathrm{d}}^{\mathrm{T}}(x(t_k))\tilde{\sigma}_{\mathrm{d}}(x(t_k))}\mathrm{tr}\,\tilde{W}_{\mathrm{d}}(t_k)\Big[\varphi_{\mathrm{d}}(x(t_k))-\tilde{W}_{\mathrm{d}}^{\mathrm{T}}(t_k)\tilde{\sigma}_{\mathrm{d}}(x(t_k))\Big]\tilde{\sigma}_{\mathrm{d}}^{\mathrm{T}}(x(t_k))\\
&+\tfrac{a}{c+\tilde{\sigma}_{\mathrm{d}}^{\mathrm{T}}(x(t_k))\tilde{\sigma}_{\mathrm{d}}(x(t_k))}\mathrm{tr}\Big[\varphi_{\mathrm{d}}^{\mathrm{T}}(x(t_k))-\tilde{\sigma}_{\mathrm{d}}^{\mathrm{T}}(x(t_k))\tilde{W}_{\mathrm{d}}(t_k)\Big]\\
&\cdot\Big[\varphi_{\mathrm{d}}(x(t_k))-\tilde{W}_{\mathrm{d}}^{\mathrm{T}}(t_k)\tilde{\sigma}_{\mathrm{d}}(x(t_k))\Big],
\end{aligned}
\tag{8.35}
$$

where in (8.35) we used $\ln a-\ln b=\ln\frac{a}{b}$ and $\ln(1+d)\leq d$ for $a,b>0$, and $d>-1$, respectively, and $\frac{\tilde{\sigma}_{\mathrm{d}}^{\mathrm{T}}\tilde{\sigma}_{\mathrm{d}}}{c+\tilde{\sigma}_{\mathrm{d}}^{\mathrm{T}}\tilde{\sigma}_{\mathrm{d}}}<1$. Furthermore, note that $\tilde{\sigma}_{\mathrm{d}}^{\mathrm{T}}(x)\tilde{\sigma}_{\mathrm{d}}(x)\leq nx^{\mathrm{T}}x$.

Now, defining $\Theta\triangleq\frac{1}{\alpha\gamma_{\mathrm{d}}^2}(B_{\mathrm{d}}^{\mathrm{T}}PB_{\mathrm{d}})^2$, it follows from (8.35) that

$$
\begin{aligned}
&\Delta V(x(t_k),\hat{W}_{\mathrm{c}}^{\mathrm{T}}(t_k),\hat{W}_{\mathrm{d}}^{\mathrm{T}}(t_k))\\
&\leq\Big[-x^{\mathrm{T}}(t_k)R_{\mathrm{d}}x(t_k)-\beta x^{\mathrm{T}}(t_k)x(t_k)-\alpha[x^{\mathrm{T}}(t_k)x(t_k)-\gamma_{\mathrm{d}}^2\varphi_{\mathrm{d}}^{\mathrm{T}}(x(t_k))\varphi_{\mathrm{d}}(x(t_k))]\\
&\quad-\Big[\varphi_{\mathrm{d}}^{\mathrm{T}}(x(t_k)),\tilde{\sigma}_{\mathrm{d}}^{\mathrm{T}}(x(t_k))\tilde{W}_{\mathrm{d}}(t_k)\Big]\begin{bmatrix}\alpha\gamma_{\mathrm{d}}^2I_n & B_{\mathrm{d}}^{\mathrm{T}}PB_{\mathrm{d}}\\ B_{\mathrm{d}}^{\mathrm{T}}PB_{\mathrm{d}} & \Theta\end{bmatrix}\begin{bmatrix}\varphi_{\mathrm{d}}(x(t_k))\\ \tilde{W}_{\mathrm{d}}^{\mathrm{T}}(t_k)\tilde{\sigma}_{\mathrm{d}}(x(t_k))\end{bmatrix}\\
&\quad+\tilde{\sigma}_{\mathrm{d}}^{\mathrm{T}}(x(t_k))\tilde{W}_{\mathrm{d}}(t_k)\Theta\tilde{W}_{\mathrm{d}}^{\mathrm{T}}(t_k)\tilde{\sigma}_{\mathrm{d}}(x(t_k))\\
&\quad+\tilde{\sigma}_{\mathrm{d}}^{\mathrm{T}}(x(t_k))\tilde{W}_{\mathrm{d}}(t_k)B_{\mathrm{d}}^{\mathrm{T}}PB_{\mathrm{d}}\tilde{W}_{\mathrm{d}}^{\mathrm{T}}(t_k)\tilde{\sigma}_{\mathrm{d}}(x(t_k))\Big]\left[1+x^{\mathrm{T}}(t_k)Px(t_k)\right]^{-1}\\
&\quad-\tfrac{a}{c+\tilde{\sigma}_{\mathrm{d}}^{\mathrm{T}}(x(t_k))\tilde{\sigma}_{\mathrm{d}}(x(t_k))}\tilde{\sigma}_{\mathrm{d}}^{\mathrm{T}}(x(t_k))\tilde{W}_{\mathrm{d}}(t_k)\tilde{W}_{\mathrm{d}}^{\mathrm{T}}(t_k)\tilde{\sigma}_{\mathrm{d}}(x(t_k))\\
&\quad+\tfrac{a}{c+\tilde{\sigma}_{\mathrm{d}}^{\mathrm{T}}(x(t_k))\tilde{\sigma}_{\mathrm{d}}(x(t_k))}\varphi_{\mathrm{d}}^{\mathrm{T}}(x(t_k))\varphi_{\mathrm{d}}(x(t_k))\\
&\leq-\frac{x^{\mathrm{T}}(t_k)R_{\mathrm{d}}x(t_k)}{1+x^{\mathrm{T}}(t_k)Px(t_k)}\\
&\quad-\frac{\tilde{\sigma}_{\mathrm{d}}^{\mathrm{T}}(x(t_k))\tilde{W}_{\mathrm{d}}(t_k)\tilde{R}_{\mathrm{d}1}(x(t_k))\tilde{W}_{\mathrm{d}}^{\mathrm{T}}\tilde{\sigma}_{\mathrm{d}}(x(t_k))}{(c+\tilde{\sigma}_{\mathrm{d}}^{\mathrm{T}}(x(t_k))\tilde{\sigma}_{\mathrm{d}}(x(t_k)))(1+x^{\mathrm{T}}(t_k)Px(t_k))}\\
&\quad-\frac{\varphi_{\mathrm{d}}^{\mathrm{T}}(x(t_k))\tilde{R}_{\mathrm{d}2}(x(t_k))\varphi_{\mathrm{d}}(x(t_k))}{(c+\tilde{\sigma}_{\mathrm{d}}^{\mathrm{T}}(x(t_k))\tilde{\sigma}_{\mathrm{d}}(x(t_k)))(1+x^{\mathrm{T}}(t_k)Px(t_k))},
\end{aligned}
\tag{8.36}
$$

where

$$\begin{aligned}\tilde{R}_{\mathrm{d}1}(x) &\triangleq a(1+x^{\mathrm{T}}Px)I_m-(B_{\mathrm{d}}^{\mathrm{T}}PB_{\mathrm{d}}+\Theta)(c+\tilde{\sigma}_{\mathrm{d}}^{\mathrm{T}}(x)\tilde{\sigma}_{\mathrm{d}}(x))\\ &\geq a(1+x^{\mathrm{T}}Px)I_m-B_{\mathrm{d}}^{\mathrm{T}}PB_{\mathrm{d}}\Big(I_m+\tfrac{1}{\alpha\gamma_{\mathrm{d}}^2}B_{\mathrm{d}}^{\mathrm{T}}PB_{\mathrm{d}}\Big)(c+nx^{\mathrm{T}}x)\\ &\geq 0,\quad x\in\mathcal{D}_{\mathrm{c}},\end{aligned}\tag{8.37}$$

and

$$\begin{aligned}\tilde{R}_{\mathrm{d}2}(x) &\triangleq \beta\gamma_{\mathrm{d}}^2(c+\tilde{\sigma}_{\mathrm{d}}^{\mathrm{T}}(x)\tilde{\sigma}_{\mathrm{d}}(x))I_m-B_{\mathrm{d}}^{\mathrm{T}}PB_{\mathrm{d}}(c+\tilde{\sigma}_{\mathrm{d}}^{\mathrm{T}}(x)\tilde{\sigma}_{\mathrm{d}}(x))-a(1+x^{\mathrm{T}}Px)I_m\\ &\geq (c+\tilde{\sigma}_{\mathrm{d}}^{\mathrm{T}}(x)\tilde{\sigma}_{\mathrm{d}}(x))\Big(\beta\gamma_{\mathrm{d}}^2-\lambda_{\max}(B_{\mathrm{d}}^{\mathrm{T}}PB_{\mathrm{d}})-a\frac{1+x^{\mathrm{T}}Px}{c+\tilde{\sigma}_{\mathrm{d}}^{\mathrm{T}}(x)\tilde{\sigma}_{\mathrm{d}}(x)}\Big)I_m\\ &\geq 0,\quad x\in\mathcal{D}_{\mathrm{c}}.\end{aligned}\tag{8.38}$$

Hence, the Lyapunov difference given by (8.36) yields

$$\begin{aligned}\Delta V(x(t_k),\hat{W}_{\mathrm{c}}^{\mathrm{T}}(t_k),\hat{W}_{\mathrm{d}}^{\mathrm{T}}(t_k)) &\leq -\frac{x^{\mathrm{T}}(t_k)R_{\mathrm{d}}x(t_k)}{1+x^{\mathrm{T}}(t_k)Px(t_k)}\\ &\quad-\frac{\tilde{\sigma}_{\mathrm{d}}^{\mathrm{T}}(x(t_k))\tilde{W}_{\mathrm{d}}(t_k)\tilde{R}_{\mathrm{d}}(x(t_k))\tilde{W}_{\mathrm{d}}^{\mathrm{T}}\tilde{\sigma}_{\mathrm{d}}(x(t_k))}{(c+\tilde{\sigma}_{\mathrm{d}}^{\mathrm{T}}(x(t_k))\tilde{\sigma}_{\mathrm{d}}(x(t_k)))(1+x^{\mathrm{T}}(t_k)Px(t_k))}\\ &\leq -\frac{x^{\mathrm{T}}(t_k)R_{\mathrm{d}}x(t_k)}{1+x^{\mathrm{T}}(t_k)Px(t_k)}\\ &\leq 0,\quad k\in\overline{\mathbb{Z}}_+.\end{aligned}\tag{8.39}$$

Next, let

$$\tilde{\mathcal{D}}_\alpha\triangleq\Big\{(x,\tilde{W}_{\mathrm{c}}^{\mathrm{T}},\tilde{W}_{\mathrm{d}}^{\mathrm{T}})\in\mathbb{R}^n\times\mathbb{R}^{m_{\mathrm{c}}\times ns_{\mathrm{c}}}\times\mathbb{R}^{m_{\mathrm{d}}\times ns_{\mathrm{d}}}:V(x,\tilde{W}_{\mathrm{c}}^{\mathrm{T}},\tilde{W}_{\mathrm{d}}^{\mathrm{T}})\leq\alpha\Big\},\tag{8.40}$$

where α is the maximum value such that $\tilde{\mathcal{D}}_\alpha\subseteq\mathcal{D}_{\mathrm{c}}\times\mathbb{R}^{m_{\mathrm{c}}\times ns_{\mathrm{c}}}\times\mathbb{R}^{m_{\mathrm{d}}\times ns_{\mathrm{d}}}$. Since $\Delta V(x(t_k),\,\hat{W}_{\mathrm{c}}^{\mathrm{T}}(t_k),\hat{W}_{\mathrm{d}}^{\mathrm{T}}(t_k))\leq 0$ for all $(x(t_k),\hat{W}_{\mathrm{c}}^{\mathrm{T}}(t_k),\hat{W}_{\mathrm{d}}^{\mathrm{T}}(t_k))\in\tilde{\mathcal{D}}_\alpha$ and $k\in\overline{\mathbb{Z}}_+$, it follows that $\tilde{\mathcal{D}}_\alpha$ is positively invariant. Next, since $\tilde{\mathcal{D}}_\alpha$ is positively invariant, it follows that

$$\mathcal{D}_\alpha\triangleq\Big\{(x,\hat{W}_{\mathrm{c}}^{\mathrm{T}},\hat{W}_{\mathrm{d}}^{\mathrm{T}})\in\mathbb{R}^n\times\mathbb{R}^{m_{\mathrm{c}}\times ns_{\mathrm{c}}}\times\mathbb{R}^{m_{\mathrm{d}}\times ns_{\mathrm{d}}}:(x,\hat{W}_{\mathrm{c}}^{\mathrm{T}}-W_{\mathrm{c}}^{\mathrm{T}},\hat{W}_{\mathrm{d}}^{\mathrm{T}}-W_{\mathrm{d}}^{\mathrm{T}})\in\tilde{\mathcal{D}}_\alpha\Big\}\tag{8.41}$$

is also positively invariant. Now, it follows from Theorem 2.1 of [51] that (8.34) and (8.39) imply that the solution $(x(t), \hat{W}_{\mathrm{c}}^{\mathrm{T}}(t), \hat{W}_{\mathrm{d}}^{\mathrm{T}}(t)) \equiv (0, W_{\mathrm{c}}^{\mathrm{T}}, W_{\mathrm{d}}^{\mathrm{T}})$ to (8.22)–(8.24) and (8.30)–(8.32) is Lyapunov stable. Furthermore, since $R_{\mathrm{c}} > 0$ and $\mathcal{W} = \emptyset$, it follows from Theorem 8.1, with $\mathcal{R} = \mathcal{M} = \{(x, \hat{W}_{\mathrm{c}}^{\mathrm{T}}, \hat{W}_{\mathrm{d}}^{\mathrm{T}}) \in \mathbb{R}^n \times \mathbb{R}^{m_{\mathrm{c}} \times s_{\mathrm{c}}} \times \mathbb{R}^{m_{\mathrm{d}} \times s_{\mathrm{d}}} : x = 0\}$, that $x(t) \to 0$ as $t \to \infty$ for all $x_0 \in \mathbb{R}^n$. □

Remark 8.1. Note that the conditions in Theorem 8.2 imply partial asymptotic stability, that is, the solution $(x(t), \hat{W}_{\mathrm{c}}^{\mathrm{T}}(t), \hat{W}_{\mathrm{d}}^{\mathrm{T}}(t)) \equiv (0, W_{\mathrm{c}}^{\mathrm{T}}, W_{\mathrm{d}}^{\mathrm{T}})$ of the overall closed-loop system is Lyapunov stable and $x(t) \to 0$ as $t \to \infty$. Hence, it follows from (8.22) and (8.23) that $\dot{\hat{W}}_{\mathrm{c}}^{\mathrm{T}}(t) \to 0$ as $t \to \infty$. Furthermore, if $x(t)$, $t \geq 0$, intersects $\mathcal{Z}_x$ infinitely many times, then it follows from (8.24) and (8.25) that $\hat{W}_{\mathrm{d}}(t_k^+) - \hat{W}_{\mathrm{d}}(t_k) \to 0$ as $k \to \infty$.

Remark 8.2. Since the Lyapunov function used in the proof of Theorem 8.2 is a class $\mathcal{K}_\infty$ function, in the case where the neural network approximation holds in $\mathbb{R}^n$, the control law (8.20) and (8.21) ensures global asymptotic stability with respect to x. However, the existence of a global neural network approximator for an uncertain nonlinear map cannot in general be established. Hence, as is common in the neural network literature, for a given arbitrarily large compact set $\mathcal{D}_{\mathrm{c}} \subset \mathbb{R}^n$, we assume that there exists an approximator for the unknown nonlinear map up to a desired accuracy (in the sense of (8.11) and (8.12)). In the case where $\Delta_{\mathrm{c}}(\cdot)$ and $\Delta_{\mathrm{d}}(\cdot)$ are continuous on $\mathbb{R}^n$, it follows from the Stone-Weierstrass theorem that $\Delta_{\mathrm{c}}(\cdot)$ and $\Delta_{\mathrm{d}}(\cdot)$ can be approximated over an arbitrarily large compact set $\mathcal{D}_{\mathrm{c}}$. In this case, our neuroadaptive hybrid controller guarantees semiglobal partial asymptotic stability.

Remark 8.3. Note that the neuroadaptive hybrid controller (8.20) and (8.21) can be constructed to guarantee partial asymptotic stability using standard *linear* H_∞

theory. Specifically, it follows from standard continuous-time H_∞ theory [143] that $\|G_{\mathrm{c}}(s)\|_\infty < \gamma_{\mathrm{c}}$, where $G(s) = E_{\mathrm{c}}(sI_n - A_{\mathrm{cs}})^{-1}B_{\mathrm{c}}$ and E_{c} is such that $E_{\mathrm{c}}^{\mathrm{T}}E_{\mathrm{c}} = I_n + R_{\mathrm{c}}$, if and only if there exists a positive-definite matrix P satisfying the bounded real Riccati equation (8.16). It is important to note that $\gamma_{\mathrm{c}} > 0$ and $\gamma_{\mathrm{d}} > 0$, which characterize the approximation error (8.13) and (8.14), respectively, over $\mathcal{D}_{\mathrm{c}}$, can be made arbitrarily large provided that we take a large number of basis functions in the parameterization of the uncertainty $\Delta_{\mathrm{c}}(\cdot)$ and $\Delta_{\mathrm{d}}(\cdot)$. In this case, noting that $\frac{1+x^{\mathrm{T}}Px}{c+[x\otimes\sigma_{\mathrm{d}}(x)]^{\mathrm{T}}[x\otimes\sigma_{\mathrm{d}}(x)]}$ in (8.18) is a bounded positive function, it can be shown that there always exist α and β such that the conditions (8.16)–(8.19) are satisfied.

It is important to note that the hybrid adaptive control law (8.20)–(8.25) does *not* require explicit knowledge of the optimal weighting matrices W_{c}, W_{d}, and the positive constants α and β. Theorem 8.2 simply requires the existence of W_{c}, W_{d}, α, and β such that (8.16) and (8.17) hold. Furthermore, no specific structure on the nonlinear dynamics $f_{\mathrm{c}}(x)$ and $f_{\mathrm{d}}(x)$ is required to apply Theorem 8.2 other than the assumption that $f_{\mathrm{c}}(x)$ and $f_{\mathrm{d}}(x)$ are continuously differentiable and that the approximation error of the uncertain system nonlinearities lie in a small gain-type norm bounded conic sector. Finally, in the case where the pair $(A_{\mathrm{d}}, B_{\mathrm{d}})$ is in controllable canonical form and R_{d} in (8.17) is diagonal, it follows that

$$A_{\mathrm{ds}} = \left[\begin{array}{c} A_0 \\ 0_{m_{\mathrm{d}}\times n} \end{array} \right],$$

where $A_0 \in \mathbb{R}^{(n-m_{\mathrm{d}})\times n}$ is a known matrix of zeros and ones capturing the multivariable controllable canonical form representation [24], and hence, the update law (8.25) is simplified as

$$\Delta\hat{W}_{\mathrm{d}}^{\mathrm{T}}(t) = \tfrac{1}{c+[x(t)\otimes\sigma_{\mathrm{d}}(x(t))]^{\mathrm{T}}[x(t)\otimes\sigma_{\mathrm{d}}(x(t))]}B_{\mathrm{d}}^{\dagger}\Delta x(t)[x(t)\otimes\sigma_{\mathrm{d}}(x(t))]^{\mathrm{T}}, \quad x(t)\in\mathcal{Z}_x, \tag{8.42}$$

since $B_{\mathrm{d}}^{\dagger}A_{\mathrm{ds}} = 0$.

8.4. Illustrative Numerical Example

In this section, we present a numerical example to demonstrate the utility of the proposed neural hybrid adaptive control framework for hybrid adaptive stabilization. Specifically, consider the nonlinear uncertain controlled hybrid system given by (8.1) and (8.2) with $n = 2$, $x = [x_1, x_2]^{\mathrm{T}}$,

$$f_{\mathrm{c}}(x) = \begin{bmatrix} x_2 \\ \hat{f}_{\mathrm{c}}(x) \end{bmatrix}, \quad G_{\mathrm{c}}(x) = \begin{bmatrix} 0 \\ b_{\mathrm{c}} \end{bmatrix}, f_{\mathrm{d}}(x) = \begin{bmatrix} -x_1 + x_2 \\ \hat{f}_{\mathrm{d}}(x) \end{bmatrix}, \quad G_{\mathrm{d}}(x) = \begin{bmatrix} 0 \\ b_{\mathrm{d}} \end{bmatrix}, \tag{8.43}$$

where $\hat{f}_{\mathrm{c}} : \mathbb{R}^2 \to \mathbb{R}$ and $\hat{f}_{\mathrm{d}} : \mathbb{R}^2 \to \mathbb{R}$ are unknown, continuously differentiable functions. Furthermore, assume that the resetting set $\mathcal{Z}_x$ is given by

$$\mathcal{Z}_x = \{x \in \mathbb{R}^2 : \mathcal{X}(x) = 0,\, x_2 > 0\}. \tag{8.44}$$

Here, we assume that $f_{\mathrm{c}}(x)$ and $f_{\mathrm{d}}(x)$ are unknown and can be written in the form of (8.7) and (8.8) with

$$A_{\mathrm{c}} = A_{\mathrm{d}} = \begin{bmatrix} 0 & 1 \\ 0 & 0 \end{bmatrix},$$

$\Delta f_{\mathrm{c}}(x) = [0, \hat{f}_{\mathrm{c}}(x)]^{\mathrm{T}}$, $\Delta f_{\mathrm{d}}(x) = [0, \hat{f}_{\mathrm{d}}(x)]^{\mathrm{T}}$, $B_{\mathrm{c}} = [0, b_{\mathrm{c}}]^{\mathrm{T}}$, $B_{\mathrm{d}} = [0, b_{\mathrm{d}}]^{\mathrm{T}}$, $G_{\mathrm{cn}}(x) = G_{\mathrm{dn}}(x) = 1$. We assume that $\Delta f_{\mathrm{c}}(x)$ and $\Delta f_{\mathrm{d}}(x)$ are unknown and can be written as $\Delta f_{\mathrm{c}}(x) = B_{\mathrm{c}}\delta_{\mathrm{c}}(x)$ and $\Delta f_{\mathrm{d}}(x) = B_{\mathrm{d}}\delta_{\mathrm{d}}(x)$, where $\delta_{\mathrm{c}}(x) = \frac{1}{b_{\mathrm{c}}}\hat{f}_{\mathrm{c}}(x)$ and $\delta_{\mathrm{d}}(x) = \frac{1}{b_{\mathrm{d}}}\hat{f}_{\mathrm{d}}(x)$.

Next, let $K_{\mathrm{c}} = \frac{1}{b_{\mathrm{c}}}[k_{\mathrm{c}1}, k_{\mathrm{c}2}]$ and $K_{\mathrm{d}} = \frac{1}{b_{\mathrm{d}}}[k_{\mathrm{d}1}, k_{\mathrm{d}2}]$, where $k_{\mathrm{c}1}$, $k_{\mathrm{c}2}$, $k_{\mathrm{d}1}$, and $k_{\mathrm{d}2}$ are arbitrary scalars, such that

$$A_{\mathrm{cs}} = A_{\mathrm{c}} + B_{\mathrm{c}}K_{\mathrm{c}} = \begin{bmatrix} 0 & 1 \\ k_{\mathrm{c}1} & k_{\mathrm{c}2} \end{bmatrix},$$

$$A_{\mathrm{ds}} = A_{\mathrm{d}} + B_{\mathrm{d}}K_{\mathrm{d}} = \begin{bmatrix} 0 & 1 \\ k_{\mathrm{d}1} & k_{\mathrm{d}2} \end{bmatrix}.$$

Now, with the proper choice of $k_{\mathrm{c}1}$, $k_{\mathrm{c}2}$, $k_{\mathrm{d}1}$, and $k_{\mathrm{d}2}$, it follows from Theorem 8.2 that if there exists $P > 0$ satisfying (8.16) and (8.17), then the neural hybrid adaptive feedback controller (8.20) and (8.21) guarantees $x(t) \to 0$ as $t \to \infty$. Specifically, here

we choose $k_{c1} = -1$, $k_{c2} = -1$, $k_{d1} = -0.2$, $k_{d2} = -0.5$, $\gamma_c = 10$, $\gamma_d = 20$, $b_c = 3$, $b_d = 1.4$, $c = 1$, $\alpha = 1$, $\sigma_d(x) = [\tanh(0.1x_2), \ldots, \tanh(0.6x_2)]^T$, and

$$R_c = \begin{bmatrix} 2.6947 & 2.4323 \\ 2.4323 & 5.8019 \end{bmatrix}, \quad R_d = \begin{bmatrix} 8.0196 & 2.0334 \\ 2.0334 & 1.0569 \end{bmatrix}, \tag{8.45}$$

so that P satisfying (8.16) and (8.17) is given by

$$P = \begin{bmatrix} 10.0196 & 2.0334 \\ 2.0334 & 12.7523 \end{bmatrix}.$$

With $\hat{f}_c(x) = -a_1x_1 - a_2(x_1^2 - a_3)x_2$, $\hat{f}_d(x) = -x_2 - a_4x_1^2 - a_5\frac{x_2^3}{1+x_2^2} - a_6x_2^3$, $a_1 = 1$, $a_2 = 2$, $a_3 = 1$, $a_4 = -5$, $a_5 = -2$, $a_6 = 8$, $Y = 0.02I_3$, $\sigma_c(x) = \left[\frac{1}{1+e^{-\lambda_1 x_1}}, \ldots, \frac{1}{1+e^{-3\lambda_1 x_1}}, \frac{1}{1+e^{-\lambda_2 x_2}}, \ldots, \frac{1}{1+e^{-3\lambda_2 x_2}}\right]$, and initial conditions $x(0) = [1, 1]^T$, $\hat{W}_c^T(0) = 0_{1\times 6}$, and $\hat{W}_d^T(0) = 0_{1\times 6}$, Figure 8.2 shows the phase portraits of the uncontrolled and controlled hybrid system. Figure 8.3 shows the state trajectories and the control signals versus time. Finally, Figure 8.4 shows the adaptive gain history versus time.

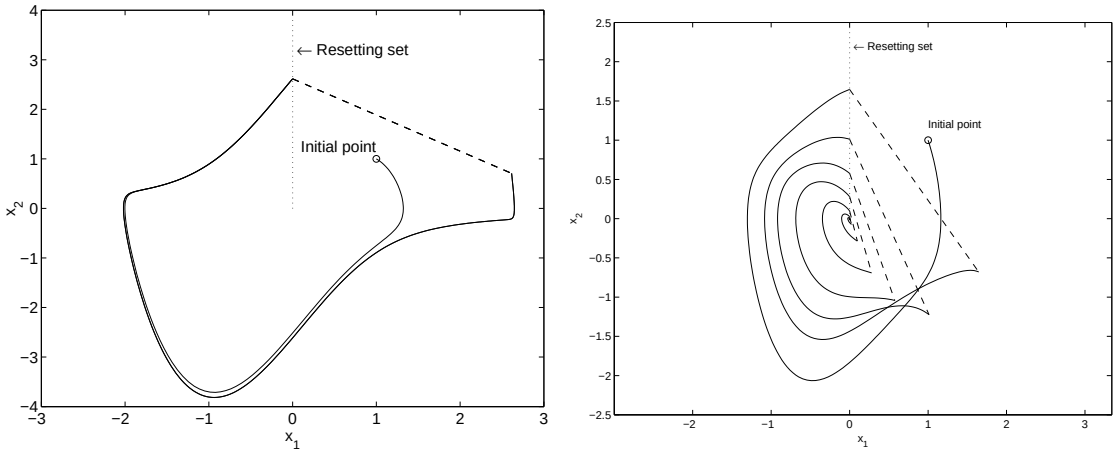

Figure 8.2: Phase portraits of uncontrolled and controlled hybrid system

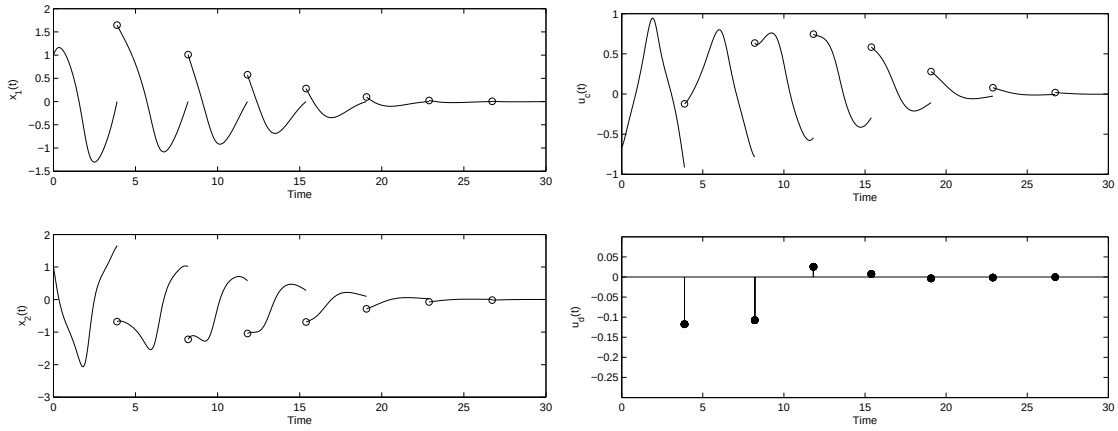

Figure 8.3: State trajectories and control signals versus time

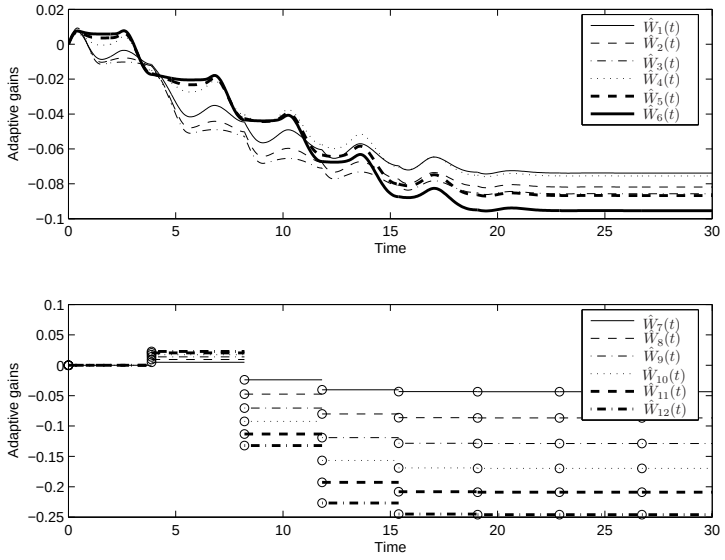

Figure 8.4: Adaptive gain history versus time

Chapter 9

Concluding Remarks and Recommendations for Future Research

9.1. Conclusion

In this dissertation, we have developed a novel adaptive and neuroadaptive architecture for nonlinear uncertain dynamical systems. We primarily focused on modification of neural network based adaptive control methods since neural networks have been extensively used for adaptive system identification as well as adaptive and neuroadaptive control of highly uncertain systems. The goal of adaptive and neuroadaptive control is to achieve system performance without excessive reliance on system models. To improve robustness and the speed of adaptation of adaptive and neuroadaptive controllers several controller architectures have been proposed in the literature. The proposed framework involves a novel controller architecture with additional terms in the update laws that are constructed using a moving window of the integrated system uncertainty. These terms can be used to identify the ideal system weights of the neural network as well as effectively suppress system uncertainty. Linear and nonlinear parameterizations of the system uncertainty are considered and state and output feedback neuroadaptive controllers are developed. Furthermore, we extend the developed framework to discrete-time dynamical systems. To illustrate the efficacy of the proposed approach we applied our results to an aircraft model

with wing rock dynamics, a spacecraft model with unknown moment of inertia, and an unmanned combat aerial vehicle undergoing actuator failures, and compared our results with standard neuroadaptive control methods.

Next, we addressed a neuroadaptive control problem for a specific class of nonlinear uncertain systems of a specific structure and properties; namely, nonnegative and compartmental dynamical systems. As discussed in the Introduction, nonnegative and compartmental dynamical systems play a key role in understanding numerous processes in biological and physiological sciences. These systems are derived from mass and energy balance considerations and are comprised of homogeneous interconnected microscopic subsystems or compartments which exchange variable quantities of material via intercompartmental flow laws. Since biological and physiological systems have numerous input, state, and output properties related to conservation, dissipation, and transport of mass and energy, nonnegative and compartmental systems are remarkably effective in describing the phenomenological behavior of these dynamical systems. The range of applications of nonnegative and compartmental systems is not limited to biological and medical systems. We used the developed framework to automatically control anesthetic drug delivery to control the depth of anesthesia in the face of system uncertainty, hemorrhage, hemodilution, and noisy EEG measurements.

Furthermore, a neuroadaptive output feedback control architecture for nonlinear nonnegative dynamical systems with input amplitude and integral constraints was developed. The proposed approach was used to control the infusion of the anesthetic drug propofol for maintaining a desired constant level of depth of anesthesia for noncardiac surgery in the face of infusion rate constraints and a drug dosing constraint over a specified period. In addition, we used the aforementioned neuroadaptive control architecture to control lung volume and minute ventilation with input pressure constraints that also accounts for spontaneous breathing by the patient. Specifically, we

develop a pressure- and work-limited neuroadaptive controller for mechanical ventilation based on a nonlinear multi-compartmental lung model. The control framework does not rely on any averaged data and is designed to automatically adjust the input pressure to the patient's physiological characteristics capturing lung resistance and compliance modeling uncertainty. Moreover, the controller accounts for input pressure constraints as well as work of breathing constraints. The effect of spontaneous breathing is incorporated within the lung model and the control framework.

Finally, a neural network hybrid adaptive control framework for nonlinear uncertain hybrid dynamical systems was developed. The proposed hybrid adaptive control framework is Lyapunov-based and guarantees partial asymptotic stability of the closed-loop hybrid system; that is, asymptotic stability with respect to part of the closed-loop system states associated with the hybrid plant states. A numerical example is provided to demonstrate the efficacy of the proposed hybrid adaptive stabilization approach.

9.2. Recommendations for Future Research

In future research, we propose to extend our neuroadaptive control schemes for improving control system performance. High performance integrated control systems satisfying multiple design criteria and real-world hardware constraints is imperative in light of the increasingly complex nature of dynamical systems. In this regard, we propose to merge our neuroadaptive control framework with intelligent control methods using fast learning algorithms to further advance control system design for clinical pharmacology.

Recently, several modification schemes for adaptive and neuroadaptive control methods, including Q-modification developed in this dissertation, have been proposed

in the literature. These schemes involve an augmentation of classical update laws with different constraints imposed on the update weights. Such modifications are intended to serve different purposes in the adaptive control algorithms, such as, for example, fast learning of the uncertainty, maintaining desired gain and phase margins of the closed-loop system, capturing of uncertainties with time-varying ideal weights, etc. It is a problem of a significant theoretical and practical importance to consider combinations of the existing modifications of the update laws and study the optimality of the composite schemes. This is particularly necessary to achieve transient behavior improvements for adaptive and neuroadaptive control schemes.

Another perspective topic related to neuroadaptive control is neural networks with non-constant size and time-varying structure. Such neural networks have a potential for more efficient and computationally low-cost schemes. In addition, neuroadaptive control of stochastic systems is a fruitful area of research of substantial practical and theoretical importance.

The complex highly uncertain and hostile environment of surgery places stringent performance requirements for closed-loop set-point regulation of multiple physiological variables. For example, during cardiac surgery, blood pressure control is vital and is subject to numerous highly uncertain exogenous disturbances. Vasoactive and cardioactive drugs are administered resulting in large disturbance oscillations to the system (patient). The arterial line may be flushed and blood may be drawn, corrupting sensor blood pressure measurements. Low anesthetic levels may cause the patient to react to painful stimuli, thereby changing system (patient) response characteristics. The flow rate of vasodilator drug infusion may fluctuate causing transient changes in the infusion delay time. Hemorrhage, patient position changes, cooling and warming of the patient, and changes in anesthesia levels will also effect system (patient) response characteristics.

In light of the complex and highly uncertain nature of system (patient) response characteristics under surgery requiring controls, it is not surprising that reliable system models for many high performance drug delivery systems are unavailable. In the face of such high levels of system uncertainty, robust controllers may unnecessarily sacrifice system performance whereas adaptive controllers are clearly appropriate since they can tolerate far greater system uncertainty levels to improve system performance. Hence, adaptive and neuroadaptive control schemes for addressing cardiovascular function and anesthesia can have a significant potential to further improve the quality of medical care.

The EEG signal and its derivatives has been one of the main methods for quantifying sedation. However, while the EEG measurement produces a reliable signal in operating room, in the ICU, it has a number of drawbacks which can limit its usefulness and reliability. In particular, in the ICU, the EEG signal can be severely degraded by noise. While proper filtering of EEG signal helps to alleviate this problem, other features such as the dependance of the EEG signal on certain medical conditions and medications limit its applicability for monitoring consciousness. In this case, other measures are necessary which can give a much more accurate estimate of patient sedation levels. In particular, a compound index incorporating the BIS signal, the mean arterial pressure (MAP) values, motion activity measurements using actigraphy, breathing/ventilation dyssynchrony, and digital imaging may offer a far better measure for quantifying sedation. Such a technology has a tremendous potential to improve and facilitate medical care, decrease health care cost, and reduce work load for the medical staff. This can be a very fruitful area for further research.

References

[1] D. Y. Abramovitch, R. L. Kosut, and G. F. Franklin, "Adaptive control with saturating inputs," in *Proc. IEEE Conf. Decision and Control*, Athens, Greece, pp. 848–852, 1986.

[2] D. Aeyels and J. Peuteman, "A new asymptotic stability criterion for nonlinear time-variant differential equations," *IEEE Trans. Autom. Contr.*, vol. 43, no. 7, pp. 968–971, 1998.

[3] D. H. Anderson, *Compartmental Modeling and Tracer Kinetics*. Berlin, Germany: Springer-Verlag, 1983.

[4] P. J. Antsaklis and A. Nerode, eds., "Special issue on hybrid control systems," *IEEE Trans. Autom. Control*, vol. 43, no. 4, 1998.

[5] K. J. Åström and B. Wittenmark, *Adaptive Control*. Reading, MA: Addison-Wesley, 1989.

[6] J. M. Bailey, "Management of the hemodynamically unstable patient," vol. 20, lesson 12, ed. F. Moya, Miami, 2000.

[7] J. M. Bailey and W. M. Haddad, "Drug-dosing control in clinical pharmacology: Paradigms, benefits, and challenges," *Contr. Syst. Mag.*, vol. 25, pp. 35–51, 2005.

[8] J. Bailey, W. Haddad, J. Im, and T. Hayakawa, "Adaptive and neural network adaptive control of depth of anesthesia during surgery," in *Proc. Amer. Contr. Conf.*, Minneapolis, MN, pp. 3409–3414, 2006.

[9] D. D. Bainov and P. S. Simeonov, *Systems with Impulse Effect: Stability, Theory and Applications*. England: Ellis Horwood Limited, 1989.

[10] J. J. Batzel and H. T. Trana, "Modeling instability in the control system for human respiration: Applications to infant non-REM sleep," *Applied Math. and Comput.*, vol. 110, no. 1, pp. 1–51, 2000.

[11] J. W. Bellville and G. M. Attura, "Servo control of general anesthesia," *Science*, vol. 126, pp. 827–830, 1957.

[12] A. Berman, M. Neumann, and R. J. Stern, *Nonnegative Matrices in Dynamic Systems*. New York: Wiley, 1989.

[13] A. Berman and R. J. Plemmons, *Nonnegative Matrices in the Mathematical Sciences*. New York, NY: Academic Press, 1979.

[14] D. S. Bernstein and D. C. Hyland, "Compartmental modeling and second-moment analysis of state space systems," *SIAM J. Matrix Anal. Appl.*, vol. 14, pp. 880–901, 1993.

[15] S. P. Bhat and D. S. Bernstein, "Lyapunov analysis of semistability," in *Proc. Amer. Control Conf.*, San Diego, CA, pp. 1608–1612, June 1999.

[16] R. G. Bickford, "Automatic electroencephalographic control of general anesthesia," *Electroencephalographic Clin. Neurophysiol.*, vol. 2, pp. 93–96, 1950.

[17] R. W. Brockett, "Asymptotic stability and feedback stabilization," in *Differential Geometric Control Theory* (R. W. Brockett, R. S. Millman, and H. J. Sussmann, eds.), pp. 181–191, Boston, MA: Birkhauser, 1983.

[18] C. I. Byrnes and A. Isidori, "Asymptotic stabilization of minimum phase nonlinear systems," *IEEE Trans. Autom. Control*, vol. 36, no. 10, pp. 1122–1137, 1991.

[19] A. J. Calise, N. Hovakimyan, and M. Idan, "Adaptive output feedback control of nonlinear systems using neural networks," *Automatica*, vol. 37, no. 8, pp. 1201–1211, 2001.

[20] A. J. Calise, Y. Shin, and M. D. Johnson, "A comparison study of classical and neural network based adaptive control of wing rock," in *Proc. AIAA Guidance, Navigation and Control Conference*, Providence, RI, June 2004.

[21] V. Chellaboina, S. P. Bhat, and W. M. Haddad, "An invariance principle for nonlinear hybrid and impulsive dynamical systems," *Nonlinear Anal.: Theory Methods Appl.*, vol. 53, pp. 527–550, 2003.

[22] V. Chellaboina, W. M. Haddad, J. M. Bailey, and H. Li, "Limit cycle stability analysis of a multi-compartment model for a pressure-limited respirator and lung mechanics system," in *Proc. Amer. Contr. Conf.*, New York, NY, pp. 2024–2029, 2007.

[23] V. Chellaboina and W. M. Haddad, "A unification between partial stability and stability theory for time-varying systems," *Contr. Syst. Mag.*, vol. 22, pp. 66–75, 2002. Erratum, vol. 23, p. 101, 2003.

[24] C.-T. Chen, *Linear System Theory and Design*. New York: Holt, Rinehart, and Winston, 1984.

[25] F. C. Chen and H. K. Khalil, "Adaptive control of nonlinear systems using neural networks," *Int. J. Control*, vol. 55, no. 6, pp. 1299–1317, 1992.

[26] F. C. Chen and H. K. Khalil, "Adaptive control of a class of nonlinear discrete-time systems using neural networks," *IEEE Trans. Autom. Contr.*, vol. 40, no. 5, pp. 791–807, 1995.

[27] J. Y. Choi and J. A. Farrell, "Adaptive observer backstepping control using neural networks," *IEEE Trans. Neural Networks*, vol. 12, no. 5, pp. 1101 –1112, 2001.

[28] P. S. Crooke, J. J. Marini, and J. R. Hotchkiss, "Modeling recruitment maneuvers with a variable compliance model for pressure controlled ventilation," *Journal of Theoretical Medicine*, vol. 4, no. 3, pp. 197–207, 2002.

[29] P. De Leenheer and D. Aeyels, "Stability properties of classes of cooperative systems," *IEEE Trans. Autom. Contr.*, vol. 46, no. 12, pp. 1996–2001, 2001.

[30] P. De Leenheer and D. Aeyels, "Stabilization of positive linear systems," *Syst. Control Lett.*, vol. 44, pp. 259–271, 2001.

[31] H. Deng, H.-X. Lin, and Y.-H. Wu, "Feedback-linearization-based neural adaptive control for unknown nonaffine nonlinear discrete-time systems," *IEEE Trans. Neural Networks*, vol. 19, no. 9, pp. 1615–1625, 2008.

[32] M. M. Duarte and K. S. Narendra, "Combined direct and indirect approach to adaptive control," *IEEE Trans. Autom. Contr.*, vol. 34(10), pp. 1071–1075, 1989.

[33] R. G. Eckenhoff and J. S. Johansson, "On the relevance of "clinically relevant concentrations" of inhaled anesthetics in in vitro experiments," *Anesthesiology*, vol. 91, no. 3, pp. 856–860, 1999.

[34] S. Fabri and V. Kadirkamanathan, "Dynamic structure neural networks for stable adaptive control of nonlinear systems," *IEEE Trans. Neural Networks*, vol. 7, no. 5, pp. 1151–1166, 1996.

[35] L. Farina and S. Rinaldi, *Positive Linear Systems: Theory and Applications*. New York, NY: John Wiley & Sons, 2000.

[36] D. M. Foster and M. R. Garzia, "Nonhierarchical communications networks: An application of compartmental modeling," *IEEE Trans. Communications*, vol. 37, pp. 555–564, 1989.

[37] W. Gao and R. R. Selmic, "Adaptive neural network output feedback control of nonlinear systems with actuator saturation," in *Proc. IEEE Conf. Dec. Contr.*, Seville, Spain, pp. 5522–5527, December 2005.

[38] S. S. Ge, T. H. Lee, G. Y. Li, and J. Zhang, "Adaptive NN control for a class of discrete-time non-linear systems," *Int. J. Contr.*, vol. 76, no. 4, pp. 334–354, 2003.

[39] A. Gentilini, M. Rossoni-Gerosa, C. W. Frei, R. Wymann, M. Morari, A. M. Zbinden, and T. W. Schnider, "Modeling and closed-loop control of hypnosis by means of bispectral index (BIS) with isoflurane," *IEEE Trans. Biomed. Eng.*, vol. 48, pp. 874–889, 2001.

[40] S. S. Ge and C. Wang, "Adaptive neural control of uncertain MIMO nonlinear systems," *IEEE Trans. Neural Networks*, vol. 15, no. 3, pp. 674 –692, 2004.

[41] P. S. Glass, M. Bloom, L. Kearse, C. Rosow, P. Sebel, and P. Manberg, "Bispectral analysis measures sedation and memory effects of propofol, midazolam, isoflurane, and alfentanil in normal volunteers," *Anesthesiology*, vol. 86, pp. 836–847, 1997.

[42] P. S. Glass, D. K. Goodman, B. Ginsberg, J. G. Reves, and J. R. Jacobs, "Accuracy of pharmacokinetic model-driven infusion of propofol," *Anesthesiology*, vol. 71, p. A277, 1989.

[43] P. S. A. Glass and I. J. Rampil, "Automated anesthesia: Fact or fantasy?," *Anesthesiology*, vol. 95, pp. 1–2, 2001.

[44] K. Godfrey, *Compartmental Models and Their Applications*. New York: Academic, 1983.

[45] G. C. Goodwin and K. S. Sin, *Adaptive filtering prediction and control*. Englewood Cliffs, NJ: Prentice-Hall, 1984.

[46] W. M. Haddad, J. M. Bailey, T. Hayakawa, and N. Hovakimyan, "Neural network adaptive output feedback control for intensive care unit sedation and intraoperative anesthesia," *IEEE Trans. Neural Networks*, vol. 18, pp. 1049–1066, 2007.

[47] W. M. Haddad and V. Chellaboina, "Stability and dissipativity theory for nonnegative dynamical systems: A unified analysis framework for biological and physiological systems," *Nonlinear Analysis: Real World Appl.*, vol. 6, pp. 35–65, 2005.

[48] W. M. Haddad and V. Chellaboina, *Nonlinear Dynamical Systems and Control: A Lyapunov-Based Approach*. Princeton, NJ: Princeton University Press, 2008.

[49] W. M. Haddad, V. Chellaboina, and Q. Hui, *Nonnegative and Compartmental Dynamical Systems.* Princeton, NJ: Princeton University Press, 2010.

[50] W. M. Haddad, V. Chellaboina, and N. A. Kablar, "Nonlinear impulsive dynamical systems part I: Stability and dissipativity," *Int. J. Contr.*, vol. 74, pp. 1631–1658, 2001.

[51] W. M. Haddad, V. Chellaboina, and S. G. Nersesov, *Impulsive and Hybrid Dynamical Systems: Stability, Dissipativity, and Control*. Princeton, NJ: Princeton University Press, 2006.

[52] W. M. Haddad and T. Hayakawa, "Adaptive control for nonlinear nonnegative dynamical systems," *Automatica*, vol. 40, pp. 1637–1642, 2004.

[53] W. M. Haddad, T. Hayakawa, and J. M. Bailey, "Adaptive control for nonnegative and compartmental dynamical systems with applications to general anesthesia," *Int. J. Adapt. Control Signal Process.*, vol. 17, pp. 209–235, 2003.

[54] W. M. Haddad, T. Hayakawa, and J. M. Bailey, "Adaptive control for nonlinear compartmental dynamical systems with applications to clinical pharmacology," *Sys. Contr. Lett.*, vol. 55, pp. 62–70, 2006.

[55] W. M. Haddad, T. Hayakawa, S. G. Nersesov, and V. Chellaboina, "Hybrid adaptive control for nonlinear impulsive dynamical systems," *Int. J. Adapt. Control Signal Process.*, vol. 19, no. 6, pp. 445–469, 2005.

[56] W. M. Haddad, K. Y. Volyanskyy, and J. Bailey, "Neuroadaptive output feedback control for automated anesthesia with noisy EEG measurements," *IEEE Trans. Contr. Syst. Tech.*, to appear.

[57] T. Hayakawa, W. M. Haddad, J. M. Bailey, and N. Hovakimyan, "Passivity-based neural network adaptive output feedback control for nonlinear nonnegative dynamical systems," *IEEE Trans. Neural Networks*, vol. 16, pp. 387–398, 2005.

[58] T. Hayakawa, W. M. Haddad, and N. Hovakimyan, "Neural network adaptive control for nonlinear uncertain dynamical systems with asymptotic stability guarantees," *IEEE Trans. Neural Networks*, vol. 19, pp. 80–89, 2008.

[59] T. Hayakawa, W. M. Haddad, N. Hovakimyan, and J. M. Bailey, "Neural network adaptive dynamic output feedback control for nonlinear nonnegative systems using tapped delay memory units," in *Proc. Amer. Contr. Conf.*, Boston, MA, July 2004.

[60] A. V. Hill, "The possible effects of the aggregation of the molecules of haemoglobin on its dissociation curves," *J. Physiol.*, vol. 40, pp. iv–vii, 1910.

[61] N. Hovakimyan, F. Nardi, A. Calise, and N. Kim, "Adaptive output feedback control of uncertain nonlinear systems using single-hidden-layer neural networks," *IEEE Trans. Neural Networks*, vol. 13, no. 6, pp. 1420–1431, 2002.

[62] Q. Hui, W. M. Haddad, V. Chellaboina, and T. Hayakawa, "Adaptive control of mammillary drug delivery systems with actuator amplitude constraints and system time delays," *Eur. J. Control*, vol. 11, pp. 586–600, 2005.

[63] K. J. Hunt, D. Sbarbaro, R. Zbikowski, and P. J. Gawthrop, "Neural networks for control: A survey," *Automatica*, vol. 28, pp. 1083–1112, 1992.

[64] C.-L. Hwang and C.-H. Lin, "A discrete-time multivariable neuro-adaptive control for nonlinear unknown dynamic systems," *IEEE Trans. Syst. Man Cybern.*, vol. 30, no. 6, pp. 865–877, 2000.

[65] P. Ioannou and P. Kokotovic, "Instability analysis and improvement of robustness of adaptive control," *Automatica*, vol. 20, no. 5, pp. 583–594, 1984.

[66] P. A. Ioannou and J. Sun, *Robust Adaptive Control*. Upper Saddle River, NJ: Prentice-Hall, 1996.

[67] A. Isidori, *Nonlinear Control Systems*. New York: Springer-Verlag, 1995.

[68] E. F. Ismail, S. J. Kim, and M. R. Salem, "Direct effects of propofol on myocardial contractility in situ canine hearts," *Anesthesiology*, vol. 79, pp. 964–972, 1992.

[69] J. A. Jacquez, *Compartmental Analysis in Biology and Medicine*. Ann Arbor, MI: Univ. Michigan Press, 1985.

[70] J. A. Jacquez and C. P. Simon, "Qualitative theory of compartmental systems," *SIAM Rev.*, vol. 35, pp. 43–79, 1993.

[71] S. Jagannathan, "Control of a class of nonlinear discrete-time systems using multilayer neural networks," *IEEE Trans. Neural Networks*, vol. 12, no. 5, pp. 1113–1120, 2001.

[72] S. Jagannathan, *Neural Network Control of Nonlinear Discrete-Time Systems*. Boca Raton, FL: CRC Press, 2006.

[73] S. Jagannathan and F. L. Lewis, "Discrete-time neural net controller for a class of nonlinear dynamical systems," *IEEE Trans. Autom. Contr.*, vol. 41, no. 11, pp. 1693–1699, 1996.

[74] S. Jagannathan and F. L. Lewis, "Multilayer discrete-time neural-net controller with guaranteed performance," *IEEE Trans. Neural Networks*, vol. 7, no. 1, pp. 107–130, 1996.

[75] J. W. Johansen and P. S. Sebel, "Development and clinical application of electroencephalographic bispectrum monitoring," *Anesthesiology*, vol. 93, pp. 1336–1340, 2000.

[76] S. P. Kárason and A. M. Annaswamy, "Adaptive control in the presence of input constraints," *IEEE Trans. Autom. Control*, vol. 39, pp. 2325–2330, 1994.

[77] M. Kaya and J. Li, "Modeling aspect of hemorrhage and hemodilution," in *Proc. IEEE Conf. Dec. Contr.*, 28th Annual Northeast, pp. 177–178, 2002.

[78] T. Kazama, K. Ikeda, K. Morita, M. Kikura, M. Doi, T. Ikeda, and T. Kurita, "Comparison of the effect site KeOs of propofol for blood pressure and EEG bispectral index in elderly and young patients," *Anesthesiology*, vol. 90, pp. 1517–1527, 1999.

[79] T. Kazama, T. Kurita, K. Morita, J. Nakata, and S. Sato, "Influence of hemorrhage on propofol pseudo-steady state concentration," *Anesthesiology*, vol. 97, pp. 1156–1161, 2002.

[80] H. K. Khalil, *Nonlinear Systems*. Upper Saddle River, NJ: Prentice-Hall, 2 ed., 1996.

[81] M. C. Khoo, R. E. Kronauer, K. P. Strohl, and A. S. Slutsky, "Factors inducing periodic breathing in humans: A general model," *Journal of Appl. Physiol.*, vol. 53, pp. 644–659, 1982.

[82] B. S. Kim and A. J. Calise, "Nonlinear flight control using neural networks," *AIAA J. Guid. Contr. Dyn.*, vol. 20, no. 1, pp. 26–33, 1997.

[83] M. Krstić, I. Kanellakopoulos, and P. V. Kokotović, *Nonlinear and Adaptive Control Design*. New York: Wiley, 1995.

[84] V. Lakshmikantham, D. D. Bainov, and P. S. Simeonov, *Theory of Impulsive Differential Equations*. Singapore: World Scientific, 1989.

[85] T. P. Laubscher, W. Heinrichs, and N. Weiler, "An adaptive lung ventilation controller," *IEEE Trans. Biomed. Eng*, vol. 41, no. 1, pp. 51–59, 1994.

[86] E. Lavretsky and N. Hovakimyan, "Stable adaptation in the presence of input constraints," *Sys. Contr. Lett.*, vol. 56, pp. 722–729, 2007.

[87] E. Lavretsky, N. Hovakimyan, and A. J. Calise, "Upper bounds for approximation of continuous-time dynamics using delayed outputs and feedforward neural networks," *IEEE Trans. Autom. Control*, vol. 48, pp. 1606–1610, 2003.

[88] E. Lavretsky and N. Hovakimyan, "Positive μ-modification for stable adaptation in the presense of input constraints," in *Proc. Amer. Contr. Conf.*, Boston, MA, pp. 2545–2550, July 2004.

[89] E. Lavretsky and K. Wise, "Adaptive flight control for manned / unmanned military aircraft," 2005 (unpublished).

[90] A. Leonessa, W. M. Haddad, T. Hayakawa, and Y. Morel, "Adaptive control for nonlinear uncertain systems with actuator amplitude and rate saturation constraints," *Int. J. Adapt. Control Signal Process.*, vol. 23, pp. 73–96, 2009.

[91] A. U. Levin and K. S. Narendra, "Control of nonlinear dynamical systems using neural networks: Controllability and stabilization," *IEEE Trans. Neural Networks*, vol. 4, no. 2, pp. 192 –206, 1993.

[92] F. L. Lewis, S. Jagannathan, and A. Yesildirak, *Neural Network Control of Robot Manipulators and Nonlinear Systems*. London, U.K.: Taylor & Francis, 1999.

[93] F. L. Lewis, A. Yesildirek, and K. Liu, "Multilayer neural-net robot controller with guaranteed tracking performance," *IEEE Trans. Neural Networks*, vol. 7, no. 2, pp. 388 –399, 1996.

[94] D. A. Linkens, M. F. Abbod, and J. E. Peacock, "Clinical implementation of advanced control in anaesthesia," *Trans. Inst. Meas. Control*, vol. 22, pp. 303–330, 2000.

[95] L. Lin, P. N. Nikiforuk, and M. M. Gupta, "Fast neural learning and control of discrete-time nonlinear systems," *IEEE Trans. Syst. Man Cybern.*, vol. 25, no. 3, pp. 478–488, 1995.

[96] B. Marsh, M. White, N. Morton, and G. N. Kenny, "Pharmacokinetic model driven infusion of propofol in children," *Brit. J. Anaesth.*, vol. 67, pp. 41–48, 1991.

[97] L. Martin, *Pulmonary Physiology in Clinical Practice.* St. Louis, MO: C.V. Mosby, 1987.

[98] A. S. Morse, C. C. Pantelides, S. Sastry, and J. M. Schumacher, eds., "Special issue on hybrid control systems," *Automatica*, vol. 35, no. 3, 1999.

[99] E. Mortier, M. Struys, T. De Smet, L. Versichelen, and G. Rolly, "Closed-loop controlled administration of propofol using bispectral analysis," *Anaesthesia*, vol. 53, pp. 749–754, 1998.

[100] R. J. Mulholland and M. S. Keener, "Analysis of linear compartmental models for ecosystems," *J. Theoret. Biol.*, vol. 44, pp. 105–116, 1974.

[101] M. Muzi, R. A. Berens, J. P. Kampine, and T. J. Ebert, "Venodilation contributes to propofol-mediated hypotension in humans," *Aneth. Analg.*, vol. 74, pp. 877–883, 1992.

[102] K. Narendra and A. Annaswamy, "A new adaptive law for robust adaptation without persistent excitation," *IEEE Trans. Autom. Contr.*, vol. 32, no. 2, pp. 134–145, 1987.

[103] K. S. Narendra and A. M. Annaswamy, *Stable Adaptive Systems.* Englewood Cliffs, NJ: Prentice-Hall, 1989.

[104] K. S. Narendra and K. Parthasarathy, "Identification and control of dynamical systems using neural networks," *IEEE Trans. Neural Networks*, vol. 1, pp. 4–27, 1990.

[105] J. Park and I. Sandberg, "Universal approximation using radial basis function networks," *Neural Computation*, vol. 3, pp. 246–257, 1991.

[106] A. N. Payne, "Adaptive one-step-ahead control subject to an input-amplitude constraint," *Int. J. Control*, vol. 43, pp. 1257–1269, 1986.

[107] G. Plourde, "BIS EEG monitoring: What it can and cannot do in regard to unintentional awareness," *Can. J. Anesth.*, vol. 49, p. R12, 2002.

[108] M. Polycarpou, "Stable adaptive neural control scheme for nonlinear systems," *IEEE Trans. Autom. Contr.*, vol. 41, no. 3, pp. 447–451, 1996.

[109] M. Polycarpou and P. Ioannou, "Modeling, identification, and stable adaptive control of continuous-time nonlinear dynamical systems using neural networks," in *Proc. Amer. Contr. Conf.*, pp. 36–40, June 1992.

[110] I. J. Rampil, "A primer for EEG signal processing in anesthesia," *Anesthesiology*, vol. 89, no. 4, pp. 980–1002, 1998.

[111] H. L. Royden, *Real Analysis.* New York: Macmillan, 1988.

[112] A. M. Samoilenko and N. Perestyuk, *Impulsive Differential Equations*. Singapore: World Scientific, 1995.

[113] W. Sandberg, "On the mathematical foundations of compartmental analysis in biology, medicine and ecology," *IEEE Trans. Circuits Syst.*, vol. 25, pp. 273–279, 1978.

[114] R. Sanner and J. Slotine, "Gaussian networks for direct adaptive control," *IEEE Trans. Neural Networks*, vol. 3, no. 6, pp. 837–864, 1992.

[115] T. W. Schnider, C. F. Minto, and D. R. Stanski, "The effect compartment concept in pharmacodynamic modelling," *Anaes. Pharmacol. Rev.*, vol. 2, pp. 204–213, 1994.

[116] M. Schwager and A. Annaswamy, "Direct adaptive control of multi-input plants with magnitude saturation constraints," in *Proc. IEEE Conf. Dec. Contr.*, Seville, Spain, pp. 783–788, December 2005.

[117] H. Schwilden, J. Schutler, and H. Stoeckel, "Closed-loop feedback control of methohexital anesthesia by quantitative EEG analysis in humans," *Anesthesiology*, vol. 67, pp. 341–347, 1987.

[118] H. Schwilden and H. Stoeckel, "Quantitative EEG analysis during anesthesia with isoflurane in nitrous oxide at 1.3 and 1.5 MAC," *Brit. J. Anaesth.*, vol. 59, pp. 738–745, 1987.

[119] J. C. Scott, K. V. Ponganis, and D. R. Stanski, "EEG quantification of narcotic effect: The comparative pharmacodynamics of fentanyl and alfentanyl," *Anesthesiology*, vol. 62, pp. 234–241, 1985.

[120] P. S. Sebel, E. Lang, I. J. Rampil, P. White, R. C. M. Jopling, N. T. Smith, P. S. Glass, and P. Manberg, "A multicenter study of bispectral electroencephalogram analysis for monitoring anesthetic effect," *Anesth. Analg.*, vol. 84, no. 4, pp. 891–899, 1997.

[121] S. Seshagiri and H. Khalil, "Output feedback control of nonlinear systems using rbf neural networks," *IEEE Trans. Neural Networks*, vol. 11, no. 1, pp. 69–79, 2000.

[122] A. Sidi, P. Halimi, and S. Cotev, "Estimating anesthetic depth by electroencephalography during anesthetic induction and intubation in patients undergoing cardiac surgery," *J. Clin. Anesth.*, vol. 2, pp. 101–107, 1990.

[123] J. C. Sigl and N. G. Chamoun, "An introduction to bispectral analysis for the electroencephalogram," *J. Clin. Monit.*, vol. 10, pp. 392–404, 1994.

[124] D. D. Siljak, *Large-Scale Dynamic Systems*. New York: North-Holland, 1978.

[125] C. Sinderby, P. Navalesi, and J. Beck, "Neural control of mechanical ventilation in respiratory failure," *Natural Medicines*, vol. 5, no. 12, pp. 1433–1436, 1999.

[126] J.-J. E. Slotine and W. Li, "Composite adaptive control of robot manipulators," *Automatica*, vol. 25(4), pp. 508–519, 1989.

[127] J.-J. E. Slotine and W. Li, *Applied Nonlinear Control*. Englewood Cliffs, NJ: Prentice-Hall, 1991.

[128] E. D. Sontag and Y. Wang, "On characterizations of the input-to-state stability property," *Syst. Control Lett.*, vol. 24, pp. 351–359, 1995.

[129] J. Spooner, M. Maggiore, R. Ordonez, and K. Passino, *Stable Adaptive Control and Estimation for Nonlinear Systems: Neural and Fuzzy Approximator Techniques*. New York, NY: John Wiley & Sons, 2002.

[130] M. Struys, M. Coppens, N. De Neve, E. Mortier, A. Doufas, J. Van Bocxlaer, and S. Shafer, "Influence of administration rate on propofol plasma-effect site equilibration.," *Anesthesiology*, vol. 107, no. 3, pp. 386–396, 2007.

[131] M. Struys, T. De Smet, L. Versichelen, S. Van de Vilde, R. Van den Broecke, and E. Mortier, "Comparison of closed-loop controlled administration of propofol using BIS as the controlled variable versus "standard practice" controlled administration," *Anesthesiology*, vol. 95, pp. 6–17, 2001.

[132] G. Tao, *Adaptive Control Design and Analysis*. New York: Wiley, 2003.

[133] M. J. Tobin, *Principles and Practice of Mechanical Ventilation*. New York: McGraw-Hill, 1994.

[134] R. N. Upton, G. I. Ludrook, C. Grant, and A. Martinez, "Cardiac output is a determinant of the initial concentration of propofol after short-term administration," *Aneth. Analg.*, vol. 89, pp. 545–552, 1999.

[135] M. Vidyasagar, *Nonlinear Systems Analysis*. Englewood Cliffs, NJ: Prentice-Hall, 1993.

[136] K. Y. Volyanskyy, A. J. Calise, and B.-J. Yang, "A novel Q-modification term for adaptive control," in *Proc. Amer. Contr. Conf.*, Minneapolis, MN, pp. 4072–4076, June 2006.

[137] K. Y. Volyanskyy, A. J. Calise, B.-J. Yang, and E. Lavretsky, "An error minimization method in adaptive control," in *Proc. AIAA Guidance, Navigation and Control Conference*, Keystone, CO, August 2006.

[138] K. Y. Volyanskyy, W. M. Haddad, and A. J. Calise, "A new neuroadaptive control architecture for nonlinear uncertain dynamical systems: Beyond σ- and e-modifications," *IEEE Trans. Neural Networks*, vol. 20, no. 11, pp. 1707–1723, 2009.

[139] K. Volyanskyy, W. M. Haddad, and A. J. Calise, "A new neuroadaptive control architecture for nonlinear uncertain dynamical systems: Beyond σ- and e-modifications," in *Proc. IEEE Conf. Dec. Contr.*, Cancun, Mexico, pp. 80–85, December 2008.

[140] E. R. Weibel, *Morphometry of the Human Lung*. New York: Academic Publishers, 1963.

[141] J. B. West, *Respiratory Physiology*. Philadelphia: Lippincott Williams & Wilkins, 2008.

[142] M. White and G. N. C. Kenny, "Intravenous propofol anaesthesia using a computerised infusion system," *Anesthesia*, vol. 45, pp. 204–209, 1990.

[143] J. C. Willems, "Least squares stationary optimal control and the algebraic Riccati equation," *IEEE Trans. Autom. Control*, vol. 16, pp. 621–634, 1971.

[144] M. Younes, *Principles and Practice of Mechanical Ventilation*, ch. Proportional Assist Ventilation. In Tobin M. J. (ed.), pp. 349–369. New York: McGraw-Hill, 1994.

[145] M. Younes, A. Puddy, and D. Roberts, "Proportional assist ventilation. Results of an initial clinical trial," *American Review of Respiratory Desease*, vol. 145, pp. 121–129, 1992.

[146] C. Zhang and R. J. Evans, "Amplitude constrained adaptive control," *Int. J. Control*, vol. 46, pp. 53–64, 1987.

[147] X. S. Zhang, R. J. Roy, and E. W. Jensen, "EEG complexity as a measure of depth of anesthesia for patients," *IEEE Trans. Biomed. Eng.*, vol. 48, pp. 1424–1433, 2001.